Cranfield University

Marco Nunez

Design Exploration
for
Engineering Design Optimisation

An Aircraft Conceptual Perspective

School of Engineering

Department of Aircraft Engineering

PhD Thesis

Academic Year 2010-2011

Supervisor: Prof. Marin D. Guenov

November 2010

Cranfield University

School of Engineering

Department of Aircraft Engineering

PhD Thesis

Academic Year 2010-2011

Marco Nunez

Design Exploration for Engineering Design Optimisation

An Aircraft Conceptual Perspective

Supervisor: Prof. Marin D. Guenov

November 2010

This thesis is submitted in partial fulfilment of the requirements for the Degree of Doctor of Philosophy

"Exploration is really the essence of the human spirit."

Frank Borman

Abstract

Most of the efforts in optimisation so far have been focused on the development of novel or the improvement of existing numerical methods for an effective computation of optimal solutions. Particular attention has been put on balancing multiple conflicting objectives, handling the interaction between different disciplines, reducing computational cost and managing uncertainty. Nonetheless, specific issues of this design methodology still remain to be properly addressed. In this research, attention is concentrated on advancing engineering optimisation as a tool for design exploration. The work is put in the context of conceptual aircraft design.

The overall aim of the present research is to develop a methodology that allows the designer to effectively conduct an exploration and analysis of alternative design solutions via a set of methods that can be used separately or conjointly.

The initial part of the thesis introduces two novel methods for assisting the formulation of an optimisation problem, which generally is assumed to be given *a priori*. Nonetheless, the correctness of the optimisation statement, which is not addressed by established optimisation methods, turns out to be decisive for the feasible design set determination. The designer is thus provided with an adaptive formulation of functional and design-variable constraints, which allows the exploration of further promising solutions initially not contained in the feasible design set. Meaningless results or the loss of important solutions can therefore be partially avoided.

In a second instance, attention is focused on the visualisation needs for design exploration. A suitable visualisation methodology has been developed to make the large multidimensional results of complex design optimisation procedures fully readable and explanatory. This is achieved by integrating advanced visualisation techniques which

provide the designer with diverse perspectives of the data under study and allow him/her to conduct a number of analysis tasks on it, without the need to be an expert in numerical optimisation methods.

Last, but not least, a methodology to address conceptual design change problems is proposed. The decision-maker is enabled to formally state the new design requirements and priorities introduced by the conceptual change via an adequate problem reformulation. All the data previously collected can thus be re-used and exploited to drive an effective exploration of alternative design solutions through design space regions of interest.

The evaluation of the proposed methodologies has been carried out with a number of test cases. Analytical examples have been used for the assessment of effectiveness, whereas codes representative of aircraft sizing procedures have been adopted to evaluate the methodologies functionality. A visualisation user interface prototype has also been developed for demonstration and evaluation purposes.

Acknowledgements

I would like to express my sincere gratitude to Prof. Marin D. Guenov for his invaluable guidance and patience, as well as for the opportunity to work with him. I also thank my past and present colleagues: Aditya, Atif, Jeremy, Libish, Mattia, Paolo, Varun, Vis and Yves.

A very special thanks goes to Cinzia for being on my side with her indispensable support and encouragement throughout all these years, each and every day. Without you it would have been completely different if not impossible.

I would like to warmly thank my parents and Fabrizio, who have always supported me in every possible way, notwithstanding the distance between us. I also would like to express my gratitude to all the rest of my family for the motivation and determination they provided me.

Finally, my gratefulness goes to the BC (members and semi-members). All the memories of past battles have been precious, not mentioning the northern campaigns.

Contents

List of Figures ... viii

List of Tables …. xvii

Abbreviations …. xx

1 Introduction ... 1

1.1. Problem Area ... 1

1.2. Research Aims and Objectives ... 2

1.3. Overview of Thesis ... 3

2 Literature Review ... 5

2.1. Engineering Design Optimisation ... 5

2.2. Problem Formulation ... 7

2.2.1. Search Region Definition ... 7

2.2.2. Non-rigid Constraints ... 10

2.3. Suitable Visualisation Techniques for Design Optimisation ... 11

2.3.1. Multidimensional Data Visualisation ... 12

2.3.2. Carpet Plots ... 16

2.3.3. Recent Developments in MOO Visualisation ... 17

2.3.4. Pareto Frontier Exploration via Approximations 18
2.3.5. Uncertainty Visualisation in Robust Design Optimisation 20
2.4. Design Change 22
2.5. Bayesian Global Optimisation 24
2.5.1. The Response Surface Model 24
2.5.2. Infill Sampling Criteria 29
2.5.3. Stop Criteria 33
2.6. Summary and Conclusions 34

3 Formulation of Optimisation Problems 36

3.1. Introduction 36
3.2. Proposed Method for an Adaptive and Efficient Setup of the Search Region .. 38
3.2.1. Terminology 39
3.2.2. Under-Determined and Over-Determined Search Regions 41
3.2.3. Restriction Criterion 42
3.2.4. Relaxation Criterion 44
3.2.5. Hybrid Optimisation 47
3.2.6. Implementation of ASOM 50
3.2.7. Analytical Example 52
3.3. Local Relaxation Method for Non-rigid Constraints 58
3.3.1. Problem Formulation and Assumptions 58
3.3.2. Proposed Relaxation Method 58
3.3.3. Analytical Example 62
3.4. Summary and Conclusions 66

4 Visual Exploration and Analysis of Design Solutions 68

4.1. Introduction 68

4.2. Visual Exploration of Alternative Design Solutions 69

4.3. Proposed Visualisation Methodology 71

4.3.1. Visualisation Techniques 72

4.3.2. Visualisation Interfaces 74

4.3.3. Operation of the Visualisation Interfaces 81

4.3.4. Robust Optimisation Data Visualisation 86

4.4. Summary and Conclusions 88

5 Exploration of Design Alternatives to Address Conceptual Design Changes ... 89

5.1. Introduction 89

5.2. Problem Definition and Assumptions 91

5.3. Proposed Method 94

5.3.1. Surrogate Model Phase 97

5.3.2. Problem Reformulation Phase 99

5.3.3. Design Exploration Phase 102

5.4. Analytical Example 104

5.5. Isocontours of Objectives and Constraints 112

5.6. Summary and Conclusions 118

6 Application Example - Aircraft Conceptual Design Optimisation 120

6.1. Introduction 120

6.2. Test Case Description 121

6.3. Adaptive Search Optimisation 122

6.4. Visual Exploration of Optimisation Results 128

6.5. Introduction of Minor Design Changes Affecting Conceptual Design 134

6.6. Summary and Conclusions 144

7 Summary and Conclusions 146

7.1. Introduction 146

7.2. Summary of Research 146

7.3. Contributions to Knowledge 148

7.4. Future Work 149

References ……. 151

Appendix A Parallel Coordinates Plot and Scatter Plot Matrix 168

Appendix B An Example of the Effects of Correcting the Search Region on the Optimal Solutions Set 176

Appendix C An Example of the Effects of Relaxing a Soft Constraint on the Optimal Solutions Set 183

Appendix D Engineering Change Problems that can Potentially Affect Aircraft Conceptual Design 188

List of Figures

Figure 1. Shown in orange and blue are the non-dominated and feasible solutions sets of a generic optimisation problem formulated as in Problem (1) with n=2, J=2, and I=2..... 6

Figure 2. Typical types of distributions: (a) Valid distribution, with a peak located in the central area of the normalised search region and a low density of samples near the bounds; (b) Invalid distribution, with the peak located in vicinity of the upper bound; (c) Invalid distribution, with the peak located in vicinity of the lower bound [53]..... 9

Figure 3. Procedure for adaptive search region proposed by Jeong et al. [53]. 10

Figure 4. Representation of four three-dimensional points through the Cartesian-coordinate system and a parallel coordinate plot. The point values per each dimension are specified on the table above..... 12

Figure 5. Scatter plot matrix displaying a satellite design dataset [111]. 14

Figure 6. Representation of the same dataset considered in Appendix A by means of the self-organising maps. The basic idea is that, through a learning process, the map is organised in such a way that all the cells close to each other represent all the inputs having similar features. The representation of any dataset is thus obtained via a set of two-dimensional plots, as many as the dimensions of the problem at hand. Each data sample is represented by a cell, which has always the same space position within all the plots. Each self-organising map is associated to a particular dimension and the values of its cells are encoded according to their colour-bar located besides the map..... 15

Figure 7. Example of the carpet plots of two different design points, one in red and the other in blue. Hatching denotes inadmissible side of constraint curves [82]. 17

Figure 8. Visualisation scheme proposed by Rangavajhala et al. [90]. The exploration of the robust Pareto cloud can be conducted in the mean objective space by varying the filter

tolerances tol_J, tol_h and tol_g associated to objective variation σ_J, probability of equality constraint satisfaction PCS_h, and probability of inequality constraint satisfaction PCS_g, respectively. 21

Figure 9. Comparison of the robust and deterministic results of an aircraft MOO problem. By considering the mean objective space *MTOW-RA*, the mean and variance of the solutions are represented by the red points and yellow ellipses for the robust Pareto cloud, and by the green points and blue ellipses for the deterministic Pareto front (after conducting an *a posteriori* uncertainty analysis) [43]..... 21

Figure 10. Different change types. In contrast to *change ripples* and *change blossoms*, that finish within the required time t, *change avalanches* can behave like *blossoms* over a longer, or represent an uncontrolled increment of changes [28]. 22

Figure 11. Typical curves with time for a generic product development cycle [92]. The shape of the curve will vary depending on a number of factors, e.g. the project at hand, design strategy, technologies, etc. 23

Figure 12. An example of response surface for a simple one-dimensional function $f(x)$. The real objective function is visualised in green, and the black dots identify the points where it has been sampled. The red line represents a potential predictor that fits such observations, and its standard error is depicted in blue below. 27

Figure 13. Diagnostic plots: (a) the *actual function values versus cross-validated predictions*, (b) the *standardized cross-validated residuals versus cross-validated predictions*..... 29

Figure 14. An example of response surface for a simple one-dimensional function $f(x)$. The response surface is visualised in green, and the black dots identify the points where $f(x)$ has been sampled. The predictor standard error is depicted in blue and the red line represents the current best sampled function value. 30

Figure 15. Notation taken into consideration in relation with the *i-th* variable search region..... 40

Figure 16. The analysis of each variable distribution reveals if its corresponding search region is (a) valid, (b) under-determined, or (c) over-determined. The lower and upper adaptive bounds of the variable are represented by green lines, while the black part of the histogram represents the fraction of feasible samples out of the entire set of sampled points (in red)..... 41

Figure 17. Notation adopted for the restriction criterion. 43

Figure 18. Probability bounds on normal and gamma distributions. 46

Figure 19. Comparison of the error trend for the Matlab function fmincon and the SPSA algorithm (averaged over 100 independent simulations). The proposed hybrid optimisation terminates the SPSA optimisation after obtaining a first considerable error decrement, switching to fmincon (in blue) to carry out the final phase of the optimisation search..... 50

Figure 20. Flowchart of the tasks that take place for each individual optimisation run. The variables bounds to be considered for the optimisation procedure starting from the *j-th* starting point are adequately determined by analysing the variables distributions of the overall feasible points previously evaluated. Note that the *i-th* design-variable can turn out to be over-determined with respect to its lower bound, and under-determined with respect to its upper-bound, and vice versa..... 52

Figure 21. The bump function in two dimensions [57]..... 53

Figure 22. An example of ASOM results from solving problem (42) considering twenty starting points..... 55

Figure 23. An example of resulting adaptive variables bounds for problem (43)..... 57

Figure 24. The four figures represent conceptually the four possible cases that may occur when relaxing a constraint of the same amount ε. Attention is here focused on the identification of the cases as in *d)*, where a significant improvement of the objective can be achieved via a minor relaxation of one constraint. 60

Figure 25. Conceptual representation of the proposed relaxation method. 61

Figure 26. Proposed loop to handle the relaxation of multiple constraints. 62

Figure 27. Results obtained for Problem (47) by using the Matlab algorithm fmincon on six different starting points, which are represented by the green triangles. The proposed method for constrain relaxation was subsequently used for the solutions characterized by constraint activation. The contours of the objective f and constraints g_1 and g_2 are given by the red, black and blue lines, respectively. 63

Figure 28. Magnified view of the optimisation procedures started from the points A, C and D along with the respective constraint(s) relaxation execution..... 65

Figure 29. Default visualisation of the *IEVI*. The three most relevant data perspectives in optimisation problems are shown via the below-described interfaces: *ESI* (top-right window), *SDTI* (top-left window) and *MDVI* (bottom window). 75

Figure 30. Two magnified examples of the visualisation flexibility allowed in *ESI*. The feasible, non-feasible and non-dominated sets of points have been identified by means of *Filtering* and are represented through green points, grey points and yellow squares, respectively. 76

Figure 31. Visualisation of the points obtained through the manual *Selective PCP Ranges* function for *Filtering*. In this case, the solutions within the ranges x_1=[0,0.5] and f=[-0.67334,- 0.4] are highlighted in the *ESI* through cyan x-markers. 78

Figure 32. Scatter plot matrix (*SPM*). 79

Figure 33. Visualisation of solutions for a conceptual aircraft design optimisation. The sets of feasible, non-feasible and non-dominated points are depicted in the *ESI* considering the same graphical notation of Figure 30. In the same interface, it is shown how any solution of interest can be interactively selected, updating in real time the two other interfaces. The designer is thus allowed to assess the satisfaction of performance and to conduct a numerical analysis of the selected point on the *SDTI* and *MDVI* respectively. 80

Figure 34. An example of an alternative use of the *SDTI* for a generic optimisation problem, offering a three-dimensional plot of the filtered data depicted in Figure 31. It is also shown how the interactive selection of points can be facilitated by zooming-in on the filtered solutions, as displayed in the *ESI*. 81

Figure 35. Comparison of three solutions interactively selected on the *ESI* from the clusters of points for which the objective function f is within the range [-0.67367,- 0.2]. 82

Figure 36. Visualisation of the solutions that meet a tighter constraint $g(\mathbf{x}) \leq 3$ by using the *Selective PCP Ranges Filtering* function. 83

Figure 37. Study of the non-feasible set of points. For this problem, from the analysis of the *PCP*, it is evident that no-improvement on the objective function f can be achieved via a relaxation of the constraint g. 84

Figure 38. Identification of the design points for which the constraint g is active. 85

Figure 39. Shown in the *SDTI* is the adopted robustness visualisation in the mean space of objectives/constraints for a RDO problem [43]. 87

Figure 40. Summary flowchart of the proposed exploration methodology to address conceptual design changes. 95

Figure 41. In this elementary example, the hypothetical original formulation of a one-dimensional problem consists of a single objective $f(x)$ and a single constraint $g(x) \leq 0$. The design change to accommodate is assumed to be formulated as a correction on the lower bound of *x*, which renders unfeasible the optimal point previously found (red square). The surrogate model $\hat{f}(x)$ to be used will fit all the evaluations earlier computed (black points), allowing to approximate the system elsewhere along with a prediction error estimation. Once the predictor accuracy is ensured, if necessary, via additional observations (blue triangles), the new feasible region(s) where to focus design exploration can hence be identified (in orange). 97

Figure 42. The goal attainment method with two generic objectives F_1 and F_2 [114][67]. 101

Figure 43. Relaxation concept for the proposed constraint-handling approach, comparing for a generic constraint $g_i(x) \leq 0$ the search regions corresponding to: (a) constraint satisfaction based only on the function prediction $\hat{g}_i(x)$; (b) constraint satisfaction based on the function prediction $\hat{g}_i(x)$ and its associated error $s_i(x)$. 104

Figure 44. Surrogate models of *f*(x) and *g*(x). 105

Figure 45. Diagnostic plots for the surrogate models of *f*(x) and *g*(x). 106

Figure 46. Trend of the extended expected improvement function that yielded the first six evaluations conducted by considering the weighting coefficient vector (53). 108

Figure 47. Solution found by considering the weighting coefficient vector (54). 109

Figure 48. Trend of the extended expected improvement function that yielded the first three evaluations conducted by considering the weighting coefficient vector (55). 111

Figure 49. Summary of the alternative solutions obtained with three different *a priori* articulations of preferences. The green crosses, the orange triangle and the red squares represent the design solutions identified by considering the weighting coefficient vectors

(53),(54) and (55) respectively. The green x-markers, blue points and black points represent the sets of starting optimisation points, initial function observations and additional evaluations required for model validation, respectively. 112

Figure 50. Basic concept behind the proposed isocontour method. 115

Figure 51. Isocontour for the single degree-of-freedom problem (ω_d,m) taken into consideration in de Weck [21], where 35 isopoints were computed with a tolerance of 1% and a discretization of the design space based on 441 points via the non-gradient algorithm *Exhaustive Search*. The application of the method proposed here by the author within the same variable ranges required 310 total evaluations for the identification of the depicted 36 isopoints, with a tolerance of 0.1%. 116

Figure 52. Displayed in red are the isocontours associated with 5 points (depicted in cyan) randomly selected across the design space of Problem (42). 117

Figure 53. Distributions of the overall and feasible point sets, which are portrayed in red and black, respectively. The black and red vertical lines in the variable histograms represent the borders of the feasible and infeasible distributions..... 125

Figure 54. Comparison of the Pareto front obtained by means of ASOM (in green) with respect to the optimal points computed without ASOM by considering as bounds the adaptive and frozen bounds (in red and blue) given in Table 12. 126

Figure 55. Distributions of the Pareto points displayed in Figure 54 by adopting the same colour notation. 128

Figure 56. Default optimisation data visualisation..... 129

Figure 57. Optimisation data visualisation by means of *Filtering*. The colour notation shown in the *Filtering settings* panel is used to identify the sets of feasible, infeasible, and non-dominated design points. 130

Figure 58. Interactive selection of points on the *ESI* with a real-time visualisation update in the remaining interfaces. In this case, the selected point is identified in the *BPR-Awing* sub-space of the problem through an orange cross-symbol in the *SDTI*, whereas its exact numerical value for each dimension of the design and objective spaces are given in the *PCP* displayed in the *MDVI*. 131

Figure 59. One example of the visual exploration tasks that can be conducted by using the *Selective PCP Ranges Filtering* function in the *PCP*. The design points for which the constraint *Kff* is active are identified in the *ESI* and *SDTI* through cyan x-markers..... 132

Figure 60. Analysis of Pareto solutions. 133

Figure 61. Example of the data visualisation via *discipline-dependent techniques* in the *SDTI* by representing the carpet plot corresponding to the design selected in a magnified inset of the objective space displayed in the *ESI*. Displayed in red are possible performance constraints that are not satisfied. 133

Figure 62. Setup of the design sub-region to be explored in addressing the design change problem taken into account. 135

Figure 63. Isocontours of objectives and constraints. 139

Figure 64. Identification of the obtained solutions in the objective space..... 143

Figure 65. Parallel coordinates plot of a dataset of 75 aircraft belonging to 11 different categories and considering 8 parameters, which are encoded by the table of Figure 67 along with their corresponding value ranges. 170

Figure 66. Graphics enhancement obtained by performing the above-described analysis techniques for the analysis of parallel coordinate plots. The identification of the aircraft categories is depicted through the colour of the polylines..... 171

Figure 67. Individual visualisation of the different aircraft categories and code of the parameters names displayed in Figure 65 and Figure 66. 173

Figure 68. A possible interactive interface in which any bivariate plot selected by the user is magnified below the main diagonal. This example is also representative of those situations in which the user may be interested in identifying the equation which best describes the overall pattern of the relationship between two parameters (e.g., linear, quadratic, cubic, exponential, sinusoidal, etc.) [125]. 175

Figure 69. Pareto fronts of Optimisation Nº1 and Optimisation Nº2. The two optimisation procedures were carried out within similar search regions, whose settings are specified in Table 31 177

Figure 70. Comparison of the design parameters distributions of Optimisation Nº1 and Optimisation Nº2, where the entire set of evaluated points and the set of feasible points are represented in red and black respectively. The green lines represent the variables bounds considered throughout the optimisation procedures; whereas the dashed blue lines identify the lower and higher feasible sampled values of each variable distribution, which in some cases are not visible. It is important to notice how, normally, such lines coincide. Nonetheless, it may happen that either the sampled set of feasible points turns out to be narrower than the imposed corresponding search region (variable *tuc* and *Mach_crz*), or the optimiser occasionally samples design solutions located beyond the variables bounds (variable *Awing*). 182

Figure 71. F.A.R. take-off runway length requirements (standard day) –model 777-200 (baseline airplane) [1]. 184

Figure 72. Distribution of field lengths at major European airports [51]. 184

Figure 73. Future distribution of flights [15]. 185

Figure 74. Pareto fronts of Optimisation Nº3 and Optimisation Nº4. Displayed besides each one of the considered points of Optimisation Nº4 is the corresponding *tofl* value. 186

List of Tables

Table 1. Setup of the frozen and adaptive bounds for the optimisation of the bump function in two variables..... 53

Table 2. Coordinates and value of the objective function for the feasible optimum located within the initial search region established in Table 1 (Point N°1) and the corresponding set of semi-infeasible optimal points..... 53

Table 3. The first column on the left-side contains the design solutions obtained via fmincon for Problem (47), where each subscript identifies the relative starting point. The remaining columns show, from left to right, the solution coordinates (x_1 and x_2), the corresponding objective value (f) and Lagrange multipliers (λ_1 and λ_2), the estimated gains ($\lambda_1\tilde{\varepsilon}_1$ and $\lambda_2\tilde{\varepsilon}_2$) in the objective due to a maximum relaxation of the constraints and the resulting values of left-side of inequality (46) ($\frac{-\Delta f_1}{f}$ and $\frac{-\Delta f_2}{f}$)..... 63

Table 4. Coordinates and objective values of the new design points obtained via a constraint relaxation of Problem (47). The first column on the left hand side identifies the three cases analysed in Figure 28 through the letter-subscript, standing for the corresponding starting point. The superscripts *R1* and *R2,* instead, denote the solution coordinates and objective value resulting after a relaxation of *g1* and *g2* respectively.... 66

Table 5. Deterministic visualisation methodology matrix..... 73

Table 6. Comparison of x* with the solutions found by considering the weighting coefficient vector (53). The values that represent the best attainment of each of the four goals are highlighted in grey..... 108

Table 7. Comparison of x* with the solution found by considering the weighting coefficient vector (54)..... 109

Table 8. Comparison of x* with the solutions found by considering the weighting coefficient vector (55)..... 111

Table 9. Isopoints computed from $\bar{\mathbf{x}}$=[4.5594425,3.0524488]..... 118

Table 10. Test case nomenclature..... 121

Table 11. Conceptual aircraft design optimisation formulation..... 122

Table 12. Setup of the frozen and adaptive bounds..... 122

Table 13. Final adaptive bounds..... 123

Table 14. Design to be changed $\mathbf{x}^*$..... 134

Table 15. Definition of the design sub-space to explore..... 134

Table 16. Goals and weighting coefficients vectors considered for the first hypothetic design change scenario..... 136

Table 17. Variable values of the solutions obtained for the goals and weights vectors in Table 16..... 136

Table 18. Objective and constraint values of the solutions obtained for the goals and weights vectors in Table 16..... 137

Table 19. Differences between the variable values of the explored designs and the sought point..... 137

Table 20. Differences between the objective and constraint values of the explored designs and the sought point..... 137

Table 21. Summary of the isocontours computation..... 138

Table 22. Goals and weighting coefficients vectors considered for the second hypothetic design change scenario..... 140

Table 23. Variable values of the solutions obtained for the goals and weights vectors in Table 22..... 140

Table 24. Objective and constraint values of the solutions obtained for the goals and weights vectors in Table 22..... 140

Table 25. Differences between the variable values of the explored designs and the sought point..... 140

Table 26. Differences between the objective and constraint values of the explored designs and the sought point..... 140

Table 27. Goals and weighting coefficients vectors considered for the third hypothetic design change scenario..... 141

Table 28. Variable values of the solutions obtained for the goals and weights vectors in Table 30..... 142

Table 29. Objective and constraint values of the solutions obtained for the goals and weights vectors in Table 30..... 142

Table 30. Typical breakdown of a conventional design of a medium subsonic transport aircraft..... 176

Table 31. Variables bounds setup for Optimisation Nº1 and Optimisation Nº2..... 177

Table 32. Narrow-body aircraft field performance [49][64]..... 185

Abbreviations

ASOM	–	Adaptive Search Optimisation Method
BFL	–	Balanced Field Length
CIA	–	Change Impact Analysis
DACE	–	Design and Analysis of Computer Experiments
DoE	–	Design of Experiments
ECO	–	Engineering Change Order
EGO	–	Efficient Global Optimisation
EI	–	Expected Improvement
ESI	–	Euclidean Space Interface
FAR	–	Federal Aviation Regulations
GA	–	Genetic Algorithm
GUI	–	Graphical User Interface
IEVI	–	Integrated Exploration and Visualisation Interface
MDVI	–	Multidimensional Data Visualisation Interface
MSE	–	Mean Squared Error
MOO	–	Multi-Objective Optimisation
PCP	–	Parallel Coordinates Plot
PDF	–	Probability Density Function
RDO	–	Robust Design Optimisation
RMSE	–	Root Mean Squared Error
SDTI	–	Specific Design Tools Interface
SOM	–	Self-Organising Map
SPM	–	Scatter Plot Matrix
SPSA	–	Simultaneous Perturbation Stochastic Approximation
SQP	–	Sequential Quadratic Programming
USMAC	–	Ultra Simplified Model of Aircraft
WEIF	–	Weighted Expected Improvement Function

Chapter 1

Introduction

1.1. Problem Area

The selection of the "best" or "optimum" solutions plays an essential role in many real-life engineering problems. Mathematical optimisation algorithms are no longer considered as an esoteric approach for addressing theoretical problems only [1]. They have proven to be an effective tool for the design of complex systems and processes. Most of the efforts in optimisation so far have been focused on resolving the inherent trade-offs that exist between multiple and conflicting design criteria [31][44][76], handling the interaction among different disciplines [59][23], reducing computational cost [116][71], and managing uncertainty [85][86]. Nevertheless, specific issues of this design methodology still remain to be properly addressed. Attention is concentrated in this research upon three issues outlined below, within the framework of conceptual design optimisation.

The importance of correctly formulating the problem to be solved has been emphasized by Statnikov and Matusov [108]. Broad experience has shown that although the mathematical model of engineering optimisation problems may be correct, unsatisfactory results often derive from an improper formulation [11]. This issue is not addressed by established optimisation methods and a formulation-solution cyclic process is typically required for most of the engineering applications, which takes up to 70-80% of the total time [108]. In this context, a proper definition of the functional and design-variable

constraints turns out to be fundamental for the determination of the feasible solutions set. A tight setup of such parameters may cause optimal solutions to be overlooked, while an excessively loose definition might lead to substantial or useless computational efforts and time.

A growing interest has been directed towards methods with an *a posteriori articulation of preferences* on a set of potential solution points, denoting by preference the relative importance of different objective functions [72]. Visualisation tools play an essential role for such an approach in order to allow the designer to first explore various alternatives and then select the solution that best represents his/her preferences. Large multidimensional results need therefore to be made fully readable and explanatory by conducting a number of analysis tasks via adequate visualisation aids.

Last, but not least, an important issue for consideration stems from the iterative nature of design [30][18], which is generally due to uncertainty or the lack of specific design information [124][42]. Unplanned iterations occur when unexpected design changes need to be undertaken as a result of the incomplete satisfaction of the design specifications due to process inefficiencies and/or cognitive limitations (e.g., unsuccessful execution of testing and integration activities, sudden change of customer needs and requirements [18], or the appearance of alternative highly attractive design solutions [89]). Adequate strategies are hence required for the exploration of design points that represent the best trade-offs for change accommodation with minimum disruption to the product configuration.

1.2. Research Aims and Objectives

The overall aim of the present research is to propose a strategy to address specific design exploration aspects involved in conceptual design optimisation. In particular, a set of methodologies, that can be used separately or conjointly, are to be developed in order to support the problem formulation, evaluation of results, and introduction of design changes.

The first objective of the work is to develop a method to allow an adaptive formulation of functional and design-variable constraints. This should aid the designer in efficiently stating the optimisation problem at hand without the need for iterative refinements based on successive runs. Solutions initially not contained in the feasible design set can thus be explored, preventing to some extent the computation of meaningless results or the loss of important solutions.

The second objective is to propose a suitable visualisation methodology for an effective analysis of optimisation results. The designer should be able to visually explore and trade-off promising design alternatives by performing a number of common analysis tasks aimed at selecting the most attractive solutions. Additionally, the methodology should render multidimensional results of complex design optimisation procedures fully readable and explanatory to the decision-maker, without the need for the latter to be an expert in numerical methods.

The third objective is to develop a novel methodology to address design change problems which affect conceptual design. The proposed strategy would provide a means to identify the designs that represent the best trade-offs for change accommodation with minimum disruption to the product configuration. Data previously collected should be adequately re-used to drive an efficient exploration of new alternative design solutions within design space regions of interest.

1.3. Overview of Thesis

Presented in Chapter 2 is the literature review of the research. An introduction to multi-objective optimisation problems is first provided, together with the generic problem formulation taken into consideration for this thesis. An investigation of the state-of-the-art numerical methods and strategies relevant to the present research is presented next.
Proposed in Chapter 3 are two different methods to assist the designer in stating an optimisation problem via an adaptive formulation of functional and design-variable constraints. The *Adaptive Search Optimisation Method* (ASOM) allows a recurrent

variable-bounds redefinition process to be conducted via an on-the-fly monitoring of variables distributions throughout the optimisation procedure. The second method, instead, permits to perform a controlled relaxation of functional constraints that are flexible to some degree with the intent of exploring points that could lead to a substantial improvement of single objective optimisation problems.

A novel methodology for visual exploration of design solutions is presented in Chapter 4 with the aim of supporting the designer in analysing and comparing large number of design concepts. Suitable visualisation techniques are integrated for addressing common data analysis scenarios occurring in deterministic and robust optimisation. A set of interactive visualisation interfaces provides the designer with a means to gain insight into the problem under study, as well as to build, debug, and understand the algorithms and models integrated within the optimisation architecture.

The methodology proposed to support the introduction of design changes deriving from unplanned design iterations and affecting conceptual design is described in Chapter 5. It allows to retrieve available prior computational analysis information in order to drive an exploration process by means of surrogate models and the incorporation of key concepts from the goal attainment method and Bayesian global optimisation. Also presented is a complementary method based on the computation of objective and constraint isocontours through the evaluation of design points that keep invariant desirable design performance.

The three proposed methodologies are evaluated in Chapter 6 with an aircraft sizing test case supplied by a major airframe manufacturer, demonstrating their capabilities in addressing problems of industrial relevance. The results obtained by means of ASOM are first compared with the solutions obtained via standard optimisation procedures. A demonstration of a thorough investigation of the obtained complex data structure by means of the proposed visual exploration methodology is then provided. The exploration of alternative solutions for addressing three hypothetic design change problems via the proposed strategy is finally shown.

An overall summary of the present research is given in Chapter 7, along with the main contribution to knowledge and recommendations for future work.

Chapter 2

Literature Review

2.1. Engineering Design Optimisation

In the design of complex systems and processes, *ad hoc* methods are required to manage the interaction between various disciplines and to trade-off multiple design criteria, which are often conflicting in nature. Over the past few decades, mathematical optimisation algorithms have proven to be an effective tool for engineering design, no longer being considered as an esoteric approach for addressing theoretical problems only [1]. The establishment of algorithms capable of solving progressively larger and more difficult problems has been facilitated by the enhancement of computer power and speed [6], as well as parallel programming and integration frameworks. A wide range of different optimisation procedures have been developed depending on the problem under study, where the common aim is to identify the best solutions that satisfy a given set of constraints. Most of the efforts in optimisation so far have been focused on resolving the inherent trade-offs that exist between multiple and conflicting design criteria [31][44][76], handling the interaction among different disciplines [59][23], reducing computational cost [116][71], and managing uncertainty [85][86]. Nevertheless, specific issues of this design methodology still remain to be properly addressed. Attention is concentrated in this research upon three issues outlined in the following sections within

the framework of conceptual design optimisation. The generic problem formulation taken into consideration is as follows:

$$\min_{\mathbf{x}\in S} \mathbf{F}(\mathbf{x}) = \{f_1(\mathbf{x}), f_2(\mathbf{x}), \dots, f_J(\mathbf{x})\}$$

$$\text{subject to:} \quad \mathbf{G}(\mathbf{x}) = \{g_1(\mathbf{x}), g_2(\mathbf{x}), \dots, g_I(\mathbf{x})\} \le \mathbf{0}, \tag{1}$$

$$\text{with:} \quad \mathbf{x}_{\mathbf{lb}} \le \mathbf{x} \le \mathbf{x}_{\mathbf{ub}}$$

where the J real-valued objective functions $f_j(\mathbf{x})$ are to be minimised with respect to the design vector $\mathbf{x} = [x_1, x_2, \dots, x_n]$ in the n-dimensional design space S, subject to the I functional inequality constraints $g_i(\mathbf{x})$ and $2n$ design-variable constraints (the lower and upper bounds $\mathbf{x}_{\mathbf{lb}}$ and $\mathbf{x}_{\mathbf{ub}}$, respectively).

Given in Figure 1 is a conceptual representation of the feasible and non-dominated[1] solutions sets.

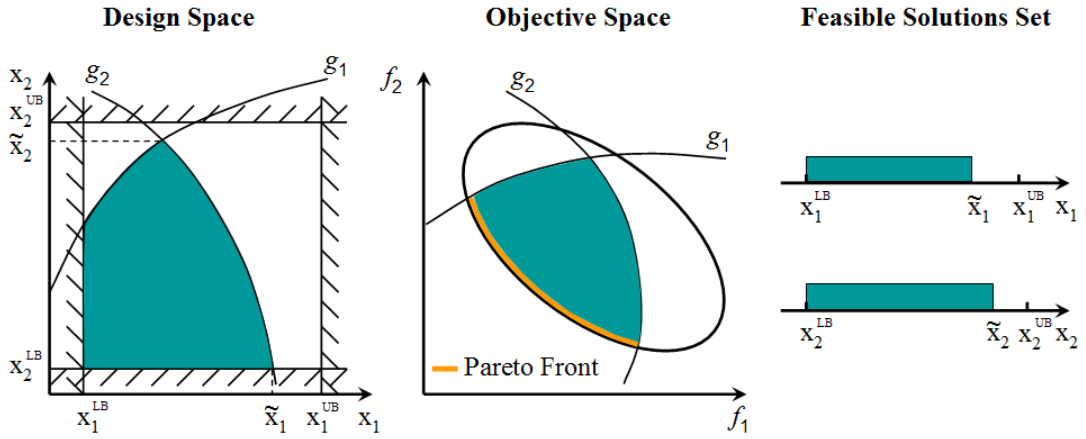

Figure 1. Shown in orange and blue are the non-dominated and feasible solutions sets of a generic optimisation problem formulated as in Problem (1) with n=2, J=2, and I=2.

[1] The set of non-dominated solutions of an optimisation problem is also referred to as Pareto front. A feasible design point is said to be Pareto optimal if no other feasible solution can improve any of the objectives without simultaneously being detrimental to other objectives.

2.2. Problem Formulation

The importance of correctly formulating the problem to be solved has been emphasized by Statnikov and Matusov [108]. Broad experience has shown that although the mathematical model of engineering optimisation problems may be correct, unsatisfactory results often derive from an improper formulation [11]. Amarger et al. [6] note that, despite the current algorithmic improvements and the availability of various powerful optimisation packages, it still remains to be far from trivial for design engineers to properly formulate optimisation models. Nonetheless, this issue is not addressed by established optimisation methods and a formulation-solution cyclic process is typically required for most of the engineering applications, which takes up to 70-80% of the total time [108]. In this context, a proper definition of the functional and design-variable constraints turns out to be fundamental for the determination of the feasible solutions set.

2.2.1. Search Region Definition

The determination of the search region within the design space is crucial in order to conduct an effective computation of optimal solutions. Formally, the search region is identified by the variables bounds specified in Equation (1):

$$x_{lb} \le x_i \le x_{ub} , \qquad \text{for } i = 1, \dots, n \tag{2}$$

where n is the dimensionality of the problem at hand. When the search region is inadequate the whole optimisation process may result to be incomplete and inefficient. If the specified variables bounds are too tight, a set of feasible points could have been cut out from the optimiser search and, as a consequence, promising optimal solutions may be overlooked. On the other hand, an excessively loose search region may lead to substantial or useless computational efforts and time.

Statnikov and Matusov [108] show the importance of adequately defining the design search region by providing few examples of how often superior solutions may not be evaluated because they lie slightly beyond the established design-variable constraints.

Therefore, they focus their efforts on the problem of obtaining information about whether it is possible to improve the optimal and feasible solution sets and, on the other hand, how much the design-variable bounds should be changed in order to achieve a certain improvement. The strategy proposed by the authors is based on the employment of the Parameter Space Investigation (PSI) method, which was created by Sobol' and Statnikov (see, e.g., Statnikov [107] and Sobol' and Statnikov [103]) for identifying correctly the feasible solutions set to optimise. This is done through three stages and requires the evaluation of a number N of trial points that mostly depends on the problem formulation, the functions involved and the number of variables taken into consideration. To correct the design-variable constraints, the authors suggest analysing the histograms of the design-variable distributions over the ranges of their variation. These provide the designer with a tool to identify the variables bounds that could be revised in order to improve the feasible and Pareto optimal solutions. Such process can be iterated several times until satisfactory results are obtained.

Jeong et al. [52] suggest a similar approach through an adaptive search region method for design optimisation. The validity of the search region is firstly assessed by analysing the probabilistic distribution of the design variables. If the search region turns out to be inadequate, it is changed adaptively. The procedure starts with the generation of the *superior population*, which is a set of samples satisfying all design constraints and assuring all objective function values are above a user-defined threshold. Thus, the search region for the *i-th* variable is considered relatively reasonable if the probability to find superior individuals outside of the current bounds is considered to be negligible. This implies that the mean of a valid distribution is located in the central area of the normalized search region and its tails are not close to the *i-th* variable bounds. In contrast, whenever a distribution is concentrated on the boundary region, the bound values of the corresponding variable should be expanded. This concept is illustrated in Figure 2.

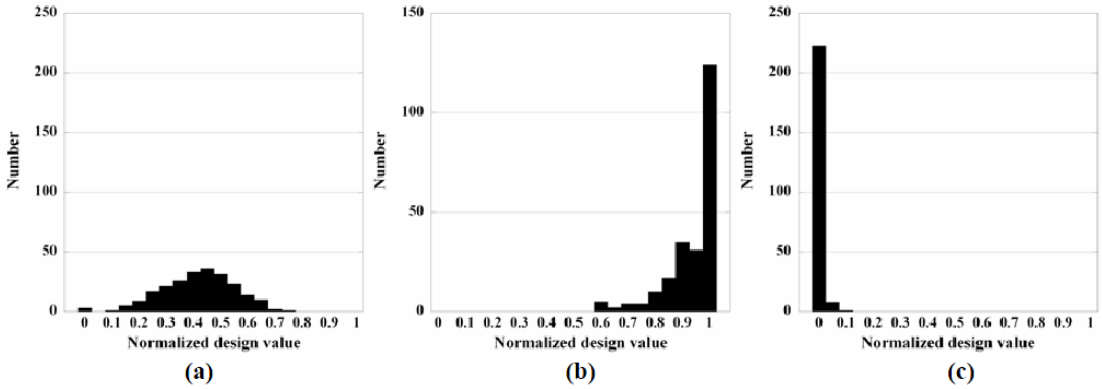

Figure 2. Typical types of distributions: (a) Valid distribution, with a peak located in the central area of the normalised search region and a low density of samples near the bounds; (b) Invalid distribution, with the peak located in vicinity of the upper bound; (c) Invalid distribution, with the peak located in vicinity of the lower bound [53].

Formally, the validity criterion proposed by Jeong et al. [52] is:

$$
\begin{aligned}
&\text{if} \quad (\eta < 0.05 \quad \text{or} \quad \eta > 0.95) \quad \text{then} \\
&\qquad \text{search region is } \textbf{invalid} \\
&\text{else} \\
&\qquad \text{if} \quad (\eta - 1.96\sigma < 0 \quad \text{or} \quad \eta + 1.96\sigma > 1) \quad \text{then} \\
&\qquad\qquad \text{search region is } \textbf{invalid} \\
&\qquad \text{else} \\
&\qquad\qquad \text{search region is } \textbf{valid} \\
&\qquad \text{endif} \\
&\text{endif}
\end{aligned}
\tag{3}
$$

where η and σ are the mean and standard deviation of the distribution in the normalised search region, respectively. Whenever the search region is invalid, it is suggested to redefine it as follows:

$$
\begin{aligned}
&\min(0, \eta - 1.96\sigma) < x < \max(1, \eta + 1.96\sigma) \qquad \text{if} \quad 0.05 < \eta < 0.95 \\
&\min(0, \eta - 1.96 w_1 \sigma) < x < \max(1, \eta + 1.96 w_2 \sigma) \qquad \text{otherwise}
\end{aligned}
\tag{4}
$$

where w_1 and w_2 are two weighting parameters used to accelerate the convergence of the search region.

Such an approach allows to define the normalised search region that would contain any normal distribution of design variables with a confidence interval of 95% [52].

Nevertheless, the distributional assumption of normality is not valid for a wide range of problems, since often the distributions of design variables turn out to be skewed or multimodal. Furthermore, similarly to the approach suggested by Statnikov and Matusov [108], the assessment of the search region validity has to be performed after the optimisation procedure is completed, as shown in Figure 3.

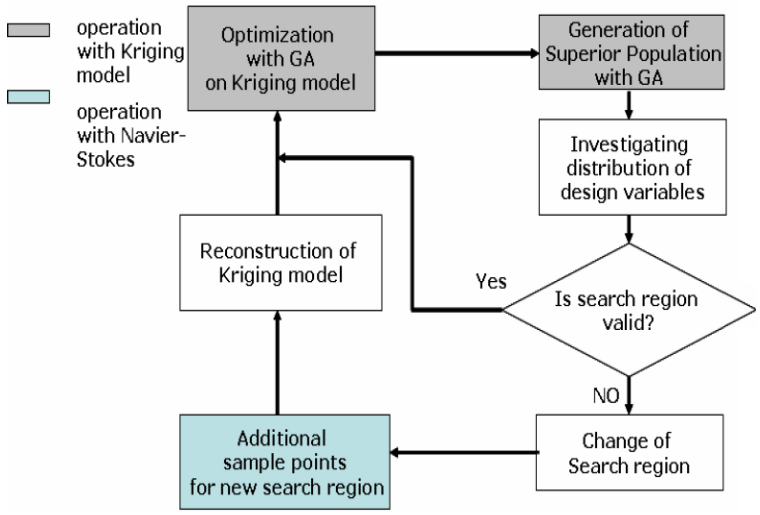

Figure 3. Procedure for adaptive search region proposed by Jeong et al. [53].

It is evident there is a need for defining an adaptive search region strategy which is capable of handling generic classes of design-variable distributions while reducing computational efforts and time by limiting the formulation-solution iterations that are inherent in the above approaches.

2.2.2. Non-rigid Constraints

The formulation of the constraints to be considered for a particular product/system design can be dictated by design criteria that may be both objective and subjective. Quantifiable (objective) figures of metric are generally employed along with an associated limit value given *a priori* (e.g. performance specifications, operational parameters, economical budget, direct operating costs, airworthiness/emissions/noise regulations, etc.). In other cases, however, the selection and formulation of optimisation constraints might be driven by non-objective factors, such as marketing strategies (based, for instance, on a *return-on-investment* estimation, or the comparison of competing products), external aspects that

must be considered because of their potential effects on the product (i.e. political, economic, technological, sociological, environmental and so forth), or simply by designers' knowledge, experience and intuition.

In an optimisation context, the formal statement of the latter class of constraints, from here on referred to as "soft" ("non-rigid" or "manageable") constraints [109], is a critical issue. Their formulation, in fact, can significantly influence the optimisation results and the subsequent design phases. On the one hand, the set of feasible solutions can drastically be reduced if unnecessary or over-stringent constraints are imposed; on the other hand, commercial penalties may subsequently arise when a fundamental requirement is overlooked.

In the attempt to include further optimal solutions potentially lying slightly beyond the imposed constraint limits, Statnikov and Matusov [108] propose the concept of *pseudocriterion*. The basic idea is that of reformulating any soft constraint of an optimisation statement as an additional objective. Such an approach allows a relaxation of the entire feasible solutions set, leaving any decision with respect to soft constraints to be made upon considerations coming from the analysis of an expanded set of evaluated solutions. However, the complexity of the objective space turns thus to be increased, which may impact on the computational cost and the selection of suitable optimisation algorithms for multi-criteria problems.

In an optimisation framework for reliability based design, Agarwal et al. [3] propose the use of homotopy[2] methods for conducting a constraint relaxation and to obtain a relaxed feasible region. A series of optimisation procedures is then carried out by gradually transforming the relaxed optimisation problem to the original one via a homotopy.

2.3. Suitable Visualisation Techniques for Design Optimisation

A major requirement for an effective visualisation technique is to be able to translate numerical datasets into simple and meaningful graphical representations in order to facilitate data analysis and understanding. Previous efforts in this field have been based

[2] Homotopy is the relation existing between two mappings in a topological space if one can be continuosly deformed into the other.

on the application of multidimensional visualisation techniques in MOO, so that both evaluation and exploration of the Pareto frontier could be performed. In some cases, well-known methods have been implemented, while in others *ad hoc* methodologies have been developed. A brief summary is presented below.

2.3.1. Multidimensional Data Visualisation

Among all the multidimensional visualisation methods, scatter plot matrices, parallel coordinates plots and self-organising maps are widely used in MOO because of their capabilities to represent large multidimensional datasets. A synopsis of their main features follows.

Parallel Coordinates Plot (PCP)

Because of their effectiveness in simultaneously displaying high-dimensional datasets on a simple two-dimensional plot, parallel coordinate plots provide both a global vision of the entire data at hand and a tool to perform a local and accurate data examination by visualising only the axes and/or the samples of interest. The key concept is displayed in Figure 4.

	X_1	X_2	X_3
Point A	1	1	1
Point B	1	5	5
Point C	8	2	7
Point D	9	9	9

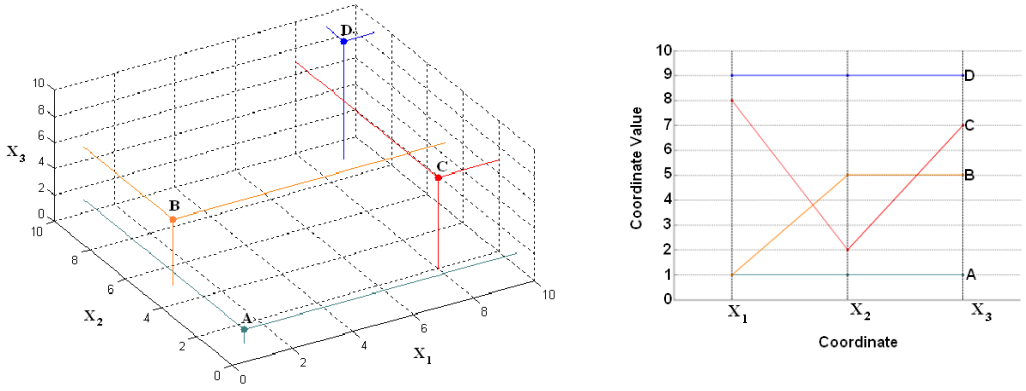

Figure 4. Representation of four three-dimensional points through the Cartesian-coordinate system and a parallel coordinate plot. The point values per each dimension are specified on the table above.

Furthermore, it allows to conduct data analysis by identifying one-dimensional features (e.g., marginal densities), two-dimensional features (e.g., correlations), and multidimensional features (e.g., clustering) [120].

Nonetheless, there are some shortcomings which must be kept in mind. Firstly, the fact that, although all the dimensions are simultaneously visualised in the plot, the entire space is not represented: since the axes are plotted side by side, the *i-th* dimension is linked at most to two other dimensions. Therefore, in an *n*-dimensional problem no information is visualised about the relationships among the *i-th* axis and the other (*n* - 3) axes which are not by its sides. This can be achieved by performing multiple permutations of the axes, in order to gain insight into the problem at hand via different perspectives of the same input dataset.

A further deficiency is the unfriendly and unfamiliar nature of this visualisation technique, in contrast with our familiarity with the Cartesian-coordinate system. Consequently, the analysis of large multidimensional datasets may result to be excessively complex and onerous for the designers who are accustomed to traditional visualisation tools. However, such a drawback can be greatly reduced via a suitable intuitive and user-friendly interface, exploiting at the same time the capabilities of the parallel coordinate plots in visualising multidimensional data. In this context, McDonnel and Mueller [74] propose the *Illustrative Parallel Coordinates* (IPC). This is a set of rendering techniques (edge-bundling, branched clusters, silhouettes, shadows, halos, faded histograms within clusters and density plots) aimed at augmenting and improving the graphical aspects of the parallel coordinate plots so that as much information as possible can be conveyed also to non-expert data analysts.

In the attempt to achieve the same goal, other approaches are based on the integration of the parallel coordinate plots with other visualisation techniques. Wegman and Luo [121], for example, suggest a coupling with the *grand tour* technique to allow the user to explore datasets which are both high-dimensional and massive in size.

Scatter Plot Matrix (SPM)

Scatter plots are well suited for discovering or checking correlations between two variables. Scatter plot matrices can be obtained by applying the same concept to every pair of the variables contained in multidimensional datasets. The systematic format of the

resulting visualisation technique allows the user to compare all the dimensions at hand with respect to each other in a simple and immediate fashion by moving along a single row/column of a matrix of bivariate graphs [50], as shown in Figure 5.

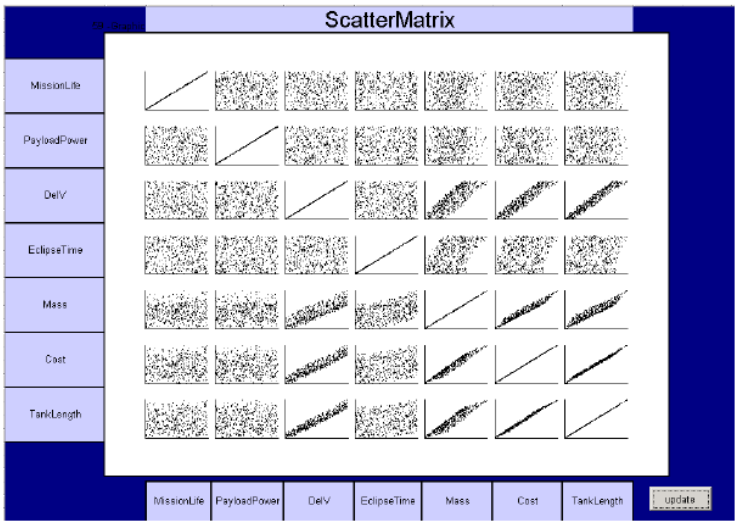

Figure 5. Scatter plot matrix displaying a satellite design dataset [111].

The main limitation is of practical nature and arises from the visualisation of datasets with a large number of dimensions. In this case, the analysis of the single scatter plots may be significantly complicated because of their number and dimensions, especially if the plot is displayed on a computer monitor. Therefore, scatter plot matrices are advisable for the visualisation of datasets containing at most 8-10 variables. This limitation can be partially addressed by integrating the half-matrix version of scatter plots with an interactive interface which allows the user to steer data analysis and to select the information to be displayed on the graph [111][126].

Self-Organising Map (SOM)

The self organising maps are an efficient technique for visualising multidimensional data [63]. Through an unsupervised learning, the cells within the maps are organised to best describe the set of input data samples and allows projecting a high-dimensional space onto bidimensional component maps. Consequently, the main capabilities of the SOMs lie in providing an appropriate technique to identify data similarities and for clustering

[25][46]. An example is provided in Figure 6 for the same dataset considered in Appendix A.

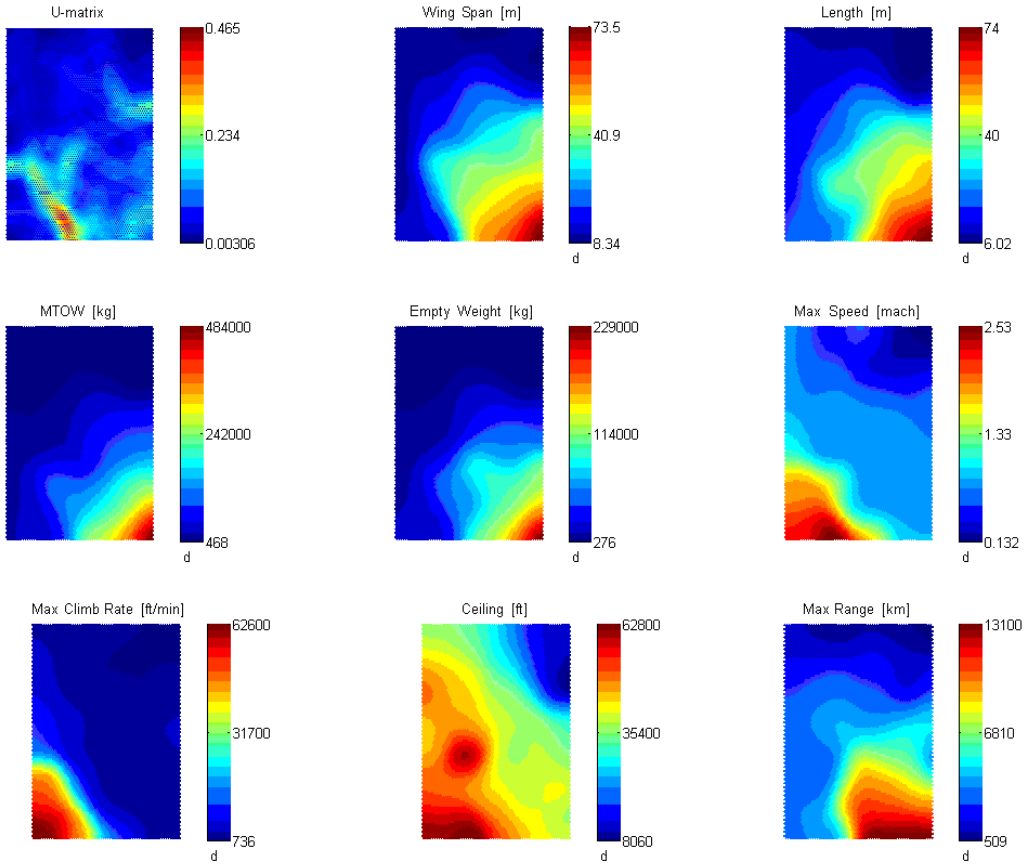

Figure 6. Representation of the same dataset considered in Appendix A by means of the self-organising maps. The basic idea is that, through a learning process, the map is organised in such a way that all the cells close to each other represent all the inputs having similar features. The representation of any dataset is thus obtained via a set of two-dimensional plots, as many as the dimensions of the problem at hand. Each data sample is represented by a cell, which has always the same space position within all the plots. Each self-organising map is associated to a particular dimension and the values of its cells are encoded according to their colour-bar located besides the map.

As regards the dimensionality of the data samples, the SOMs are not suitable for visualising high-dimensional datasets containing more than about ten variables. When dealing with a large amount of variables, either the numerical analysis of the single maps

may be significantly deteriorated because of their number and reduced dimensions, or a global perspective of the problem under study is compromised (it may be impossible to visualise all the maps simultaneously on the same sheet or screen), which may affect the identification of data clusters and relationships.

With respect to the number of input samples, the main limitation is related to the number of cells contained in the maps. The more input samples are taken into account the larger is the number of map units to consider. Therefore, such a limitation in terms of dataset size affects the PC processing capabilities: increasing the number of input samples makes the learning process more complicated, and consequently a longer time is required [118].

2.3.2. Carpet Plots

Prior to the application of computational tools in aircraft conceptual design, optimization methods were based on the development of a set of parallel layouts, each one characterized by different combinations of the design parameters. Design optimization was carried out with the help of carpet plots [69][93] by estimating the impact of parametric variations on the aircraft layout and criteria such as mission, weight and cost. A typical carpet plot provides a means of visualizing performance requirements (e.g. cruise speed, second segment climb rate, take-off and landing field length distances) as a function of parametric variables such as thrust-to-weight-ratio (T/W) and wing-loading (W/S). A point on the carpet plot represents a particular aircraft design and provides the designer with information on how performance constraints are satisfied.

In an optimisation context, carpet plots provide a straightforward and physical representation of the optimization results [82]. In the T/W-W/S space (or an equivalent parametric space), the users can immediately obtain information about the performance constraint satisfaction of the design under study.

A simultaneous visualization of multiple optimal solutions in the carpet plot would present not only a distinct location of the design points, but also a different arrangement of their respective sets of performance constraints, as shown in Figure 7. This is due to the dependence of the constraints on design parameters which are peculiar to each solution, but not explicitly represented in the T/W-W/S space.

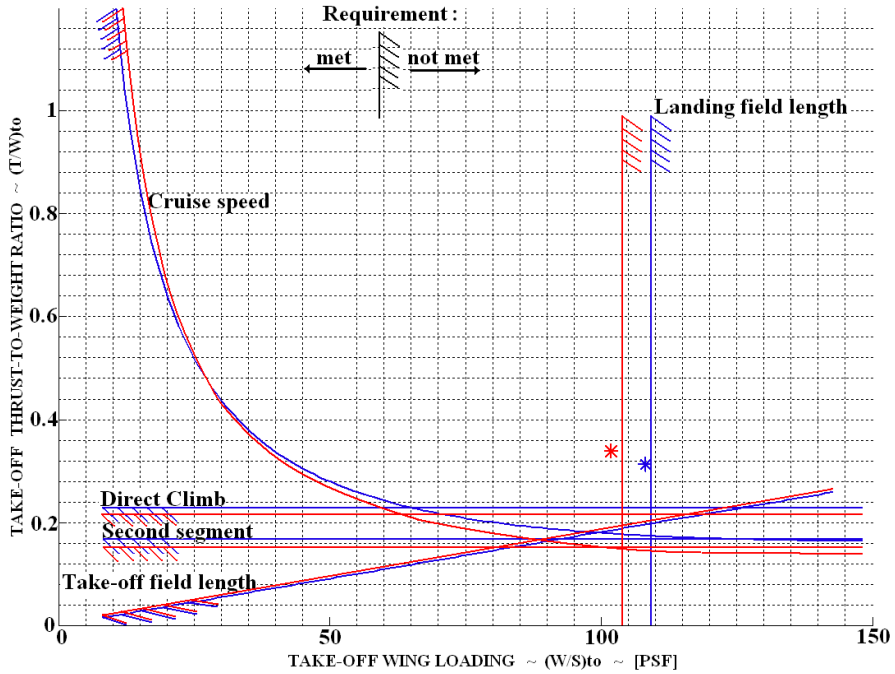

Figure 7. Example of the carpet plots of two different design points, one in red and the other in blue. Hatching denotes inadmissible side of constraint curves [82].

The integration of carpet plots in a visualization framework aimed at the exploration of optimisation results allows the designer to evaluate the design solutions with respect to a set of design constraints by using a traditional design tool without the burden of mathematical complexity.

2.3.3. Recent Developments in MOO Visualisation

Ad hoc methodologies have been developed for an effective visualisation of design optimisation data. Among them, mention can be made of the hyper-space diagonal counting (HSDC) method presented in Agrawal et al. [4]. Intended to visualize intuitively the Pareto frontier for large-scale MOO problems, this method exploits Cantor's findings in set theory which enable the representation of multidimensional Pareto surfaces in a 2-D or 3-D graph without any loss of information.

In the framework of aircraft design, several authors have also stressed the importance of representing the physical layout of the airplane to simultaneously visualize the geometrical parameters characterizing each design solution [47][5][38]. This has been achieved either by using simple parametric CAD models or schematics of the aircraft

under consideration. These representations allow the designer to immediately understand the main features of different aircraft concepts (e.g. number of engines and their location, fuselage geometry, tail and wing plants, etc). However, such visualization might only be useful for experienced designers dealing with conventional aircraft design. Furthermore, such representations can only display limited information with regard to aerodynamics, performance, civil/military regulations, design-constraints satisfaction, and so forth. Finally, it does not allow to appreciate the subtle, but still important differences between similar design solutions.

For constraint analysis and visualisation, mention should be made of the methodology presented by Deremaux et al. [26]. Through a CAD-based visualisation, the investigation of constraint behaviour is performed by intuitively displaying relevant information for each solution, such as active constraints, the sensitivity of each constraint to each of the design variables, and the identification of the constraints that drive the design. This is achieved by means of an interactive graphical user interface (GUI) composed of different windows that allows the designer to gain a better understanding of the design trade-offs made by the optimiser.

An approach to trade space exploration is presented by Yukish et al. [126], allowing users to steer further model runs in desired regions of the design space by using multidimensional visualisation tools. This is obtained through the specification of point attractors and by graphically linking all the plots together.

2.3.4. Pareto Frontier Exploration via Approximations

Among the methods for conducting a trade-off analysis on a set of optimal design solutions, mention should be made of the advantages in employing local Pareto approximation methods.

Generally, the Pareto frontier of MOO problems that are representative of real-life engineering problems cannot be described analytically because of their complexity. Numerical methods are hence required to obtain discrete Pareto solutions, which may turn out to be computationally demanding. In case that the optimisation is conducted by means of gradient-based algorithms, an advantageous strategy to extend the set of non-dominated points is offered by local approximations of the Pareto frontier. In this

framework, approximation methods that reuse gradient information obtained throughout the optimisation procedure prove to be particularly efficient in terms of computational cost. These methods allow to derive new approximated Pareto solutions in the objective space and to obtain their corresponding design vectors in the design space [115][116]. Linear and quadratic local approximations can be computed via a Taylor expansion around a differentiable Pareto point as follows:

$$f_p = f_p^* + \sum_{i=1}^{n_f} \frac{df_p}{df_i} \Delta f_i \,, \qquad \text{for} \quad p = n_f + 1, \ldots, J \tag{5}$$

$$f_p = f_p^* + \sum_{i=1}^{n_f} \frac{df_p}{df_i} \Delta f_i \; + \; \frac{1}{2} \sum_{j,k=1}^{n_f} H_{jk}^{(p)} \Delta f_j \Delta f_k \,, \qquad \text{for} \quad p = n_f + 1, \ldots, J \tag{6}$$

where $\frac{df_p}{df_i}$ and $H_{jk}^{(p)} = \frac{d^2 f_p}{df_j df_k}$ are the first and second order derivatives on the Pareto surface, whereas n_f is the dimension of the largest family of linearly independent vectors $\mathbf{P}\,\nabla f_i$, where $\mathbf{P}$ is the projection matrix onto the hyper-plane normal to all gradients of active constraints. The derivatives can be computed from the usual gradients of objectives and active constraints obtained during the optimization process. Thus further information in the vicinity of a Pareto point can be obtained at no extra computational cost. In this work, the term *optimal family* of solutions will be used to identify those designs belonging to the same local Pareto frontier and characterized by the same set of active constraints (including the active bounds of the variables).

By understanding the trade-offs between objectives, the designer is hence enabled to articulate local preferences with the aim of improving some objectives at the expense of others and simultaneously ensuring the satisfaction of inactive constraints.

A detailed description of the method along with its limitations and a strategy for detecting non-differentiable Pareto points can be found in Utyuzhnikov et al. [115] and Maginot [71].

2.3.5. Uncertainty Visualisation in Robust Design Optimisation

Generally, the visualisation of robust design optimisation (RDO) data represents a more demanding challenge in comparison with the corresponding deterministic case. On the one hand, it is due to the higher problem dimensionality deriving from the introduction of additional design parameters, typically formulated in terms of statistical variation of objectives and constraints. On the other hand, there is a need to visualise a wider diversity of information, such as constraint satisfaction probability.

A survey of uncertainty visualisation techniques to aid data analysis and decision making in a number of disciplines is presented by Pang et al. [87]. A brief review of uncertainty sources together with a classification of the possibilities in uncertainty visualisation is also presented with the intent of highlighting apparent needs in visualisation. The importance of uncertainty visualisation to support decisions is also shown by Griethe and Schumann [40] by focusing the attention on the demand for new approaches.

In the context of RDO, Mattson and Messac [73] introduce a multi-objective decision-making tool using objectives uncertainty visualisation for supporting non-deterministic concept selection. In order to enhance the trade-off among various design alternatives, Rangavajhala et al. [90] propose an approach based on the visualisation of results in terms of three uncertainty attributes: mean objective performance, variation in performance, and constraint satisfaction. The selection and analysis of different alternatives is driven by the identification of design subsets meeting specific requirements on the above attributes. The decision-making process is thus enhanced by enabling the designer to trade-off not only the mean design performance, but also the robustness of objectives and the satisfaction probability of constraints. This is achieved by means of a filtering scheme aimed at discovering desirable regions of the mean objective space from an uncertain perspective, as shown in Figure 8.

The main limitation of the above scheme is its applicability to RDO problems with a maximum of three objectives. Furthermore, it does not allow the analysis of results by considering the mean and variance of constraints separately. The latter can be addressed by means of the strategy suggested by Padulo [86], which allows the visualisation of the variance of any pair of objectives/constraints in their corresponding mean space. This is achieved by displaying around each design point an ellipse having the horizontal and

vertical semi-axis given by the standard deviations corresponding to the parameters displayed in the abscissa and ordinate directions, as illustrated in Figure 9.

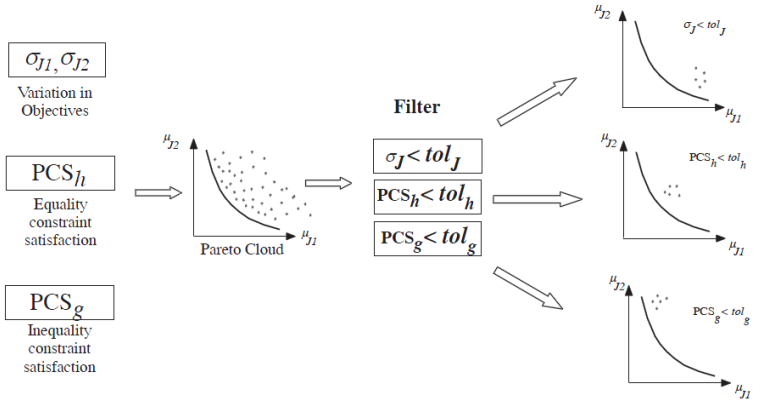

Figure 8. Visualisation scheme proposed by Rangavajhala et al. [90]. The exploration of the robust Pareto cloud can be conducted in the mean objective space by varying the filter tolerances tol_J, tol_h and tol_g associated to objective variation σ_J, probability of equality constraint satisfaction PCS_h, and probability of inequality constraint satisfaction PCS_g, respectively.

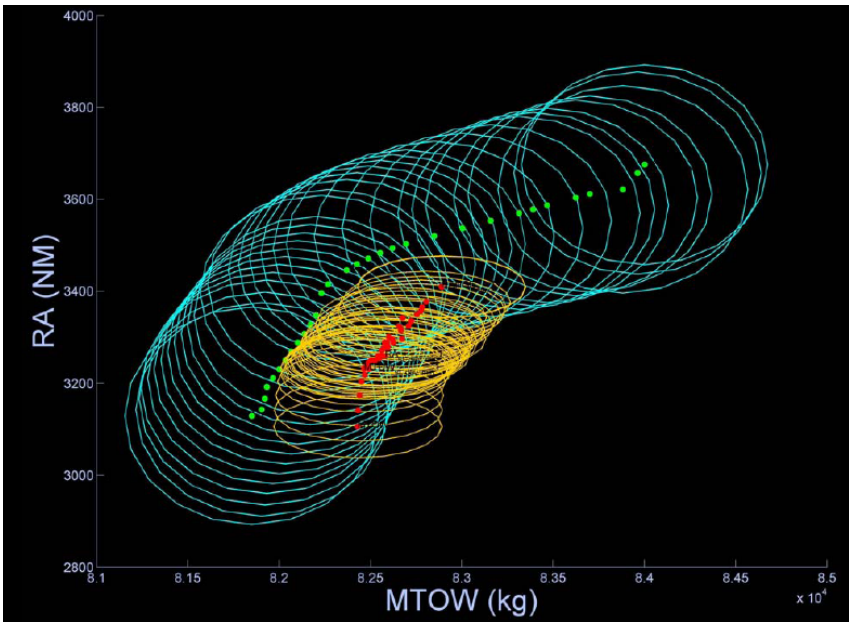

Figure 9. Comparison of the robust and deterministic results of an aircraft MOO problem. By considering the mean objective space *MTOW-RA*, the mean and variance of the solutions are represented by the red points and yellow ellipses for the robust Pareto cloud, and by the green points and blue ellipses for the deterministic Pareto front (after conducting an *a posteriori* uncertainty analysis) [43].

2.4. Design Change

This section provides an overview of design change problems occurring in engineering. The reasons for which a change may be required are various, and a number of examples are given in Appendix D. Generally, changes can be necessary when new needs and requirements emerge, or because of weaknesses or deficiencies of the design process that preclude the achievement of initially defined standards in the product [28]. Changes can also be required to modify existing designs, which could facilitate bringing innovative high value products to the market ahead of the competitors [81]; as well as to fulfil the need for mass customisation by supporting product variety [20][35].

Managing the change process is not trivial. The outcome is not always as expected or desired, especially for complex products, due to the intricate connections among design features. Even a single simple change can trigger a series of other changes, thus generating a flow of changes that propagates across the design [20]. It is therefore essential to establish effective strategies for Change Impact Analysis (CIA), so that the time, cost, and resources can be allocated to introduce it [28]. In addition to the overall number of changes required, the time each change might start being introduced together with its duration need to predicted. The illustration of different change types in Figure 10 shows the difficulty in handling the cases where not all the potential effects deriving from the accommodation of a change are captured. This leads to an increment of the number of changes as the redesign progresses, which could lead to *change avalanches* if it gets out of control.

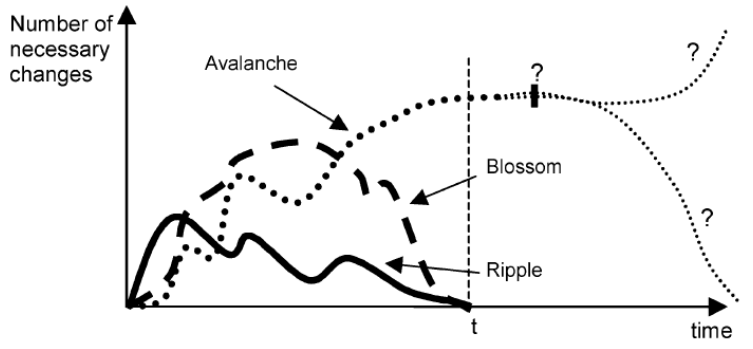

Figure 10. Different change types. In contrast to *change ripples* and *change blossoms*, that finish within the required time t, *change avalanches* can behave like *blossoms* over a longer, or represent an uncontrolled increment of changes [28].

In this context, Guenov [41] introduces an approach to trace and analyse the propagation of the knock-on effects of design and specification changes in distributed design models. A change prediction model (CPM) is suggested by Clarkson et al. [20] by combining Design Structure Matrices and risk management techniques to compute the indirect change propagation risks between design components. A probabilistic prediction of the change consequences along with a visualisation scheme of change propagation paths is instead provided by Eckert et al. [29].

The potential advantages of employing efficient CIA methods for addressing changes raised during the early stages of product lifecycle are outlined by several authors [33][48][92]. This is illustrated in Figure 11 by representing the typical cost of an Engineering Change Order (ECO) curve in relation to the product development phases.

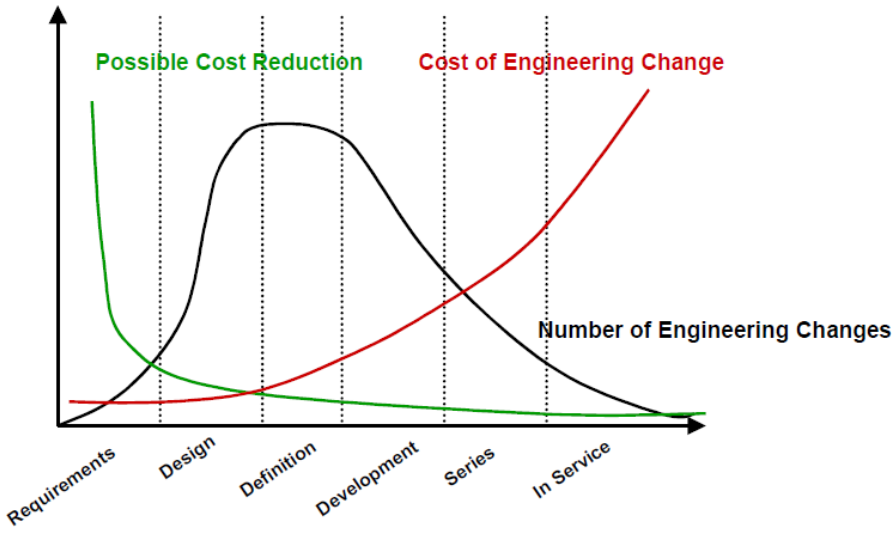

Figure 11. Typical curves with time for a generic product development cycle [92]. The shape of the curve will vary depending on a number of factors, e.g. the project at hand, design strategy, technologies, etc.

In general, the later a design change is introduced, the further it propagates and, therefore, the higher the costs are. It is therefore evident that changes should be managed and introduced early in the product life cycle. Keller et al. [58] propose an engineering change methodology to support conceptual design. It allows to analyse alternative solutions and to foresee potential problems arising from the product architecture by

predicting change propagation via connectivity models of past designs. However, the suggested approach is based on the CPM methodology as described by Clarkson et al. [20], although the components of a product may be not defined yet at conceptual stage. Moreover, the method involves the participation of different experts to obtain the data required in input.

2.5. Bayesian Global Optimisation

Analysed in this section are the salient aspects of Bayesian global optimisation methods, which allow to solve problems of the type of Equation (1) by means of response surfaces. In particular, attention if focused here on the Efficient Global Optimisation (EGO) algorithm developed by Jones et al. [56] and subsequently employed by other researches [98][100][102], which combines the use of kriging metamodels and the sampling criterion introduced by Mockus et al. [78]. Such an approach has proven to be particularly efficient also for nonlinear and multimodal models, providing an efficient trade-off between the optimisation of response surfaces (by evaluating the design points where the surrogate model is minimised) and the enhancement of the approximation (via a minimisation of the prediction error). This turns out to be particularly convenient for applications where time-consuming computer simulations are involved.

2.5.1. The Response Surface Model

During the last decades there has been a growing interest in developing fast surrogate models of objective and constraint functions used in optimisation problems. Additional advantages in using surrogate models apart from reducing computation time are outlined in the taxonomy of global optimisation methods based on response surfaces given by Jones [55]:

- All the evaluations employed to fit the surfaces can be executed in parallel.
- All the evaluations can be performed before formally stating the problem.

- All the evaluations can be reused for different formulations of the same problem (e.g., different constraint limits).
- It is possible to use all the evaluations to conduct also sensitivity analyses aimed at identifying the most important variables and to visualise input-output relationships.
- When computer models are not available, response surfaces provide a means to computationally represent the relationships between input and outputs.

Nevertheless, in some cases the generation of a satisfactory surrogate model can lead to the computation of a large number of observations, depending on the nature of the problem to be addressed. In general, it is also not clear which type of surrogate model would provide the most accurate description of any function not known *a priori*.

Among all the existing approaches for obtaining surrogate models, a method that is gaining popularity in the research community is kriging, also known as DACE (Design and Analysis of Computer Experiments). Such method has been considered in this research because of its statistical interpretation that allows to estimate the potential error of the interpolator. It will be shown how this feature turns out to be essential to Bayesian global optimisation methods. Only the main features and principles required by the reader will be explained in this chapter, referring to literature for more details [95][56][70].

Kriging is a response surface model that interpolates the evaluations with a linear combination of "basis functions" having parameters that are tuned [55]. Supposing that *m* observations have been previously evaluated on the unknown deterministic function $y(\mathbf{x})$, the corresponding surrogate model $\hat{y}(\mathbf{x})$ is expressed as the sum of a constant regression function μ and a random function (stochastic process) $\varepsilon(\mathbf{x})$:

$$\hat{y}(\mathbf{x}) = \mu + \varepsilon(\mathbf{x}) \tag{7}$$

The random function $\varepsilon(\mathbf{x})$ is assumed to have mean zero and covariance:

$$\mathrm{Cov}[\varepsilon(\mathbf{x}^i), \varepsilon(\mathbf{x}^j)] = \sigma^2 R(\mathbf{x}^i, \mathbf{x}^j) \tag{8}$$

where σ^2 is the process variance, and the correlation function R considered here is defined as:

$$R(\mathbf{x}^i, \mathbf{x}^j) = \prod_{k=1}^{n} \exp\left(-\theta_k \left| x_k^i - x_k^j \right|^{\varsigma} \right) \tag{9}$$

where the exponent $0 < \varsigma \leq 2$ (that can also vary with *k*) is an important parameter that determines the smoothness of the response prediction globally (if it is a scalar) or across dimensions (if it is a vector). Troughout the thesis it is assumed that $\varsigma = 2$, under the hypothesis of smoothness of the deterministic function $y(\mathbf{x})$ at hand [55][56]. The parameter θ_k, instead, determines the deterioration rate of the correlation in the *k-th* direction. The kriging model has therefore *n+2* parameters: $\mu, \sigma^2, \theta_1, \ldots, \theta_k$. Their estimation is obtained by fitting the model to the training data set to maximise the likelihood of the observed data. The following closed form of the predictor can thus be obtained:

$$\hat{y}(\mathbf{x}) = \hat{\mu} + \mathbf{r}' \mathbf{R}^{-1} (\mathbf{y} - \mathbf{1}\hat{\mu}) \tag{10}$$

with:

$$\hat{\mu} = \frac{\mathbf{1}' \mathbf{R}^{-1} \mathbf{y}}{\mathbf{1}' \mathbf{R}^{-1} \mathbf{1}} \tag{11}$$

where $\mathbf{r}$ is the vector whose *i-th* element is:

$$r_i(\mathbf{x}) \equiv \mathrm{Corr}[\varepsilon(\mathbf{x}), \varepsilon(\mathbf{x}^i)] \tag{12}$$

and $\mathbf{1}$ denotes an *n*-vector of ones. The key feature of kriging is that it allows to estimate the potential error in the approximation via the following equation of the mean squared error of the predictor:

$$s^2(\mathbf{x}) = \sigma^2 \left[1 - \mathbf{r}'\mathbf{R}^{-1}\mathbf{r} + \frac{\left(1 - \mathbf{1}'\mathbf{R}^{-1}\mathbf{r}\right)^2}{\mathbf{1}'\mathbf{R}^{-1}\mathbf{1}} \right] \tag{13}$$

where σ^2 can be estimated by:

$$\hat{\sigma}^2 = \frac{(\mathbf{y} - \mathbf{1}\hat{\mu})'\mathbf{R}^{-1}(\mathbf{y} - \mathbf{1}\hat{\mu})}{n} \tag{14}$$

A full derivation of the above equations can be found in Sacks et al. [95].

Equation (13) turns out to be particularly useful since it provides a means to estimate the prediction uncertainty at any point. It is consequently zero in correspondence to any observation, whereas it tends to be σ^2 for points very distant from the data [56]. Within an optimisation context, this comes to be essential in order to avoid having an erroneous representation of the tackled problem, as shown in Figure 12.

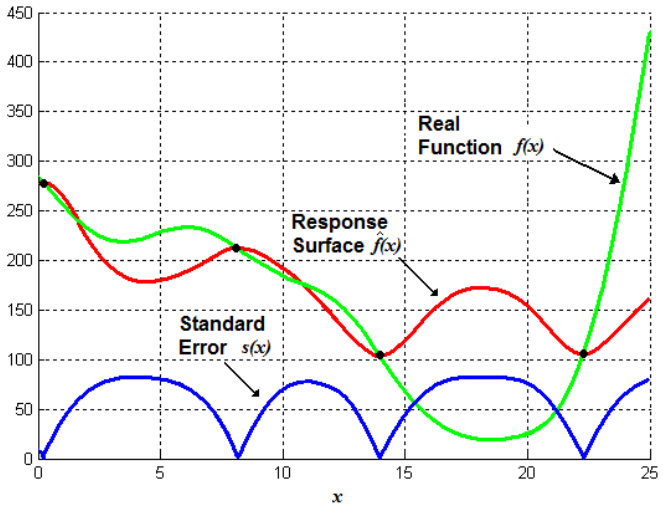

Figure 12. An example of response surface for a simple one-dimensional function $f(x)$. The real objective function is visualised in green, and the black dots identify the points where it has been sampled. The red line represents a potential predictor that fits such observations, and its standard error is depicted in blue below.

To assess the validity of the stochastic process models to be used in optimisation processes, Jones et al. [56] propose a *cross-validation procedure* to be conducted through

a series of diagnostic tests. A first check plot is given by comparing actual and predicted values of a given set of points. With the objective of avoiding the evaluation of additional points, the procedure is carried out by considering only the *m* function evaluations used to fit the model. Each evaluation is left out at a time to be then predicted by means of the surface that fits the remaining (*m*-1) points. The prediction accuracy of the model can thus be assessed by plotting the actual function values versus the cross-validated predictions. The more the points lie on a 45º line, the more accurate is the model at hand.
One more useful diagnostic test is based on computing for each observation the corresponding standardized residual, defined as the number of standard errors that the predicted valued is away from the actual value:

$$\text{standardised residual}_{\,i\text{-}th\ \text{sample}} = \frac{y(\mathbf{x_i}) - \hat{y}_{-i}(\mathbf{x_i})}{s_{-i}(\mathbf{x_i})} \tag{15}$$

where $y(\mathbf{x_i})$ and $\hat{y}_{-i}(\mathbf{x_i})$ denote the actual value and the cross-validated prediction of the *i-th* observation respectively, and $s_{-i}(\mathbf{x_i})$ represents the cross-validated standard error of the prediction at $\mathbf{x_i}$. A straightforward validation graph results from plotting all the standardized residuals versus the respective predicted function values. The model is thus considered to be accurate if all the cross-validated function predictions $\hat{y}_{-i}(\mathbf{x_i})$ are located within a certain range of the standardized residual, depending on the confidence interval that is desired[3].
An example of the diagnostic plots described above is shown in Figure 13.

[3] Generally, the interval [-3, 3] is taken into consideration for a 99.73 % confidence interval in the prediction [56].

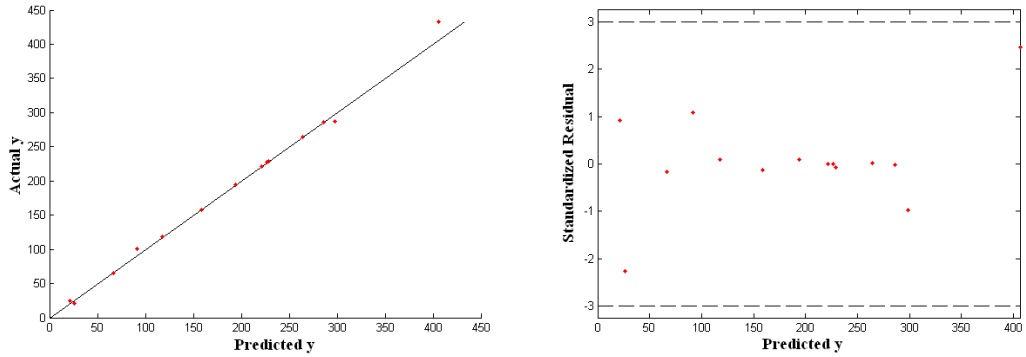

(a) (b)

Figure 13. Diagnostic plots: (a) the *actual function values versus cross-validated predictions*, (b) the *standardized cross-validated residuals versus cross-validated predictions.*

After the model has been validated, it can be used to guide the search of optimal solutions in the design space. This can be done in two different ways. On the one hand, the optimisation process can be conducted by establishing the successive system evaluations on the basis of the predicted function minimum. On the other hand, the attempt of assuring a certain accuracy of the response surface can lead to exploring points which are considerably distant from the optimal solutions. It is therefore necessary to introduce a suitable sampling criterion that balances global search (directed at searching in the design space regions with the highest standard error of the predictor) with the local search (focused on seeking promising areas of the design space identified through the predictor). A review of existing figures of merit to trade-off the two aspects mentioned above is provided in the next section.

2.5.2. Infill Sampling Criteria

The key concept is that of modelling the uncertainty about the prediction by assuming $y(\mathbf{x})$ as the realisation of a stochastic process $Y(\mathbf{x})$, which is considered to be a normally distributed random variable with mean and standard deviation given by the predictor and the associated standard error. Denoting by $\hat{y}$ and s the prediction and its standard error estimate, Y is therefore Normal($\hat{y}$,s) [56]. Such an approach allows us to estimate what is the probability of improving our current best function value $f_{min} = (y^{(1)},y^{(2)},\ldots,y^{(m)})$ that

can be associated with each point of the design space. This is illustrated in Figure 14 through a simple one-dimensional function $f(x)$, depicting the normal density function with mean and standard deviation given by the response surface at $x = 17$. Since the tail of the distribution lies beyond f_{min}, there is a probability of obtaining a better value of the function at $x = 17$.

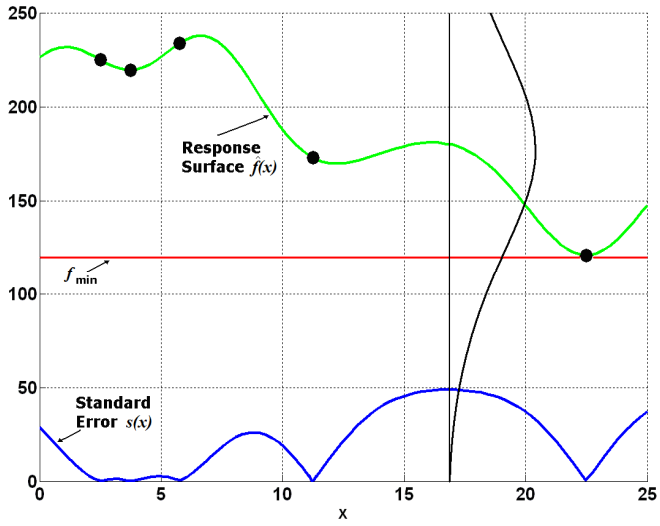

Figure 14. An example of response surface for a simple one-dimensional function $f(x)$. The response surface is visualised in green, and the black dots identify the points where $f(x)$ has been sampled. The predictor standard error is depicted in blue and the red line represents the current best sampled function value.

Such a concept can be formalised by defining the improvement at the generic point $\boldsymbol{x}$ as:

$$I(\mathbf{x}) \equiv \max\left(f_{\min} - Y(\mathbf{x}), 0\right) \tag{16}$$

which is also a random variable. Taking the expected value of $I(\mathbf{x})$ yields the probability of improvement, often referred as expected improvement:

$$\mathrm{E}\left[I(\mathbf{x})\right] \equiv \mathrm{E}\left[\max\left(f_{\min} - Y(\mathbf{x}), 0\right)\right] \tag{17}$$

that can be expressed in closed form as [56]:

$$\mathrm{E}\left[I(\mathbf{x})\right] \equiv (f_{\min} - \hat{y})\Phi\left(\frac{f_{\min} - \hat{y}}{s}\right) + s\phi\left(\frac{f_{\min} - \hat{y}}{s}\right) \tag{18}$$

where $\phi(\cdot)$ and $\Phi(\cdot)$ are the standard normal density function and the standard normal distribution function, respectively.

By analysing the terms on the right-hand side of Eq. (18), it can be noted how the probability to obtain at some point $\boldsymbol{x}$ a function value lower than f_{min} is influenced both by the predicted function value and its corresponding standard error. In fact, the first term is given by the difference between the current best minimum and the predicted value of f at $\boldsymbol{x}$, penalised by the improvement probability. The second term instead depends on the prediction error s. Consequently, the expected improvement will tend to increase in those points where $\hat{y}$ is predicted to be smaller than f_{min} and/or where the prediction uncertainty is large [99], thus providing an efficient criterion to balance global and local search. In the attempt of controlling accurately such a balance, Sóbester et al. [102] propose a weighted expected improvement function WEIF, obtained from Eq. (18) by introducing a weighting factor $w \in [0,1]$:

$$\mathrm{WEIF}(\mathbf{x}) \equiv w(f_{\min} - \hat{y})\Phi\left(\frac{f_{\min} - \hat{y}}{s}\right) + (1-w)s\phi\left(\frac{f_{\min} - \hat{y}}{s}\right) \tag{19}$$

The advantage of this weighted infill sample criterion is that setting w close to zero will emphasise the search in areas of maximum uncertainty, whereas for values close to one the search will focus on the evaluation of promising regions.

An alternative solution to control the local-global search is given by the generalized expected improvement [99][100]. Introducing a non-negative integer parameter $\bar{g}$ in the definition of the improvement at the generic point $\boldsymbol{x}$:

$$I^{\bar{g}}(\mathbf{x}) = \begin{cases} \left[f_{\min} - Y(\mathbf{x})\right]^{\bar{g}} & \text{if } Y(\mathbf{x}) < f_{\min} \\ 0 & \text{otherwise} \end{cases} \tag{20}$$

yields:

$$\mathrm{E}\left[I^{\bar{g}}(\mathbf{x})\right] = s^{\bar{g}} \sum_{k=0}^{\bar{g}} (-1)^k \binom{\bar{g}}{k} u^{\bar{g}-k} T_k \tag{21}$$

where

$$u = \frac{(f_{\min} - \hat{y})}{s}, \quad T_0 = \Phi(u), \quad T_1 = -\phi(u),$$

and

$$T_k = -u^{k-1}\phi(u) + (k-1)T_{k-2} \qquad \text{for } k > 1. \tag{22}$$

When dealing with constrained optimisation problems, it is necessary to adopt a sampling criterion that somehow acknowledges the satisfaction of the constraints to be met, as in Eq. (1). The approach suggested by Schonlau et al. [100] is based on the assumption that the predictions for all the response functions $[g_1(\mathbf{x}), \ldots, g_J(\mathbf{x})]$ acting as constraints are statistically independent. The expected improvement subject to constraints $\mathrm{E_c}[I(\boldsymbol{x})]$ is thus obtained multiplying the expected improvement criterion by the satisfaction probabilities of each constraint:

$$\mathrm{E_c}\left[I(\mathbf{x})\right] = \mathrm{E}\left[I(\mathbf{x})\right] \cdot \mathrm{P}\left(g_1(\mathbf{x}) \le 0\right) \cdot \ldots \cdot \mathrm{P}\left(g_J(\mathbf{x}) \le 0\right) \tag{23}$$

Assuming that each $g_j(\mathbf{x})$ has mean and standard deviation given by the associated predictor and its standard error, such probabilities can be estimated from the corresponding standard cumulative distribution functions. However, the optimal points of constrained optimisation problems in many instances lie along a constraint boundary or in its neighbourhood. Therefore, the disadvantage in using Eq. (23) is that the sampling of additional points is focused on the design space regions which are more likely feasible, thus preventing the evaluation of promising points located in the vicinity of constraints boundaries [98].

In the constrained case, Sóbester et al. [102] modify the WEIF as follows:

$$\mathrm{WEIF}_c(\mathbf{x}) \equiv \begin{cases} w(f_{\min} - \hat{y})\Phi\left(\dfrac{f_{\min} - \hat{y}}{s}\right) + (1-w)s\phi\left(\dfrac{f_{\min} - \hat{y}}{s}\right) \\ \text{if } s > 0 \text{ and the (approximate or exact) constraints are satisfied,} \\ 0 \\ \text{if } s = 0 \text{ or if the (approximate or exact) constraints are violated.} \end{cases} \tag{24}$$

Nevertheless, constraints satisfaction in Eq. (24) is assessed solely on the basis of the value of the constraint prediction, without acknowledging the uncertainty that is associated with it.

Sasena et al. [98] provide a review of several infill sampling criteria, along with a comparison of their efficiency and accuracy on four analytical examples establishing a set of comparison metrics. The advised strategy for restricting the evaluation of further samples in the infeasible areas of the design space is to use a penalty-adjusted expected improvement criterion. However, no advantage over the constraint satisfaction probability method was shown from preliminary tests at identifying optimal points located along the constraint boundaries.

A common approach in extending the above described principles to handle multiple objectives relies on the use of scalarizing methods to transform the original multi-objective optimisation problem to a single-objective optimisation problem. In this context, a general overview is given by Hawe and Sykulski [45] with a brief review of the state-of-the-art in infill sample criteria along with a short description of existing scalarizing algorithms that can potentially be considered for such goal. A previously uninvestigated algorithm is also demonstrated together with a list of few examples available in literature where different sampling criteria and scalarizing methods are combined to give rise to multi-objective optimisation algorithms.

2.5.3. Stop Criteria

In Bayesian global optimisation, as an alternative or complementary criterion to the specification of a time-limit [101][102] or a maximum number of function evaluations

[97], the stopping rule is normally established on the maximum value of the expected improvement function (EI). In particular, the search is terminated when the maximum EI at any given step is smaller than a tolerance value, which can be expressed either as an absolute or relative value to the current minimal function value [99][56]:

$$\begin{aligned} \max\left(\mathrm{E}\left[I(\mathbf{x})\right]\right) &< \text{Absolute Tolerance} \\ \frac{\max\left(\mathrm{E}\left[I(\mathbf{x})\right]\right)}{\left|f_{\min}\right|} &< \text{Relative Tolerance} \end{aligned} \tag{25}$$

A different stopping rule is proposed by Schonlau [99] to overcome some of the undesirable properties of the above criterion, i.e. the potential premature and late termination of the algorithm. It is based on the key concept of estimating the probability bound that the real global minimum (which is unknown) and $f_{\min}$ are no farther apart than a tolerance value δ_{tol}. The process is completed when this probability is below an established critical value $p_{crit} \in [0,1]$.

2.6. Summary and Conclusions

The literature review conducted throughout this research was summarised in this chapter. It allowed to identify the state-of-the-art of suitable methods for addressing different aspects directly or indirectly related to design exploration.

With respect to the first objective of this thesis, an investigation of current approaches aimed at supporting the formulation of optimisation problems was carried out. In particular, attention was focused on the existing strategies for defining and refining the functional and design-variable constraints. This allowed to highlight their corresponding advantages and limitations, especially in terms of assumptions and computational efforts.

With respect to the second objective, different types of visualisation techniques were investigated. The most suitable multidimensional visualisation methods for the numerical analysis of optimisation results through *discipline-independent* techniques were firstly identified, i.e. parallel coordinates plot (PCP), scatter plot matrix (SPM), and self organising map (SOM). A brief description was provided for each one, whereas further

details can be found in Appendix A for the first two techniques. The importance of analysing results via *discipline-dependent* tools was also illustrated by means of carpet plots within the context of conceptual aircraft design. The integration of different techniques was investigated by considering the recent developments in establishing *ad hoc* methodologies for MOO visualisation.

Finally, the main advantages of using surrogate models along with the principles and available infill sampling criteria of Bayesian global optimisation methods were reviewed. This allowed the identification of adequate optimisation tools to be combined with respect the third research objective. The surrogate model method taken into consideration was kriging. Its main features were described in order to highlight its capabilities to support optimisation procedures by means of available computational analysis data. The state-of-the-art investigation of infill sampling criteria was instead focused on their effectiveness in balancing global and local search, as well as in handling optimisation constraints.

The present literature review establishes the fundamentals for the development of novel numerical strategies and the definition of schemas for effectively integrating available methods to address the needs identified in design optimisation.

Chapter 3

Formulation of Optimisation Problems

3.1. Introduction

Most of the efforts in optimisation have so far been focused on the development of novel numerical methods aimed at the computation of optimal solutions. However, usually it is assumed that a correct statement of the problem is given *a priori*. In effect, the first step in an optimisation problem requires to mathematically describe the system/process to be optimised via an adequate problem formulation. The correctness of the optimisation statement, which is not addressed by established optimisation methods, turns out to be decisive to avoid obtaining meaningless results or the loss of important solutions. The set of optimal points is in fact contained in the feasible design set, which, in turn, is defined on the basis of the constraints and design-variable bounds formulation [108].

The objective of this chapter is to present two different methods developed to assist the user in stating an optimisation problem via an adaptive formulation of functional and design-variable constraints. An appropriate correction of the constraints can thus enable the exploration of further promising solutions and a reduction of computational efforts.

To this aim, considered in this chapter are those optimisation problems that can generically be formulated as follows:

$$\begin{aligned} & \min_{\mathbf{x}\in S} f(\mathbf{x}) \\ \text{subject to:} \quad & \mathbf{G}(\mathbf{x}) = \{g_1(\mathbf{x}), g_2(\mathbf{x}), \ldots, g_I(\mathbf{x})\} \leq \mathbf{0}, \\ \text{with:} \quad & \mathbf{x}_{\mathbf{lb}} \leq \mathbf{x} \leq \mathbf{x}_{\mathbf{ub}} \end{aligned} \tag{26}$$

where $f(\mathbf{x})$ is the real-valued objective function to be minimised with respect to the design vector $\mathbf{x} = [x_1, x_2, \ldots, x_n]$ in the n-dimensional design space S, subject to the I functional inequality constraints $g_i(\mathbf{x})$ and $2n$ design-variable constraints (the lower and upper bounds $\mathbf{x}_{\mathbf{lb}}$ and $\mathbf{x}_{\mathbf{ub}}$, respectively).

The first proposed method addresses the determination of the search region within the design space by means of adaptive design-variable bounds. Unsatisfactory results can, in fact, be obtained when the search region is inadequate. If the specified variables bounds are too tight, a set of feasible points could be excluded from the optimiser search and, as a consequence, optimal solutions may be overlooked. On the other hand, an excessively loose search region may lead to substantial or useless computational efforts and time. In this context, reference will be made to those cases where the search region definition is not straightforward because of some reason (e.g., problem complexity or lack of knowledge). The proposed Adaptive Search Optimisation Method (ASOM) conducts a recurrent search region refinement process in parallel with the optimisation procedure. This is achieved through an on-the-fly monitoring of design-variable distributions, which allows to update the design-variable bounds by increasingly gaining insight into the problem at hand via new function evaluations. Consequently, further optimal solutions that initially were infeasible with respect to any initial design-variable constraint now can be proposed to the designer; in addition, infeasible regions can be excluded from the optimal search with the intent of reducing computational cost.

A second method, on the other hand, has been developed to handle the functional constraints that are flexible to some degree and can be changed if necessary, which

generally are referred to as "soft" or "non-rigid" constraints [109]. The presented method is intended to conduct an exploration of initially infeasible design solutions whenever a predefined minimum improvement of the objective can be gained through a maximum relaxation of constraints established *a priori*. Promising design points beyond the original border of soft constraints can hence be identified and suggested to the designer, who can thus gain a better understanding of the problem at hand.

3.2. Proposed Method for an Adaptive and Efficient Setup of the Search Region

The Adaptive Search Optimisation Method (ASOM) has been developed to tackle those optimisation problems whose design-variable constraints setup is not evident or immediate. At first, it may appear that this is related only to those optimisation problems that are characterized by a significant lack of knowledge, such as innovative or unconventional designs. However, for most of the optimisation procedures, more than 70-85% of the total time required to solve the problem is spent on its formulation, which needs to be refined until it proves to be adequate [108]. Attention is focused here on the development of a suitable methodology to prevent promising optimal solutions from being overlooked for being slightly beyond one or more design-variable constraints that could have been adequately relaxed. Such optimal solutions will be from now onwards referred as semi-infeasible optimal points. On the one hand they are infeasible with respect to the variables bounds initially established; on the other hand they could, nonetheless, be accepted by the designer. A key aspect that needs to be considered in this context is the attempt to contain computational efforts and time in contrast with the simplest solution of the problem that would be to set the design-variable constraints as large as possible.

The proposed method is intended to support the user in adequately and effectively determining the search region of an optimisation problem by exploiting the information progressively gathered during the search process. The aim is that of enhancing the evaluation of optimal solutions via the integration of a continuous updating process of the variables bounds, which has to be conducted in parallel with the optimisation procedure. The entire approach is based on a continuous monitoring of the evaluated design points

distributions and the key idea relies on updating in real time the design search region, redefining it as close as possible to the current perceived feasible space throughout the whole optimal search process. This can be achieved via a set of adaptive variables bounds introduced in Section 3.2.1, which are corrected along the optimisation. As new points are evaluated, the search region is updated on the strength of *ad hoc* statistical criteria. By relaxing, strengthening, or leaving the variables bounds as they are on the basis of the information currently gained about the problem at hand, the whole optimisation process can consequently be enhanced. If the probability of exploring semi-infeasible points exceeds a user-defined threshold, the variables bounds can be relaxed on the strength of an adequate criterion, while the entire process can be accelerated via a suitable restriction criterion by limiting the optimiser search to the sub-region of the design space that is perceived to be feasible, thus limiting the evaluation of infeasible points.

3.2.1. Terminology

The method for an adaptive setup of the search region is based on the specification of two different set of variables bounds: the adaptive bounds and the frozen (or ultimate) bounds. The first set represents the current design-variable constraints taken into consideration at a given time of the optimisation process. Their initial value setup has to be based mainly on the designer's experience and intuition. In the case of lack of knowledge of the problem under study, it is advisable to consider adaptive bounds largely set in order to facilitate the feasible design space identification and subsequently fit the search region to it. The drawback of such strategy is the risk of a heavier computational cost for the early iterations of the optimisation process, although this is preferable rather than obtaining a reduced set of optimal solutions.

The frozen bounds, on the contrary, enforce the limit value that some variables may have for any reason[4]. The lower (upper) frozen bound of a design variable, therefore, represents the ultimate lower (upper) value that the variable at issue can have.

[4] The limit values of a variable can be dictated by physical/functional considerations, design requirements or regulations. For instance, a significant challenge in designing the A380 derived from considering the [80m x 80m x 80ft] box of maximum allowable aircraft size as an additional requirement to minimise airport infrastructure impact [8] and satisfying the requirements given by ICAO

The whole method has been developed by adopting the notation shown in Figure 15, where shown in red and black are the distributions of the entire set and the feasible set of points evaluated at a generic time of an optimisation process and projected on the *i-th* dimension x^i.

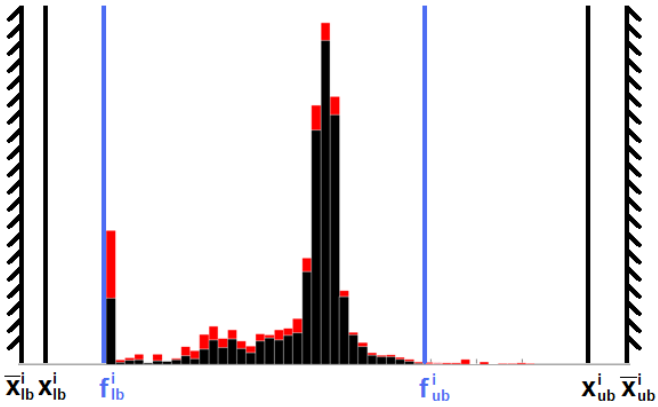

$\bar{x}^i_{lb}$	Lower Frozen Bound
x^i_{lb}	Lower Adaptive Bound
x^i_{ub}	Upper Adaptive Bound
$\bar{x}^i_{ub}$	Upper Frozen Bound

f^i_{lb}	Lower Bound of the Perceived Feasible Space $F_p{}^i$
f^i_{ub}	Upper Bound of the Perceived Feasible Space $F_p{}^i$

Figure 15. Notation taken into consideration in relation with the *i-th* variable search region.

where the superscript *i* denotes the *i-th* design variable under consideration and the subscripts *lb* and *ub* stand for *lower bound* and *upper bound* respectively.

Provided one or more feasible points exist among the overall set of computed design evaluations, the following inequality must always be satisfied for any feasible design vector **x**:

$$\bar{\mathbf{x}}_{lb} \le \mathbf{x}_{lb} \le \mathbf{f}_{lb} \le \mathbf{x} \le \mathbf{f}_{ub} \le \mathbf{x}_{ub} \le \bar{\mathbf{x}}_{ub} \tag{27}$$

[7]. Analogously, airfoils having a thickness-to-chord ratio above a certain value can not be considered because of aerodynamics reasons related to the desired range of mach cruise.

It is important to note that whereas the perceived feasible space $F_p^i = [f^i_{lb}, f^i_{ub}]$ of the *i-th* variable can be identified from the set of feasible sampled points, the real feasible space F_r^i is generally unknown.

3.2.2. Under-Determined and Over-Determined Search Regions

In general, optimisation efficiency and effectiveness can be improved by providing good starting guesses, which may limit the number of iterations to convergence and increase the likelihood of finding a global minimum rather than a local one. Nevertheless, such a strategy can not be applied to optimisation problems associated with a lack of knowledge or characterized by a significant complexity. In this context, the approach adopted here is to conduct a series of independent optimisation procedures from a number of different starting points spread all over the search region. Every single optimisation run is carried out after having assessed the effectiveness of the design search region by analysing the variables distributions of the evaluations previously computed. This allows to establish whether the search region is valid or invalid. In the first case no changes are required, whereas in the second it is necessary to relax the search region if this is under-determined, or to restrict it when over-determined. An example for the three possible types of search region is shown in Figure 16:

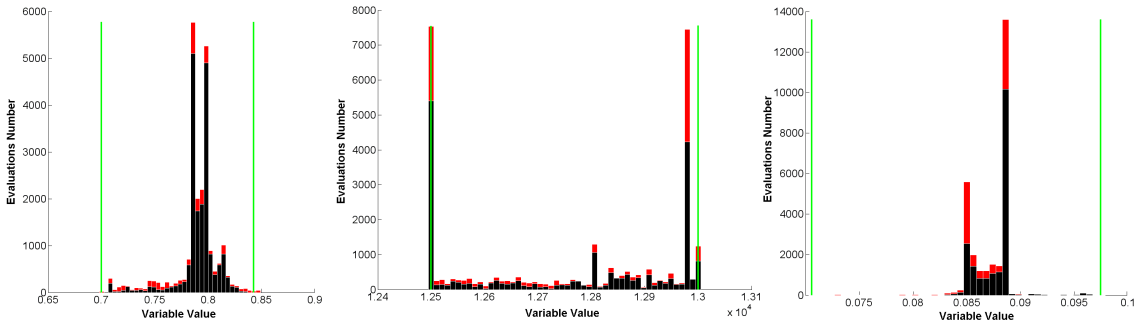

(a) (b) (c)

Figure 16. The analysis of each variable distribution reveals if its corresponding search region is (a) valid, (b) under-determined, or (c) over-determined. The lower and upper adaptive bounds of the variable are represented by green lines, while the black part of the histogram represents the fraction of feasible samples out of the entire set of sampled points (in red).

Formally, denoting the generic *i-th* variable with the superscript *i*, the search region is considered to be over-determined if:

$$x_{lb}^{i} \le f_{lb}^{i} - \alpha^{i}(f_{ub}^{i} - f_{lb}^{i}) \quad \text{or} \quad x_{ub}^{i} \ge f_{ub}^{i} - \alpha^{i}(f_{ub}^{i} - f_{lb}^{i}), \qquad \text{for } i = 1, \ldots, n \tag{28}$$

where α^{i} is the *i-th* restriction coefficient, which has to be defined as a percentage of the current perceived feasible space F_{p}^{i}. The over-determined bound(s) can be redefined on the strength of the restriction criterion proposed in Section 3.2.3.

On the other hand, the search region is considered to be under-determined for the *i-th* variable when one of the following cases occurs:

a) Throughout the optimisation process, a set of feasible design points are evaluated beyond the adaptive bounds. Consequently:

$$f_{lb}^{i} \le x_{lb}^{i} \qquad \text{or} \qquad f_{ub}^{i} \ge x_{ub}^{i}, \qquad \text{for } i = 1, \ldots, n \tag{29}$$

b) Whenever the probability that further feasible samples exist beyond the current adaptive bounds is above a threshold p_i established by the designer, thus violating one or both the following inequalities:

$$P\left\{x^{i} < x_{lb}^{i}, \quad x^{i} \in F_{r}^{i}\right\} \le p_i, \qquad P\left\{x^{i} > x_{ub}^{i}, \quad x^{i} \in F_{r}^{i}\right\} \le p_i, \qquad \text{for } i = 1, \ldots, n \tag{30}$$

Section 3.2.4 describes the proposed relaxation criterion along with a set of distribution-free probability inequalities which can provide a probability bound for (30).

3.2.3. Restriction Criterion

The restriction criterion is presented below by taking into consideration the lower adaptive bound of the *i-th* variable and assuming the notation shown in Figure 17. Analogous considerations can be extended to the upper adaptive bound case.

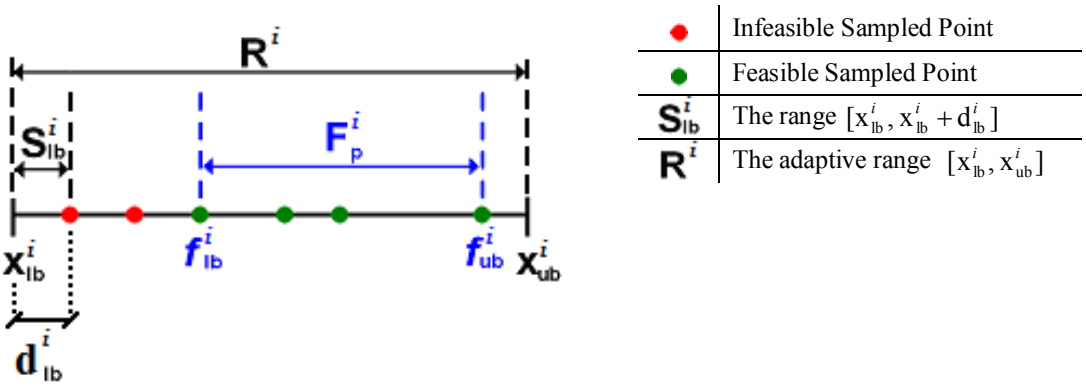

Figure 17. Notation adopted for the restriction criterion.

The range S^i_{lb} is determined by d^i_{lb}, which is the distance between the lower adaptive bound and its adjacent infeasible observation. The probability of a feasible point being in S^i_{lb} is inversely proportional to the ratio:

$$P\left(x^i \in \left[S^i_{lb} \cap F^i_r \right] \right) \propto \frac{d^i_{lb}}{(x^i_{ub} - x^i_{lb})} \quad , \qquad \text{for } i = 1, \ldots, n \tag{31}$$

Introducing a constant of proportionality ϑ^i:

$$P\left(x^i \in \left[S^i_{lb} \cap F^i_r \right] \right) = \vartheta^i \frac{d^i_{lb}}{(x^i_{ub} - x^i_{lb})} \quad , \qquad \text{for } i = 1, \ldots, n \tag{32}$$

the restriction criterion is expressed as follows:

$$\begin{aligned} &\text{if} \quad P\left(x^i \in \left[S^i_{lb} \cap F^i_r \right] \right) \le \gamma^i \\ &\qquad x^i_{lb} = x^i_{lb} + d^i_{lb} \quad , \qquad \text{for } i = 1, \ldots, n \\ &\text{end} \end{aligned} \tag{33}$$

where γ^i is the probability threshold established by the designer for the *i-th* variable. The restriction criterion has to be applied progressively to the set of infeasible sampled points adjacent to x^i_{lb} while condition (33) continues to be satisfied. As mentioned above, the criterion can similarly be extended to the upper bounds.

3.2.4. Relaxation Criterion

The proposed relaxation criterion has been developed for conducting an appropriate re-definition of under-determined search regions and enforcing inequality (27) at the same time. It can be employed in conjunction with optimisation algorithms that allow to assume the n design-variables distributions as the distributions of n random variables X_k, for k=1,…,n. An example is provided in Section 3.2.5 by considering the simultaneous perturbation stochastic approximation algorithm (SPSA). The problem at hand, therefore, can be tackled as an estimation problem of univariate tail probabilities. In other words, the adaptive bounds of any under-determined design variable x^i can be redefined according to the user-predefined probability threshold p_i and on the basis of the current feasible sampled points distribution[5]. Such a criterion has to be applied individually to any (lower/upper) design-variable bound considered to be under-determined according to the above-mentioned criteria, so that the corresponding inequality from (30) is satisfied and holds with equality.

For the generic random variable X, the following probability inequalities based on moment information have been taken here into consideration:

Chebyshev-Cantelli inequality [27]**:**

$$\mathrm{P}\{X - M_1 \geq t\} \leq \frac{\sigma_2}{\sigma_2 + t^2}, \qquad \text{for } t \geq 0 \tag{34}$$

Cantelli's inequality [12]**:**

$$\mathrm{P}\{X - M_1 \geq t\} \leq \frac{\upsilon_{2m} - \upsilon_m^2}{\upsilon_{2m} - \upsilon_m^2 + (t^m - \upsilon_m)^2}, \qquad \text{for } t \geq \left(\upsilon_{2m}/\upsilon_m\right)^{1/m} \tag{35}$$

[5] Only the distributions of the feasible points set are here taken into account rather than those of the overall points set, so that the whole optimisation process is focused on the areas of the design space which are perceived to be feasible.

Bertsimas-Popescu inequality (for $X \in R_+$) [13] [88]**:**

$$\mathrm{P}\{X > (1+t)M_1\} \le \begin{cases} \min\left(\dfrac{C_M^2}{C_M^2 + t^2}, \dfrac{1}{1+t} \cdot \dfrac{D_M^2}{D_M^2 + (C_M^2 - t)^2} \right), & \text{if } t \ge C_M^2 \\ \dfrac{1}{1+t} \cdot \dfrac{D_M^2 + (1+t)(C_M^2 - t)}{D_M^2 + (1+C_M^2)(C_M^2 - t)}, & \text{if } t < C_M^2 \end{cases}$$

$$\mathrm{P}\{X < (1-t)M_1\} \le 1 - \frac{(C_M^2 + t)^3}{\left(D_M^2 + (C_M^2 + 1)(C_M^2 + t)\right)\left(D_M^2 + (C_M^2 + t)^2\right)} \tag{36}$$

where: $C_M^2 = \dfrac{M_2 - M_1^2}{M_1^2}$ and $D_M^2 = \dfrac{M_1 M_3 - M_2^2}{M_1^4}$.

Denoting by:

$$M_m = \mathrm{E}\left[X^m\right] \quad , \quad \sigma_m = \mathrm{E}\left[\left(X - \mathrm{E}(X)\right)^m\right] \quad , \quad \upsilon_m = \mathrm{E}\left[\left|X - \mathrm{E}(X)\right|^m\right]$$

All inequalities are distribution-free so that no assumptions are required for the population probability distribution function of the design variables. For explanatory purposes, Figure 18 depicts the upper probability bounds for the tails of a normal and a gamma distribution. The choice of the appropriate inequality has to be determined by the designer conforming to his/her preferences. Cantelli's inequality provides a tight probability bound, albeit this can be computed only for those points which satisfy its constraint on *t*. Chebyshev-Cantelli and Bertisimas-Popescu inequalities generally provide a similar estimation, although the latter is sensitive to the distribution asymmetry as shown for the gamma distribution. It is important to note that although Cantelli's inequality is two-sided, generally it provides a tighter probability bound.

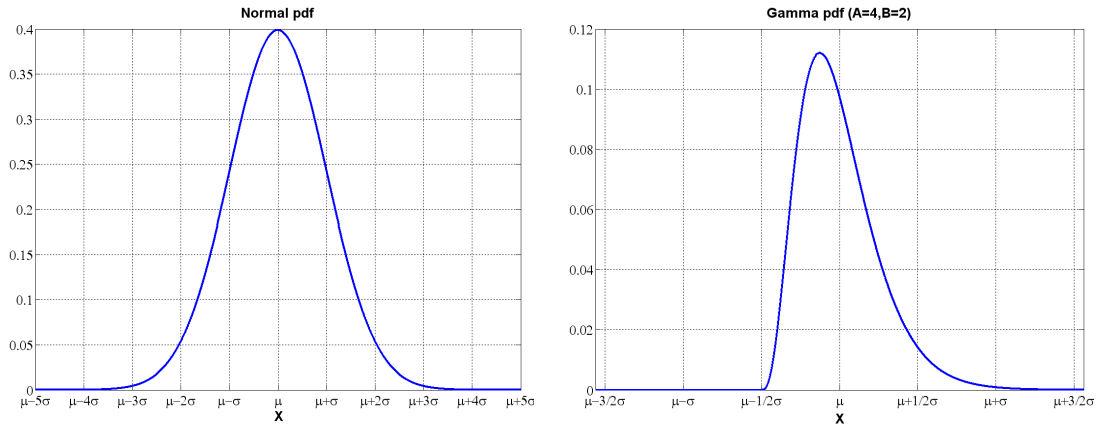

Normal PDF

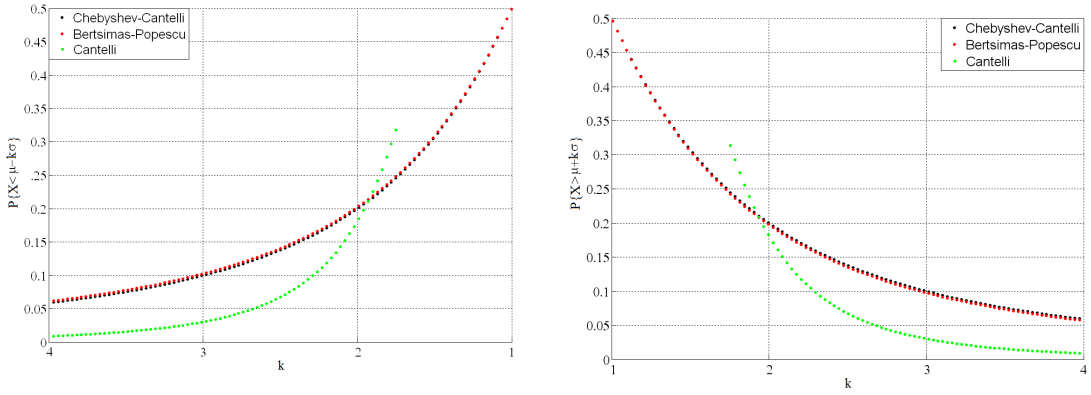

Gamma PDF (A=4, B=2)

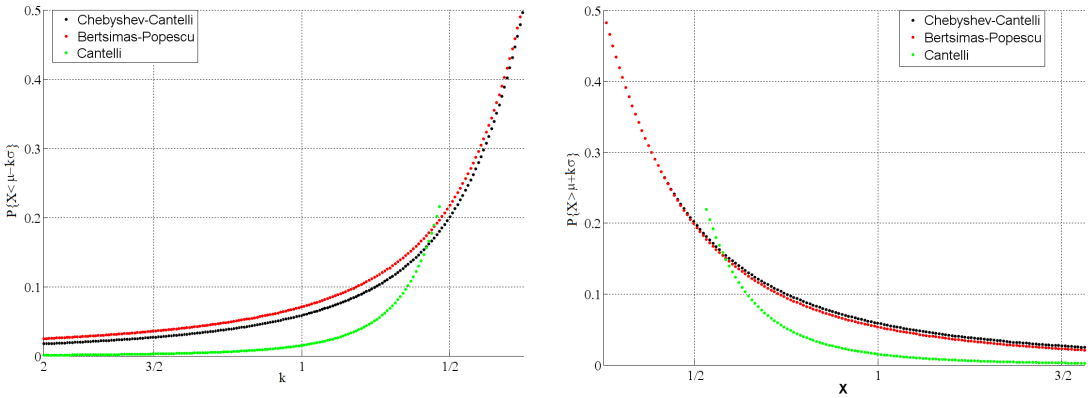

Figure 18. Probability bounds on normal and gamma distributions.

Nevertheless, the abovementioned inequalities can provide only an estimation for updating the adaptive bounds on the basis of statistical parameters of the feasible variables distributions. As a matter of consequence, it may happen that the new

theoretical adaptive bounds $\hat{x}_{lb}^{i}$ and $\hat{x}_{ub}^{i}$ do not satisfy inequality (27). Additional constraints therefore have eventually to be enforced. Formally:

Lower Adaptive Bound:	**Upper Adaptive Bound:**
if $\hat{x}_{lb}^{i} < \overline{x}_{lb}^{i}$	if $\hat{x}_{ub}^{i} > \overline{x}_{ub}^{i}$
$x_{lb}^{i} = \overline{x}_{lb}^{i}$	$x_{ub}^{i} = \overline{x}_{ub}^{i}$
elseif $\hat{x}_{lb}^{i} > f_{lb}^{i}$	elseif $\hat{x}_{ub}^{i} < f_{ub}^{i}$
if $\left(f_{lb}^{i} - \delta^{i} \cdot (f_{ub}^{i} - f_{lb}^{i})\right) \geq \overline{x}_{lb}^{i}$	if $\left(f_{ub}^{i} + \delta^{i} \cdot (f_{ub}^{i} - f_{lb}^{i})\right) \leq \overline{x}_{ub}^{i}$
$x_{lb}^{i} = f_{lb}^{i} - \delta^{i} \cdot (f_{ub}^{i} - f_{lb}^{i})$	$x_{ub}^{i} = f_{ub}^{i} + \delta^{i} \cdot (f_{ub}^{i} - f_{lb}^{i})$
else	else
$x_{lb}^{i} = \overline{x}_{lb}^{i}$	$x_{ub}^{i} = \overline{x}_{ub}^{i}$
end	end
else	else
$x_{lb}^{i} = \hat{x}_{lb}^{i}$	$x_{ub}^{i} = \hat{x}_{ub}^{i}$
end	end

for $i = 1, \ldots, n$ (37)

Where δ^{i} is a threshold expressed as a percentage of the current perceived feasible space F_p^i.

The new definition of the adaptive bounds, consequently, will derive both from the choice of the probability bound inequality and from the probability threshold established by the designer.

3.2.5. Hybrid Optimisation

Among all the optimisation methods, the simultaneous perturbation stochastic approximation (SPSA [104],[105]) algorithm can be advantageously coupled with ASOM. Such integration, first of all, allows to deal with those cases where no explicit closed-form expression of the objective function is available but only measurements of *f* at specified points of the design space are possible, also in the presence of noise. The main advantages in using SPSA, however, derive from the gradient approximation at the base of the algorithm, whose specific form for solving the constraint optimisation problem (26) is as follows [119]:

$$\mathbf{x}_{k+1} = \mathbf{x}_k - a_k \hat{\mathbf{g}}_k - a_k r_k \nabla P(\mathbf{x}_k) \tag{38}$$

where $\hat{\mathbf{g}}_k$ is the estimate of the gradient of f at the iterate $\mathbf{x}_k$, $\{a_k\}$ is a positive scalar sequence satisfying $a_k \to 0$ and $\sum_{k=1}^{\infty} a_k = \infty$, $\{r_k\}$ is an increasing sequence of positive scalar with $\lim_{k\to\infty} r_k = \infty$, and $\nabla P(\mathrm{x}_k)$ is the gradient of the penalty function $P(\mathrm{x})$ used to convert (26) into an unconstrained optimisation problem[6]. The approximation $\hat{\mathbf{g}}_k$ is obtained from only two measurements of the objective function $f(\cdot)$ based on the simultaneous and random perturbation of all the elements of the design vector around $\hat{\mathbf{x}}_k$. Formally:

$$\hat{\mathbf{g}}_{\mathbf{k}}(\hat{\mathbf{x}}_k) = \frac{f(\hat{\mathbf{x}}_k + c_k\boldsymbol{\Delta}_k) - f(\hat{\mathbf{x}}_k - c_k\boldsymbol{\Delta}_k)}{2c_k} \begin{bmatrix} 1/\Delta_{k1} \\ 1/\Delta_{k2} \\ \vdots \\ 1/\Delta_{kn} \end{bmatrix} \tag{39}$$

where Δ_{ki} is the *i-th* component of the *n*-dimensional random perturbation vector $\boldsymbol{\Delta}_k$, and $c_k \to 0$ is a positive gain sequence. Wang and Spall [119] establish the convergence of the algorithm under appropriate conditions.

Within the context of this work, the key to using the SPSA method lies in two main aspects. On the one hand, the function observations evaluated through its random search can be used to update the variables distributions at the base of ASOM, thus enabling the use of the probability inequalities described in Section 3.2.4. On the other hand, its gradient approximation technique is independent of the dimension of the problem under consideration, which makes the method particularly efficient in terms of computational resources. Nevertheless, the specific choice of the gain sequences can be not

[6] The specific choice of the gain sequences might dramatically influence the performance of the method. General implementation guidelines are given in [105] and [106].

straightforward and might dramatically influence the performance of the method. General implementation guidelines are given in [105] and [106].

Normally, a further reduction in the optimisation cost can be achieved by adopting an alternative optimisation method for the final stages of the optimisation search. After exploiting the SPSA capabilities in easily identifying the neighbourhood of a minimum $\mathbf{x}^*$, the overall optimisation procedure can be enhanced by limiting its associated asymptotic convergence. This suggests the employment of a hybrid optimisation, taking for example advantage of the second order convergence achievable by optimisation algorithms based on the sequential quadratic programming (SQP) method. Adequate switch criteria have to be established to exploit this local property of such algorithms, that requires the process to be initialised sufficiently close to $\mathbf{x}^*$ along with the satisfaction of the second order sufficient conditions at $\mathbf{x}^*$ [32]. In addition to imposing a maximum number of iterations, the SPSA procedure is terminated when the relative change in the variables is small enough for a number of consecutive iterations. Figure 19 compares the performance of the SPSA method and the SQP-based algorithm fmincon implemented in Matlab, considering the constrained optimisation problem tackled by Wang and Spall [119]. The fmincon error and the SPSA averaged error (over 100 simulations carried out independently and adopting the quadratic penalty function) are depicted in red and green respectively. It is possible to observe how the proposed hybrid algorithm tends to terminate the SPSA procedure when a first considerable error decrement has been obtained, thus switching to fmincon (visualised in blue) to finalise the optimisation. It is important to note that, in comparison to other methods, the inherent potential capabilities of SPSA in limiting computational cost depend on the problem dimensionality. Whereas the number of function evaluations required by fmincon grows with n, the SPSA algorithm needs only two measurements, independently of n. Consequently, the larger the number of variables considered, the more evident are the benefits of the proposed hybrid optimisation method.

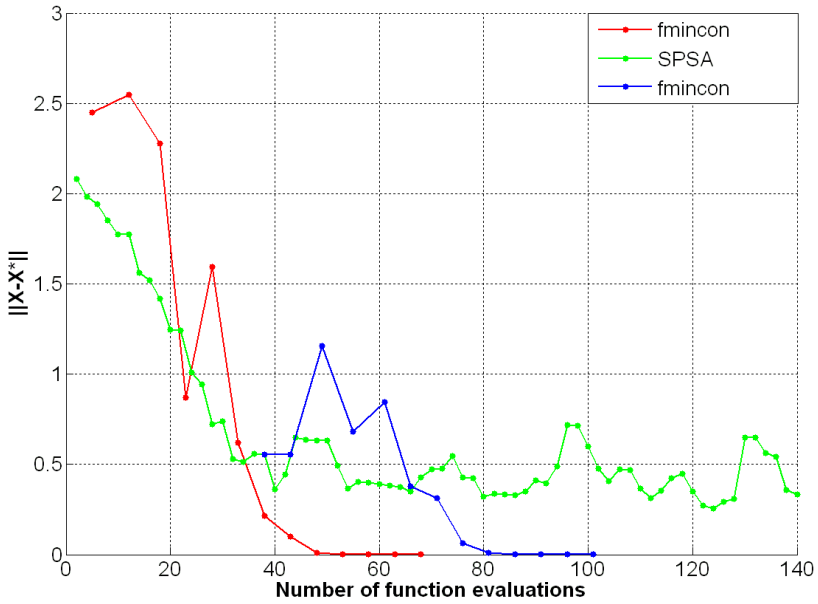

Figure 19. Comparison of the error trend for the Matlab function fmincon and the SPSA algorithm (averaged over 100 independent simulations). The proposed hybrid optimisation terminates the SPSA optimisation after obtaining a first considerable error decrement, switching to fmincon (in blue) to carry out the final phase of the optimisation search.

3.2.6. Implementation of ASOM

As mentioned in Section 3.2.2, within the framework of the problems considered here, it is assumed that independent optimisation runs are individually conducted from a number of starting points. It is also supposed that the entire collection of starting points offers the initial set of function evaluations required for the initialisation of ASOM. Provided such observations are uniformly distributed within the initial search region, the minimum number Q of starting points that is required depends on the larger of the n ratios between the constant of proportionality ϑ^i and the probability threshold γ^i. In fact, defining the average distance between samples for the *i-th* variable as follows:

$$\bar{d}^i = \frac{R^i}{(Q+1)}, \qquad \text{for } i = 1, \ldots, n \tag{40}$$

the restriction criterion (33) is applicable only if the following criterion derived from (32) and (40) is met:

$$Q \geq \max_i \left(\frac{\vartheta^i}{\gamma^i} \right) - 1 , \qquad \text{for} \quad i = 1, \ldots , n \tag{41}$$

It is important to note that Equation (41) provides a means to estimate the minimum number of observations to allow restricting the search region via the restriction criterion and under the hypothesis of a uniform distribution of the samples. An equivalent consideration of applicability for the relaxation criterion is not required, although its effectiveness is directly proportional to the number of feasible points evaluated, as it also depends on the formulation of the problem, the nature of the functions involved and the number of variables.

Once ASOM has been initialised with the evaluation of at least Q starting points, a first validity check of the current search region is carried out. In the case the search region results to be inappropriate on the strength of conditions (28), (29) and (30), then the relaxation and the restriction criteria are applied to update the bounds of the variables whose search regions are under-determined and over-determined respectively. This procedure is subsequently repeated after each optimisation execution started from a different starting point is complete. The flowchart of the method is depicted in Figure 20, which delineates the tasks that take place for each individual optimisation launched from each of the starting points obtained, for example, via a design of experiments (DoE). The search regions of all variables are analysed individually and eventually corrected in order to enforce a valid search region and the satisfaction of the inequality (27) for the subsequent individual optimisation run on the basis of the problem information gathered from all the previous evaluations.

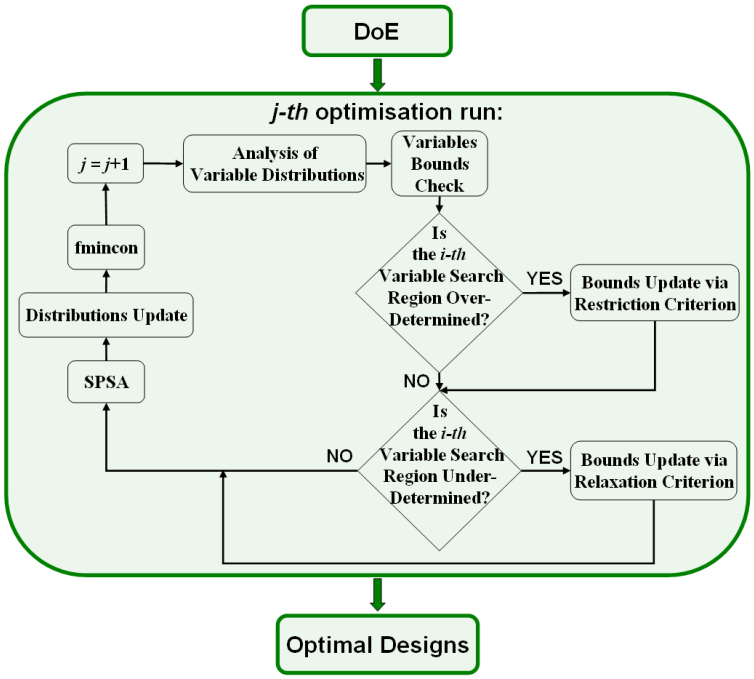

Figure 20. Flowchart of the tasks that take place for each individual optimisation run. The variables bounds to be considered for the optimisation procedure starting from the *j-th* starting point are adequately determined by analysing the variables distributions of the overall feasible points previously evaluated. Note that the *i-th* design-variable can turn out to be over-determined with respect to its lower bound, and under-determined with respect to its upper-bound, and vice versa.

3.2.7. Analytical Example

The adaptive optimisation search method has been tested with the two-dimensional bump function considered by Keane and Nair [57]:

$$\min_{\mathbf{x}\in\Re^2} f(\mathbf{x}) = -\text{abs}\left(\sum_{k=1}^{2}\cos^4(x_k) - 2\prod_{k=1}^{2}\cos^2(x_k)\right) \Bigg/ \sqrt{\sum_{k=1}^{2} k\cdot x_k^2}$$

$$\text{subject to}: \quad g(\mathbf{x}) = \sum_{k=1}^{2} x_k - 8 \le 0, \tag{42}$$

$$\text{with}: \quad 0 \le x_k \le 5 \qquad k = 1,2$$

where the variables x_k are expressed in radians. The highly bumpy nature of the function, shown in Figure 21, provides an adequate test case for ASOM in identifying further local minima located beyond the design-variable constraints initially chosen.

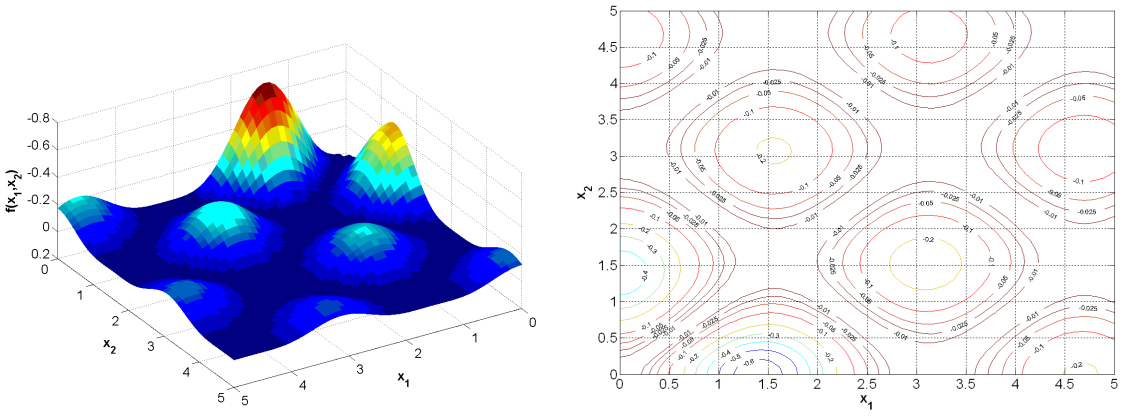

Figure 21. The bump function in two dimensions [57].

The considered setup of the optimisation problem under study is as follows:

Input Variable	**Frozen Bounds**		**Adaptive Bounds**	
	$\overline{\mathbf{x}}_{\text{lb}}$	$\overline{\mathbf{x}}_{\text{ub}}$	$\mathbf{x}_{\text{lb}}$	$\mathbf{x}_{\text{ub}}$
x_1	0	5	2	4.5
x_2	0	5	0.5	4.5

Table 1. Setup of the frozen and adaptive bounds for the optimisation of the bump function in two variables.

adopting for both variables the following ASOM parameters: $\vartheta^{1,2}=1$, $\gamma^{1,2}=0.05$, $p_{1,2}=0.05$, $\alpha^{1,2}=0.05$ and $\delta^{1,2}=0.25$.

The above definition of the frozen and adaptive bounds is representative of all those situations in which additional global minima are located slightly beyond the design-variable constraints that have been set. In this case, apart from the feasible optimum located within the initial search region, there are five further semi-infeasible optimal points, as shown in Table 2.

Optimal Points	$x_{1\ \text{optimal}}$	$x_{2\ \text{optimal}}$	$f_{\ \text{optimal}}$
Point Nº1	3.0872	1.5174	-0.2629
Point Nº2	1.5527	3.0695	-0.2145
Point Nº3	3.1272	4.6685	-0.1363
Point Nº4	4.6840	3.1040	-0.1551
Point Nº5	4.6588	0	-0.2134
Point Nº6	1.3932	0	-0.6737

Table 2. Coordinates and value of the objective function for the feasible optimum located within the initial search region established in Table 1 (Point Nº1) and the corresponding set of semi-infeasible optimal points.

Cantelli's probability inequality is adopted here, focusing attention on the case where the designer is interested in conducting a tight expansion of the design space. Whenever the requirement on the parameter t given in (35) is not satisfied, Chebyshev-Cantelli inequality is employed as an alternative.

An example of the results obtained from an optimisation run based on twenty starting points (produced by a Latin Hypercube sampling and identified by the green and red crosses, depending if they are feasible or infeasible respectively) is portrayed in Figure 22. With respect to the adaptive bounds, their initial and final values are represented by magenta and red lines, respectively, whereas their intermediate updates throughout the process are given by the set of lines with different colour shades from yellow to red. The frozen variables bounds are visualised via cyan lines, whereas the constraint under consideration is in black. The red and green points represent the feasible and infeasible points, respectively. The final design-variable distributions are displayed in the lower area of the figure, where the same meaning is associated to the different colours of the depicted lines.

In this case, three further optimal points have been found. In Figure 22 they are highlighted by blue squares. Different factors might influence the search of semi-infeasible optimal points:

- **The number of starting points.** A number of starting points are required both to identify all the feasible local minima of the problem under study and for the initialisation of ASOM. Nevertheless, the minimum quantity of starting points can not be estimated without any knowledge of the problem at hand. A small number of starting points could prevent the algorithm from expanding sufficiently any under-determined search region, thus reducing the probability of identifying all the semi-infeasible optimal points outside the initial formulation of the variables bounds. An example of this is provided in Figure 22, where the set of points located in the vicinity of the minimum $\mathbf{x} = [1.3932, 0]$ shows how the related optimal search has been obstructed and constrained to move along the adaptive bounds valid for the corresponding optimisation procedure. In general, to limit such inconvenience it may be advisable to adopt a substantial number of starting points, bearing in mind the consequent computational cost increment.

- **The distribution of the starting points.** The location of the starting points across the initial search region is another crucial factor for the ASOM effectiveness. In the event they are not uniformly scattered, semi-infeasible optimal points located in non-sampled areas of the design space might not be identified. In Figure 22 this occurs for the overlooked minimum **x** = [4.6588, 0], without any starting point in its neighbourhood.

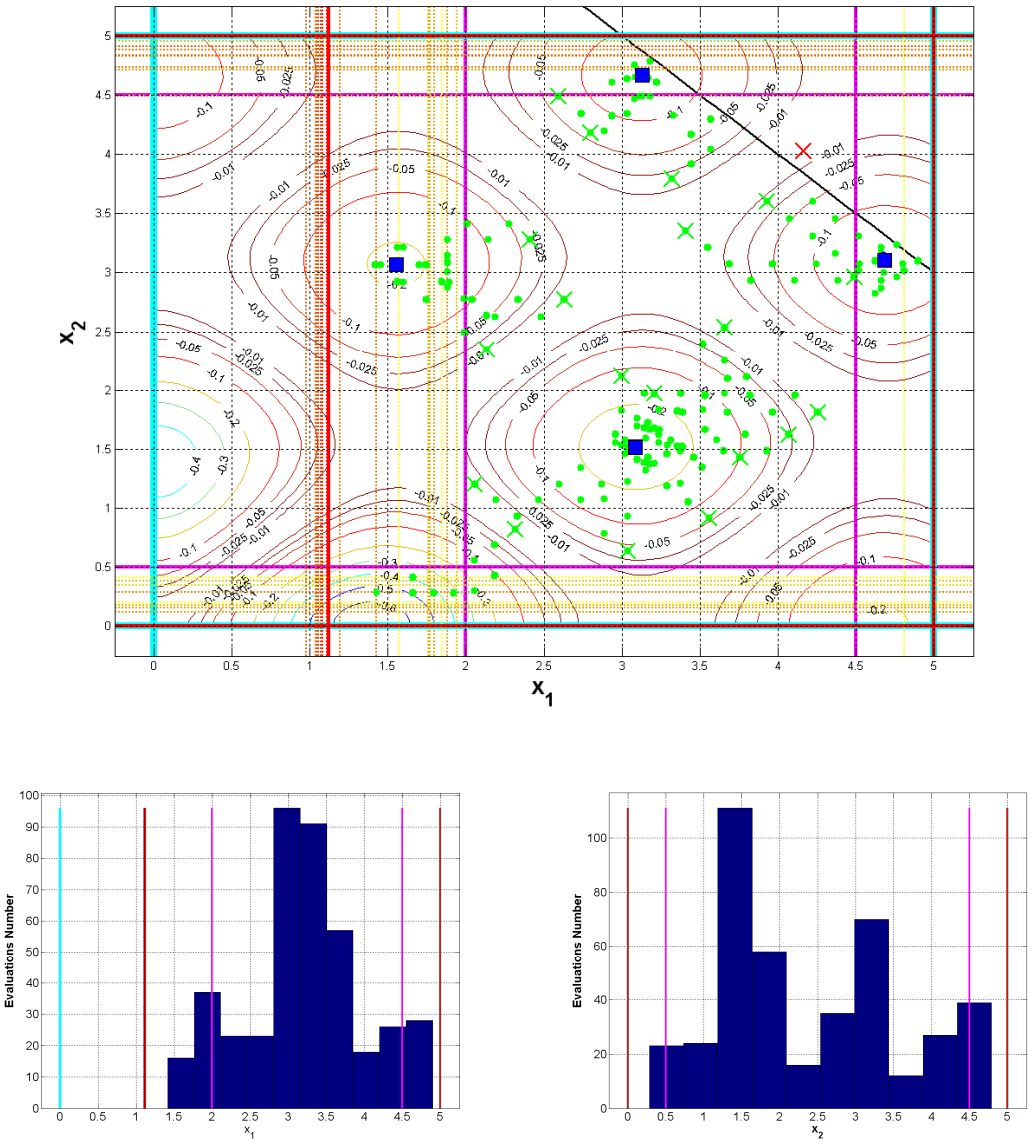

Figure 22. An example of ASOM results from solving problem (42) considering twenty starting points.

A second optimisation problem was considered to assess the capabilities of the proposed methods to cut out from the optimal search those regions of the design space presumed to be infeasible according to the parameters ϑ^i and γ^i set by the designer. The constraint in the problem formulation (42) was consequently modified to reduce the real feasible sub-region of the design space as follows:

$$\min_{\mathbf{x}\in\Re^2} f(\mathbf{x}) = -\,\mathrm{abs}\left(\sum_{k=1}^{2}\cos^4(x_k) - 2\prod_{k=1}^{2}\cos^2(x_k)\right)\Bigg/\sqrt{\sum_{k=1}^{2} k\cdot x_k^2}$$

$$\text{subject to:}\quad g(\mathbf{x}) = 3 - x_2 \le 0, \tag{43}$$

$$\text{with:}\qquad 0 \le x_k \le 5 \qquad k = 1,2$$

The same ASOM parameters specified in Problem (42) were taken into consideration. A visualisation of the above optimisation problem is shown in Figure 23 along with an example of the results obtained from its solution. The notation used is the same of Figure 22.

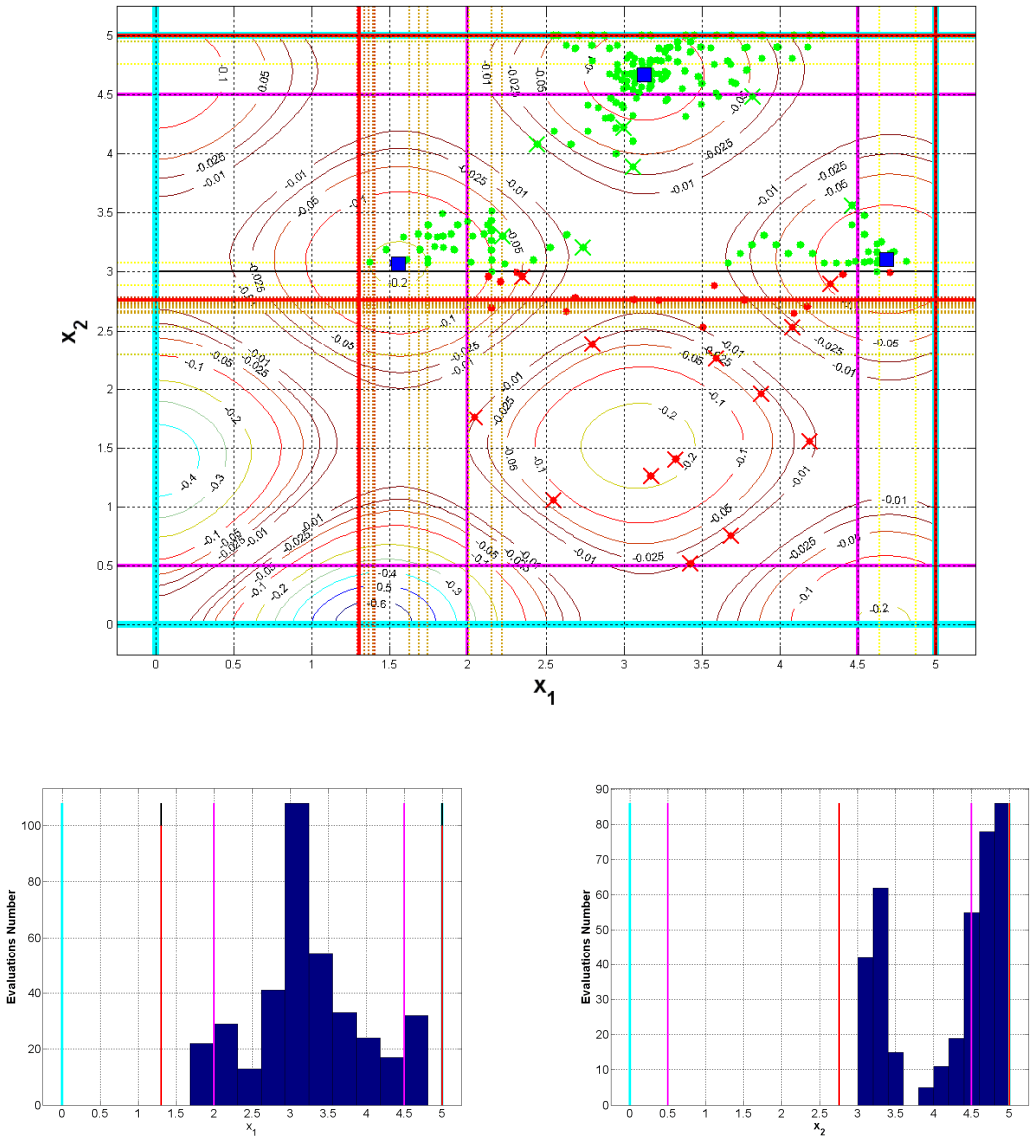

Figure 23. An example of resulting adaptive variables bounds for problem (43).

The contour plot of Figure 23 depicts the final location of the x_2 lower bound, that cuts out most of the design space area made infeasible by the constraint here considered.

3.3. Local Relaxation Method for Non-rigid Constraints

3.3.1. Problem Formulation and Assumptions

In an optimisation problem the minimisation or maximisation of objective functions might be subject to a set of functional constraints whose satisfaction restricts the values that can be assumed by the variables, thus defining the feasible design space. The determination of such region comes to be essential since it contains the Pareto front. Consequently, a tight formulation of one or more functional constraints can result in a narrow feasible design space and therefore in a reduced or empty set of optimal solutions. Constraints can be classified as "rigid" and "soft" ("non-rigid" or "manageable") [109]. The first must be accurately satisfied, and generally derive from physical/functional considerations, design requirements or regulations. Conversely, soft constraints (e.g. overall dimensions, design budget) are flexible to some degree and can be changed if necessary. It may happen, in fact, that in some cases a relaxation of a soft constraint can lead to a significant improvement of the design objectives. An example is provided in Appendix C for a conceptual aircraft design optimisation problem, demonstrating how the Pareto front can be considerably enhanced by slightly relaxing the limit value of a soft constraint. However, in other circumstances it could be not true. It is therefore necessary to identify those conditions where the relaxation of one or more soft constraints can potentially lead to a reasonable improvement of the objectives.

3.3.2. Proposed Relaxation Method

The objective of the present method is to conduct a discerning relaxation of the soft inequality constraints considered in optimisation problems formulated as in (26), with the aim of obtaining a minimum improvement on the objective defined *a priori* by the designer. In this context, it is crucial to estimate how sensitive the objective is to changes in the constraints. This information can be gained by means of the method of Lagrange multipliers. Formally, the multiplier λ_i is the derivative of the Lagrangian function with respect to the *i-th* constrain at the solution [110]. To show how λ_i measures sensitivity, let

us introduce a perturbation $\varepsilon_i>0$ on the active inequality constraint g_i. The Lagrangian of the problem is:

$$\mathcal{L}(\mathbf{x},\boldsymbol{\lambda}) = f(\mathbf{x}) - \sum_{i=1}^{I} \lambda_i (g_i(\mathbf{x}) - \varepsilon_i) \tag{44}$$

Since at solution points $\mathcal{L}(\mathbf{x}, \boldsymbol{\lambda}) = f(\mathbf{x})$ it follows that [32]:

$$\frac{df}{d\varepsilon_i} = \frac{d\mathcal{L}}{d\varepsilon_i} = \frac{\partial \mathbf{x}^T}{d\varepsilon_i} \nabla_x \mathcal{L} + \frac{\partial \boldsymbol{\lambda}^T}{d\varepsilon_i} \nabla_\lambda \mathcal{L} + \frac{d\mathcal{L}}{d\varepsilon_i} = \lambda_i \tag{45}$$

The rate of change in the objective function due to changes on a constraint is well known in economics and is expressed by means of the *shadow price* concept [96], formally defined as the amount by which the objective function value changes given a unit change on a constraint[7]. Since the shadow price for an inactive (or *nonbinding*) constraint is always zero (the corresponding multiplier is zero), only the potential effects on the objective that may derive from a relaxation of one active constraint at a time will be considered. It is also worthwhile to note that the change in the objective function is indicated to first order, and consequently it is only locally accurate.

Based on the information provided by the Lagrange multipliers, the cases where a constraint relaxation might lead to promising design improvements can thus be identified. In general, this happens when the gradient of the objective and the constraint at hand turn out to be high and low, respectively. A simple example with a one-dimensional objective f(x) and constraint g(x) is given in Figure 24.

[7] Whether an increment or a decrement of the objective value derives from a relaxation or a tightening of the constraint, depends on how the constraint is formulated (i.e., on the direction of the inequality).

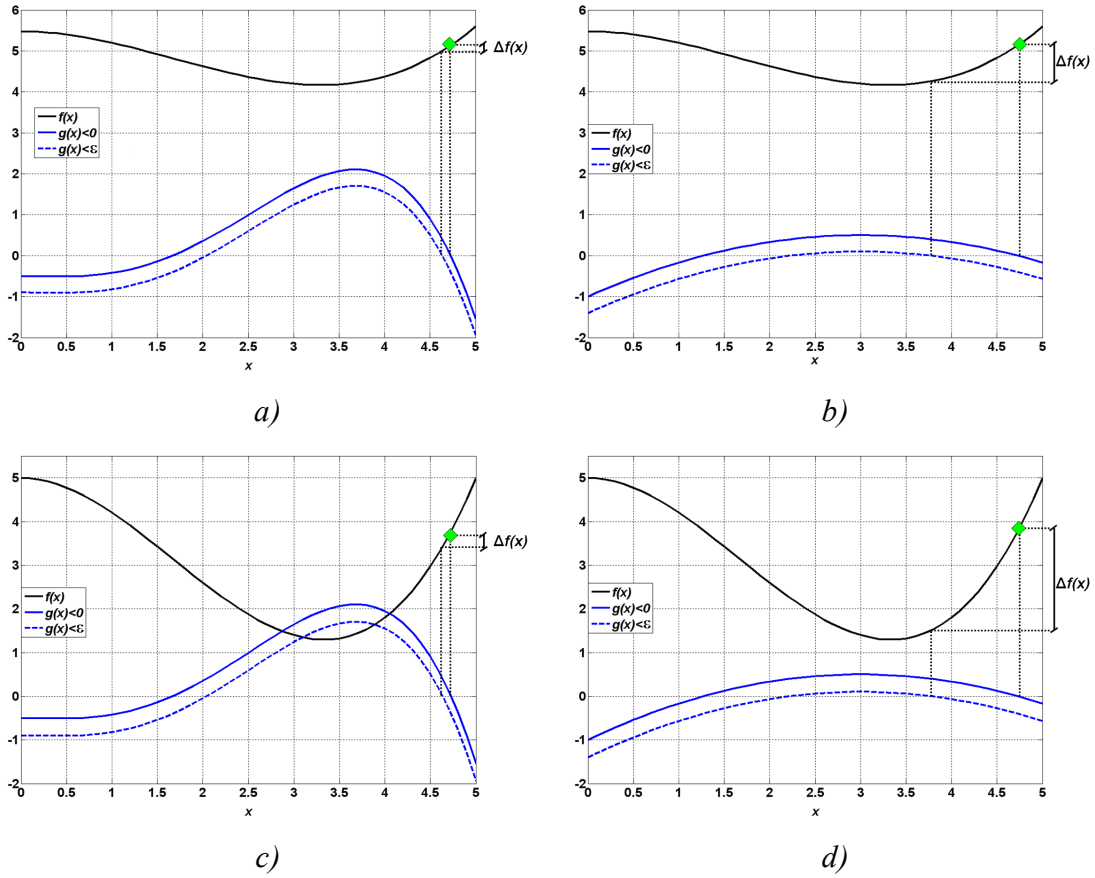

Figure 24. The four figures represent conceptually the four possible cases that may occur when relaxing a constraint of the same amount ε. Attention is here focused on the identification of the cases as in *d)*, where a significant improvement of the objective can be achieved via a minor relaxation of one constraint.

The proposed discerning relaxation of active constraints is conducted on the strength of the following parameters specified *a priori* by the user:

- α : minimum improvement of the objective as a percentage of the current objective minimum.
- $\tilde{\varepsilon}_i$: maximum relaxation allowable for the constraint g_i, for i=1,…,I.

Such set of parameters allows the introduction of a criterion to differentiate the cases of interest and enables a local relaxation of the constraints. Denoting with $\mathbf{x}^k$ a generic optimal point obtained from an optimisation procedure after k iterations and lying on the

border of the *i-th* constraint, a relaxation of g_i can be considered only if the following inequality is satisfied:

$$\frac{\Delta f_i}{f(\mathbf{x}^k)} \geq \alpha \tag{46}$$

where Δf is the predicted improvement $\lambda_i \tilde{\varepsilon}_i$ in the objective function due to a relaxation $\tilde{\varepsilon}_i$ of the constraint g_i. Figure 25 provides a graphical representation of the concept behind the above criterion, depicting the expected changes on the objective and the *i-th* constraint function at the point $\mathbf{x}^{k+1}$ corresponding to the maximum relaxation allowed on g_i.

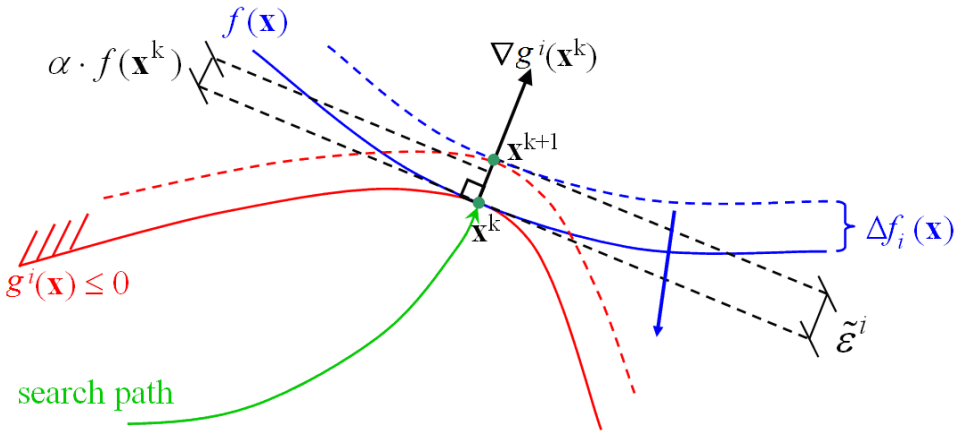

Figure 25. Conceptual representation of the proposed relaxation method.

Once a constraint is relaxed on the strength of inequality (46) satisfaction, a further optimisation procedure can be carried out considering $\mathbf{x}^k$ as starting point. However, when handling multiple constraints it may occur that the new design solution thus found activates other constraints which, in turn, can be relaxed. The relaxation of one constraint can consequently lead to the relaxation of others. Therefore, for any optimal solution it is important to scan all the active constraints and proceed with their relaxation if possible, as shown in Figure 26.

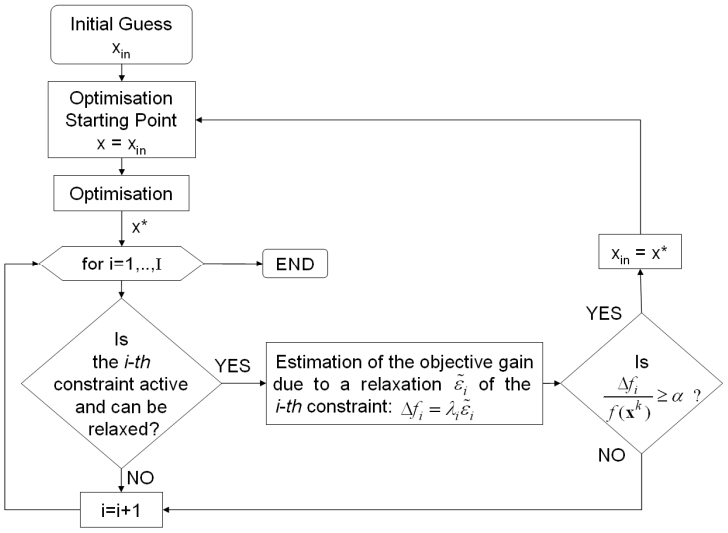

Figure 26. Proposed loop to handle the relaxation of multiple constraints.

3.3.3. Analytical Example

An example of the present relaxation method is given here by taking into consideration the objective function of Problem (42) along with the following soft constrains:

$$\min_{\mathbf{x}\in\Re^2} f(\mathbf{x}) = -\text{abs}\left(\sum_{k=1}^{2}\cos^4(x_k) - 2\prod_{k=1}^{2}\cos^2(x_k)\right)\Bigg/\sqrt{\sum_{k=1}^{2} k\cdot x_k^2}$$

$$\begin{aligned} \text{subject to:}\quad & g_1(\mathbf{x}) = 3 - x_1^2 - x_2^2 \leq 0, \\ & g_2(\mathbf{x}) = 3 - 1/5*(x_1 + 1/4)^3 - 4/5*(x_2 + 1/5)^2 \leq 0, \end{aligned} \tag{47}$$

$$\text{with:}\quad -3.5 \leq x_k \leq 3.5 \qquad k = 1,2$$

The solutions obtained via the Matlab algorithm fmincon are shown in Table 3 and portrayed in Figure 27, where the contours of the *f*, g_1 and g_2 are given by the red, black and blue lines respectively. The bold lines in blue and black depict the design space points for which the two constraints are active, whereas the dashed lines identify the contours of the active constraints after a relaxation $\tilde{\varepsilon} = [0.5, 1.25]$. The red squares are the solutions provided by fmincon after following the search paths identified by the cyan points and initiated from a number of different starting poins (represented by the green triangles). A minimum objective improvement $\alpha = 0.2$ has been taken into account.

Point	x_1	x_2	f	λ_1	λ_2	$\lambda_1\tilde{\varepsilon}_1$	$\lambda_2\tilde{\varepsilon}_2$	$\frac{\Delta f_1}{f}$	$\frac{\Delta f_2}{f}$
$\mathbf{x}^*_A$	0.0036	1.7354	-0.3858	0	0.1546	0	0.1932	0	0.5008
$\mathbf{x}^*_B$	1.5527	3.0695	-0.2145	0	0	0	0	0	0
$\mathbf{x}^*_C$	2.2014	0.0594	-0.1911	0	0.1796	0	0.2245	0	1.1748
$\mathbf{x}^*_D$	0.0067	-2.1354	-0.1686	0	0.1634	0	0.2042	0	1.2112
$\mathbf{x}^*_E$	1.5527	-3.0695	-0.2145	0	0	0	0	0	0
$\mathbf{x}^*_F$	-1.5527	-3.0695	-0.2145	0	0	0	0	0	0

Table 3. The first column on the left-side contains the design solutions obtained via fmincon for Problem (47), where each subscript identifies the relative starting point. The remaining columns show, from left to right, the solution coordinates (x_1 and x_2), the corresponding objective value (f) and Lagrange multipliers (λ_1 and λ_2), the estimated gains ($\lambda_1\tilde{\varepsilon}_1$ and $\lambda_2\tilde{\varepsilon}_2$) in the objective due to a maximum relaxation of the constraints and the resulting values of left-side of inequality (46) ($\frac{-\Delta f_1}{f}$ and $\frac{-\Delta f_2}{f}$).

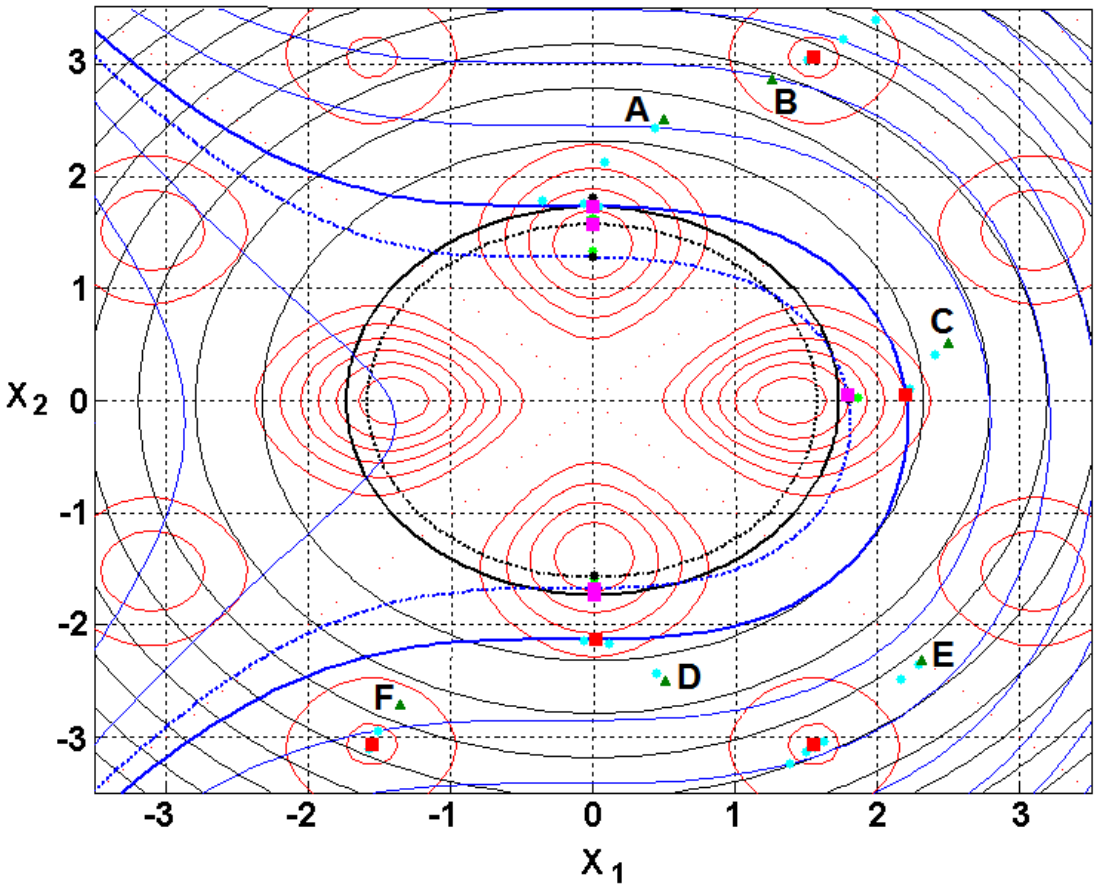

Figure 27. Results obtained for Problem (47) by using the Matlab algorithm fmincon on six different starting points, which are represented by the green triangles. The proposed

method for constrain relaxation was subsequently used for the solutions characterized by constraint activation. The contours of the objective f and constraints g_1 and g_2 are given by the red, black and blue lines, respectively.

It can be seen that only the solutions obtained from the starting points A, C and D result in the activation of a constraint (g_2, in all cases), and allow the application of the relaxation method above described. The design points obtained via further optimisation procedures (whose evaluations are illustrated via black points), conducted after the relaxation of a constraint, are represented by the magenta squares. The light green points, instead, show the estimated point for which $g_i = \tilde{\varepsilon}_i$, with i the constraint being relaxed.

For clarification purposes, a magnified view of the three cases involving constraint relaxation is presented in Figure 28. The case related to the starting point C is representative of the situations where the relaxation of only one constraint is possible. After relaxing the constraint g_2, the design solution in effect lies on the contour $g_2 = \tilde{\varepsilon}_2$. The other two cases, on the contrary, provide an example involving the relaxation of multiple constraints, where the change on one constraint can lead to the activation of another that in turn can be relaxed. With respect to the starting point A, the relaxation of the constraint g_2 does not impact on the solution provided by fmincon[8]. This is because the two constraints of the problem are tangent to each other at such point. It is only after the relaxation of g_1 that the objective function can be improved by obtaining the point P_2, which lies on the contour $g_1 = \tilde{\varepsilon}_1$, this being more stringent with respect to $g_2 = \tilde{\varepsilon}_2$. In the case of the starting point D, point P_4 is obtained after relaxing g_2 and, subsequently, P_3 via a partial relaxation of g_1, which is however hindered by the maximum relaxation $\tilde{\varepsilon}_2$ allowed on g_2.

[8] The magenta square representative of the design point obtained after a relaxation $\tilde{\varepsilon}_2$ of g_2 (point P_1) coincides with the solution given by the Matlab algorithm, therefore covering it graphically.

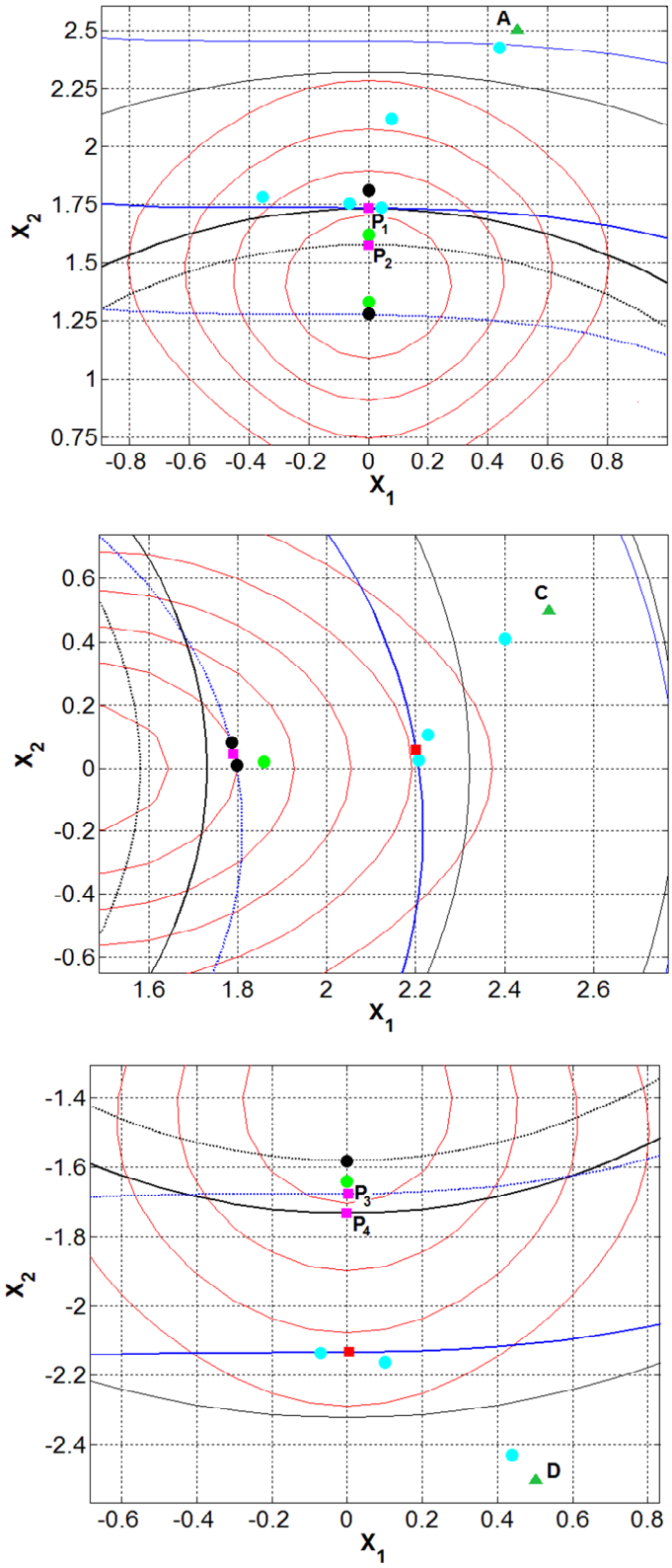

Figure 28. Magnified view of the optimisation procedures started from the points A, C and D along with the respective constraint(s) relaxation execution.

The coordinates of the new solutions and its improved objective values resulting from conducting a relaxation of one or both constraints are provided in Table 4.

Point	x_1^{R2}	x_2^{R2}	f^{R2}	x_1^{R1}	x_2^{R1}	f^{R1}
$\mathbf{x}^*_A$	0	1.7321	-0.3874	0	1.5811	-0.4471
$\mathbf{x}^*_C$	1.7912	0.0478	-0.5034	---	---	---
$\mathbf{x}^*_D$	0	-1.7321	-0.3874	0.0039	-1.6776	-0.4119

Table 4. Coordinates and objective values of the new design points obtained via a constraint relaxation of Problem (47). The first column on the left hand side identifies the three cases analysed in Figure 28 through the letter-subscript, standing for the corresponding starting point. The superscripts *R1* and *R2*, instead, denote the solution coordinates and objective value resulting after a relaxation of g_1 and g_2 respectively.

3.4. Summary and Conclusions

Proposed in this chapter are two novel methods to support the mathematical statement of optimisation problems. The overall aim is to propose a numerical strategy to conduct an adaptive formulation of functional and design-variable constraints that can be considered to be flexible to some extent, so that the feasible design set can be adequately identified and computational efforts partially reduced. The key concept to achieve this is to allow the exploration of further solutions that are located beyond the initial constraint limits and can potentially lead to a significant improvement of the optimal solutions set.

The Adaptive Search Optimisation Method (ASOM) is firstly presented for an effective determination of the search region by adaptively refining the design-variable bounds throughout the optimisation procedure. The correction of bounds is based on the strength of a continuous analysis of the distributions of the feasible evaluations via *ad hoc* statistical criteria that do not require specific distributional assumptions for the design variables. The search region can thus be relaxed, strengthened, or left unchanged on the basis of the information gained about the problem at hand through the points evaluated along the optimisation process. This enables the exploration of promising points not contained in the initial feasible design set, but located within specific design-variable ranges established by the designer. The number of infeasible evaluations is also reduced

by partially excluding from the optimiser search the areas of the design space with a low probability of containing feasible points. Both aspects contribute to reducing the formulation-cyclic iterations required for a correct problem statement

A second method is presented for handling "soft" or "non-rigid" constraints of single–objective optimisation problems. It allows to conduct an exploration of additional solutions that could potentially lead to a minimum improvement of the objective through a relaxation of constraints within specific limits established *a priori* by the designer. The fundamentals of the method are established by incorporating concepts well known in economics for expressing the rate of change in the objective function due to changes on a constraint. Promising design improvements can thus be achieved by estimating the effects on the objective deriving from a relaxation of one active constraint at a time on the basis of the information provided by the Lagrange multipliers.

The application of the proposed methods is demonstrated in this chapter with an analytical example. The capabilities of ASOM in addressing problems of industrial relevance are shown in Chapter 6 with a conceptual aircraft multi-objective optimisation test case.

Chapter 4

Visual Exploration and Analysis of Design Solutions

4.1. Introduction

Optimisation algorithms have proven to be an effective tool for design of complex engineering systems and processes. They can in fact support and enhance the identification of alternative solutions that represent the optimum trade-offs between multiple design criteria, which are often conflicting in nature.

In the context of conceptual design optimisation, a large number of design concepts have to be evaluated. An iterative process is required in order to achieve a consistent design [108], including continuous analysis, changes and improvements of the design layouts. However, the large multidimensional datasets resulting from such an approach are often too complex to be analysed and completely understood by the designers, who are accustomed to traditional visualisation tools. There is an apparent need for a suitable visualisation methodology to make the results of complex design optimisation procedures fully readable and meaningful to the designer. Appropriate visualisation strategies are also required for building, debugging and understanding algorithms and models integrated within the optimisation architecture [54].

Presented in this chapter is a novel methodology for visual exploration of design solutions with the aim of supporting the designer in analysing and comparing large number of design concepts. The expected practical effect is enabling the designer to gain an improved insight into the problem at hand through a synergistic integration of suitable visualisation techniques for addressing common data analysis scenarios occurring in deterministic and robust optimisation. The full meaning of multivariate design data is thus conveyed from different analysis perspectives via an integrated set of interactive visualisation interfaces whose overall effectiveness is expected to be greater than the sum of the individual contributions for evaluating alternative design solutions.

The foundations of the presented methodology are firstly established in Section 4.2 by outlining the standard visualisation needs and fundamental graphical aspects to be considered in engineering design optimisation at conceptual stage. The proposed methodology for visual exploration is presented in Section 4.3 for a generic MOO problem formulated as in (1), describing the techniques adopted together with the key criteria for their selection, their synergistic integration via an adequate set of visualisation interfaces, and their operation. The extension of the methodology when dealing with robust design optimisation (RDO) data is finally described.

4.2. Visual Exploration of Alternative Design Solutions

This section is intended to define the standard visualisation needs in engineering design optimisation at conceptual stage. The foundations of an adequate visualisation methodology can thus be established.

The primary objective to be achieved is the identification of the best design concepts according to the design criteria taken in consideration. In fact, as the design solutions advance step by step towards more detailed design, it becomes more difficult and expensive to introduce changes [33], as outlined in Section 2.4. Therefore, it is essential to conduct an exhaustive exploration of alternative solutions in order to obtain a good conceptual design that, in the following design phases, may require further changes but not major revisions [91].

A crucial requirement for an effective visualisation technique is to be able to translate intricate numerical datasets into simple and meaningful graphical representations with the

intent of facilitating data analysis and its understanding. A gradual and selective trade-off process on large sets of design points can thus be conducted by handling a considerable number of design parameters. Nonetheless, when dealing with multivariate data, it is important to bear in mind what is the maximum number of variables that the human being can handle simultaneously. On the strength of experimental results on the human capacity for processing information, it has been noted that by increasing the amount of *input information* the *transmitted information* increases asymptotically towards a maximum value, called the *channel capacity* of the observer. "The point seems to be that, as we add more variables to the display, we increase the total capacity, but we decrease the accuracy for any particular variable. In other words, we can make relatively crude judgments of several things simultaneously" [77]. Such cognitive ability is known as the *seven plus or minus two rule*: in our mind we can efficiently manipulate from five to nine things at the same time.

Additionally, to enable design to be conducted effectively and efficiently, in the *Total Design Activity model*, Pugh [89] recognises that various design techniques need to be used, functionally dividing them into two categories. The first, referred to as *discipline-independent techniques*, are applicable to any product or technology, such as techniques for conducting analysis, synthesis, decision making, modelling, etc. The latter, indicated as *discipline-dependent techniques*, provide additional inputs to the design process from domain-specific sources, such as stress analysis, thermodynamic analysis, information on materials, electronics, and so forth.

In engineering optimisation, moreover, it is indispensable to allow the designer to analyse not only the Pareto solutions, but also the set of feasible and infeasible designs. In the first case, the evaluation of the histograms of feasible variables distributions provides a means to assess the search region validity, as shown in Chapter 2. This offers an alternative way to manually correct the variables bounds on the strength of designer's experience and intuition, as suggested by Statnikov and Matusov [108]. The visualisation of infeasible solutions, conversely, provides a method for an *a posteriori* identification of promising design points that lie slightly beyond the contours of soft constraints.

In general, the standard visualisation needs required in engineering design optimisation at conceptual stage and taken into account in the present methodology are:

- Comparison of different designs [5][111][4] [38];
- Identification of *similar designs* [9] [126][111];
- Constraint satisfaction information [26][44][90];
- Identification of potential relationships between the parameters under consideration [111][47][46];
- Identification of ill-formulated problems [52][108].

4.3. Proposed Visualisation Methodology

A novel integrated visualisation methodology for visual exploration of design solutions is proposed with the aim of enhancing the evaluation and trade-off analysis of deterministic and robust design solutions in a MOO framework. The guidelines for using multiple views proposed by Baldonado et al. [10] have been employed for meeting the visualisation aspects and needs outlined in Section 4.2.

The present methodology is intended to advance the state-of-the-art visualisation methods for the analysis of MOO data, which are available in different commercially available software. Generally, basic analysis functions are provided, such as allowing the selection of axes and a minimum set of visualisation techniques (e.g., Global Optimisation Toolbox in Maplesoft). An interactive graphical analysis of the design space can be performed in Isight by considering (individually) different views, as well as through the identification of optimal, feasible and infeasible solutions on a table interface. An exploration of the design space from different perspectives is also provided by the VisualizationPak in PHX ModelCenter, which offers a considerable number of methods for the interpretation and navigation of multi-dimensional spaces. Nevertheless, specific visualisation needs still remain to be addressed for conducting a comprehensive analysis of optimisation results. In particular, the deployment of *discipline-dependent techniques* is required in order to effectively support the comparison of alternative solutions in complex design problems. Furthermore, a more systematic integration of multiple interactive data perspectives is

[9] *Similar designs* are those designs sharing specific criteria established by the designer, such as common variable ranges, on-target performance or the satisfaction of a particular set of constraints.

essential to evaluate high-dimensional datasets by considering different design criteria at the same time.

The basic methodology for deterministic datasets is presented in the following sub-sections. Firstly, key criteria for the selection of adequate visualisation techniques are outlined in sub-section 4.3.1 depending on the analysis scenarios and tasks at hand. Sub-section 4.3.2 describes the set of visualisation interfaces that, through a synergistic integration, provide the designer with relevant design perspectives of the data under study. Guidelines for an interactive operation of such interfaces are finally drawn in sub-section 4.3.3.

The extension of the methodology when dealing with robust design optimisation (RDO) data is ultimately described in sub-section 4.3.4.

4.3.1. Visualisation Techniques

The aim, considering the visualisation aspects and needs outlined in Section 4.2, is that the full meaning of design optimisation data is conveyed to the designer via an integration of visualisation techniques, without requiring him/her to be an expert in numerical optimisation methods. The present visualisation methodology is based on the development of a matrix that identifies the suitable visualisation techniques to be used in the context of common data analysis scenarios occurring during conceptual design optimisation. Depending on the analysis to be carried out, suitable methods have to be selected with respect to key features of the datasets to be investigated in the attempt to guarantee their full readability. All the *discipline-independent* visualisation techniques considered in the present methodology for a generic optimisation dataset are shown in Table 5. Their selection has been based on the identification of the most effective visualisation methods available in the literature for evaluating optimisation results [46][126][111][125]. In addition, the analysis tasks that can be conducted in aircraft design via carpet plots are described in the last column as an example of *discipline-dependent* tools that might be considered for specific design domains. A demonstration of the application of the present methodology to an analysis of optimal aircraft conceptual designs can be found in Nunez et al. [82], where the first three *discipline-independent* visualisation techniques (*Objective Space Visualisation, PCP and SPM*) are integrated along with carpet plots.

Table 5. Deterministic visualisation methodology matrix.

Technique / Scenario	Objective Space Visualisation	PCP	SPM	Filtering	Distribution Histograms	Carpet Plots
Visualisation of a single design point	Objective(s) values analysis	Visualisation of variables, objectives and constraints values				Performance analysis
Visualisation of a reduced number of design points (<10)	Objective(s) values comparison and analysis of design families	Comparison of design points sharing common features	Trend and correlation analysis	Analysis of design points within a specific design sub-space or objective/constraint ranges	Analysis of the corresponding distribution for any specific design parameter	Performance comparison between design points
Visualisation of a large number of design points (>10)	Objective(s) values comparison and visualisation of design families	Identification of design points sharing common features	Trend and correlation analysis	Identification of design points within a specific design sub-space or objective/constraint ranges	Analysis of the corresponding distribution for any specific design parameter	Analysis/Visualisation of the entire solutions-set distribution
Local trade-off study via Pareto approximations	Objective(s) values comparison and visualisation of design families	Identification of common features shared between the approximated solutions	Gradient information for local sensitivity analysis	Identification of the active constraints set of a Pareto frontier approximation	Analysis of the corresponding distribution for any specific design parameter	Performance visualisation of approximated Pareto frontiers
Constraint satisfaction study	Objective(s) values comparison	Study of how well constraints are satisfied		Analysis of feasible/infeasible design solutions	Distribution analysis of feasible/infeasible design solutions	Performance requirements check
Active constraints study	Visualisation of design families	Analysis of designs characterized by constraint activation. Relaxation study		Identification of potential design candidates for constraint relaxation	Distribution analysis of points located close to constraint contours	Analysis of designs characterized by constraint activation
Search region definition		Numerical analysis of optimal, feasible and infeasible sets of solutions		Analysis of the solutions located close to the variables bounds	Distribution analysis of solutions located close to the variables bounds	Performance analysis of potential design candidates for constraint relaxation

4.3.2. Visualisation Interfaces

It is author's belief that, in order to convey the full meaning of design optimisation data to the designer, an integration of visualisation techniques from Table 5 has to be carried out via a set of interactive visualisation interfaces. By coupling them synergistically, the designer can thus gain a comprehensive insight into the data under study. The effectiveness in evaluating alternative design solutions via the simultaneous analysis of specific design perspectives is consequently expected to be greater than the sum of the individual contributions of the integrated visualisation techniques.

The visual exploration of design optimisation data is conducted by means of three graphical interfaces. Each interface is focused on the representation of one of the visualisation perspectives relevant in optimisation problems: *Euclidean space representation*, *multidimensional data visualisation* and *specific design tools*. An intuitive and user-friendly implementation of such interfaces in a joint graphical user interface (GUI) is sought to further improve the visualisation of the complex information produced by design optimisation tools. The interactive selection of points on any interface triggers in real time an automatic update of the visualisation on the remaining interfaces. This provides a means to conduct in a more effective manner both the analysis of a single solution or the comparison of a number of design alternatives.

The three graphical interfaces are described below. Key concepts of the methodology are clarified and illustrated via specific screenshots of a visual exploration interface prototype developed by the author, the *Integrated Exploration and Visualisation Interface* (*IEVI*), displayed in Figure 29. Unless stated differently, all the figures of this chapter depict the results obtained from the optimisation of Problem (42) after tightening its constraint as follows:

$$g(\mathbf{x}) = \sum_{k=1}^{2} x_k \leq 4 \tag{48}$$

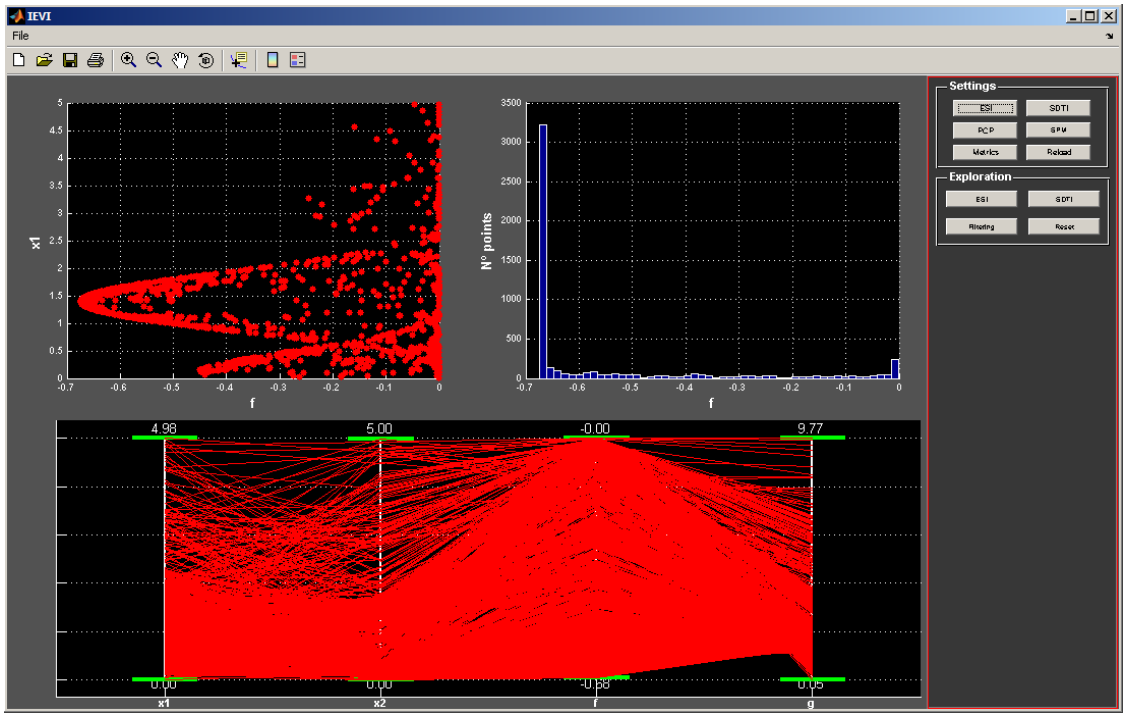

Figure 29. Default visualisation of the *IEVI*. The three most relevant data perspectives in optimisation problems are shown via the below-described interfaces: *ESI* (top-right window), *SDTI* (top-left window) and *MDVI* (bottom window).

Euclidean Space Interface (ESI)

The primary objective of the *ESI* is the representation of the objective space in a simple and conventional way for up to three objectives, providing the value of the objective functions for each alternative design point computed throughout the optimisation procedure. The visualisation of higher-dimensional objective spaces can be achieved by means of the techniques described in the *Multidimensional Data Visualisation Interface* paragraph below.

Via the integration of *Filtering*, the sets of non-dominated, feasible and infeasible solutions can be graphically highlighted in the *ESI*. Further filtering criteria can be specified in the *PCP*, as shown later on.

In the *ESI*, it is also possible to plot any pair of design parameters of interest, as shown in Figure 30. This offers a double advantage. On the one hand, it is possible to investigate the effects of any *Filtering* operation also on the design and constraint spaces. On the

other hand, the selection of points to be analysed/compared on the two other interfaces can be conducted by means of a *Filtering* process performed in the *ESI* by specifying desirable ranges of values or interactively selecting the points of interest.

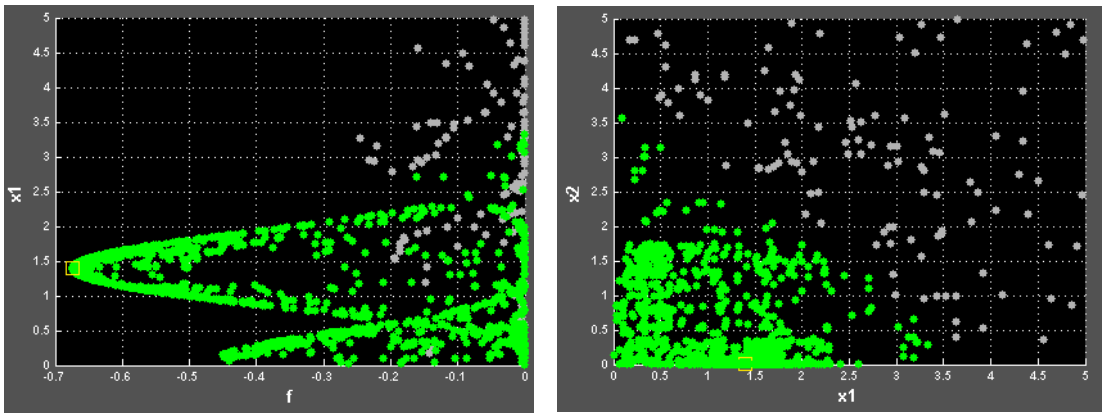

a) *b)*

Figure 30. Two magnified examples of the visualisation flexibility allowed in *ESI*. The feasible, non-feasible and non-dominated sets of points have been identified by means of *Filtering* and are represented through green points, grey points and yellow squares, respectively.

Valuable information can be rapidly obtained from the *ESI*, such as:

- The identification of the objectives minimum and maximum values for the sets of optimum or feasible points;

- The location of *similar designs* in the objective, design, and constraint spaces;

- The position of local Pareto regions, which correspond to different *optimal families* of solutions;

- The density of optimal/feasible/infeasible design solutions in a specific area of the objective, design, and constraint spaces;

- The location in the objective, design, and constraint spaces of the solutions characterized by one or more specific active constraints;

- Optimisation formulation errors.

Multidimensional Data Visualisation Interface (MDVI)

In the *MDVI*, the *PCP* is the default multidimensional visualisation technique available to the designer due to its effectiveness in visualising high-dimensional data on a simple two-dimensional plot. Moreover, this method is particularly useful for identifying relationships among the design parameters and for checking constraint satisfaction and activation.

In the *PCP* all the variables of interest are represented on the graph together. However, since the axes are plotted side by side, the *i-th* dimension is linked at most to two other dimensions. In an *n*-dimensional problem, no information is visualised about the relationships among the *i-th* axis and the other (*n*-3) axes which are not by its sides. Therefore, it is evident there is a need for implementing the *PCP* in the *MDVI* so that it is possible to permute the axes. This allows finding out different views of the problem and other possible relationships among the design parameters. Such an approach, based on a manual permutation of the axes, can be extended by firstly identifying the minimal set of permutations required to avoid duplicate adjacencies among all the *n*! possible permutations [120].

Furthermore, the user is provided with the *Filtering* function, which enables him/her to analyse only those solutions within an established range of values for any design parameter of interest (Figure 31). Additionally, it is possible to select the sets of solutions to be displayed (separately or conjointly), including: feasible points, infeasible points and non-dominated points.

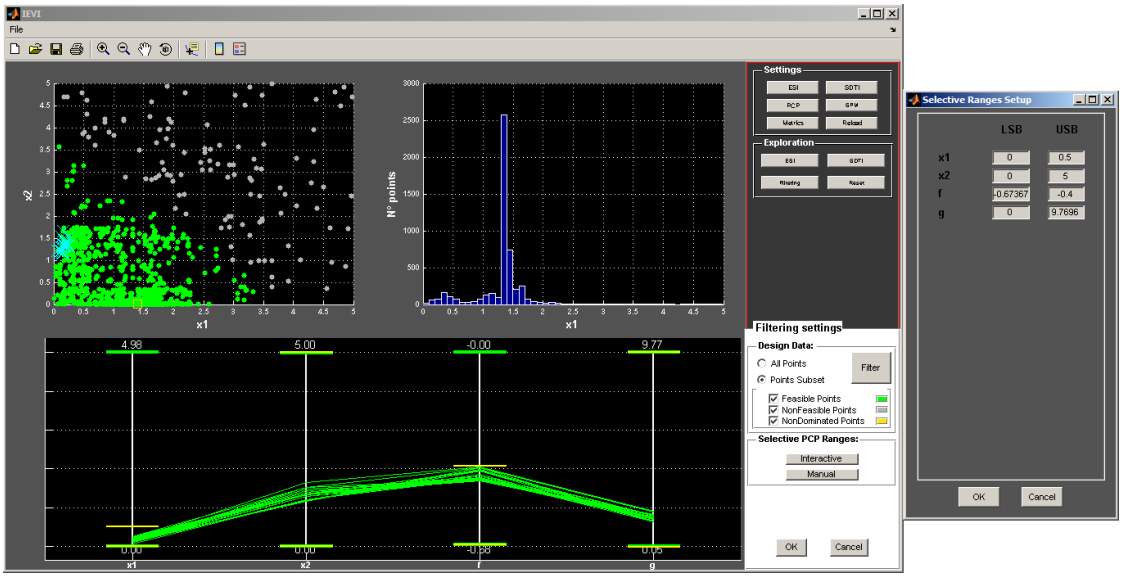

Figure 31. Visualisation of the points obtained through the manual *Selective PCP Ranges* function for *Filtering*. In this case, the solutions within the ranges x_1=[0,0.5] and f=[-0.67334,- 0.4] are highlighted in the *ESI* through cyan x-markers.

As an alternative multidimensional visualisation technique, the *SPM* is well suited for discovering or checking correlations among the data, or comparing local relationships between couples of variables, constraints and objectives (Figure 32). In this case, the *Filtering* function remains applicable, both by portraying particular sets of solutions (feasible, infeasible or optimal) and by specifying desirable ranges of values for the parameters displayed in the bivariate graphs matrix. Additionally, a numerical analysis of data can be carried out on the *SPM* in a more straightforward way on the strength of the Cartesian coordinates system. For high-dimensional datasets, however, it is necessary to analyse separately different sets of dimensions, because of the dimensional limitation of the *SPM*.

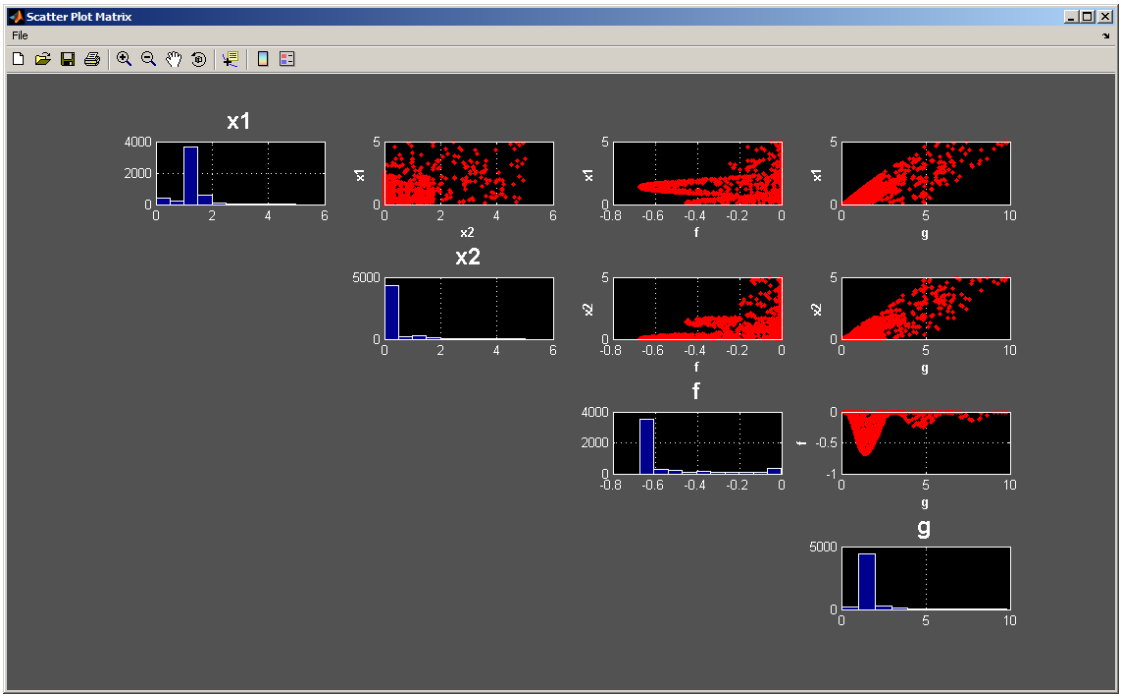

Figure 32. Scatter plot matrix (*SPM*).

Specific Design Tools Interface (SDTI)

This interface is expressly designated to conduct specific data analysis tasks in particular design domains. Therefore, the definition of the interface architecture has to be adequately defined depending on the *discipline-dependent technique(s)* to be used, along with its interaction with the other interfaces. Furthermore, a trade-off between the benefits of its integration and the corresponding complexity added to the system needs to be made, considering, for instance, the satisfaction of the rules of *diversity*, *complementarity*, *decomposition* and *parsimony* given by Baldonado et al. [10].

It has been previously outlined, as an example, the integration of carpet plots within an aircraft design optimisation framework, pointing out what are the advantages in assessing the satisfaction of performance requirements through such traditional aircraft sizing tool (Figure 33). An alternative data representation on the *SDTI* can be found in Guenov et al. [44], where multiple data views are shown conjointly for the visualisation of the Pareto set, in particular, geometry and constraint activation.

In general, the *SDTI* layout is dictated by the design context under study and the adopted visualisation strategies. For example, mention can be made of the employment of surrogate-model based visualization for design steering, as proposed by Yang et al. [123] for crashworthiness optimisation. The use of metamodel-driven visualisation for graphical design and optimisation is gaining considerable attention for overcoming many technological limitations associated with complex graphical design environments. Nevertheless, it is important to note that such a strategy represents a compromise between having a fast graphical design environment and the loss of accuracy due to the use of metamodels [68].

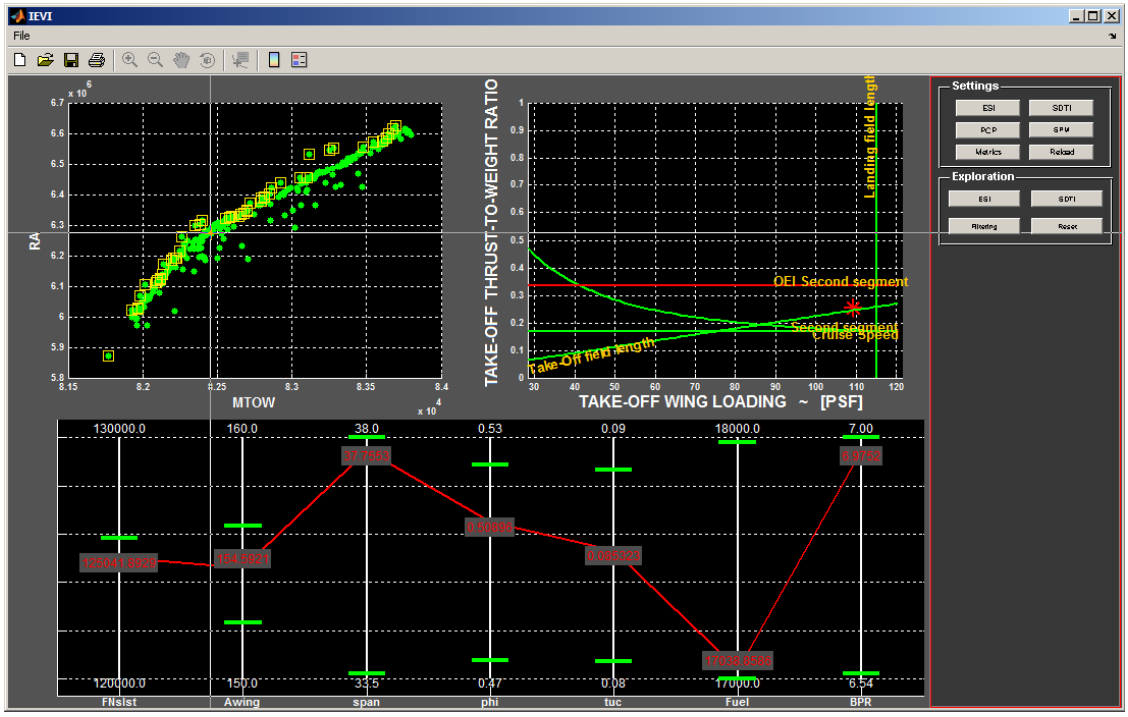

Figure 33. Visualisation of solutions for a conceptual aircraft design optimisation. The sets of feasible, non-feasible and non-dominated points are depicted in the *ESI* considering the same graphical notation of Figure 30. In the same interface, it is shown how any solution of interest can be interactively selected, updating in real time the two other interfaces. The designer is thus allowed to assess the satisfaction of performance and to conduct a numerical analysis of the selected point on the *SDTI* and *MDVI* respectively.

In the case of generic optimisation problems that do not require the use of any *discipline-dependent technique*, the *SDTI* can be used both to visualise the distribution histogram of any design parameter, or as an extension of the *ESI*. An example of the first option is portrayed in Figure 29 and Figure 31 with the distribution of the objective f and x_1; whereas the latter option is considered in Figure 34.

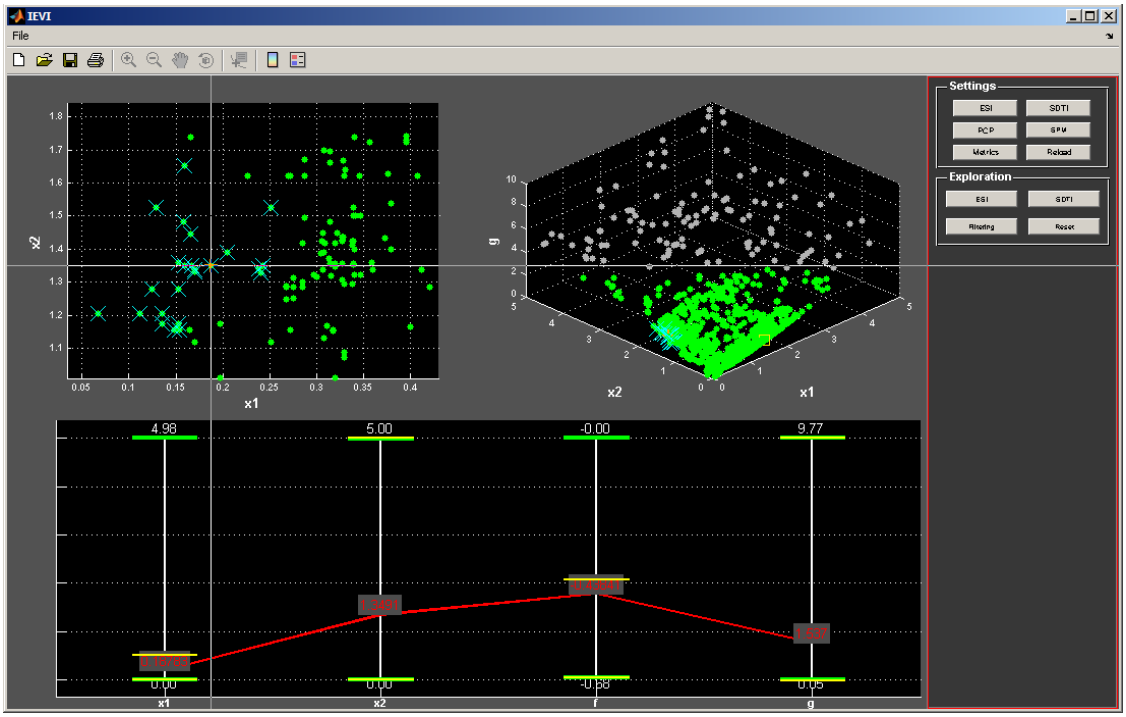

Figure 34. An example of an alternative use of the *SDTI* for a generic optimisation problem, offering a three-dimensional plot of the filtered data depicted in Figure 31. It is also shown how the interactive selection of points can be facilitated by zooming-in on the filtered solutions, as displayed in the *ESI*.

4.3.3. Operation of the Visualisation Interfaces

The exploration and analysis of design solutions has to be carried out by employing simultaneously the visualisation interfaces described above. Depending on the particular optimisation problem under study and the data analysis tasks to be conducted, Table 5 supports the selection of the most appropriate visualisation methods to employ.

The following generic analysis guidelines are provided:

Optimal Solutions Study

The evaluation of the design solutions from an objective space perspective is conducted in an intuitive manner:

- The user can choose the graphical interface to interact with amongst *ESI*, *MDVI* and *SDTI*, selecting interactively the points to be analysed. Diverse perspectives on the design(s) under consideration are provided via a simultaneous update of the visualisation on the remaining interfaces. For example, Figure 35 shows the comparison of designs that belong to three different clusters obtained by means of *Filtering*.

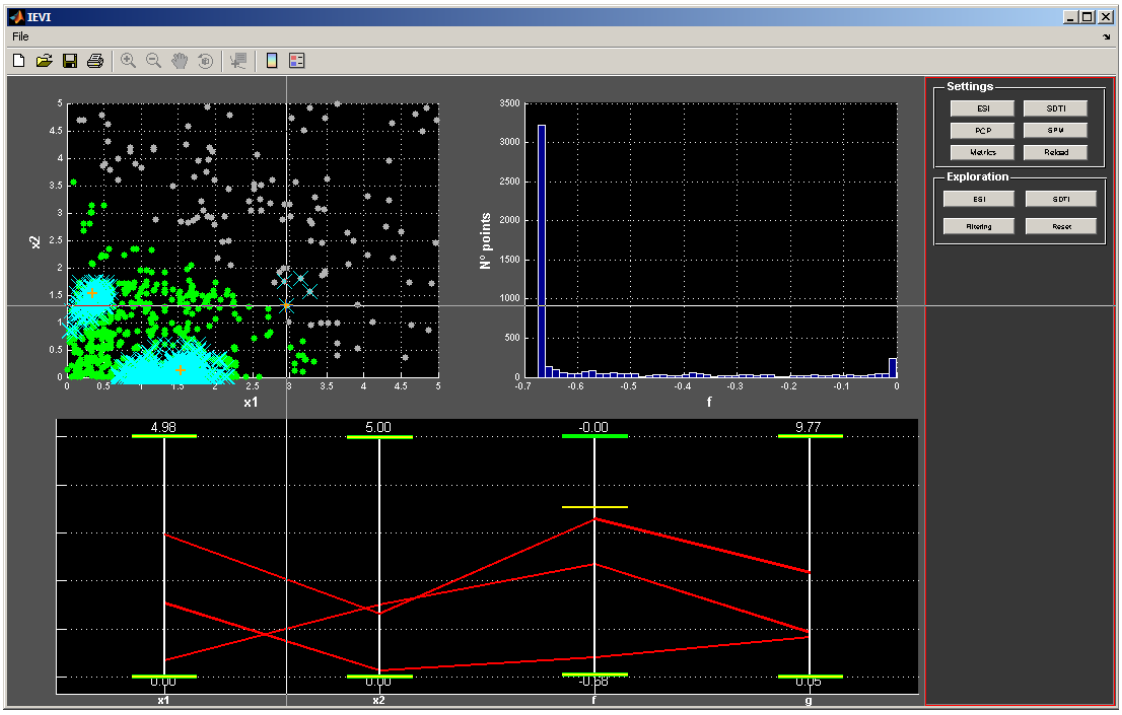

Figure 35. Comparison of three solutions interactively selected on the *ESI* from the clusters of points for which the objective function f is within the range [-0.67367,- 0.2].

- A trade-off analysis of optimal solutions can be carried out on the basis of further information in addition to the optimisation criteria, such as desirable ranges of the variables, potential figures of merit adopted in the *SDTI*, or a tighter satisfaction of constraints as shown in Figure 36.

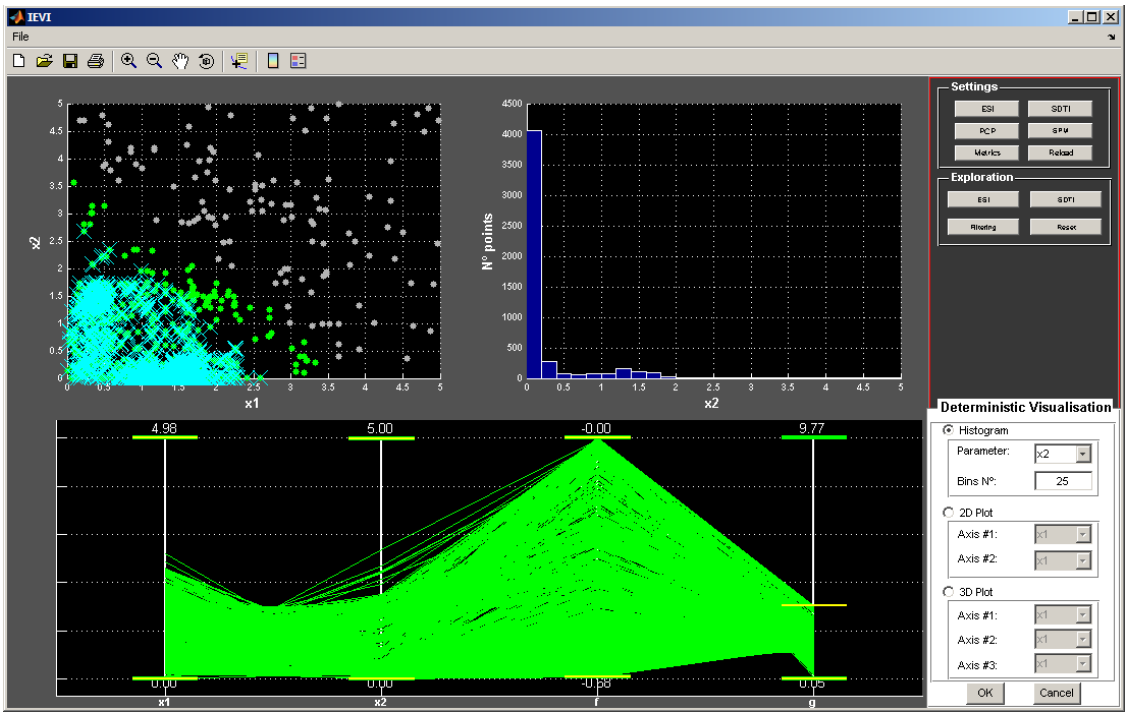

Figure 36. Visualisation of the solutions that meet a tighter constraint $g(\mathbf{x}) \leq 3$ by using the *Selective PCP Ranges Filtering* function.

- From the analysis of the infeasible points sub-sets, the designer is enabled to express precise violation thresholds for each constraint with the purpose of identifying semi-infeasible optimal points that may considerably improve one or more objectives (Figure 37). Such a procedure provides a manual alternative to the local relaxation methodology presented in Section 3.3.

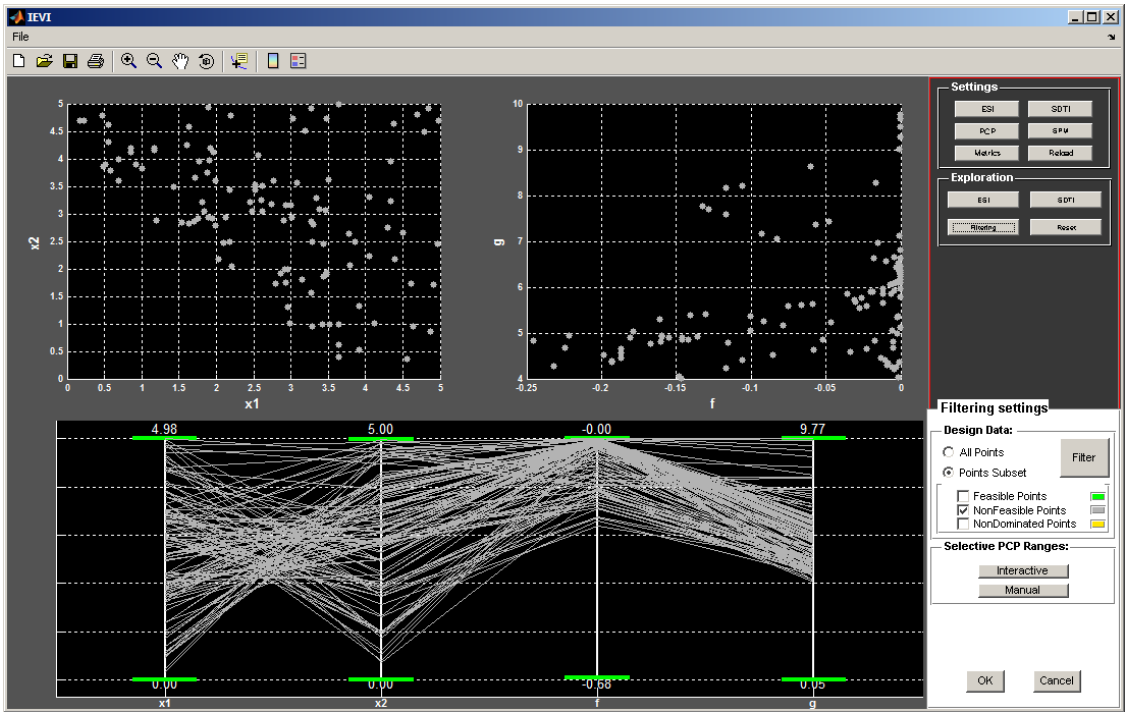

Figure 37. Study of the non-feasible set of points. For this problem, from the analysis of the *PCP*, it is evident that no-improvement on the objective function f can be achieved via a relaxation of the constraint g.

Constraint Study

A constraint behaviour analysis is required to enhance the designer's insight into the optimisation outcome. This can be achieved in two different ways:

- The user can check in the *MDVI* the satisfaction of one or more constraints for any design point $\bar{\mathbf{x}}$ by interactively selecting it in the *ESI* (Figure 33). Besides, the effect of each variable on each constraint can be conveyed both from interactively plotting multiple points in the neighbourhood of $\bar{\mathbf{x}}$ in the *ESI* (Figure 35), or from the analysis of data in the *SPM* (Figure 32).

- The decision-maker can select a constraint in the PCP in order to visualise all the solutions for which it is active in the *ESI* (and *SDTI* if applicable), as shown in Figure 38. Additional analysis criteria can be taken into account by means of

Filtering. All active and inactive constraints, for instance, can be graphically differentiated in the *ESI* by different colours and markers.

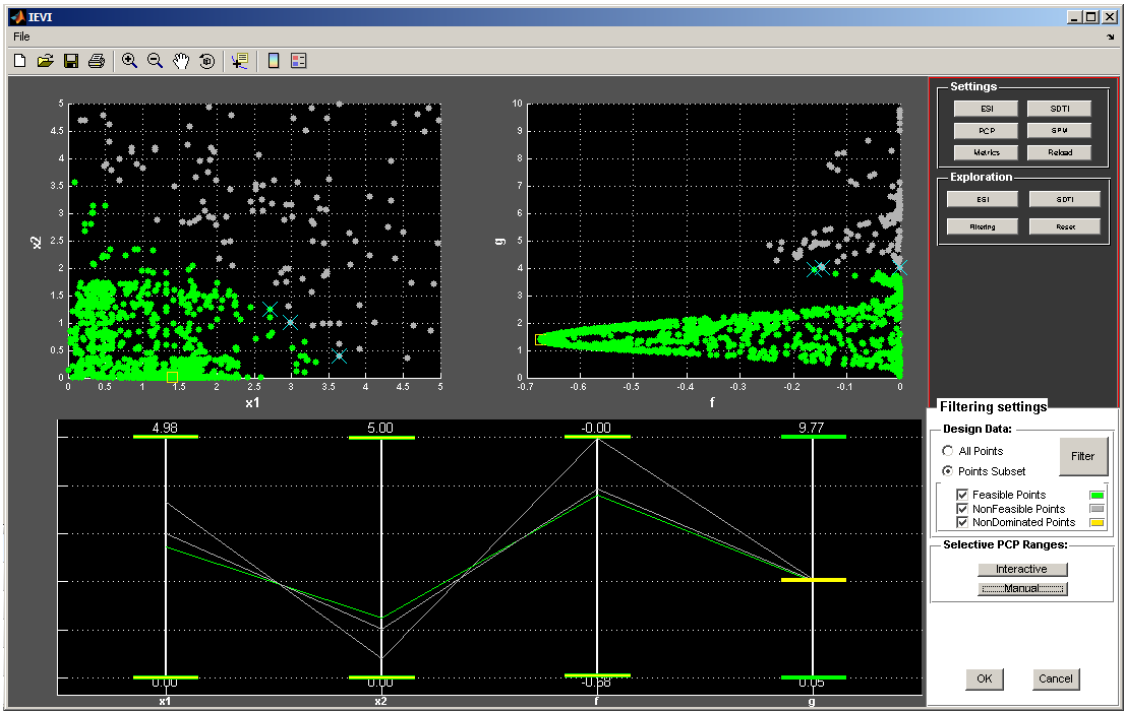

Figure 38. Identification of the design points for which the constraint *g* is active.

Both approaches allow the designer to gain a better understanding of the design, objective and constraint spaces. According to the information the user is interested in, it may be essential to discern:

- What solutions are characterized by the activation of one or more particular constraints.

- What are the active constraints that characterize each *optimal family* of solutions.

- What are the over-restrictive constraints that determine a reduced or empty set of feasible points.

- What constraints have an influence on a specific area of the design space or of the Pareto frontier.

- What variables and what range of values are determinant for the activation of each constraint.

4.3.4. Robust Optimisation Data Visualisation

This section outlines the proposed extension of the above described visualisation methodology for conducting an exploration and analysis of multi-objective robust design optimisation (RDO) solutions.

The constrained robust optimisation strategy taken into consideration in this work is based on a probabilistic uncertainty propagation approach, formally stating the uncertainty associated with the design process and parameters in terms of expectation and variance [39][85]. Problem complexity and dimensionality is therefore considerably increased by introducing additional design information, with a significant impact on the evaluation and understanding of results. In RDO, besides the search of optimal points in terms of performance, the identification of design solutions that are minimally sensitive to random fluctuations of the design variables comes to be a further fundamental design criterion. As a consequence, a suitable extension of the proposed visualisation methodology is required to allow handling higher dimensional datasets and trading-off additional design metrics.

The proposed robust visualisation enables the designer to steer the exploration of design alternatives by expressing specific analysis criteria both from a performance and from a robustness perspective. Relevant data can be first extracted by means of *Filtering* by defining desirable design attributes on the *PCP*. This allows to extend the strategy proposed by Rangavajhala et al. [90] by enabling the decision-maker to reveal the design sub-spaces that correspond to different design preferences in terms both of mean and variance of objectives and constraints. Additionally, such a scheme proves to be efficient also when single response functions are employed to handle the potentially conflicting

interaction between performance and robustness of objectives and constraints, instead of optimising their expectation and minimising, at the same time, their variance [80].

Once the design solutions of interest have been filtered on the *PCP*, the two other graphical interfaces are simultaneously updated. In a robust context, the *ESI* is intended to provide a single design perspective of two objectives/constraints among mean, variability and conjoint response (the last is applicable in case of single response functions only). A comprehensive robust viewpoint of data is instead given in the *SDTI* through the robust visualisation scheme suggested by Padulo [84], where, for each design point in the mean space of any pair of objectives/constraints, robustness is represented via ellipses, whose horizontal and vertical semi-axis are given by the corresponding standard deviations (Figure 39).

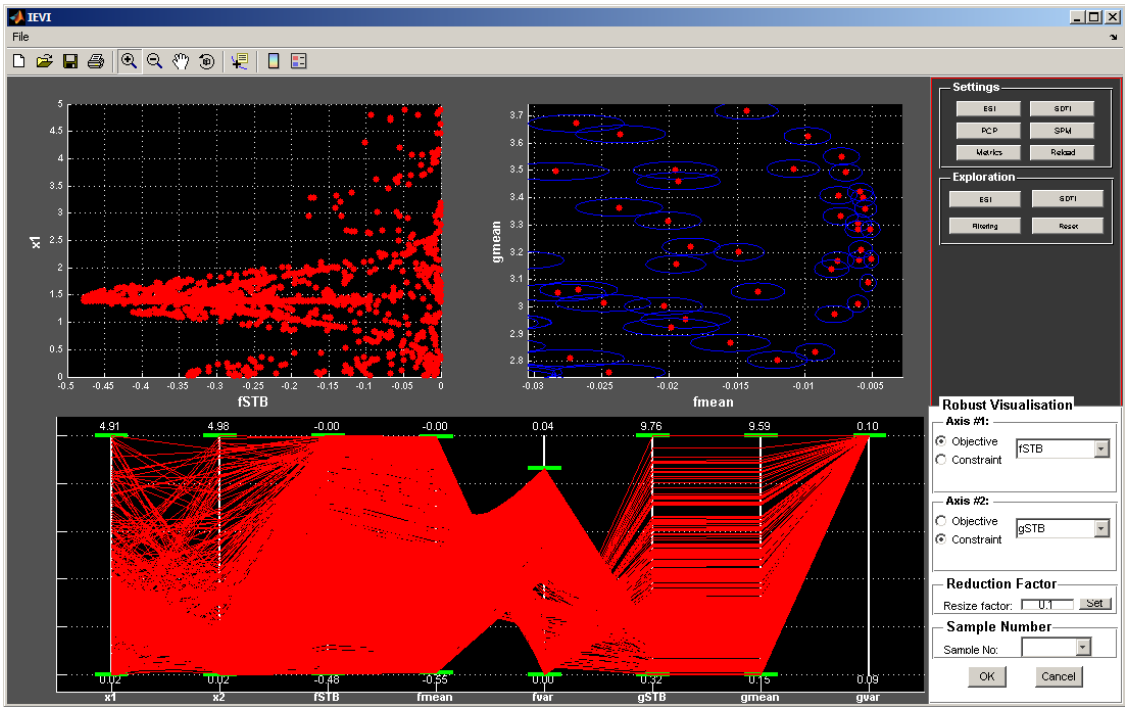

Figure 39. Shown in the *SDTI* is the adopted robustness visualisation in the mean space of objectives/constraints for a RDO problem [43].

4.4. Summary and Conclusions

Presented in this chapter is the second of the design exploration methodologies proposed in the thesis, with the aim of supporting the designer in effectively analysing and comparing large number of design concepts. The selection of the best solutions is enabled through a thorough exploration of all the computed alternatives and a trade-off analysis between multiple design criteria.

The foundations of the proposed novel methodology are established in Section 4.2, after outlining the standard visualisation requirements to be fulfilled in order to effectively convey the results of optimisation studies to the designer. Sub-section 4.3.1 describes the identified suitable visualisation techniques to achieve the sought aim, along with the criteria for their selection depending on the analysis tasks to be carried out. The integration of such techniques and their operation are presented in sub-sections 4.3.2 and 4.3.3. The extension of the methodology for robust design optimisation (RDO) is described in sub-section 4.3.4.

A visual exploration interface prototype (the *Integrated Exploration and Visualisation Interface*, *IEVI*) has been developed by the author to demonstrate the capabilities of the present methodology. The proposed approach allows to combine *discipline-independent* and *discipline-dependent techniques* required in different design contexts. The resulting synergistic integration of different data perspectives enables the designer to address common analysis scenarios occurring in design optimisation, without the need to be an expert in numerical optimisation methods. An improved insight into the problem at hand can thus be gained both through an exhaustive exploration of design solutions and by assisting the development, debugging and understanding of the employed algorithms and models.

The application of the present methodology to a conceptual aircraft optimisation test case has been demonstrated to industrial partners and within the EU CRESCENDO project, receiving particular interest and a positive feedback. A practical demonstration of the proposed methodology capabilities within the same design framework is provided in Chapter 6.

Chapter 5

Exploration of Design Alternatives to Address Conceptual Design Changes

5.1. Introduction

The inherent iterative nature of design is widely acknowledged in the engineering community [30][18][42]. The repetition of tasks may be dictated by the availability of new information (e.g. changes in input), updates of shared assumptions or the identification of errors [17]. In this framework, iterations are generally triggered by the lack or uncertainty of specific design information [124][42] (which often is expressed with the concept of *bounded-rationality*) and can be subdivided into two categories: planned and unplanned iterations. The first are predictable, can be planned in advance and are required for verifying an initial estimate or guess, or for improving the satisfaction of design specifications [18]. In aircraft sizing, an example of planned iteration is the estimation of the design take-off gross weight as a function of the fuel and

empty weights, which are initially unknown and both dependent on the total aircraft weight [91].

Unplanned iterations, conversely, occur when unexpected design revisions need to be undertaken as a result of the incomplete satisfaction of the design specifications due to process inefficiencies and/or cognitive limitations. Common causes of unforeseen iterations can be attributed to unsuccessful execution of testing and integration activities, sudden change of customer needs and requirements [18], or the appearance of alternative highly attractive design solutions [89].

In general, design iterations can be categorised as occurring either between design stages or within a design stage [18]. Attention here is focused on the first case, when, as stated by Yassine and Braha [124], "*design iterations result in changes that must propagate through the design stages, requiring upstream rework*". In particular, those cases where the introduction of design changes deriving from unplanned iterations involves the conceptual design stage can be taken into consideration. In this context, there is a need to balance two conflicting design aspects. On the one hand the required change(s) has (have) to be accommodated. On the other hand, this has to be achieved without radically changing the whole design, so that what has already been developed is still functional and, consequently, costs and time scales can be contained.

Work so far has been concentrated on modelling the extent and impact of a design change via connectivity models of the product [41][20], as well as through the identification and visualisation of change propagation paths [29].

Presented in this chapter is a novel methodology to support the introduction, within a conceptual design framework, of changes deriving from unplanned design iterations. The proposed approach is complementary to previous research in that it combines methods from design optimisation to conduct an exploration of design points that represent the best trade-offs for change accommodation with minimum disruption to the product configuration. Available prior computational analysis information is retrieved to drive an exploration process across the design space by means of surrogate models and the incorporation of key concepts from goal attainment method[36][72][19] and Bayesian global optimisation methods [56][55][98][100][102].

The background and problem definition along with the assumptions on which the methodology is based are given in Section 5.2. An overview of the proposed strategy is given in Section 5.3 for a generic MOO problem, followed by an individual description of the three phases in which it is articulated. The application of the methodology to the analytical function considered in sub-section 3.2.7 is demonstrated in Section 5.4. Finally, a novel method for the computation of objective and constraint isocontours is proposed in Section 5.5 to address design change problems through the evaluation of design points that keep invariant desirable design performance.

5.2. Problem Definition and Assumptions

This section is aimed at defining in detail the context for which the proposed methodology has been developed.

With respect to the background, a number of potential scenarios from real industrial cases can be taken into consideration. As far as the design has not evolved into much detail and the need to implement a change comes to light in the early design stages, the simplest solution is to run a further optimisation process taking into consideration a new problem formulation representative of the arisen issue. However, such a procedure can turn out to be excessively demanding and costly, especially if the whole process has been disrupted until the change cycle is accomplished. Alternatively, the approach proposed here for addressing conceptual design change problems relies on the exploitation of all the information available from prior collected datasets. It is desirable to somehow reuse all the function evaluations previously performed in order to gain insight into the new problem at hand, avoiding starting everything again from scratch. The designer's priority, de facto, is to identify the best design alternatives that on the one hand still satisfy the original design criteria considered, but on the other hand take also into account the additional requirements imposed by the arisen change.

A need for introducing a conceptual design change might come to light at different phases of the product development. Nonetheless, a common goal is that of introducing

the required change by simultaneously minimising change propagation on the remaining design parameters.
The following generic change-scenarios can be outlined:

- A detailed analysis subsequently carried out on a design system or component may reveal the need of modifying a design aspect. Example: a flight dynamics study conducted during the preliminary stage of an aircraft design might indicate the necessity of increasing ailerons area for stability reasons[10].

- The need for a manufacturing-driven change is recognised during a preliminary determination of manufacturing issues, such as material-of-choice, process-of-choice and production-tooling. In the light of the cost of changes associated with an engineering change order (ECO) with time (Figure 11), Folkestad and Johnson [33] emphasize the benefits from identifying and undertaking manufacturing design changes during the early design stages in order to achieve sustainable reductions in both time and cost.

- A variant of an existing product or an additional member of a design family is sought. This may involve the introduction of not a single but multiple modifications on a base design-layout, depending on the new design specifications[11].

---

[10] In their description of how aircraft are designed in a large organization, Bond and Ricci (1992) [16] observe that the main design decisions are refinement operations on the design, which are *negotiated* by the specialists among themselves. They give also an illustration of a typical scenario of model refinement, describing and providing some examples of the interactions among specialists to improve a design at preliminary stage by incorporating a series of changes.

[11] For example, in the attempt of improving the Spitfire wing aerodynamics for one of its numerous variants, the wing Specification No.470 was issued on 30 November 1942 [79]:
.."A new wing has been designed for the Spitfire with the following objects (1) To raise as much as possible the critical speed at which drag increases, due to compressibility, become serious. (2) To obtain a rate of roll faster than any existing fighter. (3) To reduce wing profile drag and thereby improve performance.

Further details about the potential causes that can trigger a conceptual design change problem can be found in Appendix D, where a number of real-life examples are provided, describing both the change(s) involved and the design requirements to consider.
It is important to emphasize that our efforts are focused on tackling the design change problems which affect the conceptual design stage, and represent a complementary strategy to the methods described in Section 2.4.

The assumptions on which the present methodology is based are:

- There is a need to accommodate a change on a specific design solution, obtained via an optimisation procedure carried out in the conceptual design framework, and thereafter further developed.

- The function observations computed in the above-mentioned optimisation have been stored in an allocated database.

- The new set of design solutions to be explored is assumed to be contained in the design space region where prior function evaluations were computed.

- The variables, objectives and constraints of interest regarding the problem at hand are considered to be included in the set of parameters taken into account in the stored prior evaluations. General criteria for their setup are:

The wing area has been reduced to 210 sq ft (Spiteful) and a thickness chord ratio of 13% has been used over the inner portion of the wing where the equipment is stored. Outboard the wing tapers to 8% thickness/chord at the tip…"
Considering the multiple examples of commercial passenger aircraft families, mention can be made of the A350-800 and A350-1000 designs, which, among several changes, have a fuselage shortened by 10 frames and a wing around 4% bigger with respect to the baseline A350-900, respectively [60].

- A correction of the variables bounds or a reduction of the original design space dimensionality can be carried out by identifying and removing non-significant inputs via a global sensitivity analysis [71].

- Specific constraints or objectives can not be further considered, depending on their design priority or on their local satisfaction-degree/value.

5.3. Proposed Method

The present methodology is intended to exploit the design knowledge gained via prior function evaluations with the aim of introducing a design change defined as in Section 5.2. There are two objectives:

- To explore and analyse different design alternatives which, on the one hand, are feasible according to the conceptual design problem formulation updated on the basis of the required change, and, on the other hand, minimise change propagation.

- To minimise time and computational efforts in order to optimise the whole design change process.

The achievement of the above objectives is based on a strategy that integrates a goal attainment reformulation of the problem [36] with an extension of the available criteria for dealing with nonlinear inequality constraints in Bayesian global optimisation methods [55]. The whole approach is articulated into three phases, which are described in detail in the following sub-sections. Presented below and depicted in Figure 40 is a brief summary.

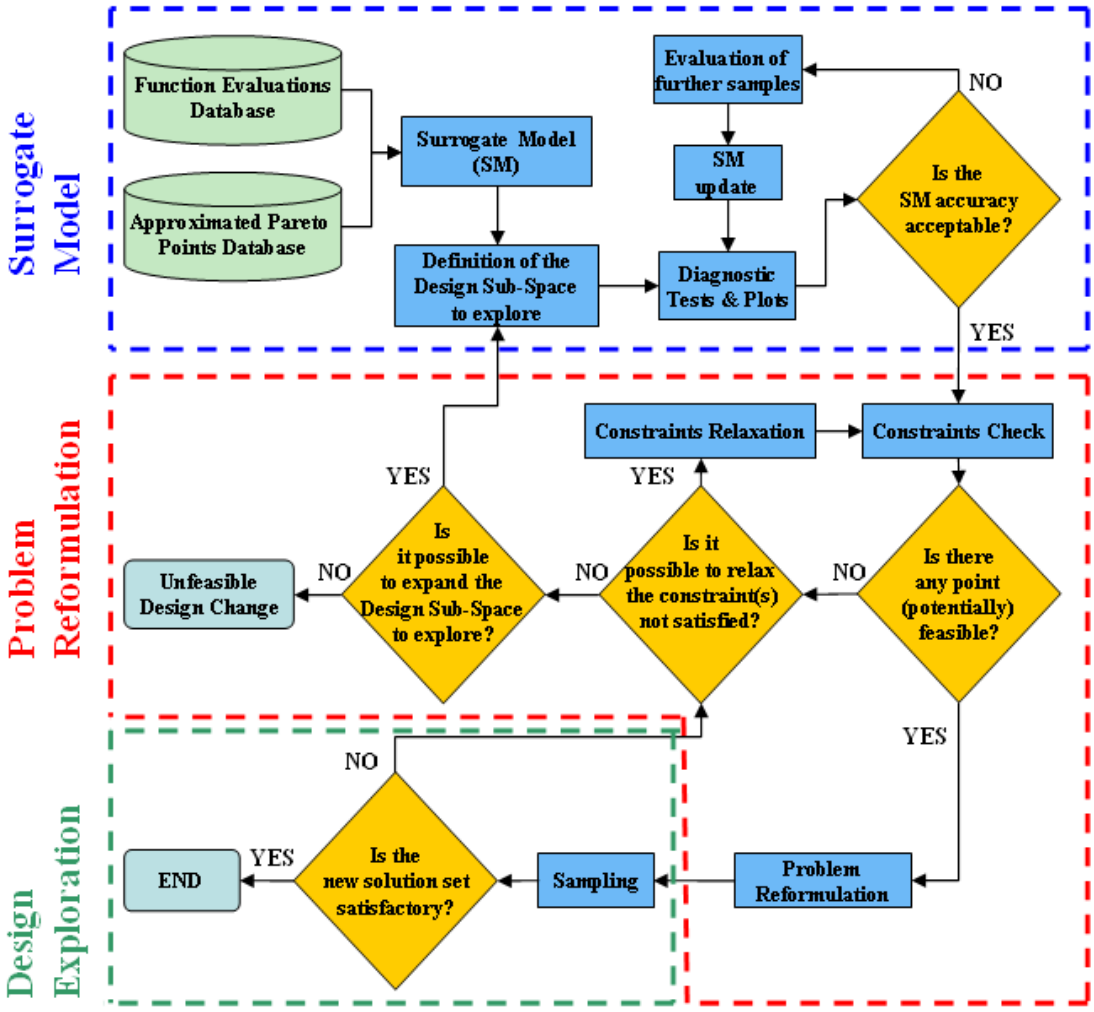

Figure 40. Summary flowchart of the proposed exploration methodology to address conceptual design changes.

In the *Surrogate Model* phase, described in Section 5.3.1, the stochastic process model outlined in Section 2.5.1 is employed to fit the set of function evaluations that is assumed to be available from previous computations. Predictions along with their associated error estimate can thus be obtained at any point, both for the objective and constraint functions, providing the designer with a global representation of the problem under study. It is important to notice at this stage, that the objective is not to build a model that is absolutely accurate, but instead summarises how the real function typically behaves. This provides one of the fundamentals of global optimisation algorithms to balance the global and local exploration of the design space, which are driven by the prediction uncertainty

(measured by the prediction standard error) and the predicted optimum (the point where the surrogate model is minimised/maximised), respectively. Regarding the set of initial evaluations required, it seems that in the literature there is not a general agreement about its size, especially when no information is available about the problem at hand. A "rule-of-thumb" is to consider a number of initial points that is roughly ten times the problem dimensionality [56]. Additional considerations and recommendations can be found in Sobester et al. [102].

The *Problem Reformulation* phase is explained in Section 5.3.2, and involves an interaction with the designer. The general behaviour of the objective and constraint functions gathered through the predictor models facilitates the identification of the most promising design sub-spaces where different trade-offs between introducing the requested change and containing change propagation can be found. On the strength of such information, the designer can therefore formally reformulate the problem as a single-objective optimisation in order to allow a local exploration of design solutions in specific areas of the design space. This is achieved by adopting the goal attainment method [36], which enables the designer to conduct an *a priori* articulation of preferences with respect to the achievement of each design parameter value. Such an approach allows to trade-off two central needs in design change problems: incorporation of the requested change and minimisation of change propagation. From a computational point of view, an additional advantage associated to the goal attainment method is that the deployment of a scalarizing optimisation approach makes applicable a wide range of sampling criteria for single-objective optimisation available in the literature [55].

Finally, Section 5.3.3 describes the basic sampling criterion that steers the evaluation process of additional design points throughout the *Design Exploration* phase with the intent of identifying the optimal solutions for the reformulated problem. In practice, the proposed strategy provides a means to conduct a double trade-off process. Firstly, the use of surrogate models and key concepts from Bayesian global optimisation allow to balance the global and local explorations above-mentioned. Secondly, the achievement of contrasting design goals can be balanced according to the preferences articulated by the designer during the problem reformulation via the goal attainment method. Particular attention here is given to assessing constraint satisfaction across the design sub-space to

be explored, so that the further evaluations can take place in feasible areas or in the vicinity of the constraint contours.

The fundamental concept of the present methodology is portrayed in Figure 41 considering a simple case where the conceptual change to be introduced can be formulated as a correction on the lower bound of the problem variable $x \in [0,7]$.

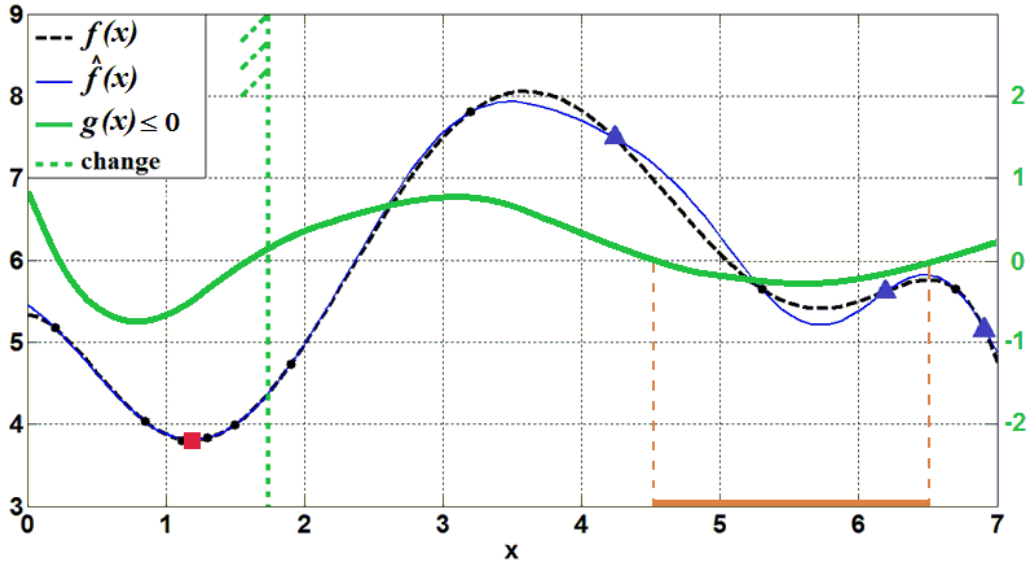

Figure 41. In this elementary example, the hypothetical original formulation of a one-dimensional problem consists of a single objective $f(x)$ and a single constraint $g(x) \le 0$. The design change to accommodate is assumed to be formulated as a correction on the lower bound of x, which renders unfeasible the optimal point previously found (red square). The surrogate model $\hat{f}(x)$ to be used will fit all the evaluations earlier computed (black points), allowing to approximate the system elsewhere along with a prediction error estimation. Once the predictor accuracy is ensured, if necessary, via additional observations (blue triangles), the new feasible region(s) where to focus design exploration can hence be identified (in orange).

5.3.1. Surrogate Model Phase

For the proposed methodology, in the first place the stochastic process model described in Section 2.5.1 is fit to a set of observations previously collected for each objective and constraint function. Within this framework, approximated function observations also can be taken into account. Jones et al. [56] describe some approaches to properly combine

low- and high-fidelity models. Such a strategy, generally referred to as multi-fidelity optimisation, turns out to be particularly effective in reducing the burden of heavy optimisation procedures without incurring a relevant model accuracy loss. Forrester et al. [34] demonstrate an optimisation strategy where a Bayesian model update criterion is coupled with an extension of the geostatistical method of *co-kriging*. Balabanov and Venter [9] describe how, under appropriate assumptions, gradient-based optimisation costs can be reduced by performing finite difference calculations using low-fidelity analysis, whereas the search points are evaluated via high-fidelity models.

The accuracy of the statistical model is ensured afterwards within the design sub-space to be explored. The definition of such region depends on the problem at hand. Generally, a sub-space in the vicinity of the design point to modify can be examined in a first instance, with the objective of minimising change propagation. The specific range to consider for each variable has to be formulated on the basis of the first rough information provided by the models, design criteria and new requirements, as well as designer's experience and intuition. In the event results turn out to be not satisfactory, the initial design sub-space can be subsequently modified.

Under the assumption that the model is sufficiently flexible to be improved, its validation is articulated into two steps and further function evaluations may be required. The first validation phase is intended to ensure that the maximum value of the mean square error (MSE) of each model is below a pre-defined threshold ξ. If not, additional function evaluations are computed by adopting, in a first instance, an infill sampling criterion based on the MSE minimisation. The point where the prediction error is maximum is successively evaluated until the prediction standard error is inferior to ξ within the established search region.

Subsequently, the validation of the model is assessed on the basis of the diagnostic test plot *actual function values versus cross-validated predictions* considered in the *cross-validation procedure* proposed by Jones et al. [56]. If the above test is not satisfactory, a further random point is evaluated in the neighbourhood of any point that represents an outlier. Alternatively, a satisfactory model accuracy can sometimes be obtained by applying a suitable transformation $\psi(y)$ to the generic dependent variable y (e.g., log or inverse) [56], although generally $\psi(y)$ is not known *a priori*.

Once the surrogate models of interest have been validated, they provide a global summary of how the objective and constraint functions behave across the specified design sub-space. A global exploration of design alternatives can thus be driven by a suitable sampling criterion, taking into account the design requirements and preferences expressed via an adequate reformulation of the problem as described in the next sub-section.

5.3.2. Problem Reformulation Phase

The exploration of alternative design solutions to accommodate the design change of interest requires a proper reformulation of the problem by balancing two central needs. On the one hand, a new design point that is feasible with respect to the requested change has to be identified. On the other hand, however, a minimisation of change propagation is sought. In practice, what is required is a trade-off between the initial design requirements and all the re-design implications that may derive from modifying the design layout selected in the conceptual phase and further developed in the subsequent design phases. Moreover, a reduction of the time and computational efforts throughout the exploration process is also of interest.

To achieve this, the suggested approach is based on a reformulation of the problem by adopting the goal attainment method proposed by Gembicki [36]. The design change problem is therefore addressed via a method with an *a priori* articulation of preferences, namely the goals $\boldsymbol{F}^* = \{f_1^*, f_2^*, ..., f_J^*, g_1^*, ..., g_I^*, x_1^*, ..., x_n^*\}$ associated with the new set of objective functions $\mathbf{F}(\mathbf{x}) = \{f_1(\mathbf{x}), f_2(\mathbf{x}), ..., f_J(\mathbf{x}), g_1(\mathbf{x}), ..., g_I(\mathbf{x}), x_1, ..., x_n\}$ that, in the generic case, is given by the J original objective functions, I inequality constraints and n design variables in Equation (1). In doing so, the design change at hand has to be formulated either as one or more goals in $\boldsymbol{F}^*$, or through a correction of the variables bounds. Formally, Problem (1) is reformulated as follows[12]:

[12] This is a comprehensive formulation of the problem that, nevertheless, can be simplified. For example, the possibility of not considering a number of variables might be evident if, from an analysis of the surrogate models, their influence results to be locally negligible. Similarly, the reformulation of the

$$\begin{aligned} & \min_{\mathbf{x}\in S} \gamma \\ \text{subject to :} \quad & F_p(\mathbf{x}) - w_p\gamma \le F_p^*, \quad p = 1,...,J+I+n, \\ \text{with :} \quad & \mathbf{x_{lb}} \le \mathbf{x} \le \mathbf{x_{ub}} \end{aligned} \tag{49}$$

where $\mathbf{w} \in \Re^p$ s.t. $w_p \ge 0, \sum_{i=1}^{p} w_i = 1,$ and $\gamma \in \Re$ is the unrestricted scalar variable to minimise, defined as the maximum over *p* of the expression [114]:

$$\frac{F_p(\mathbf{x}) - F_p^*}{w_p} \tag{50}$$

In the goal attainment method it is assumed that the values assigned to each goal can be established upon a basic understanding of the problem or the design specifications to consider [37]. In our case, the definition of the goals F_p^* has to reflect either the design change to accommodate or the design point to modify, which is intended to be retained as much as possible in the attempt to limit change propagation. The design goals not related to the change at hand are therefore dictated by the value of the objectives, constraints and variables of the original problem formulation (1) for the design point to modify. Alternatively, new goals F_p^* can be set on the basis of the information that can be gained from an analysis of the surrogate model so far obtained.

The decision-maker is enabled to control the relative degree of under- or over-achievement of the goals by means of the vector of weighting coefficients $\boldsymbol{w}=\{w_1,\ldots,w_p\}$.

---

problem can be simplified by discarding the objectives with lower priority or the constraints that locally appear to be largely satisfied. In this context, the visualisation methodology described in Chapter 4 comes to be particularly useful for the reformulation of multivariate and complex optimisation problems. The user is, in fact, allowed to conduct an exhaustive analysis of the surrogate models by plotting both the collected observations and the prediction points of interest. Moreover, the identification of the feasible design space regions can be facilitated by means of *Filtering*.

In general, the relative magnitude of w_i compared to the other weights will determine the attainment grade of the *i-th* goal F_i^*. The smaller the weight is, the smaller the degree of under- or over-attainment of the corresponding goal will be.

The advantage of reformulating the problem by adopting the goal attainment method is that it provides the means to fulfil the two needs mentioned at the beginning of this sub-section. Additionally, the goal attainment method is not subject to convexity limitations [72] and can be solved via standard optimisation procedures. Furthermore, it provides a scalarizing optimisation approach (also referred to as *methods with a priori articulation of preferences*) that makes applicable a wide range of sampling criteria for single-objective optimisation available in the literature [78][56][55][99][100][102]. A review of three alternative scalarizing methods that can be coupled with Bayesian global optimisation methods is given by Hawe and Sykulski [45].

By using different sets of weighting coefficients, alternative noninferior solutions can be obtained also for nonconvex problems [19]. This is illustrated geometrically for a two-objective minimisation problem in Figure 42, where $\boldsymbol{F}^*$ and $\boldsymbol{w}$ represent the vectors of the desired goals and the preference direction respectively.

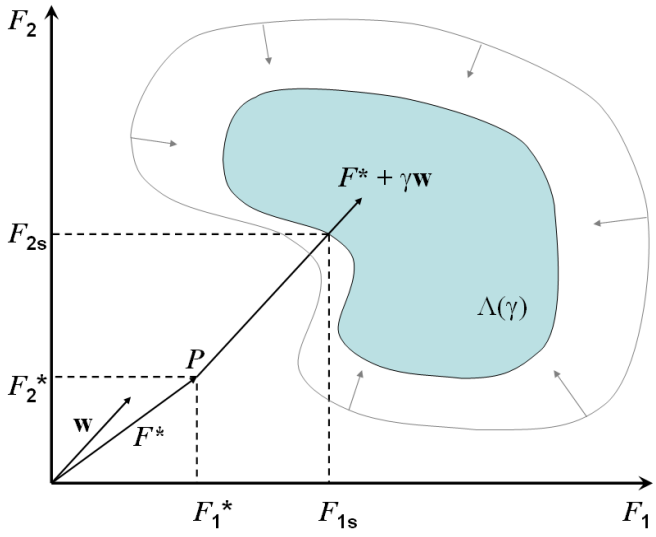

Figure 42. The goal attainment method with two generic objectives F_1 and F_2 [114][67].

The problem is equivalent to finding the closest point to the origin along the vector $\boldsymbol{F} = \boldsymbol{F}^* + \gamma \mathbf{w}$, which indicates the search direction from the goal point *P* to the feasible objective space $\Lambda(\gamma)$. Consequently, the optimal solution will be the first point $\boldsymbol{F}_s$ at which $\boldsymbol{F}$ intersects $\Lambda(\gamma)$. If the corresponding value of γ at the solution is null the desired goals have been achieved. In contrast, a negative value of γ indicates that the specified goals are attainable and an improved solution has been obtained (over-attainment in the goals); or a positive value of γ implies that the goals are unattainable (under-attainment in the goals) [67].

5.3.3. Design Exploration Phase

It is important to note that the variables bounds in Equation (49) do not necessarily need to be defined as in Problem (1) or to reflect merely a correction sought for one or more variables. They identify, in fact, the design space region that the decision-maker intends to explore in addressing a specific design change problem. In the proposed method, the evaluation process of further design points is driven across such region by an adequate sampling criterion that seeks to identify the optimal solutions for the reformulated Problem (49) by exploiting the statistical models obtained in the *Surrogate Model* phase. The integration of the models capability to make predictions with an estimate of the associated prediction error along with a suitable searching criterion provides a method to drive the exploration of optimal design alternatives. The evaluation of further samples is carried out on the strength of an extension of the criterion described in Section 2.5.2, introduced by Mockus et al. [78] and subsequently utilised by Jones and other researchers [98][100][102] as one of the fundamentals in developing Bayesian global optimisation methods.

It has been previously pointed out what are the main difficulties in constrained optimisation problems for performing further function evaluations via a sampling criterion that somehow acknowledges the satisfaction of constraints. The approach proposed here is an extension of the expected improvement criterion for a generic constrained single-objective optimisation problem with $g_i(x) \leq 0$, and can be formally stated as follows:

$$\mathrm{E}[\mathrm{I}(\mathbf{x})]_{\mathrm{c}} \equiv \begin{cases} (f_{\min} - \hat{y})\Phi\left(\dfrac{f_{\min} - \hat{y}}{s}\right) + s\phi\left(\dfrac{f_{\min} - \hat{y}}{s}\right) \\ \text{if } \; s > 0 \; \text{ and } \; \hat{g}_i - s_i \le 0, \quad \text{for all } \; i = 1, \ldots, I \\ \\ 0 \\ \text{if } \; s = 0 \; \text{ or if } \; \hat{g}_i - s_i > 0, \quad \text{for any } \; i = 1, \ldots, I \end{cases} \tag{51}$$

where s and s_i are the standard error associated with the objective prediction $\hat{y}$ and the *i-th* constraint prediction $\hat{g}_i$.

The suggested strategy, in practice, is equivalent to performing a local relaxation of each constraint g_i that is proportional to s_i. Consequently, the suggested expected improvement will be zero at the sampled points and where any of the locally relaxed constraints is not satisfied, otherwise it will be positive. This enables to assess the satisfaction of each constraint at any point of the design space not only on the strength of its predicted value (as for the WEIF proposed by Sóbester et al. [102]), but also by acknowledging the uncertainty associated with it. Moreover, the figure of merit in Equation (51) does not require the estimation of the constraints satisfaction probabilities as in the criterion presented in Schonlau [99] and Schonlau et al. [100]. Unlike the latter criterion, which may focus the sampling of additional points on the design space areas which are more likely feasible [98], the proposed sampling criterion allows the evaluation of promising points located in the vicinity of constraints boundaries as a result of their local relaxation. This constraints-handling concept is depicted in Figure 43 by considering a simple one-dimensional example, where the extension of the design space to be explored, resulting from the described constraint relaxation, is highlighted. Enabling the evaluation of all the points located close to the constraint contours offers a double advantage. Firstly, points that are predicted as infeasible, but in reality are feasible, are less likely to be overlooked because of an inaccurate approximation. This is, for instance, the case of the feasible points located in x = [4.25, 5.64]. Secondly, promising points that slightly violate one or more constraints can thus be evaluated and presented to the

designer, who may judge them as a valid alternative if a proper constraint relaxation is possible.

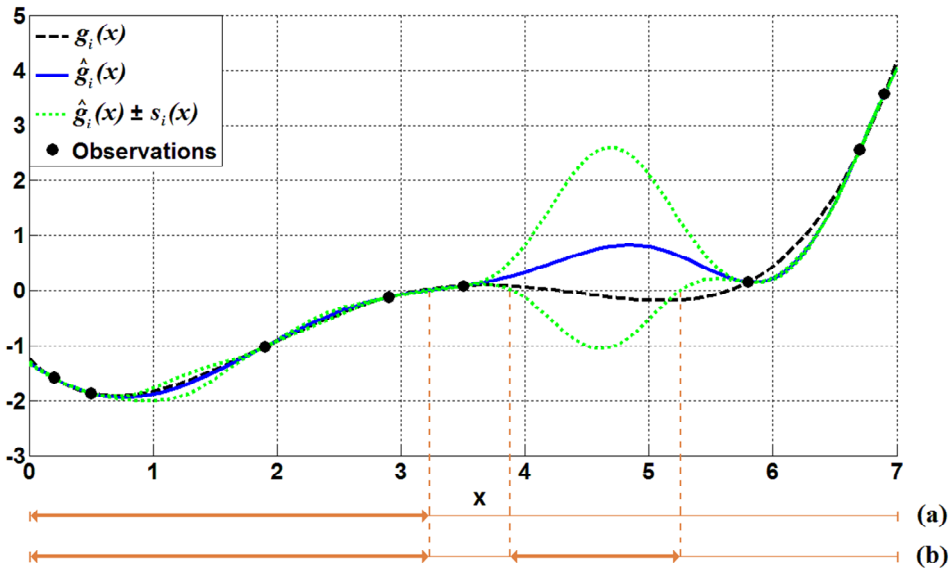

Figure 43. Relaxation concept for the proposed constraint-handling approach, comparing for a generic constraint $g_i(x) \leq 0$ the search regions corresponding to: (a) constraint satisfaction based only on the function prediction $\hat{g}_i(x)$; (b) constraint satisfaction based on the function prediction $\hat{g}_i(x)$ and its associated error $s_i(x)$.

Ultimately, a reliable stopping rule for the proposed optimisation procedure has to be chosen. A maximum number of function evaluations is expected to be specified on the basis of the second objective of the present methodology. Alternative or complementary criteria can be found in Section 2.5.3, depending on the problem at hand.

5.4. Analytical Example

The proposed method has been tested taking again into consideration the two-dimensional bump function [57] described in Section 3.2.7. It is assumed that a minor change is sought for the global minimum $\mathbf{x}^* = [1.3932, 0]$ for $x_{1,2} \in [0,5]$, which has been identified via a previous optimisation procedure, with $f(\mathbf{x}^*)$=-0.6737 and $g(\mathbf{x}^*)$=-6.6063.

The latter was conducted adopting the Matlab algorithm fmincon and considering eight different starting points, obtained via a Latin Hypercube sampling. In total, 54 distinct function evaluations were computed and stored in an allocated database. A filtering procedure was used to eliminate all the duplicated solutions, which are not allowed by the DACE toolbox [70] used in this work for the computation of surrogate models.

Firstly, in the *Surrogate Model* phase the adopted stochastic process model was fit to the stored set of function evaluations. The design sub-space to explore was set as $\mathbf{x}_{\mathbf{LB}} = [0,0]$, $\mathbf{x}_{\mathbf{UB}} = [4,4]$. The validation procedure of the model led to the evaluation of 13 additional points. A lower number of function evaluations is generally required as the examined sub-space is narrowed. Figure 44 shows the predictor model of the objective and constraint functions after being validated.

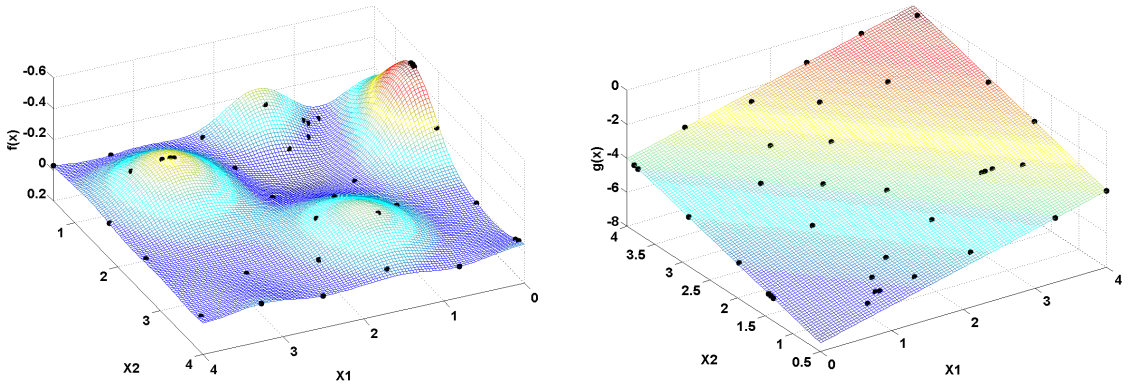

Figure 44. Surrogate models of $f(\mathbf{x})$ and $g(\mathbf{x})$.

The corresponding diagnostic tests *actual function values versus cross-validated predictions* based on the *cross-validation procedure* proposed by Jones et al. [56] are illustrated in Figure 45.

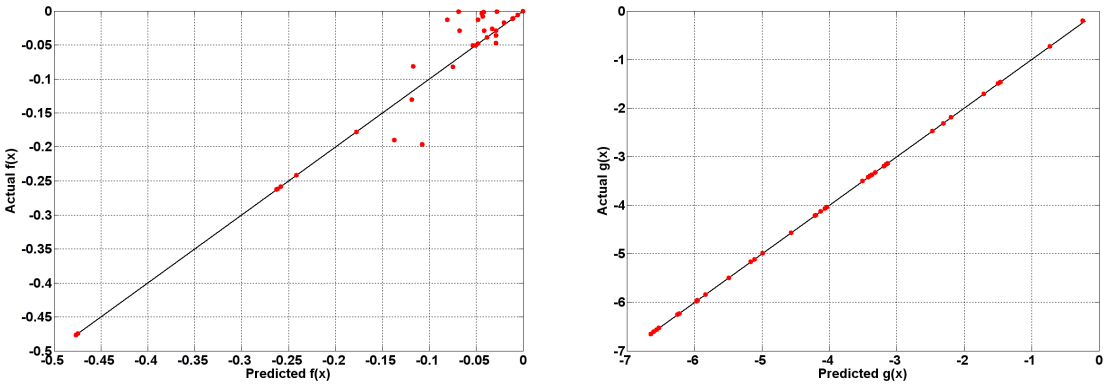

Figure 45. Diagnostic plots for the surrogate models of $f(\mathbf{x})$ and $g(\mathbf{x})$.

For explanatory purposes, regarding the *Problem Reformulation* phase let us consider the case in which the design change to introduce can be formally stated as a correction on the lower bound of the variable x_2, which is to be changed from 0 to 0.5. Other cases where the change is with respect to an objective or a constraint are shown in Chapter 6 by taking into account an industrial aircraft sizing test case. Problem (42) can be comprehensively reformulated as follows:

$$\begin{aligned}
&\text{Find} \quad \mathbf{x} \in S \quad \text{to} \quad \text{minimise} \quad \gamma, \\
&\text{subject to:} \quad F_1(\mathbf{x}) - w_1\gamma \le F_1^*, \\
&\qquad\qquad F_2(\mathbf{x}) - w_2\gamma \le F_2^*, \\
&\qquad\qquad F_3(\mathbf{x}) - w_3\gamma \le F_3^*, \\
&\qquad\qquad F_4(\mathbf{x}) - w_4\gamma \le F_4^*, \\
&\qquad\qquad \mathbf{x_{lb}} \le \mathbf{x} \le \mathbf{x_{ub}} \\
&\text{with:} \\
&\qquad\qquad \mathbf{x_{lb}} = [0, 0.5] \\
&\qquad\qquad \mathbf{x_{ub}} = [4, 4]
\end{aligned} \tag{52}$$

where the goals $\boldsymbol{F}^* = \{F_1^*, F_2^*, F_3^*, F_4^*\} = \{-0.6737,\ -6.6068,\ 1.3932,\ 0.5\}$ are the values of the objective, constraint and the variable x_1 at $\mathbf{x}^*$ along with the sought-for value of x_2, respectively.

Once the prediction models have been validated and the problem properly reformulated, alternative change solutions can be computed according to the design preferences

expressed by the designer via the weighting coefficients $\boldsymbol{w}=\{w_1,\ldots,w_4\}$. Assuming, in a first instance, that the decision-maker's interest is to minimise change propagation across all the design parameters, an equal weight has to be associated to each one of the goals, hence:

$$\boldsymbol{w}=\{0.25,0.25,0.25,0.25\} \tag{53}$$

The extended expected improvement function (51) at the beginning of the *Design Exploration* phase is portrayed in Figure 46 for the first six evaluations along with the corresponding observations collected. In addition to a maximum number of 50 iterations, an EI threshold of 1e-6 was also considered as a stopping criterion.

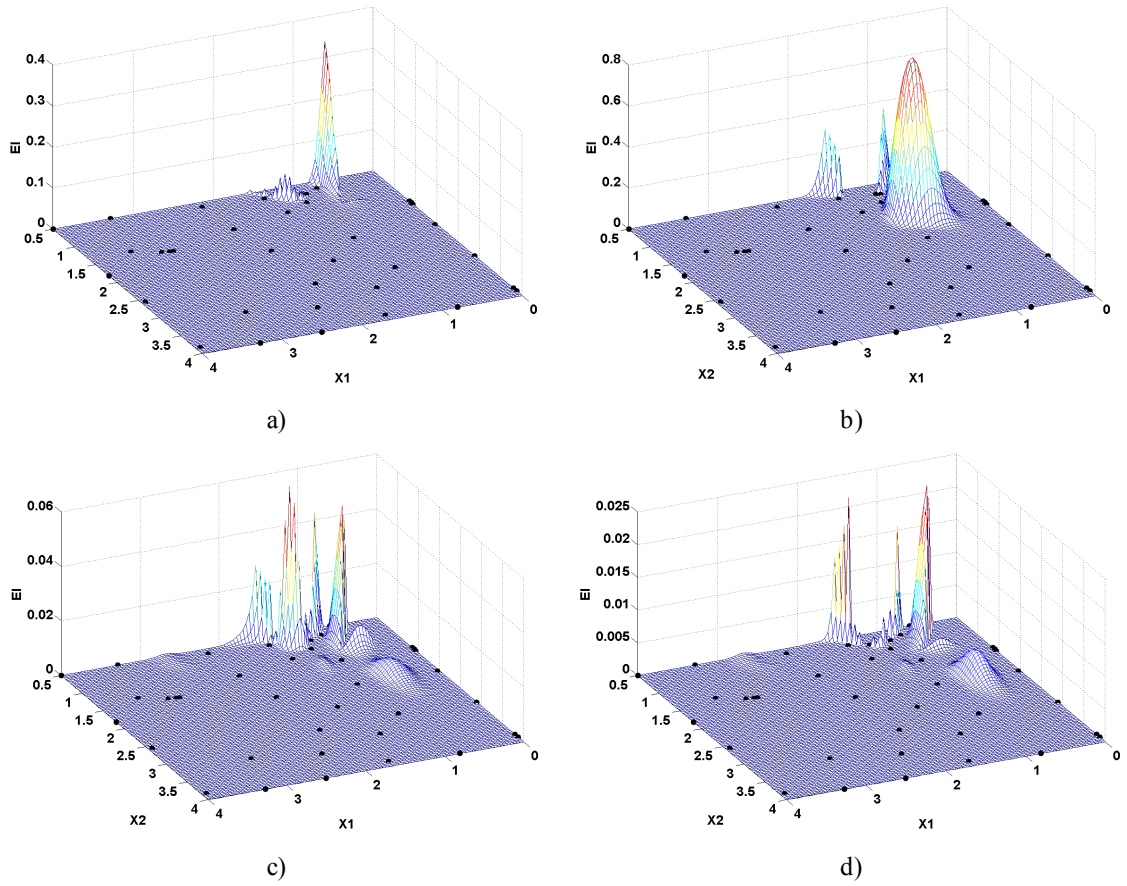

a) b)

c) d)

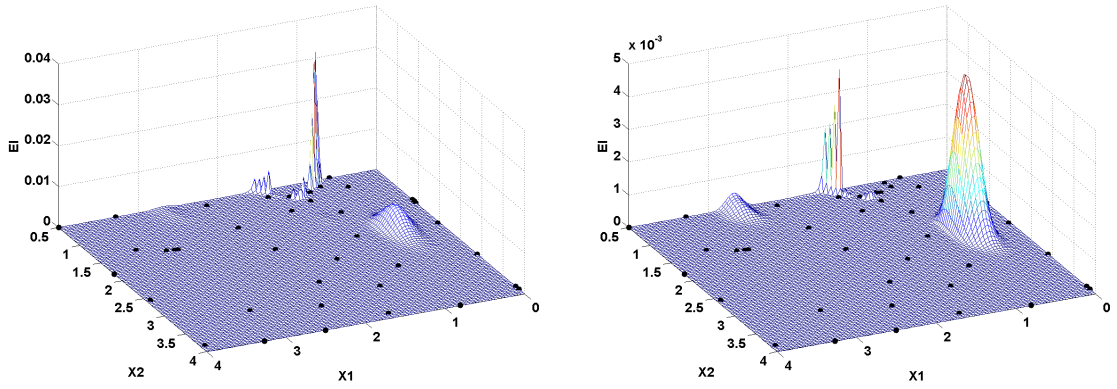

e) f)

Figure 46. Trend of the extended expected improvement function that yielded the first six evaluations conducted by considering the weighting coefficient vector (53).

Fourteen alternative change solutions were evaluated on the basis of preferences (53) and before meeting the second stopping criterion. The whole set of results is shown in Table 6, displaying the distance of each point from $\mathbf{x}^*$.

Solution	x_1	x_2	f	g	$x_1 - x_1^*$	$x_2 - x_2^*$	$f - f^*$	$g - g^*$
Point N°1	0.5937	0.5000	-0.0074	-6.9062	-0.7999	0.5000	0.6662	-0.2994
Point N°2	0.8960	1.3527	-0.0558	-5.7512	-0.4976	1.3527	0.6178	0.8556
Point N°3	1.2408	0.7780	-0.0976	-5.9811	-0.1529	0.7780	0.5760	0.6257
Point N°4	0.5104	0.7945	-0.0592	-6.6950	-0.8833	0.7945	0.6144	-0.0882
Point N°5	0.8168	0.5611	-0.0540	-6.6221	-0.5769	0.5611	0.6196	-0.0153
Point N°6	0.5126	1.9087	-0.1535	-5.5786	-0.8810	1.9087	0.5201	1.0282
Point N°7	1.4134	0.6056	-0.2567	-5.9810	0.0197	0.6056	0.4169	0.6258
Point N°8	1.3737	0.6414	-0.2213	-5.9849	-0.0200	0.6414	0.4523	0.6219
Point N°9	2.6677	0.5000	-0.0001	-4.8323	1.2740	0.5000	0.6735	1.7745
Point N°10	0.8488	0.6050	-0.0476	-6.5461	-0.5448	0.6050	0.6260	0.0607
Point N°11	1.5158	0.5000	-0.3518	-5.9842	0.1221	0.5000	0.3218	0.6226
Point N°12	0.4444	2.5859	-0.0023	-4.9697	-0.9492	2.5859	0.6713	1.6371
Point N°13	0.5656	1.2778	-0.2091	-6.1566	-0.8280	1.2778	0.4645	0.4502
Point N°14	0.5656	3.2576	-0.0161	-4.1768	-0.8280	3.2576	0.6575	2.4300

Table 6. Comparison of $\mathbf{x}^*$ with the solutions found by considering the weighting coefficient vector (53). The values that represent the best attainment of each of the four goals are highlighted in grey.

It is important to emphasise that, after having validated the prediction models to be used, the designer can explore different design solutions corresponding to different design

preferences without involving significant additional computational costs[13]. As described in Section 5.3.2, employing diverse weighting coefficients allows to obtain different results. For instance, from Table 6 it is clear that the major changes among all the solutions is with respect to the objective function value. Therefore, the designer might be interested in exploring further points that specifically minimise the change on $f(\mathbf{x})$. The vector $\boldsymbol{w}$ has then to be set accordingly, for example as follows:

$$\boldsymbol{w}=\{0.04,0.32,0.32,0.32\} \tag{54}$$

In this case, for the same stopping criteria, the *Design Exploration* phase is terminated after the evaluation of a single point, represented in Figure 47. The numerical values of the solution found are provided in Table 7.

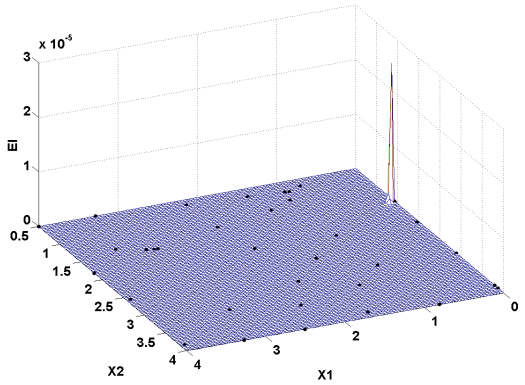

Figure 47. Solution found by considering the weighting coefficient vector (54).

Solution	x_1	x_2	f	g	$x_1 - x_1^*$	$x_2 - x_2^*$	$f - f^*$	$g - g^*$
Point Nº1	0.0241	1.3989	-0.4757	-6.5769	-1.3696	1.3989	0.198	0.0299

Table 7. Comparison of $\mathbf{x}^*$ with the solution found by considering the weighting coefficient vector (54).

[13] In the case the design sub-space is changed and further regions are to be explored, additional observations may be required for model validation purposes.

Attention should be given to the point $\bar{\mathbf{x}}=[0,1.3932]$, which would be the global optimum for Problem (42) after correcting the lower bound of the variable x_2 as considered in this section, with $f(\bar{\mathbf{x}})=-0.4764$ and $g(\bar{\mathbf{x}})=-6.6068$. It is in fact evident that, in the attempt to minimise change on the objective function, the design exploration is now focused on the identification of $\bar{\mathbf{x}}$, which turns out to be to the detriment of the value on x_1 and x_2 in particular.

In the event the designer would be interested in exploring alternative solutions by preserving as much as possible the value on x_1, a possible definition of the weighting vector could instead be:

$$\boldsymbol{w}=\{0.32,0.32,0.04,0.32\} \tag{55}$$

The extended expected improvement function for the three alternative solutions obtained in this case is depicted in Figure 48. The results are given in Table 8 along with, again, the distance of each point from $\mathbf{x}^*$.

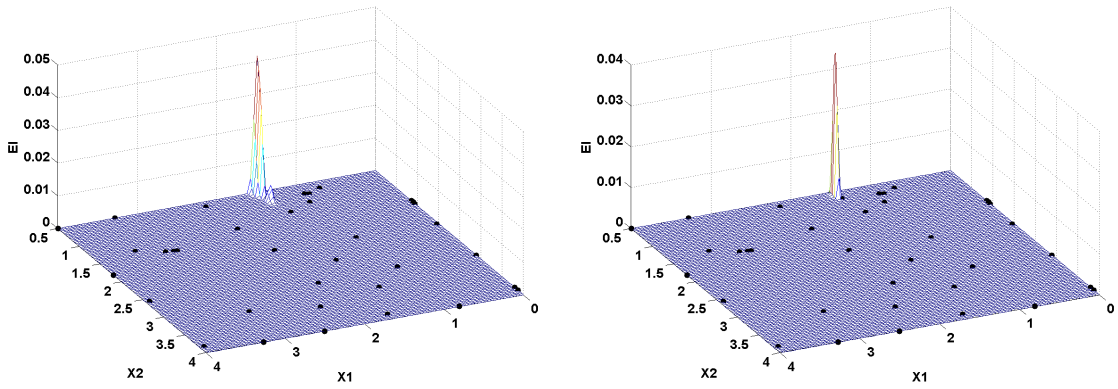

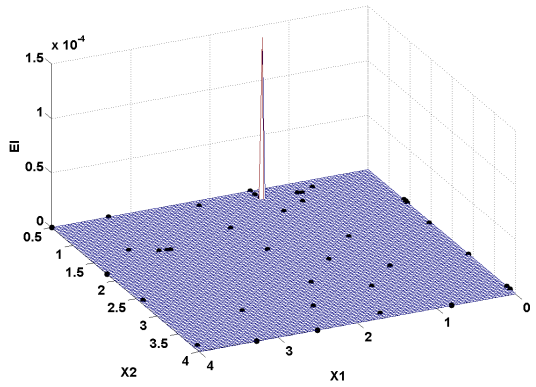

Figure 48. Trend of the extended expected improvement function that yielded the first three evaluations conducted by considering the weighting coefficient vector (55).

Solution	x_1	x_2	f	g	$x_1 - x_1^*$	$x_2 - x_2^*$	$f - f^*$	$g - g^*$
Point Nº1	1.4895	0.5010	-0.3526	-6.0094	0.0958	0.5010	0.3211	0.5974
Point Nº2	1.4893	0.6110	-0.2562	-5.8996	0.0956	0.6110	0.4175	0.7072
Point Nº3	1.4520	0.7102	-0.1781	-5.8378	0.0583	0.7102	0.4956	0.7690

Table 8. Comparison of x^* with the solutions found by considering the weighting coefficient vector (55).

The solution sets corresponding to the three different weighting coefficient vectors taken into account are summarised in Figure 49, showing the contours of $f(\mathbf{x})$ and the variables bounds under consideration.

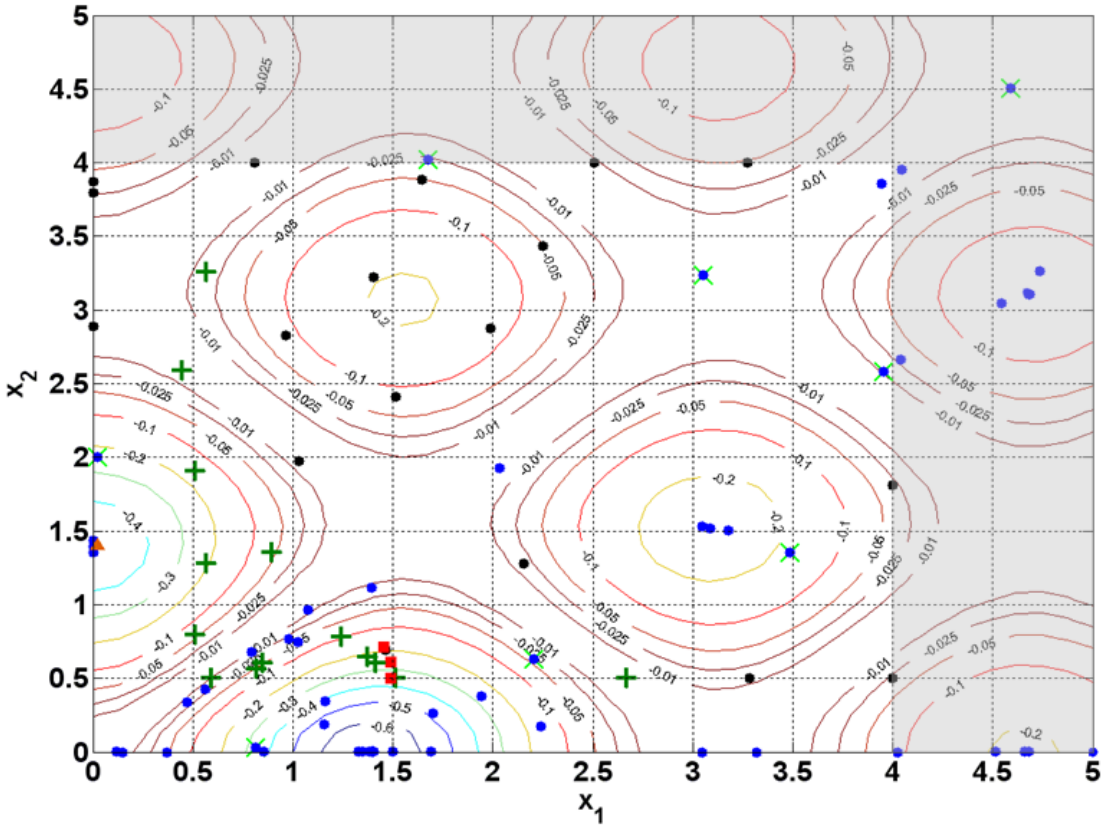

Figure 49. Summary of the alternative solutions obtained with three different *a priori* articulations of preferences. The green crosses, the orange triangle and the red squares represent the design solutions identified by considering the weighting coefficient vectors (53),(54) and (55) respectively. The green x-markers, blue points and black points represent the sets of starting optimisation points, initial function observations and additional evaluations required for model validation, respectively.

5.5. Isocontours of Objectives and Constraints

When a change of a specific design variable of a design concept is required, it might be convenient to explore all the alternative solutions that accommodate it to the detriment of another variable. Moreover, with the intent of addressing change propagation, it would be desirable to freeze, at the same time, the value of the other variables, as well specific performance achieved in terms of objectives and constraints. In the light of the three preference classes into which system requirements typically fall [75] (i.e., smaller-is-

better (SIB), larger-is-better (LIB) and nominal-is-better (NIB)), de Weck and Jones [22] illustrate the benefits that in particular cases may derive from formulating as NIB the key performance objectives that must be achieved first. This allows to extract, in the first place, the subset of solutions that satisfy the NIB requirements, to subsequently trade-off the other objectives with respect to each other.

Let us assume $\hat{\mathbf{x}} \in \Re^n$ represents a generic design point of Problem (1) for which $\mathbf{F}(\hat{\mathbf{x}}) = \{\hat{f}_1, \hat{f}_2, ..., \hat{f}_J\}$ and $\mathbf{G}(\hat{\mathbf{x}}) = \{\hat{g}_1, \hat{g}_2, ..., \hat{g}_I\}$. Setting the remaining (n-2) variables as constants, the objective is to identify the set of points $\mathbf{x}_{\mathbf{iso}} \in \Re^2$ that meet the performance $h(\hat{\mathbf{x}})$ for the generic function $h(\mathbf{x})$ among $\mathbf{F}(\hat{\mathbf{x}})$ and $\mathbf{G}(\hat{\mathbf{x}})$ within the pre-defined numerical tolerance τ^h, so that:

$$\left| \frac{h(\mathbf{x}_{\mathbf{iso}}) - h(\hat{\mathbf{x}})}{h(\hat{\mathbf{x}})} \right| \leq \frac{\tau^h}{100} \tag{56}$$

for given variables bounds $x^1_{\text{lb}} \leq x^1 \leq x^1_{\text{ub}}$ and $x^2_{\text{lb}} \leq x^2 \leq x^2_{\text{ub}}$, denoting generically by x^1 and x^2 the two independent variables at hand. A trade-off analysis of the performances formulated as NIB can thus be facilitated by plotting the corresponding isocontours in the x^1 x^2 plane, allowing the designer to assess the feasibility and the implications associated with promising design change solutions.

The key concept behind the approach proposed here is to exploit the principles and advantages of pattern search methods, which do not require any information about the gradient or higher derivatives and can be employed for non-differentiable functions [114].

The method is articulated into two iterative steps for identifying the isocontour of the generic function $h(\mathbf{x})$, namely the *Mesh Evaluation* phase and the *Search Refinement* phase.

The algorithm is initialised at the starting point $\hat{\mathbf{x}}$. At each iteration *t*, in the *Mesh Evaluation* phase the algorithm searches a set of points, called a *mesh*, which are located along the following fixed-direction vectors (or *pattern vectors*):

$$\mathbf{v}_1^{\pm} = [\pm 1,\ 0] \qquad \mathbf{v}_2^{\pm} = [0,\ \pm 1] \tag{57}$$

The local search space around $\mathbf{x}^t$ is thus partitioned into four quadrants by such a collection of vectors, as shown in Figure 50. The mesh is given by the points in the set:

$$\mathcal{L}_t \equiv \left\{ \mathbf{x} \in \Re^2 \,\middle|\, \mathbf{x} = \mathbf{x}^t + \Delta_t{}^i s^i \mathbf{v}_i^{\pm}\ ,\quad i \in \{1,2\} \right\} \tag{58}$$

where $\Delta_t{}^i > 0$ is a scalar called the mesh size factor, and s^i is a fixed parameter that takes the different scaling of the design variables into consideration [122].

A poll is hence carried out by evaluating the function *h* at the mesh points. The poll is called successful when one of the following inequalities is satisfied:

$$h(\mathbf{x}') \le h(\hat{\mathbf{x}}) \le h(\mathbf{x}'')$$

or (59)

$$h(\mathbf{x}') \ge h(\hat{\mathbf{x}}) \ge h(\mathbf{x}'')$$

for two points of the mesh $\mathbf{x}'$ and $\mathbf{x}''$ whose pattern vectors do not belong together to the bounds of the quadrant where the previous isopoint $\mathbf{x}^{t-1}$ is located. In other words, taking Figure 50 into account, $\mathbf{x}'$ and $\mathbf{x}''$ can lie only along the bounds of quadrants I, II and IV, since the previous iteration has been computed in quadrant III. In this manner the next isopoint $\mathbf{x}^{t+1}$ is assumed to be computed in the advancing search direction.

After a successful poll, the *Search Refinement* phase subsequently takes place. If condition (56) is not satisfied either by $\mathbf{x}'$ or $\mathbf{x}''$, the search of a satisfactory point $\mathbf{x}'''$ is conducted along the search direction $\overline{\mathbf{x}'\mathbf{x}''}$, assuming local continuity and unimodality of $h(\mathbf{x})$. The search then continues with $\mathbf{x}^{t+1} = \mathbf{x}'''$ and $\Delta_{t+1} = \xi \Delta_t$, where $\xi \ge 1$ is a predefined expansion factor of the mesh.

It is important to note that in the *Search Refinement* phase the aim is to identify the intersection point between the segment $\overline{\mathbf{x}'\mathbf{x}''}$ and the isocontour of $h(\mathbf{x})$ not exactly but with a tolerance τ^h. This can be achieved via a variety of ways. For instance, a simple but

effective approach is given by the bisection method, which requires only one function evaluation to repeatedly bisect $\overline{\mathbf{x}'\mathbf{x}''}$ and select the subinterval where the isocontour must lie. Alternatively, other algorithms for single-variable unconstrained optimisation may be deployed[14].

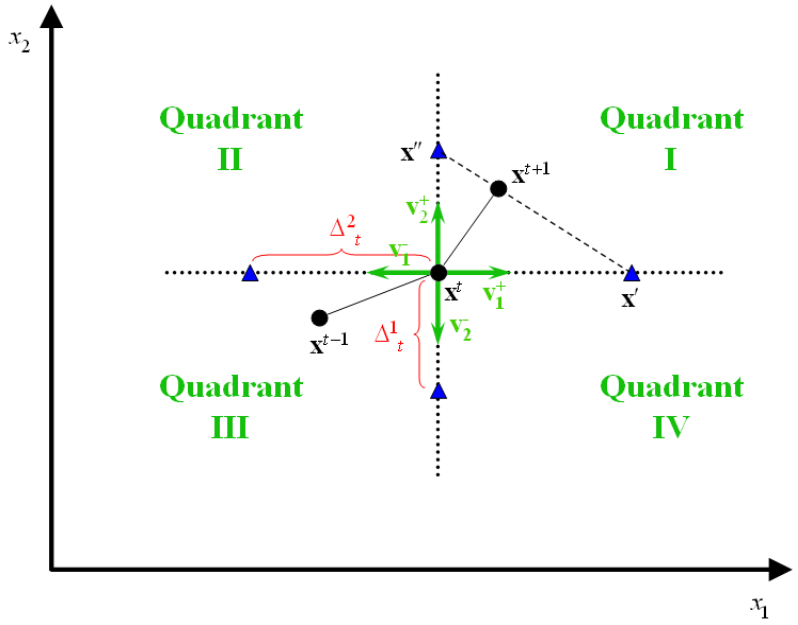

Figure 50. Basic concept behind the proposed isocontour method.

If the poll is unsuccessful, the search continues with $\mathbf{x}^{t+1}=\mathbf{x}^t$ and a reduced mesh size factor, e.g. $\Delta_{t+1} = \frac{1}{2}\Delta_t$.

With respect to algorithms based on the evaluation of grid points obtained via a discretization of the design space, the application of the suggested approach generally shows a more efficient estimation of the function isocontour in terms of computational

[14] The region-elimination methods generally offer an attractive strategy for the proposed isocontour computation method since no differentiability assumptions on $h(\mathbf{x})$ are required. Besides the bisection method, the golden search method calculates one new function evaluation per iteration, assuring a proportion of the eliminated region that is always the same and equal to 38.2%. This quantity turns out to be higher or equal to that of other methods, such as the interval halving method and the Fibonacci search [24].

cost. For comparison purposes and with the intent of providing a reference in terms of performance, the isocontour obtained for the single degree-of-freedom problem considered in de Weck [21] is shown in Figure 51. Moreover, by adopting the principles of pattern search methods, no assumptions of differentiability on $h(\mathbf{x})$ are required, which makes the method well suited for applications where derivatives are not available and finite-difference derivatives are unreliable (e.g., when the function at hand is noisy) [66].

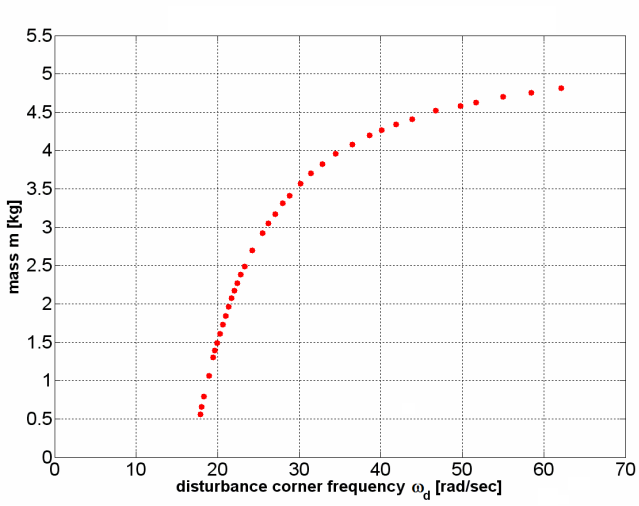

Figure 51. Isocontour for the single degree-of-freedom problem (ω_d,m) taken into consideration in de Weck [21], where 35 isopoints were computed with a tolerance of 1% and a discretization of the design space based on 441 points via the non-gradient algorithm *Exhaustive Search*. The application of the method proposed here by the author within the same variable ranges required 310 total evaluations for the identification of the depicted 36 isopoints, with a tolerance of 0.1%.

Another example of the application of the present approach is shown in Figure 52, portraying the isocountours associated with 5 points randomly selected across the design space of Problem (42), considering an accuracy of 0.001%.

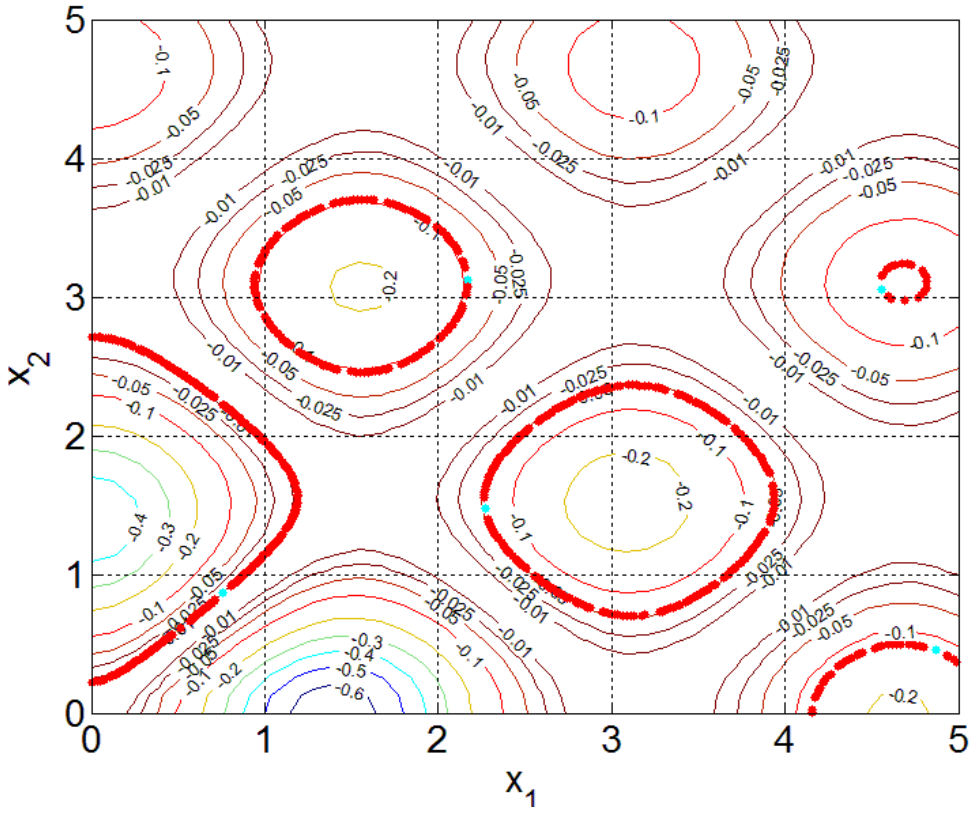

Figure 52. Displayed in red are the isocontours associated with 5 points (depicted in cyan) randomly selected across the design space of Problem (42).

Table 9 provides the details of the isopoints set obtained for the starting point $\hat{\mathbf{x}}$=[4.5594425,3.0524488], for which $f(\hat{\mathbf{x}})$=-0.1495024.

Isopoint	x_1	x_2	$f(\mathbf{x}_{iso})$	$f(\mathbf{x}_{iso}) - f(\hat{\mathbf{x}})$	$\left\lvert\frac{f(\mathbf{x}_{iso}) - f(\hat{\mathbf{x}})}{f(\hat{\mathbf{x}})}\right\rvert$
1	4.5563175	3.1493238	-0.1494372	0.0000653	0.0004365
2	4.5656925	3.1649488	-0.1496251	-0.0001227	0.0008206
3	4.5844425	3.1961988	-0.1494010	0.0001015	0.0006786
4	4.6125675	3.2180738	-0.1494970	0.0000054	0.0000364
5	4.6334008	3.2305738	-0.1493695	0.0001330	0.0008894
6	4.6740258	3.2399488	-0.1494041	0.0000983	0.0006576
7	4.7052758	3.2378655	-0.1494920	0.0000104	0.0000697
8	4.7302758	3.2295321	-0.1496494	-0.0001470	0.0009833
9	4.7896508	3.1889071	-0.1495252	-0.0000228	0.0001522

10	4.7990258	3.1732821	-0.1496242	-0.0001218	0.0008144
11	4.8146508	3.1389071	-0.1495323	-0.0000299	0.0001999
12	4.8188175	3.1097405	-0.1495342	-0.0000318	0.0002125
13	4.8125675	3.0659905	-0.1495629	-0.0000604	0.0004043
14	4.7969425	3.0316155	-0.1495276	-0.0000252	0.0001686
15	4.7823592	3.0128655	-0.1495243	-0.0000218	0.0001460
16	4.7656925	2.9961988	-0.1494288	0.0000736	0.0004922
17	4.6906925	2.9711988	-0.1496471	-0.0001447	0.0009680
18	4.6094425	2.9899488	-0.1493740	0.0001284	0.0008587
19	4.5927758	3.0066155	-0.1496046	-0.0001022	0.0006834

Table 9. Isopoints computed from $\hat{\mathbf{x}}$=[4.5594425,3.0524488].

5.6. Summary and Conclusions

A novel methodology for addressing conceptual design change problems has been introduced in this chapter. The proposed approach is based on an integration of methods from design optimisation and is proposed as a complementary strategy to the methods described in Section 2.4. The aim is to enable the designer to work out a set of new design alternatives by effectively identifying the design space areas which would allow both change incorporation and, at the same time, would limit the extent of the change.

After presenting the sought objectives, Section 5.3 provides an overview of the whole approach, introducing the three phases in which it is articulated. Firstly, in the *Surrogate Model* phase, the stochastic process model delineated in sub-section 2.5.1 is employed to fit prior collected observations, along with an adequate validation procedure. The designer is thus provided with a global understanding of the problem at hand. This enables, in the *Problem Reformulation* phase, the identification of the most promising design sub-spaces where different trade-offs between accommodating the requested change and containing change propagation can be found. An exploration of alternative design solutions can hence be conducted throughout the *Design Exploration* phase via a suitable reformulation of the problem based on the general behaviour of the objective and constraint functions. The evaluation of additional design points is driven by a sampling criterion based on a proposed extension of the figure of merit introduced by Mockus et al. [78]. In particular, the present strategy allows a local relaxation of constraints in

proportion to the standard error associated with their prediction, so that further points can be evaluated also in the vicinity of the constraint contours. This offers a double advantage within the context at hand. Firstly, points that are predicted as infeasible, but in reality are feasible, are less likely to be overlooked because of an inaccurate constraint approximation. Secondly, promising points that slightly violate one or more constraints can thus be evaluated and presented to the designer, who may judge them as a valid alternative if a proper constraint relaxation is possible.

A novel method for an efficient computation of objective and constraint isocontours is proposed in Section 5.5. It is intended to support a design exploration to accommodate, for a given design point, a change on a specific design variable to the detriment of another variable, preventing change propagation by freezing at the same time the value of the other variables. The designer is thus allowed to conduct a trade-off analysis between potential additional solutions through an evaluation of the design points that keep invariant desirable performance in terms of objectives and constraints.

An example of the application of the proposed methodology is given in this chapter by considering an analytical function. The results obtained from a test case of industrial relevance are outlined in Chapter 6, demonstrating the capabilities of the present methods in addressing more complex problems.

Chapter 6

Application Example - Aircraft Conceptual Design Optimisation

6.1. Introduction

The application of the proposed exploration methodologies to an industrial aircraft sizing test case is presented in this chapter.

A description of the test case taken into consideration is provided in Section 6.2. The application of the Adaptive Search Optimisation Method (ASOM) is then described in Section 6.3, demonstrating its capabilities to effectively improve the Pareto set by adequately re-defining the search region throughout the optimisation process. The results thus obtained are compared with the solutions obtained via standard optimisation procedures.

The visual exploration and analysis of the ASOM results through the proposed visual exploration methodology is presented in Section 6.4. It demonstrates how a thorough

investigation of complex data structures can be performed by the designer via the analysis of multiple and complementary perspectives of the problem under study. This is done by deploying the graphical user interface prototype *IEVI* presented in Chapter 4.

In Section 6.5, an exploration of alternative design points is conducted on a number of hypothetic scenarios for design change problems at conceptual stage. The application of the methodology presented in Chapter 5 is demonstrated here with the aim of computing a new set of solutions by balancing the design implications of change introduction and change propagation. It is also shown how the evaluation of additional points is conducted on the basis of the change requirements articulated by the designer, formally stated via the goals vector $\boldsymbol{F^*}$. In a second instance, the proposed isocontours method is deployed to accommodate, for a given design point, a change on a specific design variable to the detriment of another variable, while freezing the others.

The advantages, limitations and potential recommendations for each strategy are outlined in the summary and conclusions section.

6.2. Test Case Description

The adopted test case (USMAC - Ultra Simplified Model of Aircraft) has been supplied by a major airframe manufacturer as part of an EU FP6 Integrated Project [59]. It is a code developed for the evaluation and sizing of short-to-medium range commercial passenger aircraft, computing the overall performance and weights by means of 97 models and 125 design parameters. The adopted nomenclature is shown in Table 10.

Npax	Number of passengers	**Mach_crz**	Cruise mach
NpaxFront	Number of passengers per row	**alt_crz**	Cruise altitude [ft]
Naisle	Number of aisles	**alt_to**	Take-off altitude [ft]
FNslst	Sea-level static engine thrust [decaN]	**alt_app**	Approach altitude [ft]
BPR	Engine bypass ratio	**MTOW**	Maximum Take-off weight [kg]
ne	Number of engines	**RA**	Range [NM]
Awing	Wing area [m^2]	**tofl**	Take-off field length [m]
span	Wing span [m]	**vapp**	Approach speed [kts]
phi	Wing sweep angle [deg]	**vz_clb**	Climb rate [ft/min]
tuc	Wing thickness-to-chord ratio	**Kfn_cth**	Cruise thrust coefficient
Fuel	Fuel weight [kg]	**Kff**	Wing-fuselage fuel ratio

Table 10. Test case nomenclature.

Table 11 provides the original optimisation problem, which has been set as in Guenov et al. [44].

Constants	**Variables**	**Constraints**	**Objectives**
Npax = 150	FNslst = [12500,13000] decaN	tofl ≤ 2000 m	RA [NM]
NpaxFront = 6	Awing = [152,158] m^2	vapp ≤ 120 kts	to be maximised
Naisle = 1	span = [30,38] m	vz_clb ≥ 500 ft/min	
ne = 2	phi = [28,32] deg	Kfn_cth ≤ 1	MTOW [kg]
alt_crz = 35000 ft	tuc = [0.07,0.1]	Kff ≥ 0.75	to be minimised
Mach_crz = 0.82	Fuel = [17000,18000] kg		
alt_to = 0 ft	BPR = [6,7]		
alt_app = 0 ft			

Table 11. Conceptual aircraft design optimisation formulation.

6.3. Adaptive Search Optimisation

The considered setup of the optimisation problem under study is as follows:

Input Variable	**Frozen Bounds**		**Initial Adaptive Bounds**	
	$\overline{\mathbf{x}}_{lb}$	$\overline{\mathbf{x}}_{ub}$	$\mathbf{x}_{lb}$	$\mathbf{x}_{ub}$
FNslst	11875	13650	12500	13000
Awing	144.4	165.9	152	158
span	28.5	39.9	30	38
phi	26.6	33.6	28	32
tuc	0.0665	0.1050	0.07	0.1
Fuel	16150	18900	17000	18000
BPR	5.7	7.35	6	7

Table 12. Setup of the frozen and adaptive bounds.

where the frozen bounds correspond to a relaxation of 5% of the value of the lower and upper adaptive bounds. For all the variables the following ASOM parameters have been adopted: $\vartheta = 1$, $\gamma = 0.05$, $p = 0.05$, $\alpha = 0.05$ and $\delta = 0.25$.

Cantelli's probability inequality has been deployed for the relaxation criterion, switching to the Chebyshev-Cantelli inequality when the former is not applicable.

The optimisation procedure has been carried out by integrating ASOM into the DHCBI software developed by Fantini [31], considering 40 starting points produced by a Latin Hypercube sampling. The final setup of the adaptive bounds at the last optimisation

iteration is given in Table 13, where the active amongst the frozen bounds are highlighted in grey.

Input Variable	Final Adaptive Bounds	
	$\mathbf{x}_{lb}$	$\mathbf{x}_{ub}$
FNslst	11875	13650
Awing	144.4	165.9
span	33.8248	39.9
phi	26.6	33.6
tuc	0.0762	0.1027
Fuel	16150	18900
BPR	5.7	7.35

Table 13. Final adaptive bounds.

The distributions of the overall and feasible evaluations conducted via the SPSA algorithm are given in Figure 53.

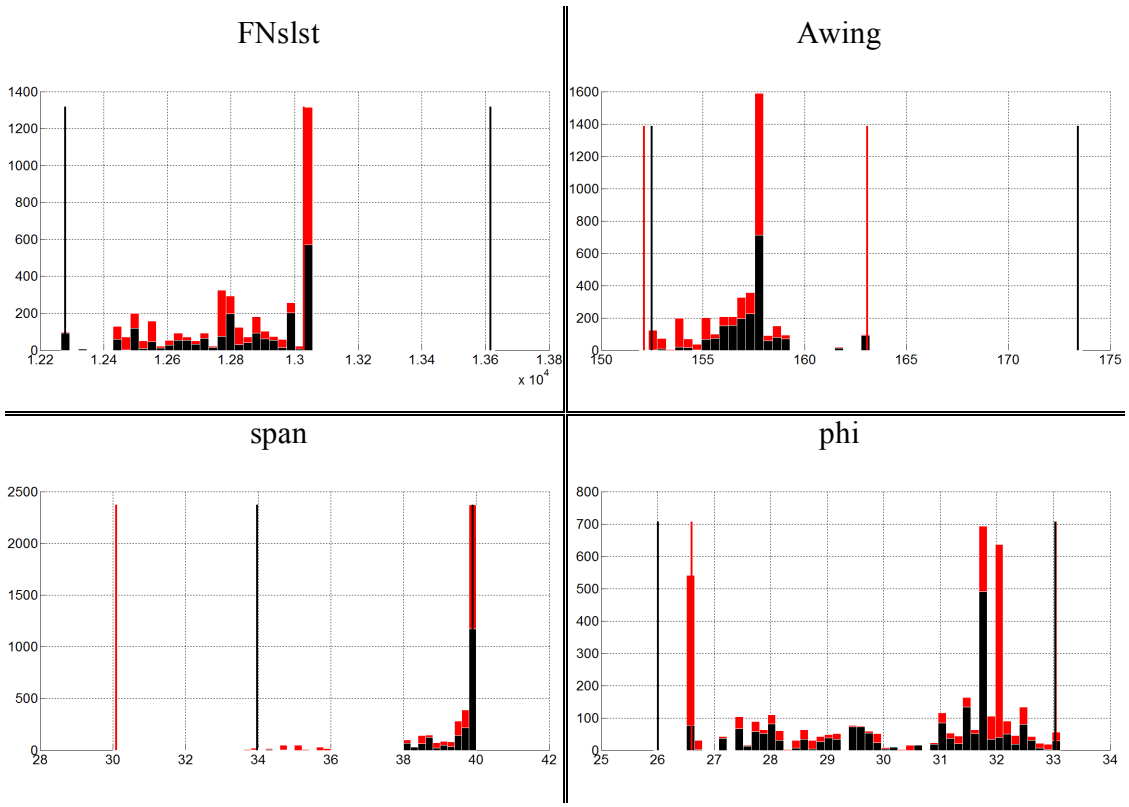

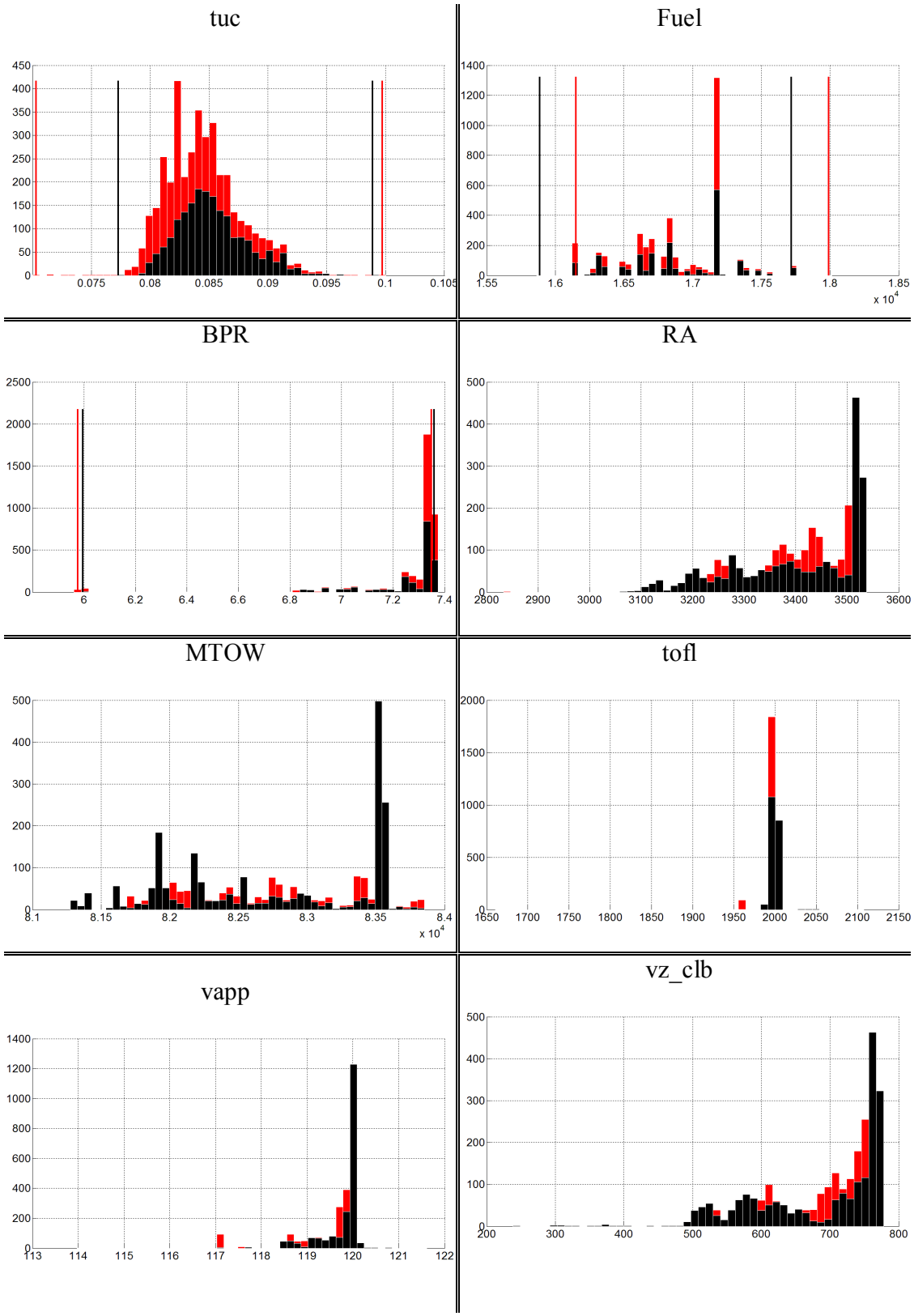
tuc
Fuel
BPR
RA
MTOW
tofl
vapp
vz_clb

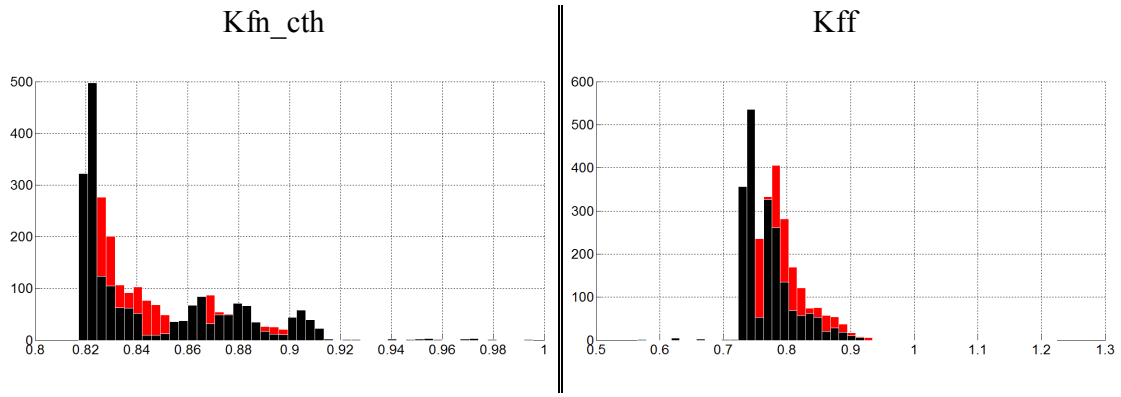

Figure 53. Distributions of the overall and feasible point sets, which are portrayed in red and black, respectively. The black and red vertical lines in the variable histograms represent the borders of the feasible and infeasible distributions.

The Pareto front that has been obtained is displayed in green in Figure 54. For comparison purposes, two additional optimisation procedures have been computed. They will be referred to as Optimisation A and Optimisation B, which have been conducted without the integration of ASOM and considering as variables bounds the adaptive and the frozen bounds given in Table 12, respectively. The corresponding Pareto fronts are visualised in Figure 54 in red (Optimisation A) and blue (Optimisation B).

The results demonstrate the capabilities of the proposed adaptive search method ASOM in enhancing the set of optimal points via a continuous redefinition of the variables bounds throughout the optimisation procedure. It is important to highlight, however, that the improvement of the Pareto front is local. This is in accordance with the aim of the method, namely the computation of further optimal solutions that may be located slightly beyond the variables bounds initially set. Consequently, the optimal set obtained by means of ASOM (in green) can be seen as an improvement of the red Pareto obtained in Optimisation A. Optimal points that are distantly located from the initial search region can not be computed because of the absence of starting points in such areas of the design space. In Figure 54 this is evident from the analysis of the blue Pareto obtained in Optimisation B, which is extended on a larger range of the criterion space.

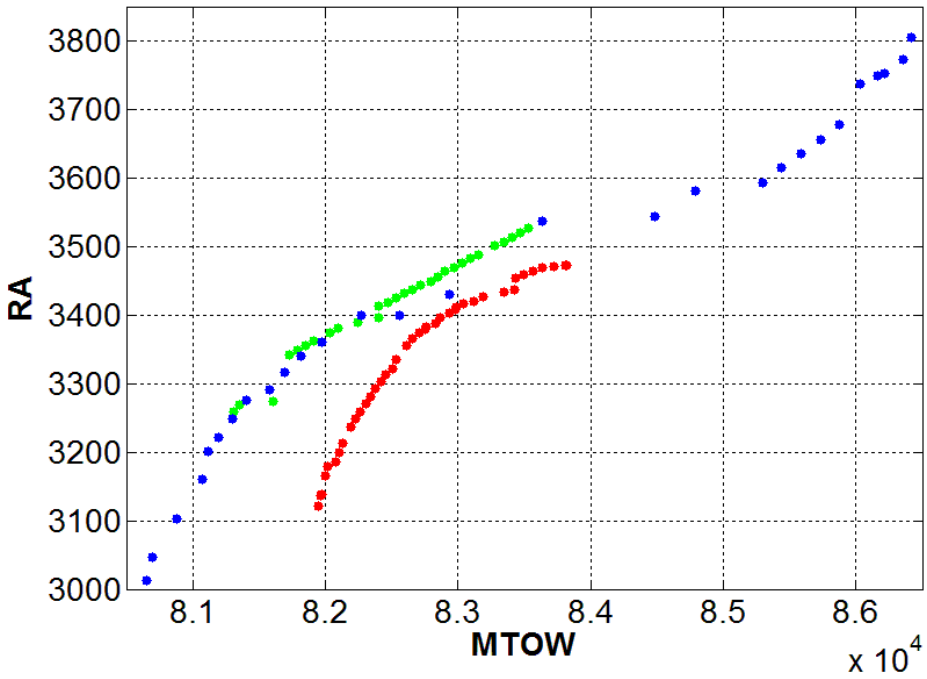

Figure 54. Comparison of the Pareto front obtained by means of ASOM (in green) with respect to the optimal points computed without ASOM by considering as bounds the adaptive and frozen bounds (in red and blue) given in Table 12.

The distributions of the three Pareto fronts under study are shown in Figure 55. It is possible to confirm that a wider distribution characterises all the design variables in the case of Optimisation B. Moreover, with the exception of *Awing*, the variables distributions obtained via ASOM show a relaxation of one or both adaptive bounds towards the bounds set for Optimisation B.

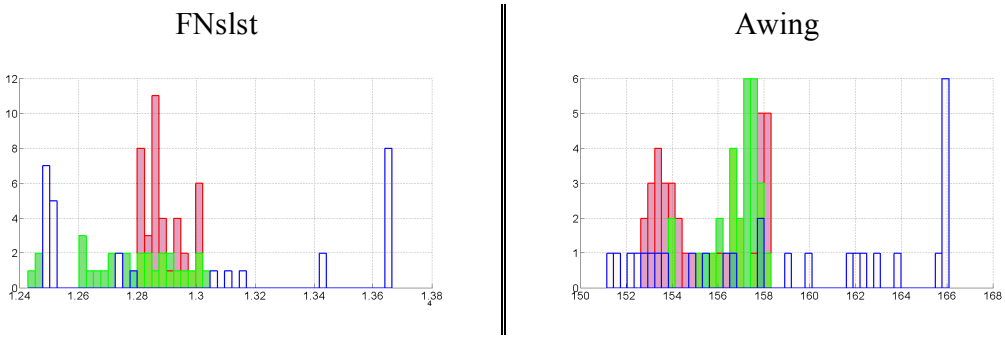

span

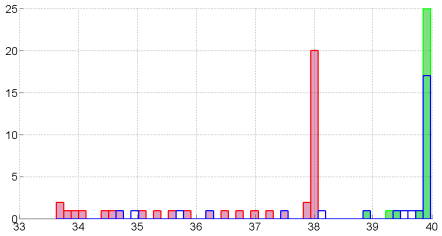

phi

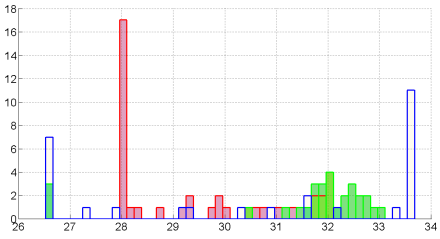

tuc

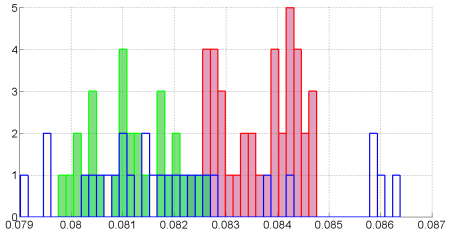

Fuel

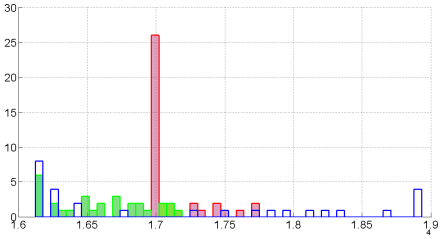

BPR

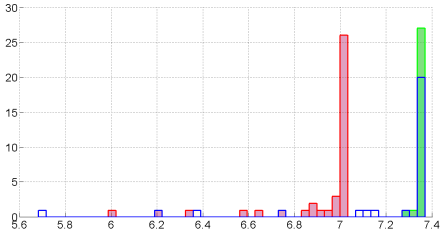

RA

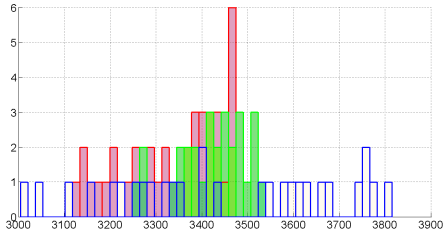

MTOW

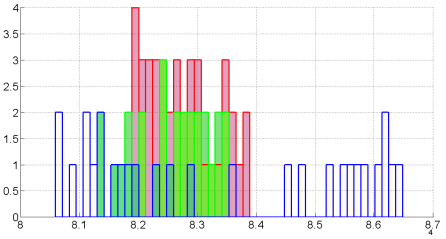

tofl

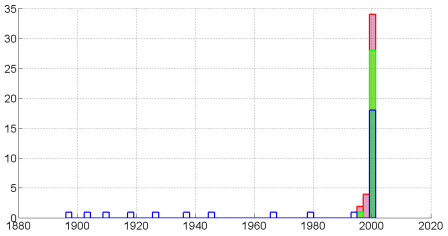

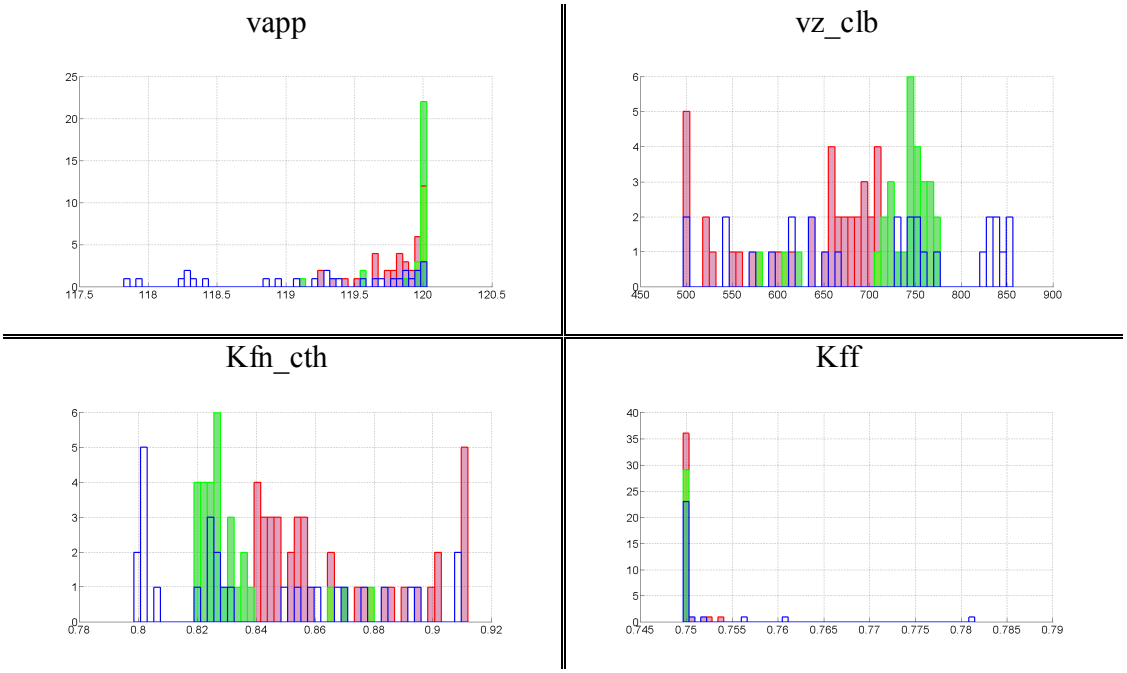

Figure 55. Distributions of the Pareto points displayed in Figure 54 by adopting the same colour notation.

A detailed analysis of the results obtained by means of the proposed adaptive search method is given in the following section.

6.4. Visual Exploration of Optimisation Results

Presented in this section is an example of the application of the visualisation methodology described in Chapter 4 for conducting a visual exploration of large multidimensional datasets deriving from MOO procedures. The whole set of function evaluations obtained from the problem addressed in the previous section (6085 samples) is analysed by means of the exploration interface prototype developed by the author, the *Integrated Exploration and Visualisation Interface* (*IEVI*). The default visualisation of the data under study is shown in Figure 56 through the representation of the objective space, *MTOW* distribution, and design space in the *Euclidean Space Interface (ESI)*,

Specific Design Tools Interface (SDTI) and *Multidimensional Data Visualisation Interface (MDVI)*.

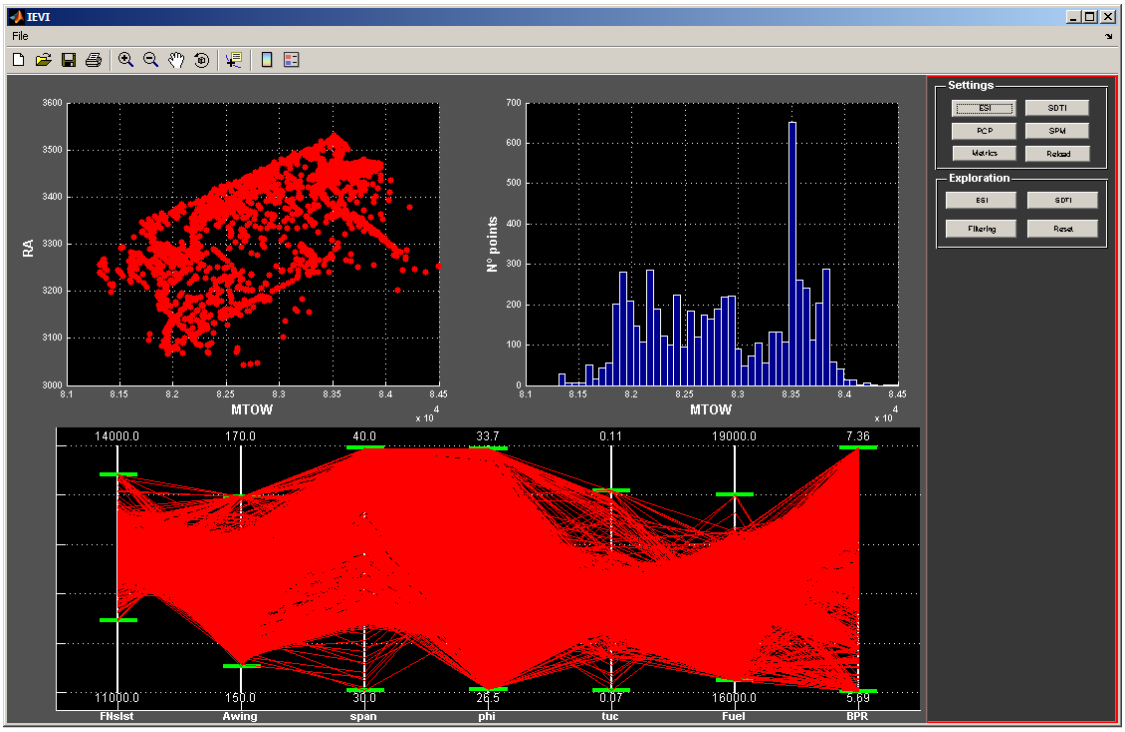

Figure 56. Default optimisation data visualisation.

The deployment of *Filtering* provides a first criterion to steer the selection of promising design solutions to be analysed. The feasible, infeasible, and non-dominated sets of points are thus graphically identified through green points, grey points and yellow squares, respectively. The same colour notation is applicable also on the *Parallel Coordinates Plot (PCP)* and is formally given in the *Filtering settings* panel, as shown in Figure 57.

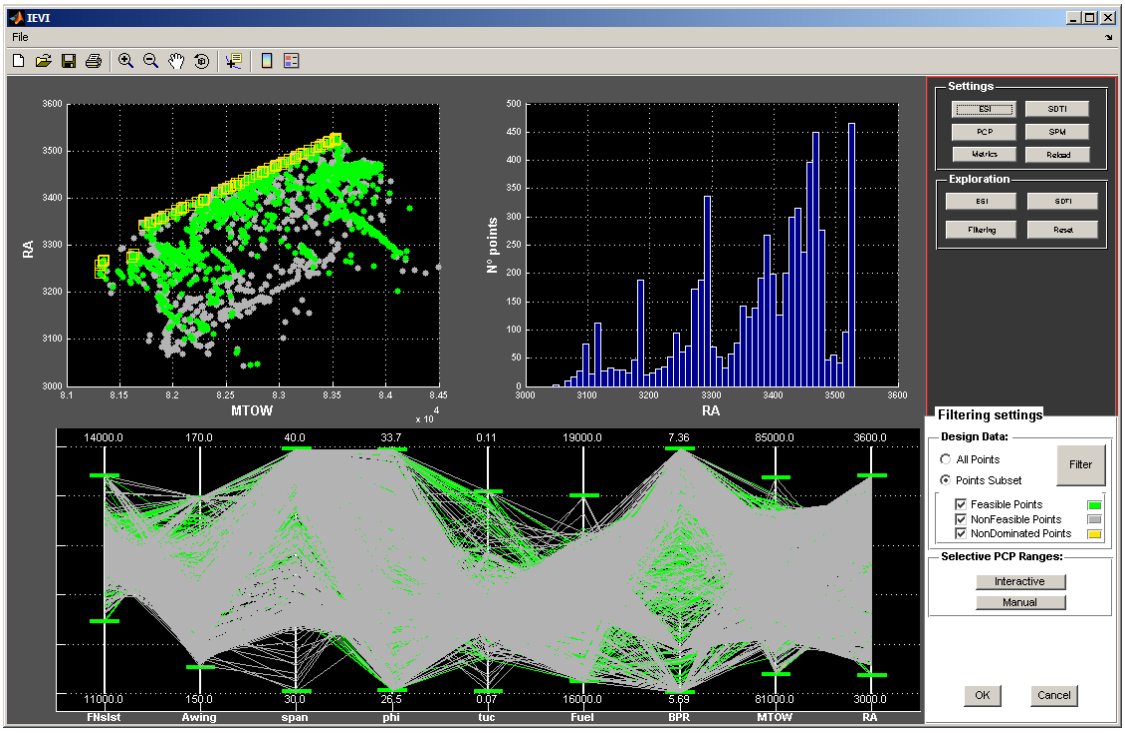

Figure 57. Optimisation data visualisation by means of *Filtering*. The colour notation shown in the *Filtering settings* panel is used to identify the sets of feasible, infeasible, and non-dominated design points.

When analysing large datasets, it is recommended to focus design exploration on one of the abovementioned sets of solutions, depending on the analysis tasks to be performed. For example, only non-dominated points may be displayed, as shown in Figure 60, or infeasible solutions might be removed from the display as in Figure 58. This provides a means to narrow down the number of design alternatives of interest, thus facilitating the interactive selection of specific design points to be individually analysed in detail. Illustrated in Figure 58 is the selection of optimal points in the *ESI*. For each selected point, the two remaining interfaces are updated simultaneously. For instance, the designer is enabled to find out what is the selection impact on any 2D/3D sub-space of the problem in the *SDTI*, comparing the chosen solution (represented by an orange cross-symbol) with respect to the other alternatives displayed. A detailed assessment of the selected point properties can instead be conducted in the *MDVI* through the analysis of the exact numerical values for the axes selected in the *PCP*.

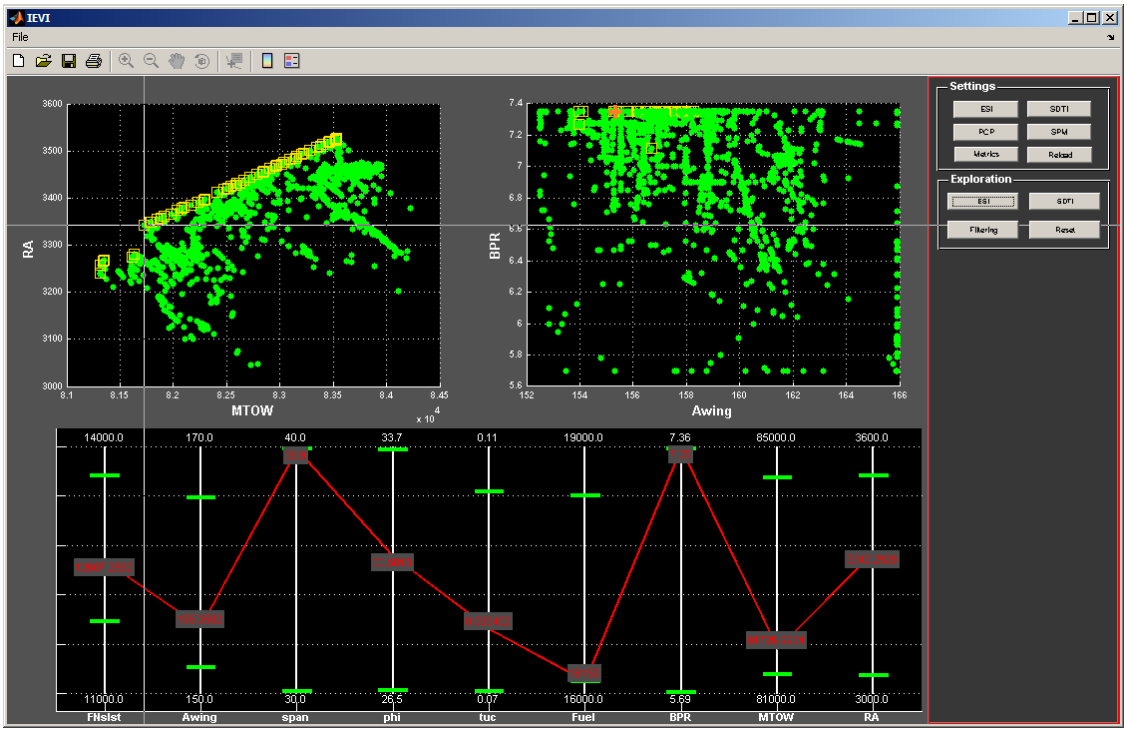

Figure 58. Interactive selection of points on the *ESI* with a real-time visualisation update in the remaining interfaces. In this case, the selected point is identified in the *BPR-Awing* sub-space of the problem through an orange cross-symbol in the *SDTI*, whereas its exact numerical value for each dimension of the design and objective spaces are given in the *PCP* displayed in the *MDVI*.

A further refinement of the results analysis process can be performed by expressing additional exploration requirements via the *Selective PCP Ranges Filtering* function. This allows the identification of all the design solutions that meet a specific range of values for any design parameter. Such function turns out to be particularly useful, for example, for the study of active constraints, as shown in Figure 59. Another practical application could be the exploration of solutions that meet one or more tighter constraints, or the influence that specific areas of the design space have on the objective space and vice versa.

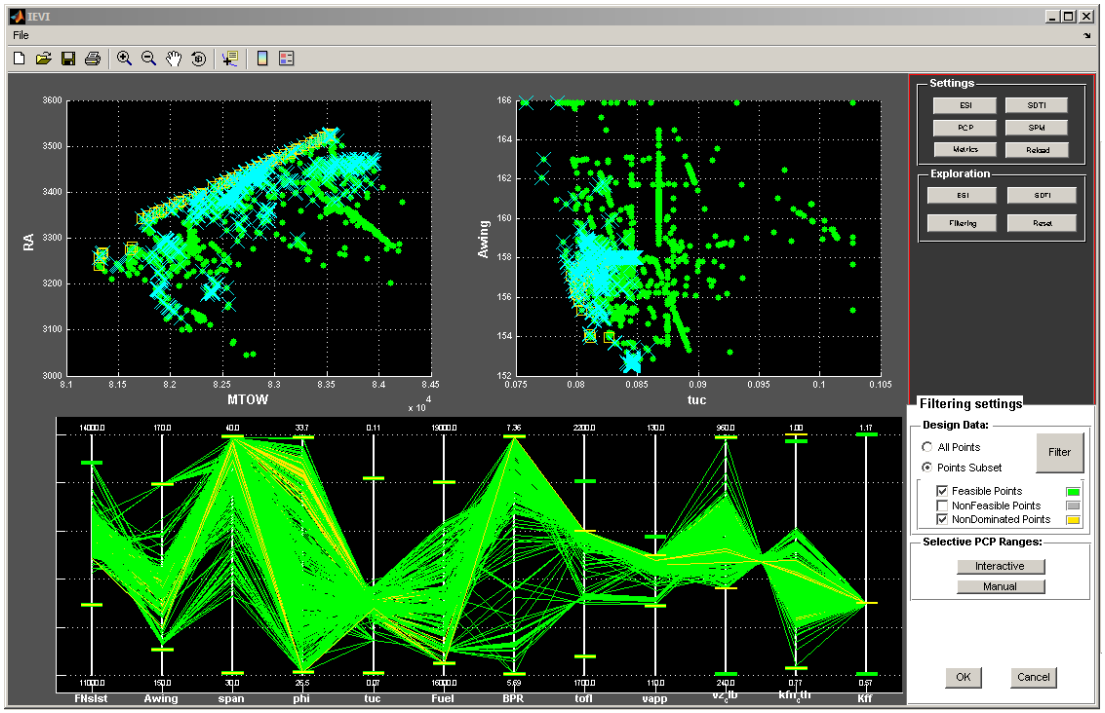

Figure 59. One example of the visual exploration tasks that can be conducted by using the *Selective PCP Ranges Filtering* function in the *PCP*. The design points for which the constraint *Kff* is active are identified in the *ESI* and *SDTI* through cyan x-markers.

One criterion that can potentially influence the trade-off analysis study on a set of design alternatives is the satisfaction grade of constraints. In this respect, a penalty weight would be attributed to those points for which constraints are active or slightly satisfied. Such information can be also used to assess the formulation of constraints and their possible relaxation. In the *SDTI* displayed in Figure 60, for example, it is evident that most of the computed optimal points are located very close to the limit value formulated for the velocity of approach ($vapp \leq 120$kts). On the other hand, the constraint on the climb rate ($vz\_clb \geq 500$ ft/min) appears to be largely met by all the Pareto points. Additionally, it can be noted that a large number of optimal designs have been computed beyond the initial adaptive bounds of various variables. This is shown in Figure 60, both qualitatively in the *PCP* (for *span* and *BPR*) and quantitatively in the *ESI* (for *Fuel* and *phi*).

Last, but not least, Figure 61 provides an example of the integration of *discipline-dependent techniques* by illustrating the carpet plot (in the *SDTI*) corresponding to any point selected in the *ESI*.

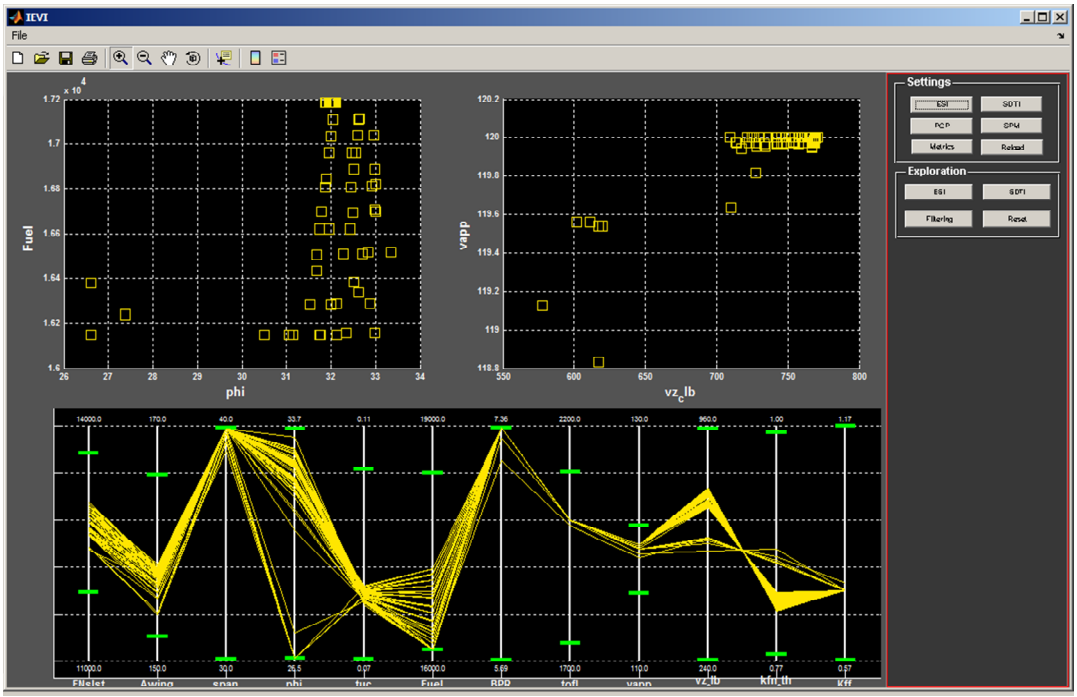

Figure 60. Analysis of Pareto solutions.

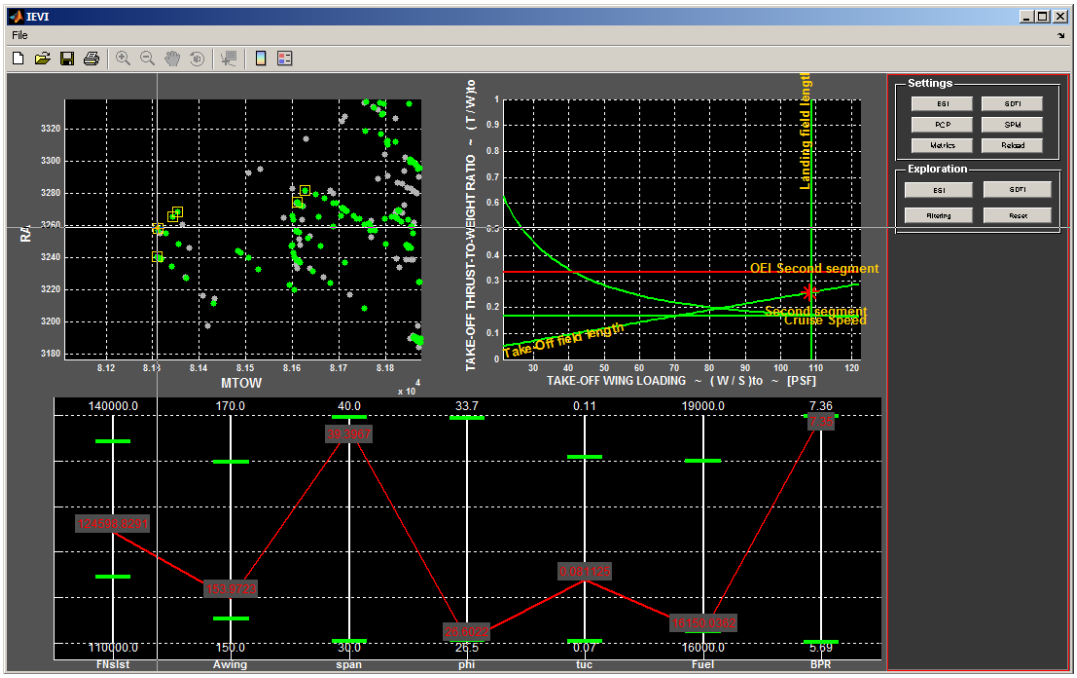

Figure 61. Example of the data visualisation via *discipline-dependent techniques* in the *SDTI* by representing the carpet plot corresponding to the design selected in a magnified inset of the objective space displayed in the *ESI*. Displayed in red are possible performance constraints that are not satisfied.

6.5. Introduction of Minor Design Changes Affecting Conceptual Design

In this section, the capabilities of the methodology proposed in Chapter 5 are demonstrated with the USMAC test case. Addressed are three hypothetic scenarios where design changes are required for the point selected in Figure 61, denoted by $\mathbf{x}^*$ and given in Table 14.

Variables	**Constraints**	**Objectives**
FNslst = 12459.8829 decaN	tofl = 1999.9888 m	RA = 3258.163 [NM]
Awing = 153.9723 m^2	vapp = 119.5601 kts	
span = 39.3967 m	vz_clb = 611.2451 ft/min	
phi = 26.6022 deg	Kfn_cth = 0.8692	MTOW = 81311.8282 [kg]
tuc = 0.0811	Kff = 0.7496	
Fuel = 16150.0362 kg		
BPR = 7.35		

Table 14. Design to be changed $\mathbf{x}^*$.

It is arbitrarily assumed in a first instance that the wing area needs to be increased, say to 156 m^2. Changes on all other parameters are to be minimised.

One of the criteria to support the definition of the design sub-space to be explored can be to allow the computation of further points in the objective-space neighbourhood of the design to be changed. For this, the proposed visualisation methodology turns out to be particularly useful by mapping a given set of points in the objective space to the design space. Defined in Table 15 is the exploration region considered on the basis of the variable ranges displayed in the right-hand side of Figure 62, which contain a desirable set of the Pareto points identified by means of *Filtering*.

FNslst = [12360 - 12677] decaN
Awing = [153.7 - 157.0] m^2
span = [38.7 - 39.9] m
phi = [26.6 - 27.8] deg
tuc = [0.079 - 0.083]
Fuel = [16149 - 16463] kg
BPR = [7.05 - 7.35]

Table 15. Definition of the design sub-space to explore.

Within such design sub-space, 79 distinct function evaluations were performed and stored throughout the optimisation procedure described in Section 6.3. The validation of the surrogate models was conducted by considering the proposed procedure, and 24 additional evaluations were required.

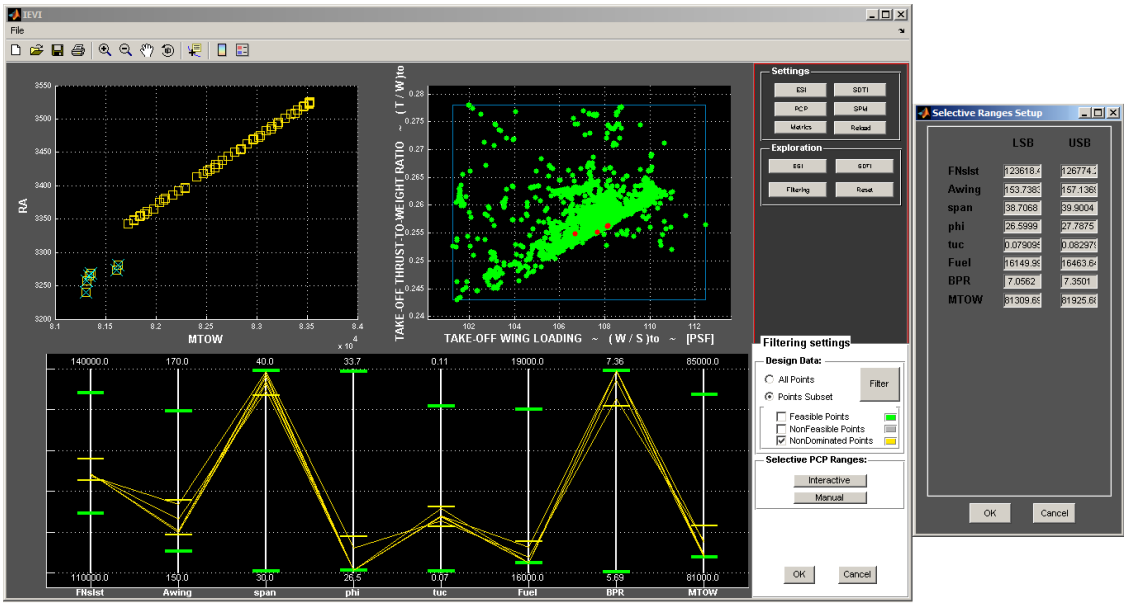

Figure 62. Setup of the design sub-region to be explored in addressing the design change problem taken into account.

The *Problem Reformulation* phase was conducted as indicated in sub-section 5.3.2 by considering the sought design values and the variables ranges given in Table 15. The goals and weighting coefficients vectors were therefore set as follows:

Parameter	**Goals**	**Weighting Coefficients**
RA	$F^*_{RA} = 3258.163$ [NM]	$w_{RA} = 0.075949$ (1/13.167)
MTOW	$F^*_{MTOW} = 81311.8282$ [kg]	$w_{MTOW} = 0.075949$ (1/13.167)
tofl	$F^*_{tofl} = 1999.9888$ [m]	$w_{tofl} = 0.075949$ (1/13.167)
vapp	$F^*_{vapp} = 119.5601$ [kts]	$w_{vapp} = 0.075949$ (1/13.167)
vz_clb	$F^*_{vz\_clb} = 611.2451$ [ft/min]	$w_{vz\_clb} = 0.075949$ (1/13.167)
Kfn_cth	$F^*_{Kfn\_cth} = 0.8692$	$w_{Kfn\_cth} = 0.075949$ (1/13.167)
Kff	$F^*_{Kff} = 0.7496$	$w_{Kff} = 0.075949$ (1/13.167)

FNslst	$F^*_{\text{FNslst}} = 12459.8829$ [decaN]	$w_{\text{FNslst}} = 0.075949$ (1/13.167)
Awing	$F^*_{\text{Awing}} = 156$ [m^2]	$w_{\text{Awing}} = 0.012658$ (1/79)
span	$F^*_{\text{span}} = 39.3967$ [m]	$w_{\text{span}} = 0.075949$ (1/13.167)
phi	$F^*_{\text{phi}} = 26.6022$ [deg]	$w_{\text{phi}} = 0.075949$ (1/13.167)
tuc	$F^*_{\text{tuc}} = 0.0811$	$w_{\text{tuc}} = 0.075949$ (1/13.167)
Fuel	$F^*_{\text{Fuel}} = 16150.0362$ [kg]	$w_{\text{Fuel}} = 0.075949$ (1/13.167)
BPR	$F^*_{\text{BPR}} = 7.35$	$w_{\text{BPR}} = 0.075949$ (1/13.167)

Table 16. Goals and weighting coefficients vectors considered for the first hypothetic design change scenario.

For the *Design Exploration* phase, a maximum number of 10 iterations (for demonstration purposes) and an EI threshold of 1e-6 were considered as stopping criteria. Shown in Table 17 and Table 18 are the values in the design space and in the objective/constraint spaces of the obtained solutions.

Solution	**FNslst [decaN]**	**Awing [m^2]**	**span [m]**	**phi [deg]**	**tuc**	**Fuel [kg]**	**BPR**
Point Nº1	12413.7723	155.2909	39.1304	26.7299	0.0823	16188.5493	7.0576
Point Nº2	12514.2720	154.4322	39.5099	27.0070	0.0809	16158.3488	7.2671
Point Nº3	12360.4763	155.5095	39.1912	26.7494	0.0806	16231.2857	7.0500
Point Nº4	12381.9779	155.2452	38.7000	26.6000	0.0809	16282.0092	7.1553
Point Nº5	12427.9335	153.9732	38.7000	26.6000	0.0811	16150.0389	7.0500
Point Nº6	12390.2049	155.6729	38.7000	26.6000	0.0802	16150.0000	7.0500
Point Nº7	12360.0000	154.7547	38.7000	26.6000	0.0807	16150.0000	7.3497
Point Nº8	12373.4535	155.2175	38.7000	26.6000	0.0804	16150.0000	7.0500
Point Nº9	12401.6466	154.3775	38.7127	26.7087	0.0809	16150.0000	7.3500
Point Nº10	12392.6792	155.9816	39.0397	27.2856	0.0802	16186.8461	7.3242

Table 17. Variable values of the solutions obtained for the goals and weights vectors in Table 16.

Solution	**MTOW [kg]**	**RA [NM]**	**tofl [m]**	**vapp [kts]**	**vz_clb [ft/min]**	**Kfn_cth**	**Kff**
Point Nº1	81387.0478	3227.2630	1993.3017	119.1041	585.0289	0.8771	0.7739
Point Nº2	81410.2602	3265.2606	1992.0532	119.5252	633.6000	0.8622	0.7499
Point Nº3	81411.6266	3247.3621	2000.1842	119.0066	580.4757	0.8778	0.7504
Point Nº4	81421.3703	3241.7373	2000.1183	119.0482	565.3548	0.8833	0.7501
Point Nº5	81215.2647	3220.5145	2000.1169	119.4708	589.8470	0.8762	0.7499
Point Nº6	81280.7084	3212.7474	1985.5658	118.8766	573.7437	0.8809	0.7499
Point Nº7	81220.7526	3232.7661	2000.2666	119.1739	564.4743	0.8837	0.7500

Point Nº8	81246.0959	3215.3671	1992.8665	119.0192	571.7611	0.8814	0.7500
Point Nº9	81234.0024	3236.8531	2000.1679	119.3478	578.1897	0.8797	0.7500
Point Nº10	81419.4492	3257.9607	1991.7120	118.9542	587.4952	0.8759	0.7500

Table 18. Objective and constraint values of the solutions obtained for the goals and weights vectors in Table 16.

The comparison between the sought point and the explored designs in terms of value differences is given in Table 19 and Table 20.

Solution	**FNslst $_{diff}$ [decaN]**	**Awing $_{diff}$ [m^2]**	**span $_{diff}$ [m]**	**phi $_{diff}$ [deg]**	**tuc $_{diff}$**	**Fuel $_{diff}$ [kg]**	**BPR $_{diff}$**
Point Nº1	-46.1106	-0.7091	-0.2663	+0.1277	+0.0012	+38.5131	-0.2924
Point Nº2	+54.3891	-1.5678	+0.1132	+0.4048	-0.0002	+8.3126	-0.0829
Point Nº3	-99.4066	-0.4905	-0.2055	+0.1472	-0.0005	+81.2495	-0.3000
Point Nº4	-77.9050	-0.7548	-0.6967	-0.0022	-0.0002	+131.9730	-0.1947
Point Nº5	-31.9494	-2.0268	-0.6967	-0.0022	+0.0000	+0.0027	-0.3000
Point Nº6	-69.6780	-0.3271	-0.6967	-0.0022	-0.0009	-0.0362	-0.3000
Point Nº7	-99.8829	-1.2453	-0.6967	-0.0022	-0.0004	-0.0362	-0.0003
Point Nº8	-86.4294	-0.7825	-0.6967	-0.0022	-0.0006	-0.0362	-0.3000
Point Nº9	-58.2363	-1.6225	-0.6840	+0.1065	-0.0002	-0.0362	+0.0000
Point Nº10	-67.2037	-0.0184	-0.3570	+0.6834	-0.0009	+36.8099	-0.0258

Table 19. Differences between the variable values of the explored designs and the sought point.

Solution	**MTOW $_{diff}$ [kg]**	**RA $_{diff}$ [NM]**	**tofl $_{diff}$ [m]**	**vapp $_{diff}$ [kts]**	**vz_clb $_{diff}$ [ft/min]**	**Kfn_cth $_{diff}$**	**Kff $_{diff}$**
Point Nº1	+75.2196	-30.9000	-6.6871	-0.4560	-26.2162	+0.0079	+0.0243
Point Nº2	+98.4320	+7.0976	-7.9356	-0.0349	+22.3549	-0.0070	+0.0003
Point Nº3	+99.7984	-10.8009	+0.1954	-0.5535	-30.7694	+0.0086	+0.0008
Point Nº4	+109.5421	-16.4257	+0.1295	-0.5119	-45.8903	+0.0141	+0.0005
Point Nº5	-96.5635	-37.6485	+0.1281	-0.0893	-21.3981	+0.0070	+0.0003
Point Nº6	-31.1198	-45.4156	-14.423	-0.6835	-37.5014	+0.0117	+0.0003
Point Nº7	-91.0756	-25.3969	+0.2778	-0.3862	-46.7708	+0.0145	+0.0004
Point Nº8	-65.7323	-42.7959	-7.1223	-0.5409	-39.4840	+0.0122	+0.0004
Point Nº9	-77.8258	-21.3099	+0.1791	-0.2123	-33.0554	+0.0105	+0.0004
Point Nº10	+107.6210	-0.2023	-8.2768	-0.6059	-23.7499	+0.0067	+0.0004

Table 20. Differences between the objective and constraint values of the explored designs and the sought point.

The designer is provided with a set of different alternatives to address the design change problem at hand. The solution that best accommodates the sought change in *Awing*

(+1.31%) turns out to be Point Nº10. Minor changes involve most of the remaining design parameters, although an increment of 0.28% and 0.13% are required on *Fuel* and *MTOW*, respectively. However, an improvement of 0.41% is achieved on *tofl*, whereas *vz_clb* remains to be largely satisfied notwithstanding its reduction of 3.88%.

Alternatively, the proposed isocontour approach can be deployed for the exploration of design solutions that may introduce the required change in *Awing* to the detriment of any other variable, ensuring at the same time desirable performance in terms of objectives and constraints. Depicted in Figure 63 are the isocontours of all the objectives and constraints passing through $\mathbf{x}^*$ (Table 14) in the plane *FNslst-Awing*. The details of their computation are provided in Table 21.

Parameter	Initial Mesh $[\Delta_t^1 s^1, \Delta_t^2 s^2]$	Tolerance	Total Evaluations	Nº Isopoints
MTOW	[10 decaN, 0.5 m^2]	1 kg	254	32
RA	[10 decaN, 0.5 m^2]	0.1 NM	826	98
tofl	[10 decaN, 0.5 m^2]	0.1 m	345	40
vapp	[10 decaN, 0.5 m^2]	0.01 kts	753	102
vz_clb	[10 decaN, 0.5 m^2]	0.1 ft/min	290	28
Kfn_cth	[10 decaN, 0.5 m^2]	0.001	94	15
Kff	[10 decaN, 0.5 m^2]	0.001	606	100

Table 21. Summary of the isocontours computation.

There are two further aspects that need to be mentioned. Firstly, the isocontours of *Kfn_cth* and *vz_clb* can be considered in this particular case to be coincident, as well as in the case of *MTOW* and *tofl*. Moving along these lines gives us the advantage of preserving two performances (within their corresponding tolerances) instead of one. Secondly, within the considered *FNslst* range of [12000 – 13000] decaN, the requested value of *Awing* can be achieved only by freezing the values of one of the pairs of abovementioned parameters (either *Kfn_cth* and *vz_clb*, or *MTOW* and *tofl*). Other performance may be assured only for lower (*RA*) or larger (*vapp*) values of *FNslst*.

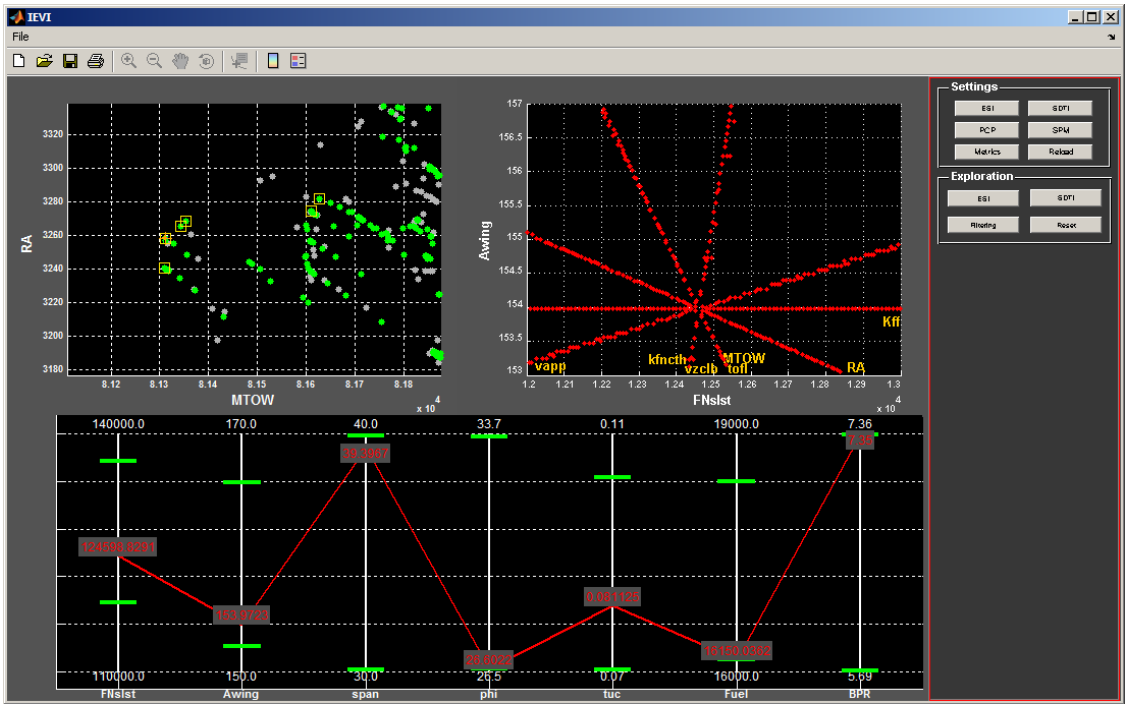

Figure 63. Isocontours of objectives and constraints.

A second hypothetic design change scenario was taken into consideration by assuming that, apart form the increment requested for *Awing*, a reduction of *tofl* to 1900 m is also required. To address it, the goals and weighting coefficients vectors were redefined as follows:

Parameter	**Goals**	**Weighting Coefficients**
RA	$F^*_{RA} = 3258.163$ [NM]	$w_{RA} = 0.081967$ (1/12.2)
MTOW	$F^*_{MTOW} = 81311.8282$ [kg]	$w_{MTOW} = 0.081967$ (1/12.2)
tofl	$F^*_{tofl} = 1900$ [m]	$w_{tofl} = 0.0081967$ (1/122)
vapp	$F^*_{vapp} = 119.5601$ [kts]	$w_{vapp} = 0.081967$ (1/12.2)
vz_clb	$F^*_{vz\_clb} = 611.2451$ [ft/min]	$w_{vz\_clb} = 0.081967$ (1/12.2)
Kfn_cth	$F^*_{Kfn\_cth} = 0.8692$	$w_{Kfn\_cth} = 0.081967$ (1/12.2)
Kff	$F^*_{Kff} = 0.7496$	$w_{Kff} = 0.081967$ (1/12.2)
FNslst	$F^*_{FNslst} = 12459.8829$ [decaN]	$w_{FNslst} = 0.081967$ (1/12.2)
Awing	$F^*_{Awing} = 156$ [m^2]	$w_{Awing} = 0.0081967$ (1/122)
span	$F^*_{span} = 39.3967$ [m]	$w_{span} = 0.081967$ (1/12.2)

phi	$F^*_{phi} = 26.6022$ [deg]	$w_{phi} = 0.081967$ (1/12.2)
tuc	$F^*_{tuc} = 0.0811$	$w_{tuc} = 0.081967$ (1/12.2)
Fuel	$F^*_{Fuel} = 16150.0362$ [kg]	$w_{Fuel} = 0.081967$ (1/12.2)
BPR	$F^*_{BPR} = 7.35$	$w_{BPR} = 0.081967$ (1/12.2)

Table 22. Goals and weighting coefficients vectors considered for the second hypothetic design change scenario.

The rest of the setup parameters were not modified.

One solution has thus been obtained. Its variable and objective/constraint values are given in Table 23 and Table 24.

Solution	FNslst [decaN]	Awing [m^2]	span [m]	phi [deg]	tuc	Fuel [kg]	BPR
Point N°1	12677.0000	157.0000	38.7000	26.6000	0.0795	16150.0000	7.0500

Table 23. Variable values of the solutions obtained for the goals and weights vectors in Table 22.

Solution	MTOW [kg]	RA [NM]	tofl [m]	vapp [kts]	vz_clb [ft/min]	Kfn_cth	Kff
Point N°1	81532.8646	3200.4884	1935.2027	118.602	635.1924	0.8642	0.7494

Table 24. Objective and constraint values of the solutions obtained for the goals and weights vectors in Table 22.

The solution is compared with the sought point in Table 25 and Table 26.

Solution	FNslst $_{diff}$ [decaN]	Awing $_{diff}$ [m^2]	span $_{diff}$ [m]	phi $_{diff}$ [deg]	tuc $_{diff}$	Fuel $_{diff}$ [kg]	BPR $_{diff}$
Point N°1	+217.1170	+1.0000	-0.6967	-0.0022	-0.0016	-0.0362	-0.3000

Table 25. Differences between the variable values of the explored designs and the sought point.

Solution	MTOW $_{diff}$ [kg]	RA $_{diff}$ [NM]	tofl $_{diff}$ [m]	vapp $_{diff}$ [kts]	vz_clb $_{diff}$ [ft/min]	Kfn_cth $_{diff}$	Kff $_{diff}$
Point N°1	+221.0364	-57.6746	+35.2027	-0.9581	+23.9473	-0.0050	-0.0002

Table 26. Differences between the objective and constraint values of the explored designs and the sought point.

In this case, the additional pursuit of the second change objective (*tofl*) resulted in an over-attainment of the requested valued for *Awing* (+0.63%). Moreover, a considerable increment was necessary with respect to the sought values of *FNslst* (+1.74%) and *MTOW* (+0.27%), together with a significant reduction of 1.77% for *RA*.

A third scenario was finally analysed in the light of those cases where the exploration of further solutions in the objective space areas with a low density of Pareto points is formulated as a design change problem. Let us thus assume that, containing as much as possible the design features of $\mathbf{x}^*$, the designer is interested in the computation of solutions in the neighbourhood of the point [81500 kg, 3300 NM] in the objective space (see Figure 63). The goals and weighting coefficients vectors can therefore be defined as follows:

Parameter	**Goals**	**Weighting Coefficients**
RA	$F^*_{RA} = 3300$ [NM]	$w_{RA} = 0.005494$ (1/182)
MTOW	$F^*_{MTOW} = 81500$ [kg]	$w_{MTOW} = 0.005494$ (1/182)
tofl	$F^*_{tofl} = 1999.9888$ [m]	$w_{tofl} = 0.082418$ (1/12.133)
vapp	$F^*_{vapp} = 119.5601$ [kts]	$w_{vapp} = 0.082418$ (1/12.133)
vz_clb	$F^*_{vz\_clb} = 611.2451$ [ft/min]	$w_{vz\_clb} = 0.082418$ (1/12.133)
Kfn_cth	$F^*_{Kfn\_cth} = 0.8692$	$w_{Kfn\_cth} = 0.082418$ (1/12.133)
Kff	$F^*_{Kff} = 0.7496$	$w_{Kff} = 0.082418$ (1/12.133)
FNslst	$F^*_{FNslst} = 12459.8829$ [decaN]	$w_{FNslst} = 0.082418$ (1/12.133)
Awing	$F^*_{Awing} = 153.9723$ [m^2]	$w_{Awing} = 0.082418$ (1/12.133)
span	$F^*_{span} = 39.3967$ [m]	$w_{span} = 0.082418$ (1/12.133)
phi	$F^*_{phi} = 26.6022$ [deg]	$w_{phi} = 0.082418$ (1/12.133)
tuc	$F^*_{tuc} = 0.0811$	$w_{tuc} = 0.082418$ (1/12.133)
Fuel	$F^*_{Fuel} = 16150.0362$ [kg]	$w_{Fuel} = 0.082418$ (1/12.133)
BPR	$F^*_{BPR} = 7.35$	$w_{BPR} = 0.082418$ (1/12.133)

Table 27. Goals and weighting coefficients vectors considered for the third hypothetic design change scenario.

The solutions obtained are shown in Table 28 and Table 29, and visualised in the objective space in Figure 64.

Solution	FNslst [decaN]	Awing [m^2]	span [m]	phi [deg]	tuc	Fuel [kg]	BPR
Point Nº1	12419.9317	155.2771	39.7979	26.6000	0.0806	16212.9448	7.3500
Point Nº2	12399.0854	157.0000	38.7000	26.6000	0.0796	16177.7627	7.3500
Point Nº3	12439.0820	156.4153	38.7225	26.6000	0.0798	16150.0000	7.0776
Point Nº4	12430.8816	154.7818	38.7000	26.6000	0.0811	16292.5960	7.3265
Point Nº5	12423.4814	155.3113	39.3226	26.9951	0.0804	16150.0000	7.3500
Point Nº6	12425.4972	155.0310	39.8922	26.8793	0.0807	16197.8212	7.3066
Point Nº7	12360.0000	157.0000	39.9000	26.6000	0.0795	16150.0000	7.3500
Point Nº8	12421.0789	155.3455	39.9000	26.6000	0.0809	16284.3367	7.0500
Point Nº9	12504.6958	156.8268	38.7000	27.6943	0.0830	16150.0000	7.3500
Point Nº10	12428.1448	156.1230	39.2564	26.9765	0.0800	16150.0000	7.0500

Table 28. Variable values of the solutions obtained for the goals and weights vectors in Table 30.

Solution	MTOW [kg]	RA [NM]	tofl [m]	vapp [kts]	vz_clb [ft/min]	Kfn_cth	Kff
Point Nº1	81473.0253	3275.5760	1996.2084	119.1462	604.2699	0.8705	0.7500
Point Nº2	81398.6873	3225.2458	1971.7620	118.4551	562.7572	0.8845	0.7499
Point Nº3	81353.8309	3210.1270	1971.1925	118.6607	582.0925	0.8786	0.7499
Point Nº4	81445.5907	3253.3927	2000.0336	119.2387	574.8333	0.8808	0.7499
Point Nº5	81371.4209	3258.8218	1992.1079	119.1568	601.8176	0.8716	0.7500
Point Nº6	81466.4735	3281.7970	1999.9834	119.2903	615.7182	0.8667	0.7500
Point Nº7	81455.6452	3260.8663	1980.8984	118.5320	588.5861	0.8749	0.7496
Point Nº8	81569.8768	3275.0031	2000.0353	119.1432	609.5826	0.8684	0.7506
Point Nº9	81502.4854	3224.8870	1968.6395	118.8035	593.1720	0.8756	0.7959
Point Nº10	81402.0466	3237.0355	1981.4789	118.8718	603.3069	0.8711	0.7500

Table 29. Objective and constraint values of the solutions obtained for the goals and weights vectors in Table 30.

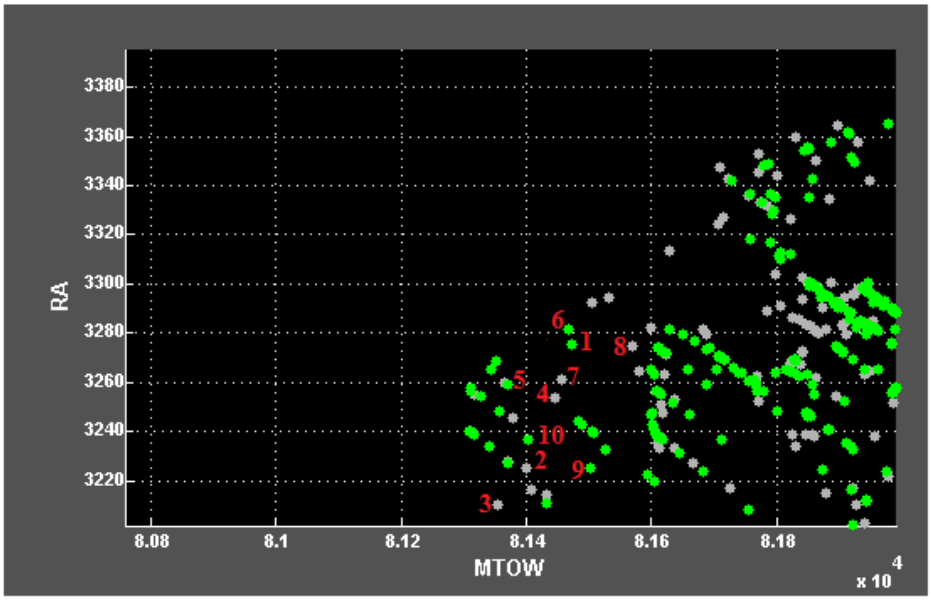

Figure 64. Identification of the obtained solutions in the objective space.

Considering the three scenarios, it can be verified that the proposed relaxation approach for constraint handling allows the computation of points located in the vicinity of constraint limits. This is particularly evident for *Kff*. In some cases it led to the evaluation of points slightly infeasible (e.g. points Nº 2, 3, 4, and 7 in Table 29). In the current context, however, such constraint violation can be considered as a minor change propagation among constraints to allow the accommodation of required changes. Hence, the designer may permit a minor relaxation of particular constraints if one of the explored alternatives represents a promising solution.

Ultimately, mention should be made of some design-variable values of the solutions in Table 28. Numerous points are located along or in the vicinity of the considered design sub-space bounds. Therefore, in the event none of the explored alternatives is considered to be satisfactory, it may be convenient, if possible, to relax the exploration design sub-space before considering a reformulation of the goals vector.

6.6. Summary and Conclusions

In this chapter, the integrated application of the three exploration methodologies proposed is shown. Their capabilities are demonstrated by taking into consideration a multi-objective optimisation problem with a test case provided by industrial partners and described in Section 6.2.

The Adaptive Search Optimisation Method (ASOM) presented in Chapter 3 was firstly deployed in Section 6.3 to conduct an adaptive definition of the search region throughout the optimisation procedure. This allowed a controlled relaxation of the search region into feasible areas of the design space, as well as a partial exclusion of infeasible regions from the optimisation search. It has been shown that the resulting improvement of the Pareto front is local, due to the capture of optimal points located slightly beyond the initial variables bounds, as intended. Future work can be focused on the improvement of the Pareto front on a larger range of the criterion space, either through an optimal setup of the SPSA parameters, or via the development of further hybrid algorithms.

In a second instance, the analysis of the ASOM results was conducted in Section 6.4 by means of the visual exploration methodology presented in Chapter 4. The graphical user interface prototype *IEVI* was deployed to demonstrate the interactive use of multiple integrated data views in addressing a number of common analysis tasks required for the assessment of optimisation results. The practical advantages in using the *Filtering* function were highlighted for the study of subsets of points corresponding to specific analysis criteria (e.g. satisfaction/activation/tightening of constraints, identification of *optimal families* of solutions). It was also shown that the trade-off study of optimisation results can be enhanced through the interactive selection of design points of interest, thus allowing both an individual detailed analysis of solutions, as well as the comparison of different alternatives. An example of the integration of *discipline-dependent techniques* was given with the visualisation of carpet plots in the *SDTI*.

Finally, in Section 6.5, the capabilities of the third exploration methodology proposed in Chapter 5 were demonstrated with the same test case for three hypothetic design change scenarios. The use of the proposed visual exploration methodology to facilitate the definition of the design sub-space to explore was firstly illustrated. This can be potentially enhanced by directing future work efforts on the visualisation of the surrogate

models at hand, which would help the identification of promising design basins where to focus the whole exploration process. The search of additional design solutions was then concentrated on tackling each one of the scenarios, demonstrating the method capabilities in addressing the change of variables, objectives and constraints. An arbitrary example of the setup of the goals and weight coefficients vectors was provided in each case. The resulting explored sets of points indicate the different design alternatives to accommodate a desirable change. Their computation proved also the capabilities of the proposed relaxation approach for constraint handling in evaluating points located in the vicinity of constraint limits.

Chapter 7

Summary and Conclusions

7.1. Introduction

This chapter concludes the main body of the thesis. A summary of the work is first provided in Section 7.2. The main contributions of research are then summarised in Section 7.3. The recommendations for future work are finally discussed in Section 7.4.

7.2. Summary of Research

The research presented in this thesis has been conducted to develop an effective design exploration methodology in the context of conceptual engineering design optimisation. Three specific needs have been identified, which led to the definition of the research objectives.

Work was first concentrated on developing an effective visualisation methodology for the analysis and exploration of optimisation results. An approach based on the use of multiple data views was taken into consideration to enable the designer to address common data analysis scenarios occurring in deterministic and robust optimisation. To

this aim, a state-of-the-art investigation was firstly conducted to identify the most suitable visualisation techniques. A specific set of interactive visualisation interfaces was thus established to synergistically integrate both *discipline-independent* and *discipline-dependent* techniques. Particular attention was focused on allowing the designer to gain insight into the problem at hand without the need to be an expert in numerical optimisation methods. The methodology was also intended to support the definition of optimisation architectures by building, debugging, and understanding the algorithms and models to be used.

In a second stage, the research efforts were aimed at addressing other aspects of design exploration in engineering optimisation, which are mainly related to *what-if* scenarios.

To support the formulation of optimisation problems, attention was focused on enhancing the statement of functional and design-variable constraints that may be considered as flexible to some degree or not straightforward for some reason, e.g. problem complexity or lack of knowledge. With respect to the variables bounds, it was demonstrated that even a minor relaxation of one design-variable constraint can potentially lead to a significant improvement of the Pareto front (Appendix B). In other cases, instead, computational efforts could be reduced by partially excluding infeasible regions of the design space via an adequate tightening of specific variables bounds. Similar considerations were also made with respect to the limits of functional constraints (Appendix C). To tackle such issues, the development of a numerical method for an adaptive formulation of functional and design-variable constraints was undertaken.

Finally, an effective methodology to assist the introduction of changes affecting conceptual design was sought. It would provide a means to explore different design alternatives for accommodating changes deriving from unplanned iterations, which may arise because of the inherent iterative nature of design processes. Additionally, available prior computational analysis information should be reused to minimise computational efforts and time, especially when the whole design process has been disrupted until the change cycle is accomplished. To achieve this, research was centred on the development and integration of adequate methods from design optimisation to address three major issues: reuse and exploitation of prior evaluations, problem reformulation by considering the new design requirements causing the change, and efficient exploration of design

solutions representing the best trade-offs for change accommodation with minimum disruption to the product configuration.

The development of the three methodologies was carried out by considering an analytical example. Their evaluation was conducted with an aircraft sizing test case supplied by a major airframe manufacturer, with the intent of demonstrating the applicability in addressing problems of industrial relevance.

7.3. Contributions to Knowledge

The main contributions of the present thesis to the research in engineering design can be summarised as follows:

- A novel method for an adaptive formulation of design-variable constraints throughout the optimisation process. It enables a recurrent re-definition of any variables bounds on the strength of the analysis of the distributions of the feasible evaluations via *ad hoc* statistical criteria that do not require specific distributional assumptions for the design variables. This allows to both enhance the Pareto front computation through the exploration of further points initially not contained in the feasible design set, as well as to reduce the re-formulation iterations required for a correct statement of optimisation problems.

- The introduction of a synergistic integration of suitable visualisation techniques to address common data analysis scenarios occurring in design optimisation. It allows an interactive analysis of large multidimensional datasets to effectively support the evaluation and comparison of results, the identification of points that best satisfy specific design criteria, and the development, debugging and understanding of algorithms and models. Different data perspectives are provided by combining *discipline-independent* and *discipline-dependent* techniques, without the need for the user to be an expert in numerical optimisation methods.

- A novel strategy to address design change problems in the context of conceptual design. The exploration of solutions that best balance the accommodation of the required change while limiting its propagation is achieved through the integration of key concepts from global attainment and Bayesian global optimisation methods. Furthermore, the use of surrogate models allows to retrieve and re-use any available prior computational analysis information.

- The extension of the expected improvement criterion of Bayesian global optimisation methods for constraints handling. The evaluation of points located in the vicinity of constraint boundaries is possible by means of a local relaxation of constraints in proportion to the standard error associated with their prediction.

- A computationally efficient method for the computation of objectives and constraints isocontours. By exploiting the principles and advantages of pattern search methods, no assumptions of differentiability are required, which makes the method well suited for applications where derivatives are not available and finite-difference derivatives are unreliable. Furthermore, the application of the suggested approach generally shows a more efficient and accurate isocontours computation with respect to algorithms based on the evaluation of grid points obtained via a discretization of the design space.

7.4. Future Work

Future work can be directed on enhancing the capabilities of ASOM to allow an improvement of the Pareto front on a larger range of the criterion space. To achieve this, an adequate setup of the SPSA parameters, or the development of further hybrid algorithms may be considered.

The proposed method for a local relaxation of soft constraints has been developed for single-objective optimisation problems. Suitable numerical strategies could be identified for its extension to the multi-objective case. Particular attention should be focused on

addressing those situations where the relaxation of a soft-constraint may lead to the improvement of one objective, but to the detriment of others.

With respect to the present visualisation methodology for the analysis of optimisation results, it might be convenient to contemplate the possibility of partially allowing to change on-the-fly the formulation of robust objectives and constraints. This would be particularly advantageous for the visualisation of any RDO objective/constraint $h(\mathbf{x})$ formulated by using loss or utility functions within a given distributional assumption, as suggested by Padulo [86]. The effects of considering a different satisfaction probability and alternative assumptions on the output distributions can thus be explored for any design solution through the re-estimation of the coefficient k_h.

Lastly, the proposed isocontours method could be extended to enable the computation of robust objectives and constraints isocontours. A potential strategy is via the integration of adequate uncertainty propagation algorithms which would allow to exploit the evaluations conducted during the *Mesh Evaluation* phase to estimate the propagation of input uncertainty to model outputs.

References

[1] 777-200/300 Airplane Characteristics for Airport Planning, Boeing Commercial Airplanes, Document D6-58329, Revision C, December 2008. http://www.boeing.com/commercial/cmo/freighter.html. (accessed 12th July 2009).

[2] Adeli, H., Ed. (1994). *Advances in Design Optimization*, Chapman and Hall, London.

[3] Agarwal, H., Gano, S.E., Renaud, J.E., Perez, V.M. and Watson, L.T. (2007), Homotopy methods for constraint relaxation in unilevel reliability based design optimization. *Engineering Optimization*, Vol. 41, No 6, pp. 593-607.

[4] Agrawal, G., Lewis, K., Chugh, K., Huang, C.-H., Parashar, S., and Bloebaum, C. L. (2004). Intuitive Visualization of Pareto Frontier for Multi-Objective Optimization in n-Dimensional Performance Space. In: *10th AIAA/ISSMO Multidisciplinary Analysis and Optimization Conference*, Albany, New York, 30 August - 1 September 2004.

[5] Antoine, N.E. and Kroo, I.M. (2005). Framework for Aicraft Conceptual Design and Environmental Performance Studies. *AIAA Journal*, Vol. 43, No. 10, pp. 2100-2109.

[6] Amarger, R.J., Biegler, L.T. and Grossmann, I.E. (1992). An automated modelling and reformulation system for design optimization. *Computers & Chemical Engineering*, Vol. 16, No. 7, pp. 623-636.

[7] Anon, Annex 14 to the Convention on International Civil Aviation, Vol. I: Aerodrome Design and Operations, ICAO, 2004.

[8] Anon, The Second Meeting of the Regional Airspace Safety Monitoring Advisory Group (RASMAG/2), Review of the report of the Eighth Meeting of the FANS Interoperability Team (FIT/8) of the Informal Pacific ATC Coordinating Group (IAPCG), International Civil Aviation, Bangkok, Thailand, 4-8 October 2004.

[9] Balabanov, V.O. and Venter G. (2004). Multi-Fidelity Optimization with High-Fidelity Analysis and Low-Fidelity Gradients. In: *10th AIAA/ISSMO Multidisciplinary Analysis and Optimization Conference*, Albany, New York, 20 August – 1 September 2004.

[10] Baldonado, M.Q.W., Woodruff, A. and Kuchinsky, A. (2000). Guidelines for Using Multiple Views in Information Visualization. In: *Proceedings of the working conference on advanced visual interfaces*, Palermo, Italy, May 2000, pp. 110-119.

[11] Balling, R. (1999). Design by shopping: a new paradigm?. In: *Proceedings of the Third World Conference of Structural and Multidisciplinary Optimization (WCSMO-3)*, Buffalo, NY, 17-21 May 1999, Vol. 1. Cited in: Xiaolong, Z., Simpson, T., Frecker, M. and Lesieutre, G. (2010). Supporting knowledge exploration and discovery in multi-dimensional data with interactive multiscale visualisation. *Journal of Engineering Design*, First published on: 23 June2010.

[12] Bennett, G. (1965). Upper bounds on the moments and probability inequalities for the sum of independent, bounded random variables. *Biometrika*, Vol. 52, No.3-4, pp. 559-569.

[13] Bertsimas, D. and Popescu, I. (2005). Optimal Inequalities in Probability Theory: A Convex Optimization Approach. *SIAM Journal on Optimization*, Vol. 15, No. 3, pp. 780-804.

[14] Birch, N.T. (2000). 2020 vision: the prospects for large civil aircraft propulsion. *The Aeronautical Journal*, Vol. 104, No. 1038, pp. 347-352.

[15] Boeing Commercial Airplanes, Current Market Outlook 2008-2027. http://www.boeing.com/commercial/cmo/freighter.html. (accessed 22th September 2009).

[16] Bond, A. H. and Ricci, R.J. (1992). Cooperation in Aircraft Design. *Research in Engineering Design*, Vol. 4, pp. 115-130.

[17] Braha, D. and Bar-Yam, Y. (2004). Topology of large-scale engineering problem-solving networks. *Physical Review E*, Vol. 69.

[18] Braha, D. and Maimon, O. (1998). *A Mathematical Theory of Design: Foundations, Algorithms, and Applications*. Kluwer Academic Publishers, Norwell, MA, USA.

[19] Chen, Y.L. and Liu C.-C. (1994). Multiobjective VAR planning using the goal-attainment method". In: *IEE Proceedings on Generation, Transmission and Distribution*, Vol. 141, No. 3, pp. 227-232.

[20] Clarkson, P.J., Simons, C. and Eckert, C. (2001). Predicting change propagation in complex design". In: *Proceedings of ASME Design Engineering Technical Conferences & Computers and Information in Engineering Conference*, Pittsburgh, Pennsylvania, September 9-12 2001.

[21] De Weck, O.L. (2001). *Multivariable Isoperformance Methodology for Precision Opto-Mechanical Systems*. PhD Thesis, Massachusetts Institute of Technology, Cambridge.

[22] De Weck, O.L. and Jones, M.B. (2006). Isoperformance: Analysis and Design of Complex Systems with Desired Outcomes. *Systems Engineering*, Vol. 9, No. 1.

[23] De Weck, O., Agte, J., Sobieszczanski-Sobieski, J., Arendsen, P., Morris, A. and Spieck, M. (2007). State-of-the-Art and Future Trends in Multidisciplinary Design Optimization. In: *Proceedings of the 48th AIAA/ASME/ASCE/AHS/ASC Structures, Structural Dynamics, and Materials Conference*, Honolulu, Hawaii, 23-26 April 2007.

[24] Deb, K. (1995). *Optimization for engineering design: algorithms and examples*, Prentice-Hall of India Private Limited, New Delhi.

[25] Demuth, H. and Beale M. (2001). *Neural Network Toolbox (For Use with MATLAB)*, The MathWorks, User's Guide version 4.

[26] Deremaux, Y., Willcox, K. and Haimes, R. (2003). Physically-Based, Real-Time Visualization and Constraint Analysis in Multidisciplinary Design Optimization, AIAA Paper 3876.

[27] Devroye, L., Györfi, L., and Lugosi G. (1996). *A probabilistic Theory of Pattern Recognition*, Springer-Verlag, New York.

[28] Eckert, C., Clarkson, P.J. and Zander, W. (2004). Change and customisation in complex engineering domains. *Research in Engineering Design*, Vol. 15, pp. 1-21.

[29] Eckert, C.M., Keller, R., Earl, C. and Clarkson, P.J. (2006). Supporting change process in design: Complexity, prediction and reliability. *Reliability Engineering and System Safety*, Vol. 91, No. 12, pp.1521-1534.

[30] Evbuomwan, N.F.O., Sivaloganathan, S. and Jebb, A. (1996). A survey of design philosophies, models, methods and systems. *Journal of Engineering Manufacture*, Vol. 210, pp. 301-320.

[31] Fantini, P. (2007). *Improving the Effectiveness of Multi-Disciplinary Design Optimization at the Aircraft Conceptual Design Phase*. Ph.D. Thesis, Aerospace Engineering Department, Cranfield University, UK.

[32] Fletcher, R. (1987). *Practical Methods of Optimization*, 2nd ed., John Wiley and Sons, New York.

[33] Folkestad, J.E. and Johnson, R.L. (2002). Integrated rapid prototyping and rapid tooling (IRPRT). *Integrated Manufacturing Systems*, Vol. 13, No. 2, pp. 97-103.

[34] Forrester, A.I.J., Sobester, A. and Keane, A.J. (2007). Multi-fidelity optimization via surrogate modelling. In: *Proceedings of the Royal Society A*, Vol. 463, No. 2088, pp. 3251-3269.

[35] Fricke, E. and Schulz, A.P. (2005). Design for changeability (DfC): Principles To Enable Changes in Systems Throughout Their Entire Lifecycle. *Systems Engineering*, Vol. 8, No. 4, pp. 342-359.

[36] Gembicki, F.W. (1974). *Performance and Sensitivity Optimization: A Vector Index Approach*. PhD Thesis, Case Western Research University, Cleveland, OH.

[37] Gembicki, F.W. and Haimes, Y.Y. (1975). Approach to Performance and Sensitivity Multiobjective Optimization: The Goal Attainment Method. *IEEE Transactions on Automatic Control*, Vol. 20, No. 6, pp. 769-771.

[38] Grasmeyer, J.M. (1999). Multidisciplinary Design Optimization of a Transonic Strut-Braced Wing Aircraft. In: *37th AIAA Aerospace Sciences Meeting and Exhibit*, Reno, NV, January 11-14.

[39] Green, L.L. Lin, H.Z. and Khalessi, M.R. (2002). Probabilistic methods for uncertainty propagation applied to aircraft design. In: *Proceedings of 20th AIAA Applied Aerodynamics Conference*, St. Louis, MO, June 24-26 2002.

[40] Griethe, H. and Schumann, H. (2005). Visualizing Uncertainty for Improved Decision Making. In: *Proceeding of the 4th International Conference on Perspectives in Business Informatics Research (BIR'05)*, Skøde, Sweden.

[41] Guenov, M.D. (1996). Modeling Design Change Propagation in an Integrated Design Environment. *Computer Modeling and Simulation in Engineering*, Vol. 1, pp. 353-367.

[42] Guenov, M.D. and Barker, S.G. (2005). Application of Axiomatic Design and Design Structure Matrix to the Decomposition of Engineering Systems. *Journal of Systems Engineering*, Vol. 8, No. 1, pp. 29-40.

[43] Guenov, M.D., *PRELUDE – PREliminary and Unconventional DEsign for Global Aircraft*, VIVACE Forum-3, Toulouse, 17-19 October 2007. http://www.vivaceproject.com/content/forum3/forum3.php (accessed 12th September 2010).

[44] Guenov, M., Fantini, P., Balachandran, L., Maginot, J., Padulo, M. and Nunez, M. (2010). Multidisciplinary Design Optimization Framework for the Pre Design Stage. *Journal of Intelligent and Robotic Systems*, Vol. 59, No. 3-4, pp. 223-240.

[45] Hawe, G. and Sykulski, J. (2008). Scalarizing cost-effective multi-objective optimization algorithms made possible with kriging. *The International Journal for Computation and Mathematics in Electrical and Electronic Engineering*, Vol. 27, No. 4, pp. 836-844.

[46] Holden, C.M.E. (2004). *Visualization Methodologies in Aircraft Design Optimization*. PhD Thesis, School of Engineering Sciences, University of Southampton.

[47] Holden, C.M.E. and Keane, A.J. (2004). Visualization Methodologies in Aircraft Design. In: *10th AIAA/ISSMO Multidisciplinary Analysis and Optimization Conference*, Albany, New York, 30 August - 1 September 2004.

[48] Iqbal, L.U. and Sullivan, J.P. (2008). Application of an Integrated Approach to the UAV Conceptual Design. In: *46th AIAA Aerospace Sciences Meeting and Exhibit*, Reno, Nevada, 7-10 January 2008.

[49] Jackson, P. (Ed.), *Jane's All the World's Aircraft 2006-2007*, Jane's Information Group, Alexandria, VA, USA, 2006.

[50] Jacoby, W. G. (1998). *Statistical graphics for visualizing multivariate data*, Sage Publications, Thousand Oaks, CA.

[51] Jenkinson, L.R., Simpkin, P. and Rhodes, D. (1999). *Civil Jet Aircraft Design*, Arnold, London.

[52] Jeong, S., Obayashi, S. and Yamamoto, K. (2006). A Kriging-based probabilistic method with an adaptive search region. *Engineering Optimization*, Vol. 38, No. 5, pp. 541-555.

[53] Jeong, S., Yamamoto, K. and Obayashi, S. (2004). Kriging-Based Probabilistic Method for Constrained Multi-Objective Optimization Problem, AIAA Paper 2004-6437.

[54] Jones, C.V. (1994). Visualization and Optimization. *ORSA Journal on Computing*, Vol. 6, No. 3, pp. 221-257.

[55] Jones, D.J. (2001). A Taxonomy of Global Optimization Methods Based on Response Surfaces. *Journal of Global Optimization*, Vol. 21, pp. 345-383.

[56] Jones, D.R., Schonlau, M. and Welch, W.J. (1998). Efficient global optimization of expensive black-box functions. *Journal of Global Optimization*, Vol. 13, pp. 455-492.

[57] Keane, A. J. and Nair, P. B. (2005). *Computational Approaches for Aerospace Design: The Pursuit of Excellence*, John-Wiley and Sons, New York.

[58] Keller, R., Eckert, C.M. and Clarkson, P.J. (2008). Using an engineering change methodology to support conceptual design. *Journal of Engineering Design*, Vol. 20, No. 6, pp. 571-587.

[59] Kesseler, E. and Guenov, M.D. [Eds.] (2010). Advances in collaborative civil aeronautical multidisciplinary design optimization. *Progress in Astronautics and Aeronautics*, Vol. 233, American Institute of Aeronautics and Astronautics, Reston, VA.

[60] Kingsley-Jones, M., "Airbus focuses on family commonality as it begins A350-800 detailed design", *Flight International*, 28 April 2010 (online). http://www.flightglobal.com/articles/2010/04/28/341139/airbus-focuses-on-family-commonality-as-it-begins-a350-800-detailed.html (accessed 07 November 2010).

[61] Kingsley-Jones, M., "Most XWB customers' endorse A350-800 rethink: Airbus", *Flight International*, 29 April 2010 (online). http://www.flightglobal.com/articles/2010/04/29/341140/most-xwb-customers-endorse-a350-800-rethink-airbus.html (accessed 07 November 2010).

[62] Kingsley-Jones, M., "Airbus poised to start building new higher weight A380 variant", *Flight International*, 19 May 2010 (online). http://www.flightglobal.com/articles/2010/05/18/341926/airbus-poised-to-start-building-new-higher-weight-a380.html (accessed 07 November 2010).

[63] Kohonen, T. (1990). The Self-Organizing Map. In: *Proceedings of the IEEE*, Vol. 78, No. 9, pp.1464.1480.

[64] Lambert, M. (Ed.), *Jane's All the World's Aircraft 1993-1994*, Jane's Information Group, Alexandria, VA, USA, 1993.

[65] Lee, J.J., Lukachko, S.P., Waitz, I.A. and Schafer, A. (2001). Historical and Future Trends in Aircraft Performance, Cost, and Emissions. *Annual Review of Energy Environment*, Vol. 26, pp. 167-200.

[66] Lewis, R.M., Torczon, V. and Trosset, M.W. (1998). Why Pattern Search Works. Technical report, NASA/CR-1998-208966, ICASE Report No. 98-57.

[67] Liao, W.B., Chen, Y.L. and Wang, S.C. (2002). Goal-attainment method for optimal multi-objective harmonic filter planning in industrial distribution systems.

In: *IEE Proceedings on Generation, Transmission and Distribution*, Vol. 149, No. 5, pp. 557-563.

[68] Ligetti, C., Simpson, T.W., Frecker, M., Barton, R.R. and Stump, G. (2003). Assessing the Impact of Graphical Design Interfaces on Design Efficiency and Effectiveness. *Journal of Computing and Information Science in Engineering*, Vol. 3, No. 2, pp. 144-154.

[69] Loftin, L.K.. Jr. (1980). *Subsonic Aircraft: Evolution and the Matching of Size to Performance*, NASA, Reference Publication 1060.

[70] Lophaven, S.N., Nielsen, H.B. and Søndergaard, J. (2002). DACE: A Matlab Kriging Toolbox. Technical Report IMM-TR-2002-12, Technical University of Denmark.

[71] Maginot, J. (2007). *Sensitivity Analysis for Multidisciplinary Design Optimisation*. PhD Thesis, Cranfield University, Cranfield, UK.

[72] Marler, R.T. and Arora, J.S. (2004). Survey of multi-objective optimization methods for engineering. *Structural and Multidisciplinary Optimization*, Vol. 26, No. 6, pp. 369-395.

[73] Mattson, C. and Messac, A. (2005). Pareto Frontier Based Concept Selection Under Uncertainty, with Visualization. *Optimization and Engineering*, Vol. 6, pp. 85-115.

[74] McDonnell, K. T. and Mueller, K. (2008). Illustrative Parallel Coordinates. *Computer Graphic Forum (Special Issue on Proceedings of the Eurographics/IEEE-VGTC Symposium on Visualization 2008)*, Vol. 27, No. 3, pp. 1031-1038.

[75] Messac, A. (1996). Physical programming: Effective Optimization for Computational Design. *AIAA Journal*, Vol. 34, pp. 149-158.

[76] Messac, A., Ismail-Yahaya, A. and Mattson, C.A. (2003). The normalized normal constraint method for generating the Pareto frontier. *Structural and Multidisciplinary Optimization*, Vol. 25, No. 2, pp. 86-89.

[77] Miller, G. A., (1956). The Magical Number Seven, Plus or Minus Two. *The Psychological Review*, Vol. 63, pp. 81-97.

[78] Mockus, J., Tiesis, V. and Zilinskas, A. (1978). The application of Bayesian methods for seeking the extremum. In: *Towards Global Optimisation*, L.C.W. Dixon and G.P. Szego, eds., Vol. 2, pp. 117-129, North Holland, Amsterdam.

[79] Morgan, E. B. and Shacklady, E. (1987). *Spitfire: The History*, Key Publishing Ltd, Stamford, England.

[80] Murphy, T.E., Tsui, K.-L. and Allen, J.K. (2005). A review of robust design methods for multiple responses. *Research in Engineering Design*, Vol. 16, pp. 118-132.

[81] Murray, C.J. (1998), "Design cycles shrink", Design News (online). http://www.designnews.com/article/11923-Design_cycles_shrink.php (accessed 07 November 2010).

[82] Nunez, M., Maginot, J., Padulo, M. and Guenov, M., (2009). Integrated Exploration and Visualization of Optimal Aircraft Conceptual Designs. In: *50th AIAA/ASME/ASCE/AHS/ASC Structures, Structural Dynamics and Materials Conference*, 4-7 May, Palm Springs, California.

[83] Owen, K. (2001). *Concorde, story of a supersonic pioneer*, Science Museum, London.

[84] Padulo, M. (2008), Internal Report, Cranfield University (unpublished report).

[85] Padulo, M., Campobasso, M.S. and Guenov, M.D. (2007). Comparative analysis of uncertainty propagation methods for robust engineering design. In: *International Conference on Engineering Design ICED'07*, Paris, August 28-31 2007.

[86] Padulo, M. (2009). *Computational Engineering Design Under Uncertainty: an aircraft conceptual design perspective*. PhD Thesis, Cranfield University, Cranfield, UK.

[87] Pang, A.T., Wittenbrink, C.M. and Lodha, S.K. (1997). Approaches to uncertainty visualisation. *The Visual Computer*, Vol. 13, pp. 370-390.

[88] Popescu, I. (1999). *Applications of Optimization in Probability, Finance and Revenue Management*. Ph.D Thesis, Applied Mathematics Department and Operations Research Center, MIT, Cambridge, MA.

[89] Pugh, S. (1990). *Total design: integrated methods for successful product engineering*, 1st edition, Addison-Wesley, England.

[90] Rangavajhala, S., Mullur, A.A. and Messac, A. (2006). Uncertainty Visualization in Multiobjective Robust Design Optimization. In: *2nd AIAA Multidisciplinary Design Optimization Specialist Conference*, Newport, Rhode Island, 1-4 May 2006.

[91] Raymer, D.P. (1992). *Aircraft Design: A Conceptual Approach*, 2nd ed., AIAA Educational Series, ISBN 0-930403-51-7.

[92] Riviere, A. (2004). *Aircraft components impact analysis: state of the art*, VIVACE D1.2.2_2 (online). http://www.vivaceproject.com/content/aircraft/cia_full.pdf (accessed 07 November 2010).

[93] Roskam, J. (1979). *Airplane Design: Part I, Preliminary Sizing of Airplanes*, Roskam Aviation and Engineering Corp., Ottawa, KS.

[94] Rothman, A. and Ray S., "Airbus Dresses Plane as Shark to Take Bite Out of Boeing Market", June 2010 (online). http://www.bloomberg.com/news/2010-06-03/airbus-dresses-up-a321-plane-as-shark-to-take-bite-out-of-boeing-s-market.html (accessed 04 June 2010)

[95] Sacks, J., Welch, W.J., Mitchell, T.J. and Wynn, H.P. (1989). Design and Analysis of Computer Experiments. *Statistical Science*, Vol. 4, No. 4, pp.409-423.

[96] Sarker, R.A. and Newton, C.S. (2008). *Optimization Modelling: A Practical Approach*, CRC Press.

[97] Sasena, M.J. (2002). *Flexibility and Efficiency Enhancements for Constraint Global Design Optimization with Kriging Approximations*. PhD Thesis, University of Michigan, USA.

[98] Sasena, M.J., Papalambros, P. and Goovaerts, P. (2002). Exploration of Metamodeling Sampling Criteria for Constrained Global Optimization. *Engineering Optimization*, Vol. 34, pp. 263-278.

[99] Schonlau, M. (1997). *Computer Experiments for Global Optimization*. PhD Thesis, University of Waterloo, Canada.

[100] Schonlau, M., Welch, W.J. and Jones, D.R. (1998). Global versus local search in constrained optimization of computer models. In: *New Developments and Applications in Experimental Design* (edited by N. Flournoy, W. F. Rosenberger and W.K. Wong), Institute of Mathematical Statistics, Vol. 34, pp. 11-25. Also available as Technical Report RR-97-11 (1997), Institute for Improvement in Quality and Productivity, University of Waterloo, Canada

[101] Sóbester, A. (2003). *Enhancements to Global Design Optimization Techniques*. PhD Thesis, University of Southampton, UK.

[102] Sóbester, A., Leary, S.J. and Keane, A.J. (2005). On the Design of Optimization Strategies Based on Global Response Surface Approximation Models. *Journal of Global Optimization*, Vol. 33, pp. 31-59.

[103] Sobol', I.M. and Statnikov, R.B. (1981). *The Choice of Optimal Parameters in Multicriteria Problems*, Nauka, Moscow (in Russian). Cited in: Statnikov, R.B. and Matusov, J.B. (1995). *Multicriteria Optimization and Engineering*, Chapman & Hall, New York.

[104] Spall, J.C. (1998). An Overview of the Simultaneous Perturbation Method for Efficient Optimization. *Johns Hopkins APL Technical Digest*, Vol. 19, pp. 482-492.

[105] Spall, J.C. (1998). Implementation of the simultaneous perturbation algorithm for stochastic optimisation. *IEEE Transactions on Aerospace and Electronic Systems*, Vol. 34, No. 3, pp. 817-823.

[106] Spall, J.C. (1998). *Introduction to stochastic search and optimization: estimation, simulation and control*, John Wiley & Sons, Hoboken, New Jersey.

[107] Statnikov, R.B. (1978). Solution of multicriteria machines design problems on the basis of parameters space investigation. In: *Multicriteria Decision-Making Problems*, ed. J.M. Gvishiani and S.V. Yemelyanov, pp. 148-155, Mashinostroyeniye, Moscow (in Russian). Cited in: Statnikov, R.B. and Matusov, J.B. (1995). *Multicriteria Optimization and Engineering*, Chapman & Hall, New York.

[108] Statnikov, R.B. and Matusov, J.B. (1995). *Multicriteria Optimization and Engineering*, Chapman & Hall, New York.

[109] Statnikov, R.B., Bordetsky, A. and Statnikov, A. (2009). Management of constraints in optimization problems. *Nonlinear Analysis: Theory, Methods & Applications*, Vol. 71, No. 12, pp. 967-971.

[110] Strang, G. (1991). *Calculus*, Wellesley-Cambridge Press, Wellesley, MA.

[111] Stump, G. M., Simpson, T. W., Yukish, M. and Bennett, L. (2002). Multidimensional visualization and its application to a design by shopping paradigm. In: *9th AIAA/ISSMO Sympossium on Multidisciplinary Analysis and Optimization*, Atlanta, GA, 4-6 September 2002.

[112] Sukhoi Company (JSC). http://sukhoi.org/ (accessed 04 November 2010).

[113] Torenbeek, E. (1982). *Synthesis of Subsonic Airplane Design*, Kluwer Academic Publishers, Dordrecht, The Netherlands.

[114] The MathWorks, Inc., (2007), "Optimization Toolbox 4 User's Guide".

[115] Utyuzhnikov, S.V., Maginot, J., and Guenov, M. (2006). Local Pareto Analyzer for Preliminary Design. In: *Proceedings of the 25th International Congress of the Aeronautical Sciences*, ICAS, Stockholm, Sweden.

[116] Utyuzhnikov, S.V., Maginot, J., and Guenov, M. (2007). Local Approximation of Pareto Surface. In: *Proceedings of the World Congress on Engineering*, Vol. 2, IAENG, Hong Kong, pp. 898-903.

[117]Utyuzhnikov, S., Maginot, J., and Guenov, M. (2008). Local Pareto approximation for multiobjective optimization. *Engineering Optimization*, Vol. 40, No. 9, pp. 821-847.

[118] Vesanto, J., Himberg J., Alhoniemi E.,and Parhankangas J., *SOM Toolbox for Matlab 5*, SOM Toolbox Team, Helsinki University of Technology, http://www.cis.hut.fi/projects/somtoolbox/ (accessed 23 June 2010)

[119] Wang, I. and Spall, J.C. (2003). Stochastic optimization with inequality constraints using simultaneous perturbations and penalty functions. In: *Proceedings of the 42nd IEEE Conference on Decision and Control*, Vol. 16, pp.3808-3813.

[120] Wegman, E. J. (1990). Hyperdimensional data analysis using parallel coordinates, *Journal of the American Statistical Association*, Vol. 85, pp. 664-675.

[121] Wegman, E. J. and Luo, Q. (1997). High dimensional clustering using parallel coordinates and the grand tour. *Computing Science and Statistics*, Vol. 28, pp. 352-360.

[122] Wetter, M. and Wright, J. (2003). Comparison of a generalized pattern search and a genetic algorithm optimization method. In: *8th International IBPSA Conference*, Eindhoven, Netherlands.

[123] Yang, R.J., Li, G., Gu, L. and Soto, C.A. (2004). Application of High Performance Computing and Visualization to Crashworthiness Design Optimization. In: *10th AIAA/ISSMO Multidisciplinary Analysis and Optimization Conference*, Albany, New York, 30 August – 1 September 2004.

[124] Yassine, A. and Braha, D. (2003). Complex Concurrent Engineering and the Design Structure Matrix Method. *Concurrent Engineering: Research and Application*, Vol. 11, No. 3, pp. 165-176.

[125] Young, F. W., Valero-Mora P. M., Friendly M. (2006). *Visual Statistics: Seeing Data with Dynamic Interactive Graphics*, John Wiley and Sons.

[126] Yukish, M., Stump, G. and Lego, S. (2007). Visual steering and trade space exploration. In: *2007 IEEE Aerospace Conference*, 3-10 March 2007.

Appendix A

Parallel Coordinates Plot and Scatter Plot Matrix

This appendix is intended to provide a more exhaustive description and few examples of the two multidimensional visualisation methods integrated in the methodology proposed in Chapter 4 and implemented in the Integrated Exploration and Visualisation Interface (IEVI). Further details can be found in the literature [46][50][120][125].
To highlight their key features and capabilities, a dataset of 75 aircraft belonging to 11 different categories and including 8 variables is considered.

Parallel Coordinates Plot

Unlike the traditional Cartesian-coordinate system in which the axes are represented mutually perpendicular, parallel coordinates plots are based on the idea of representing the dimensions by a set of vertical parallel axes, as many as the dimensions of the input vectors and usually equally spaced [46][125]. Such technique is particularly useful for the visualisation of high-dimensional data on a simple two-dimensional plot, representing all the parameters simultaneously on the same graph: a point $P \in R^n$ is visualised as a polyline characterized by n vertices located on the vertical axes, with the position of the *i-th* vertex established by the *i-th* coordinate of the point. Consequently, plotting an entire dataset of multidimensional points will produce a graph consisting of as many polylines as the number of samples, each one made up of $(n - 1)$ segments.
This technique provides a means for clustering, enabling the users to identify subsets of samples which are characterized by common features (e.g., all those samples whose values for one or more dimensions are within specific ranges) or the relationships existing among the design parameters.

As for most visualisation techniques, data normalization is a simple but very important aspect that must be considered to ensure that all the dimensions have the same weight in the plot. In those cases where the considered parameters have values within ranges that are very different from one another, normalisation of input data allows to prevent that the axis having the highest values turn out to be predominant on the plot, making the visualisation of other parameters not visible or clear.

For large datasets, the corresponding parallel coordinate plot may be not clear, and it could be extremely difficult to identify any data structure or pattern because of the polylines overlapping. In order to tackle this problem, Young et al. [125] suggest to repeatedly apply the following actions:

- **Brushing the plot**, searching data subsets characterized by a common trace-line profile;
- **Changing the colour** of the polylines belonging to the same subset, in order to distinguish them from the other subsets;
- **Hiding the identified subsets** during the analysis of the remaining polylines, so that the search of other more hidden subsets can be carried out more easily by reducing the amount of trace lines to analyse.

This three-step process should be performed several times until all the clusters can be identified within the whole input data.

Figure 65 illustrates the parallel coordinates visualisation of the multidimensional dataset mentioned earlier, giving a practical example of the analysis actions described above. The parameters names are encoded by the table of Figure 67, and data have been normalised (scaling the values of each parameter within the range [0 1]) before being plotted.

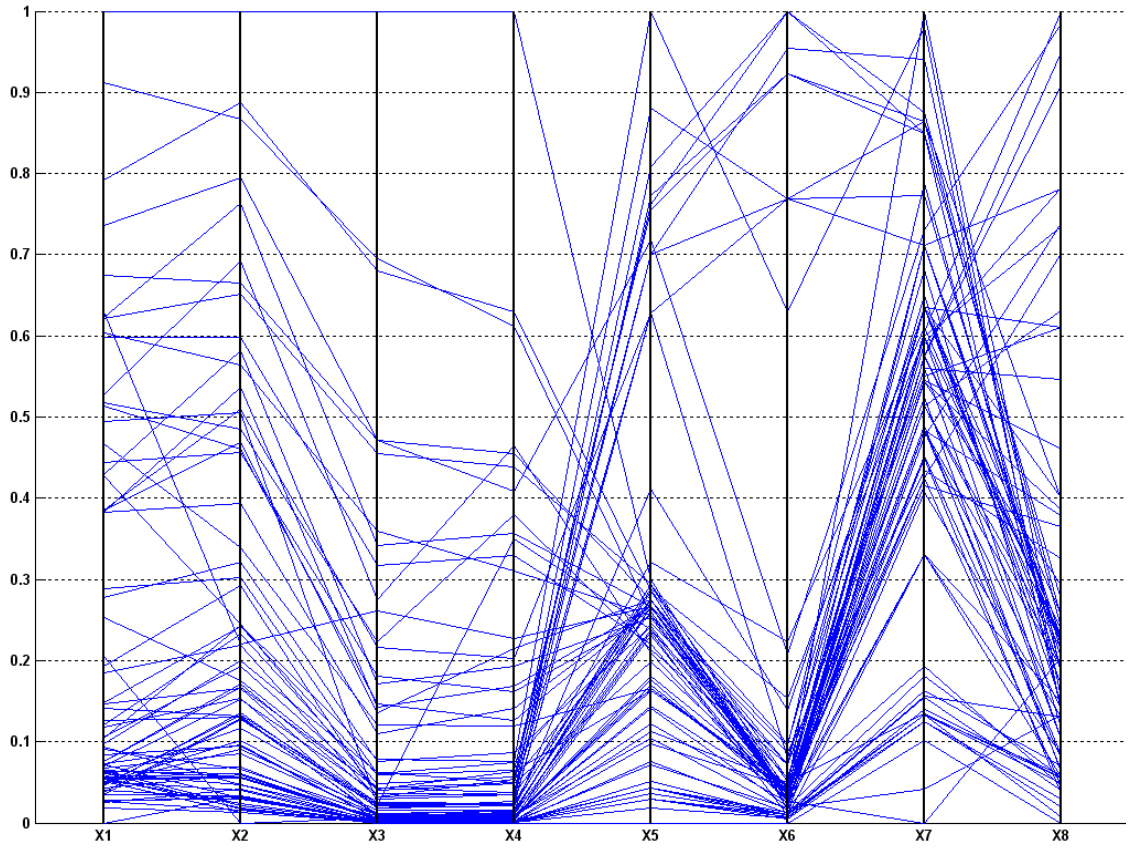

Figure 65. Parallel coordinates plot of a dataset of 75 aircraft belonging to 11 different categories and considering 8 parameters, which are encoded by the table of Figure 67 along with their corresponding value ranges.

The analysis of Figure 65 is clearly complex and only a limited amount of information can be conveyed to the user (e.g., the range of values and few relationships among the parameters displayed in the plot). However, the entire data analysis can be simplified by performing the three analysis techniques earlier mentioned, as shown in Figure 66:

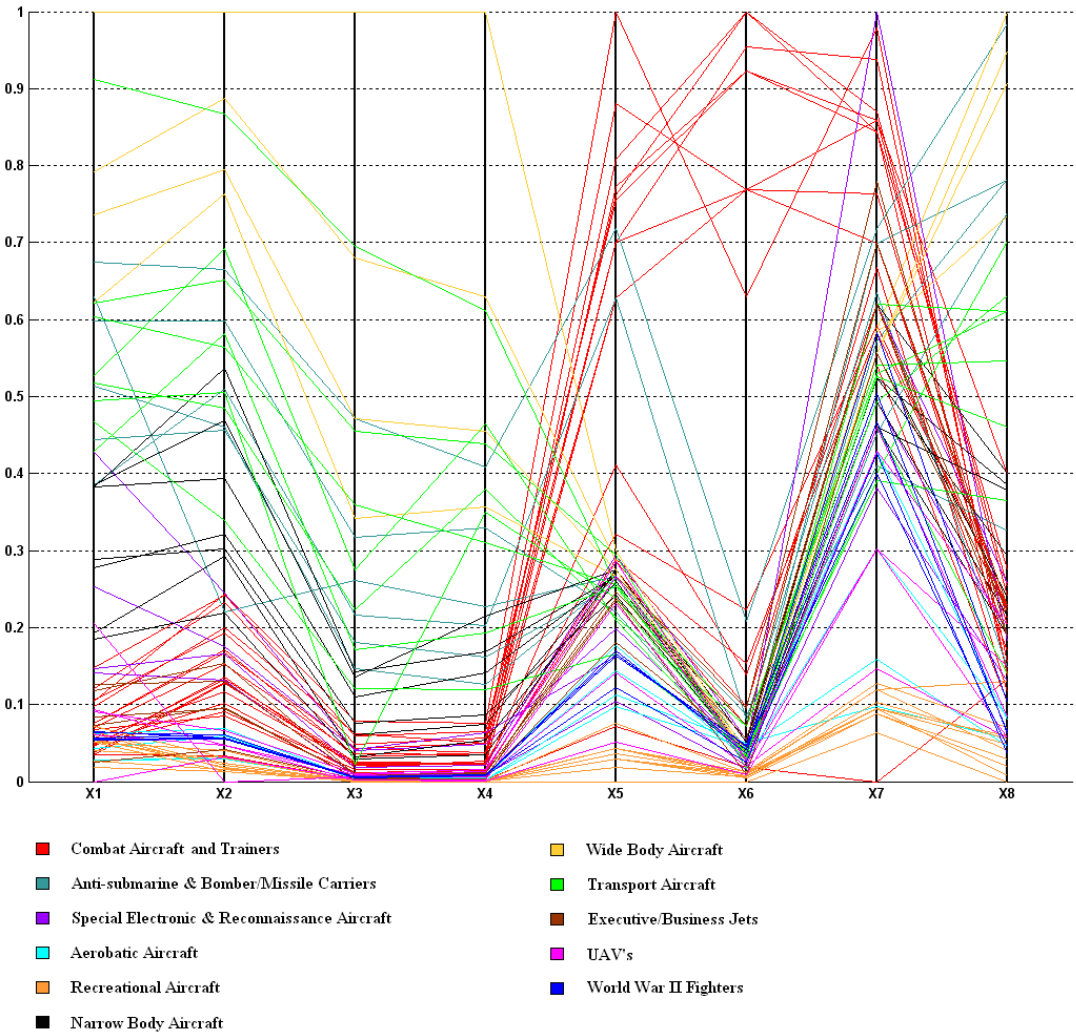

Figure 66. Graphics enhancement obtained by performing the above-described analysis techniques for the analysis of parallel coordinate plots. The identification of the aircraft categories is depicted through the colour of the polylines.

The individual visualisation of the different categories within the input data allows to highlight the features that are inherent to each subset, as illustrated in Figure 67.


Combat Aircraft & Trainers
1
0.9
0.8
0.7
0.6
0.5
0.4
0.3
0.2
0.1
0
X1 X2 X3 X4 X5 X6 X7 X8

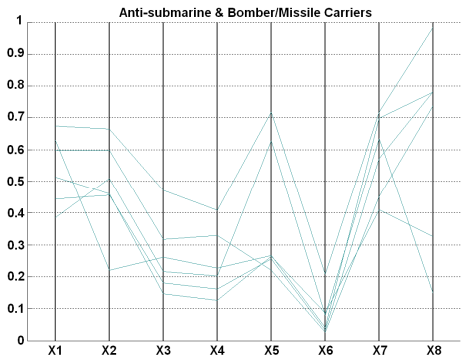
Anti-submarine & Bomber/Missile Carriers
1
0.9
0.8
0.7
0.6
0.5
0.4
0.3
0.2
0.1
0
X1 X2 X3 X4 X5 X6 X7 X8

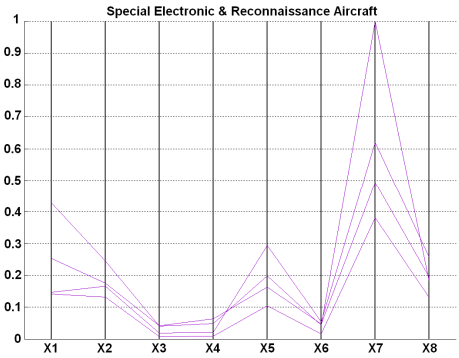
Special Electronic & Reconnaissance Aircraft
1
0.9
0.8
0.7
0.6
0.5
0.4
0.3
0.2
0.1
0
X1 X2 X3 X4 X5 X6 X7 X8

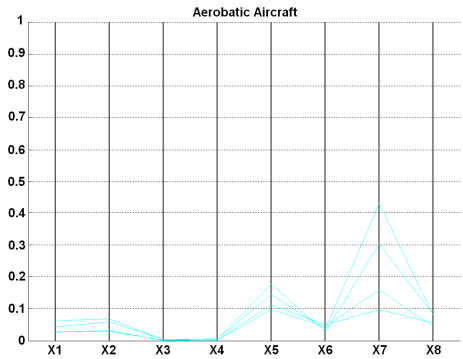
Aerobatic Aircraft
1
0.9
0.8
0.7
0.6
0.5
0.4
0.3
0.2
0.1
0
X1 X2 X3 X4 X5 X6 X7 X8

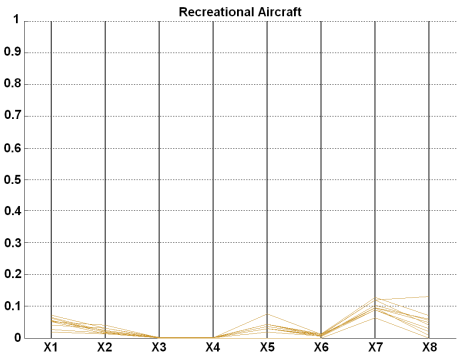
Recreational Aircraft
1
0.9
0.8
0.7
0.6
0.5
0.4
0.3
0.2
0.1
0
X1 X2 X3 X4 X5 X6 X7 X8

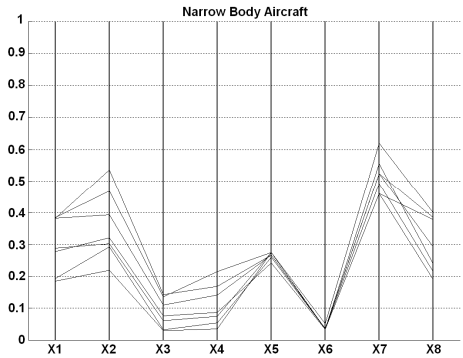
Narrow Body Aircraft
1
0.9
0.8
0.7
0.6
0.5
0.4
0.3
0.2
0.1
0
X1 X2 X3 X4 X5 X6 X7 X8

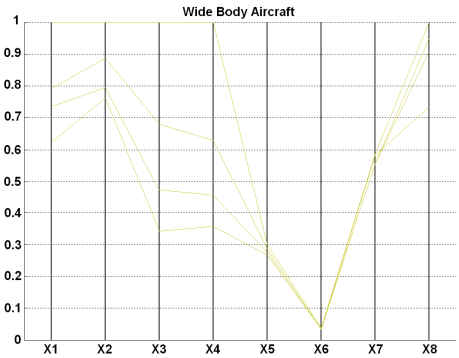
Wide Body Aircraft
1
0.9
0.8
0.7
0.6
0.5
0.4
0.3
0.2
0.1
0
X1 X2 X3 X4 X5 X6 X7 X8

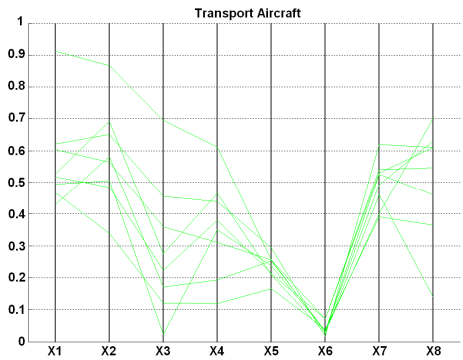
Transport Aircraft
1
0.9
0.8
0.7
0.6
0.5
0.4
0.3
0.2
0.1
0
X1 X2 X3 X4 X5 X6 X7 X8

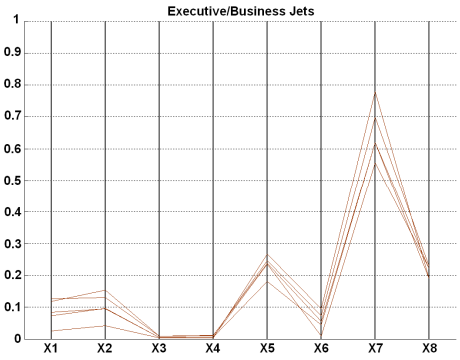

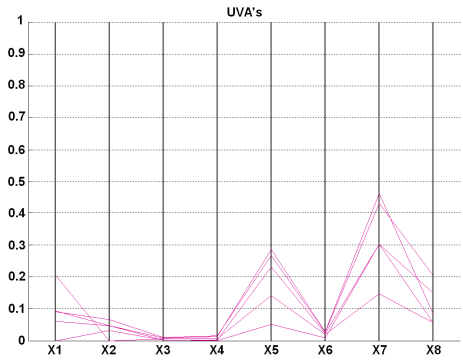

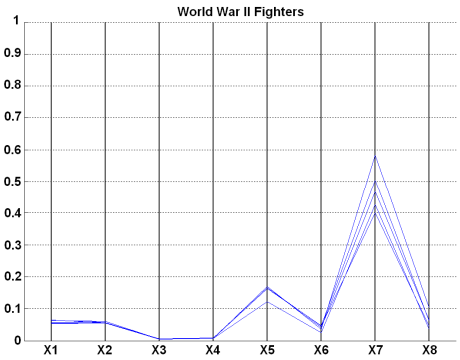

Axis	Parameter	Range
X_1	Wing Span	[5.7 - 79.8] [m]
X_2	Length	[4.6 - 79] [m]
X_3	MTOW	[181 - 583000] [kg]
X_4	Empty Weight	[88.5 - 286000] [kg]
X_5	Max Speed	[0.06 – 2.83] [mach]
X_6	Max Climb Rate	[300 - 65000] [ft/min]
X_7	Ceiling	[6000 - 68900] [ft]
X_8	Max Range	[129 - 14177] [km]

Figure 67. Individual visualisation of the different aircraft categories and code of the parameters names displayed in Figure 65 and Figure 66.

Scatter Plot Matrix

A scatter plot is a graph in which the observations for a pair of parameters are shown in a bidimensional space via axes drawn perpendicularly to each other (Cartesian coordinates). The resulting scattering of points allows the user to reveal any relationship between the parameters under study, distributions shape, possible data patterns, clusters and outliers.

A scatter plot matrix is a square and symmetric matrix made up of bidimensional scatter plots showing the relationship between every pair of parameters of a multidimensional database [125][50]. For a *k*-parameters dataset the plot contains *k* rows and columns, each one representing a different dimension. The cell identified by the intersection of row *i* and column *j* contains the bivariate plot having the *i-th* parameter on the vertical axis and the *j-th* parameter on the horizontal axis. The scatter plot matrix is therefore symmetric about

its diagonal: the panel *j-i* has the same parameters of the panel *i-j*, but with their relative axes reversed.

This method is a very simple technique to visualise and analyse datasets containing a large amount of samples and several parameters. The systematic visualisation format of the *k(k-1)* distinct two-dimensional views through the off-diagonal cells makes the identification of bivariate relationships within multivariate data easier: all the relationships of the *i-th* parameter with all of the other dimensions are represented in the panels contained within the *i-th* row (or column) of the scatter plot matrix.

Since each pair of parameters is represented twice within two different cells, one above and one below the main diagonal, it can seem that the scatter plot matrix provides redundant information. An alternative is the so-called half-matrix version, or draftsman's display, which visualises only the off-diagonal bivariate plots above or below the main diagonal. In contrast to the main advantage of gaining a more concise data visualisation, there are two main drawbacks with respect to this variant. First, all the relationships of a particular parameter are not any more displayed only on the corresponding row or column, with the exception of the first and last parameters (represented by the plots on the last column and the first row in the case of the upper triangular matrix). Second, visual processing of information can be influenced by the disposition of the parameters in the plot axes. For example, in some occasions it can be easier to identify a relationship between two parameters X_i and X_j when they are represented on the vertical and horizontal axis respectively rather than when their positions are reversed.

According to the user's analysis objectives and personal customisation, the basic scatter plot matrix can be modified and enriched by displaying further information [125]. Common approaches are based on the use of the diagonal cells to display one-dimensional data features (e.g., univariate distributions).

However, too much information or graphical enhancements can overshadow features of the data, overloading the information-processing skills of the user. It is recommended to represent data without excessive information, looking for a data visualisation as simple as possible.

Theoretically, there is not any limitation as regards the dimension *k* of an input dataset visualised by a scatter plot matrix. Simply, the larger is *k* the larger is the matrix. However, even if all the data is visualised simultaneously in a unique plot, it can be very difficult to manage all the information displayed. For this reason, it is recommended to consider at most 8-10 parameters. A possible solution to increase such number could be represented by an interactive graph which, for example, magnifies and furnishes a greater amount of information about any cell selected by the user. Figure 68 illustrates an example of a potential user interface implemented on the basis of such idea.

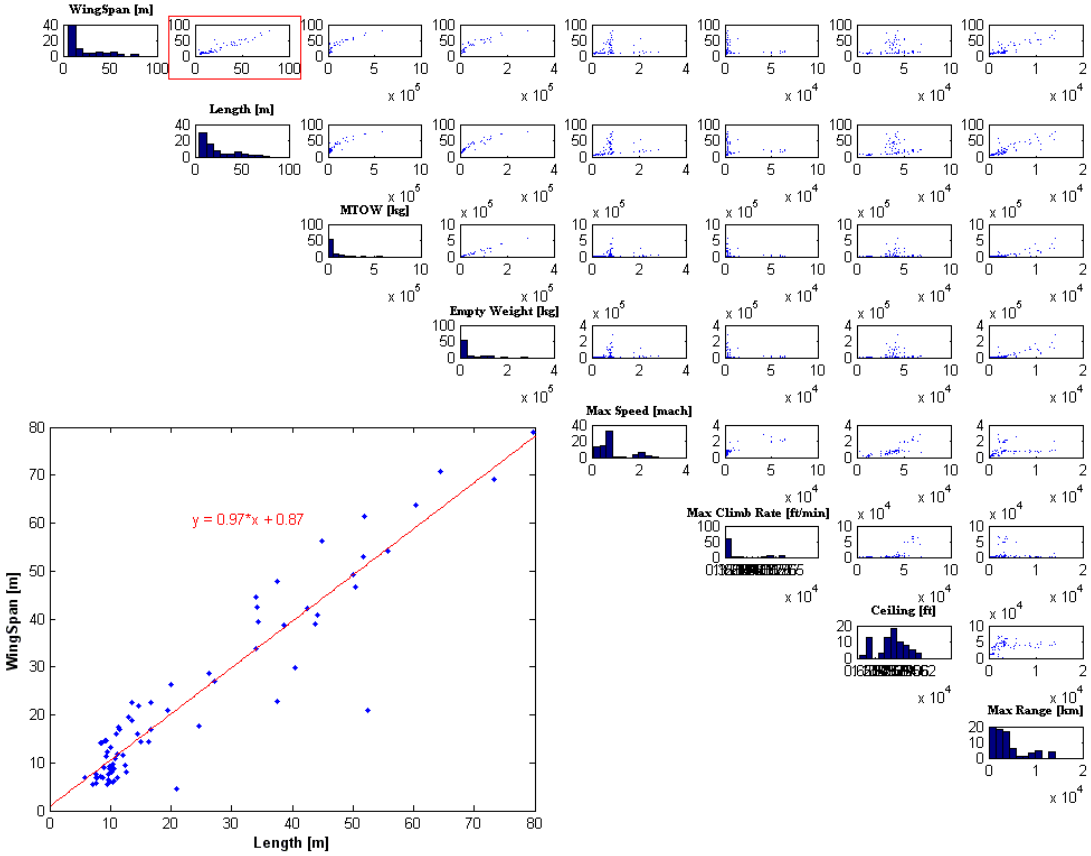

Figure 68. A possible interactive interface in which any bivariate plot selected by the user is magnified below the main diagonal. This example is also representative of those situations in which the user may be interested in identifying the equation which best describes the overall pattern of the relationship between two parameters (e.g., linear, quadratic, cubic, exponential, sinusoidal, etc.) [125].

Appendix B

An Example of the Effects of Correcting the Search Region on the Optimal Solutions Set

The choice of the aircraft layout during the conceptual phase is crucial for the initial weight prediction, whose minimisation is a paramount issue because of its impact on numerous disciplines (e.g. aerodynamics, propulsion, structures) and on total operating costs. A rough weight breakdown of a conventional design of a medium subsonic transport aircraft [113] is shown in Table 30 as a function of MTOW:

OEW	61% MTOW
Payload	22% MTOW
Fuel	17% MTOW (5% reserve, 12% trip fuel)

Table 30. Typical breakdown of a conventional design of a medium subsonic transport aircraft.

In general, aircraft costs are associated with the operational empty weight (OEW)[15]. It is evident that the effort in minimising MTOW and maximising the range (fuel) for a constant payload is an emblematic example of a multi-objective optimisation with conflicting design objectives. Its solution relies on the search of aircraft configurations for which a reduction in MTOW can be obtained by reducing mainly the OEW in order to limit significant detriments on fuel, guaranteeing at the same time the specified payload.

The following example, representative of the abovementioned problem, highlights the importance of choosing adequately the search region for an optimisation procedure. For the test case described in Chapter 6 two optimisations where conducted by considering

[15] For example, the estimated cost for a jet-propelled transport aircraft for the 1973-1975 period was approximately 220-265 dollars per kg of OEW [113].

the sets of design-variable constraints described in Table 31. To show how sensible optimal results can be, depending on the choice of the design-variable constraints, the search regions taken into consideration for the two optimisations are exactly the same except for the lower bound of the variable *Awing*, which has been relaxed of 1.31%. The corresponding Pareto fronts obtained are depicted in Figure 69.

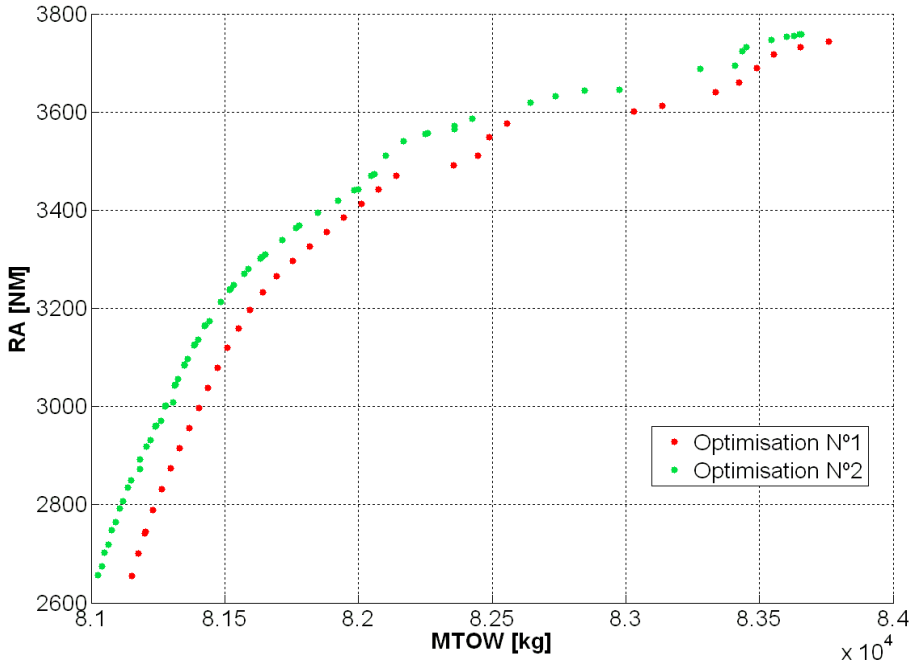

Figure 69. Pareto fronts of Optimisation N°1 and Optimisation N°2. The two optimisation procedures were carried out within similar search regions, whose settings are specified in Table 31.

Input Variable	Optimisation N°1		Optimisation N°2	
	x_{lb}	x_{ub}	x_{lb}	x_{ub}
FNslst [decaN]	12500	13000	12500	13000
Awing [m^2]	152	158	150	158
span [m]	30	38	30	38
phi [deg]	28	32	28	32
tuc	0.07	0.1	0.07	0.1
Fuel [kg]	17000	18000	17000	18000
BPR	5	8.5	5	8.5
Mach_crz	0.7	0.9	0.7	0.9

Table 31. Variables bounds setup for Optimisation N°1 and Optimisation N°2.

If the designer is particularly interested in minimising the MTOW rather than maximising the range in order to cut costs, s/he would consider the points placed in the lower left-hand corner of the graph. In this perspective, at a first sight it may not appear evident there is any significant improvement by considering the optimal solutions of Optimisation Nº2 in terms of MTOW reduction. For example, by considering the extreme points of the two optimal sets, the MTOW difference is approximately 125 kg, which is a cut of only 0.15% of the value obtained via Optimisation Nº1. However, for the same points, the increase in range for an equal MTOW is 180-190 NM, which is a considerable increase of 6.78-7.15% on the values of Optimisation Nº1.

Another fundamental issue in defining the search region is the coupling amongst all the design variables taken into consideration. Generally, the correction of the bounds on a variable affects the distribution of the feasible solutions set on the remaining variables. This is shown in Figure 70, where the distributions of all the design parameters considered in the two optimisations described above are compared. Considering the distributions of the points evaluated during the Optimisation Nº1, it is evident that in the case of the variable *Awing* the great majority of feasible points are concentrated near the lower bound, whereas occasional points have been evaluated elsewhere. It is therefore natural to consider the possibility that further feasible (potentially optimal) points can be obtained by relaxing the constraint on the lower bound of this variable. This is precisely the motivation behind the setup of Optimisation Nº2, moving only the lower bound of *Awing* from 152 to 150 [m^2]. The resulting effects on the new distributions for the other variables are shown in the same figure. Relevant consequences, for example, are evident on *Fuel* and *FNslst*, whose distributions now present new peaks in the central area of the respective search regions. A relevant effect is also evident in the neighbourhood of the *Awing* upper bound.

	Optimisation Nº1	**Optimisation Nº2**
Variable: *FNslst*	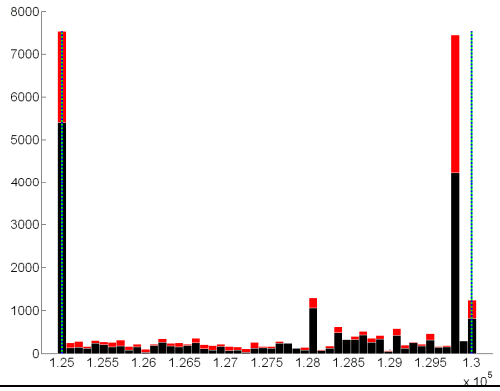	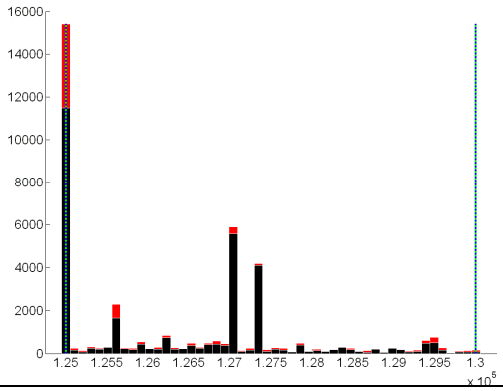
Variable: *BPR*	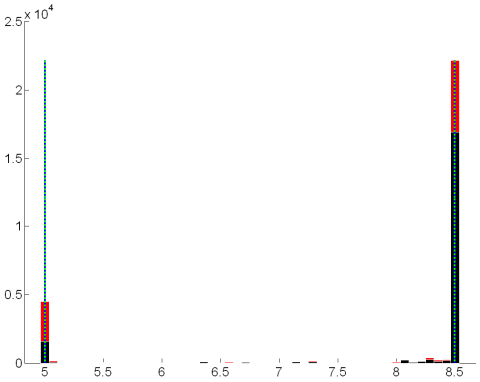	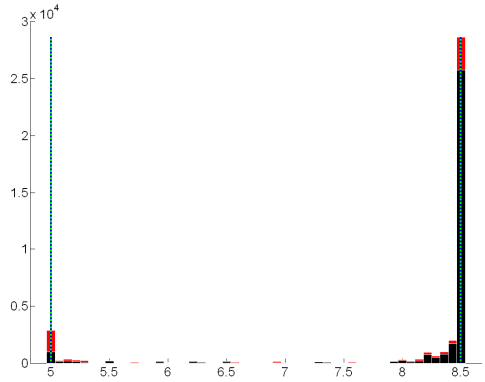
Variable: *Awing*	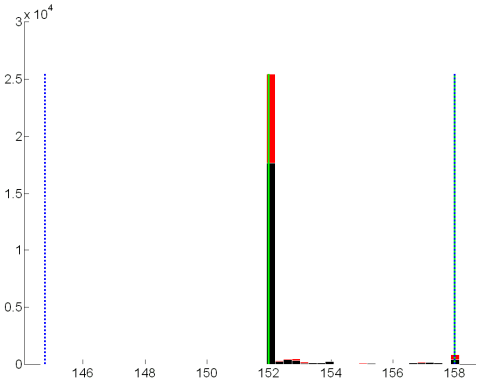	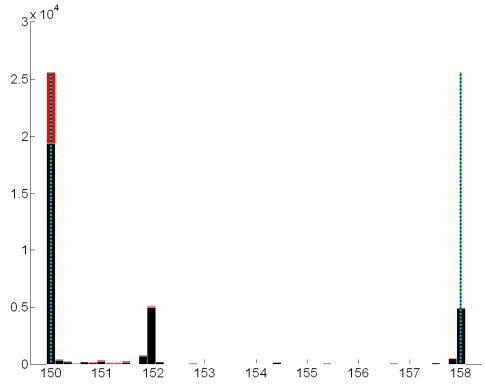

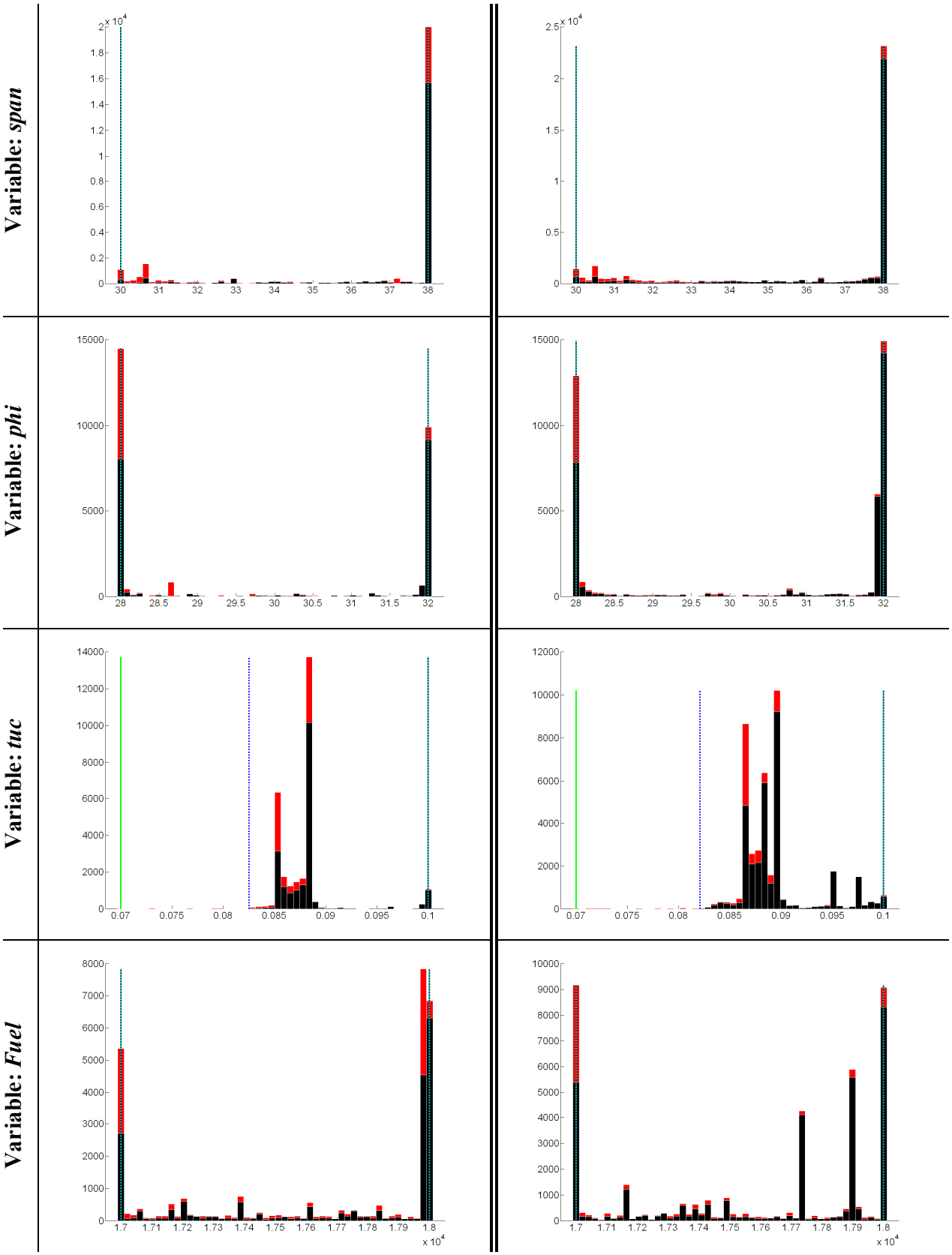
Variable: span
Variable: phi
Variable: tuc
Variable: Fuel

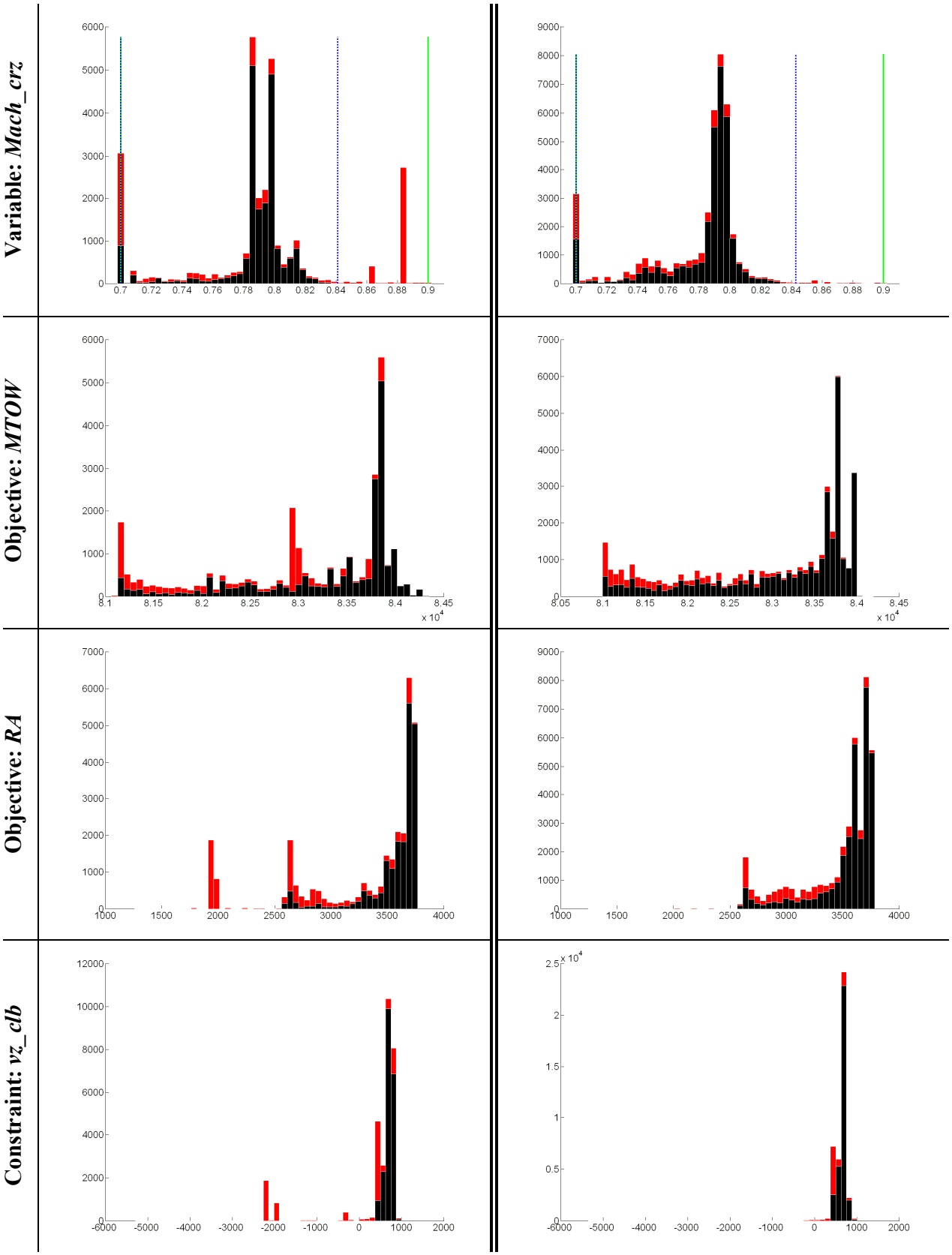
Variable: Mach_crz
Objective: MTOW
Objective: RA
Constraint: vz_clb

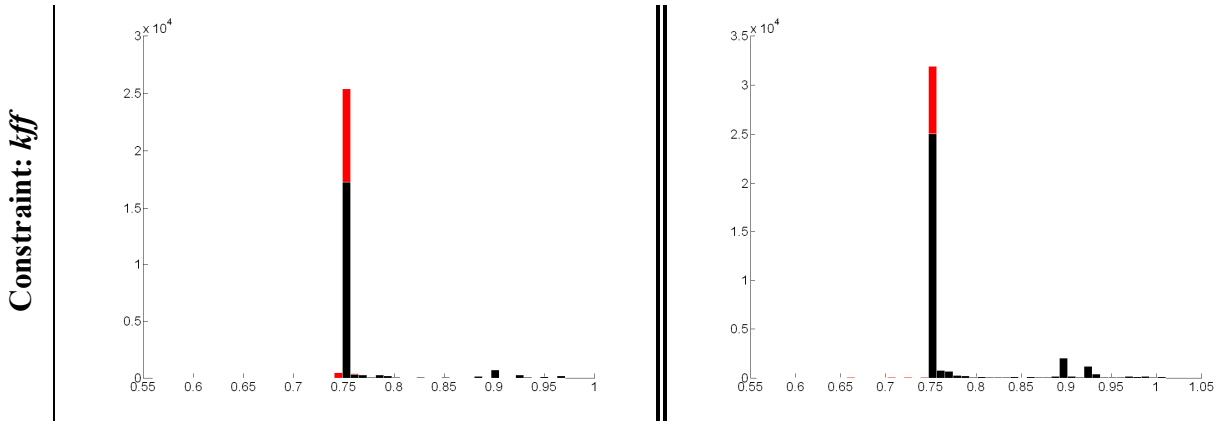

Figure 70. Comparison of the design parameters distributions of Optimisation Nº1 and Optimisation Nº2, where the entire set of evaluated points and the set of feasible points are represented in red and black respectively. The green lines represent the variables bounds considered throughout the optimisation procedures; whereas the dashed blue lines identify the lower and higher feasible sampled values of each variable distribution, which in some cases are not visible. It is important to notice how, normally, such lines coincide. Nonetheless, it may happen that either the sampled set of feasible points turns out to be narrower than the imposed corresponding search region (variable *tuc* and *Mach_crz*), or the optimiser occasionally samples design solutions located beyond the variables bounds (variable *Awing*).

Appendix C

An Example of the Effects of Relaxing a Soft Constraint on the Optimal Solutions Set

Take-off field length (*tofl*) is one of the critical performance constraints of aircraft design. Due to its direct influence on the aircraft configuration this is generally part of the initial design specifications. The enforcement of a certain take-off field length may dictate the aircraft wing area, the size of the engine required, or the performance of the high-lift system.

In terms of airworthiness regulations, one of the most important design criteria is given by the Balanced Field Length (BFL) that expresses the safety requirements to account for the event of one-engine-out take-off. Such a performance parameter is a function of brake-release gross weight and ambient conditions (temperature and airport altitude). Therefore, the same aircraft can be operated in airports with different runway lengths and ambient conditions by adequately setting its take-off weight (payload and fuel).

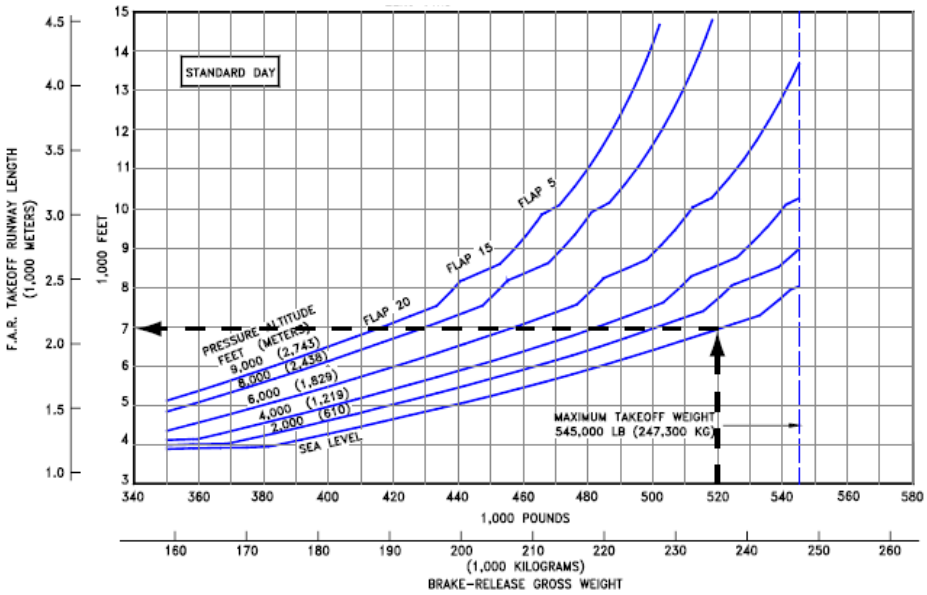

Figure 71. F.A.R. take-off runway length requirements (standard day) –model 777-200 (baseline airplane) [1].

A more stringent constraint on take-off field length may be considered when a gain in the number of airports from which the airplane is able to operate is sought, thus increasing its operational flexibility and consequently its market potential. From an economical perspective, the runway length requirement comes to be a trade-off. An excessive take-off field length can result on a considerable reduction of the available airports, whereas its minimisation can significantly raise design costs. Considering runways information for UK, French and German major airports, the 50 cumulative percentage corresponds to a field length of around 2100 m, as shown in Figure 72.

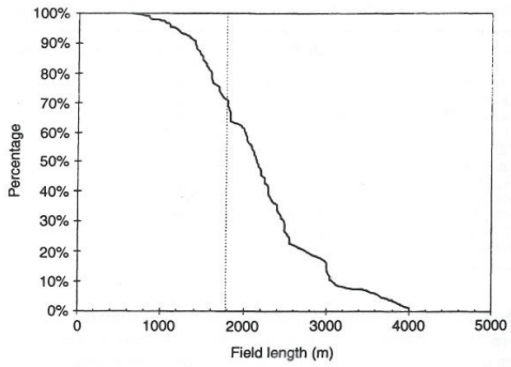

Figure 72. Distribution of field lengths at major European airports [51].

During the early stages of design, key criteria for the requirements specification might be given by non-technical considerations such as the commercial transport market outlook, in particular by examining long-term forecasts for airplanes demand and market growth rates. For example, according to the market predictions by Boeing shown in Figure 73, the sectors of narrow-body seem to gain more and more importance in the commercial transport of next generation. This may happen both to sustain the expected increment of number of passengers (~5% per year) and because of the fleet reshaping already stared by many airliners, which are investing on new aircraft that match more closely the routes they fly in order to reduce the costs of old and low-efficient airplanes associated with today's high fuel prices.

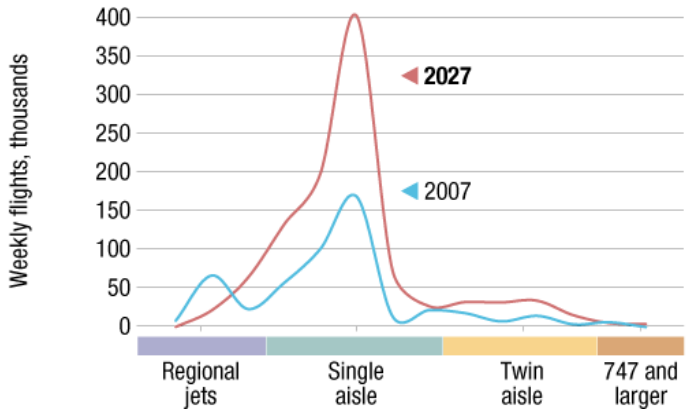

Figure 73. Future distribution of flights [15].

This example is aimed at highlighting the consequences that may potentially arise when dealing with non-rigid constraints. The scenario under analysis is the field performance specification for a conceptual design of a narrow-body commercial aircraft. For comparison purposes, the average field lengths required by some current narrow-body aircraft are provided in Table 32.

Aircraft	Avro RJ-85	Embraer RJ 135ER	Airbus A 318	Airbus A 321	Boeing 737-800	MD 82
Take-Off Field Length (*tofl*) [m]	1564	1700	1670	2220	2100	2315

Table 32. Narrow-body aircraft field performance [49][64].

Considering again the test case described in Chapter 6 two optimisations where conducted. They will be here referred as Optimisation Nº3 and Optimisation Nº4. The two problem formulations are the same except for the limit values established for the take-off field length constraint, which has been relaxed of 100 meters on Optimisation Nº4. The Pareto fronts obtained in both cases are shown in Figure 74. From the analysis of the results it turns out that for all the optimal points of Optimisation N º3 the *tofl* constraint can be assumed to be active, while this happens for less than 40% of the optimal solutions found in Optimisation Nº4. Supposing again that the designer is more interested in minimising *MTOW* rather than maximising range, s/he will be more attracted by the points placed in the lower left-hand corner of the graph. The main benefits resulting from a relaxation of the *tofl* constraint regard the points of Optimisation Nº3 characterized by a *MTOW* within the range [82300-82600] kg. The *MTOW* reduction for an equal *Range* obtained for those points via the Optimisation Nº4 is about 300 kg (-0.36%), and the gain in *Range* for an equal *MTOW* is 80-90 NM (+2.45-2.8%).

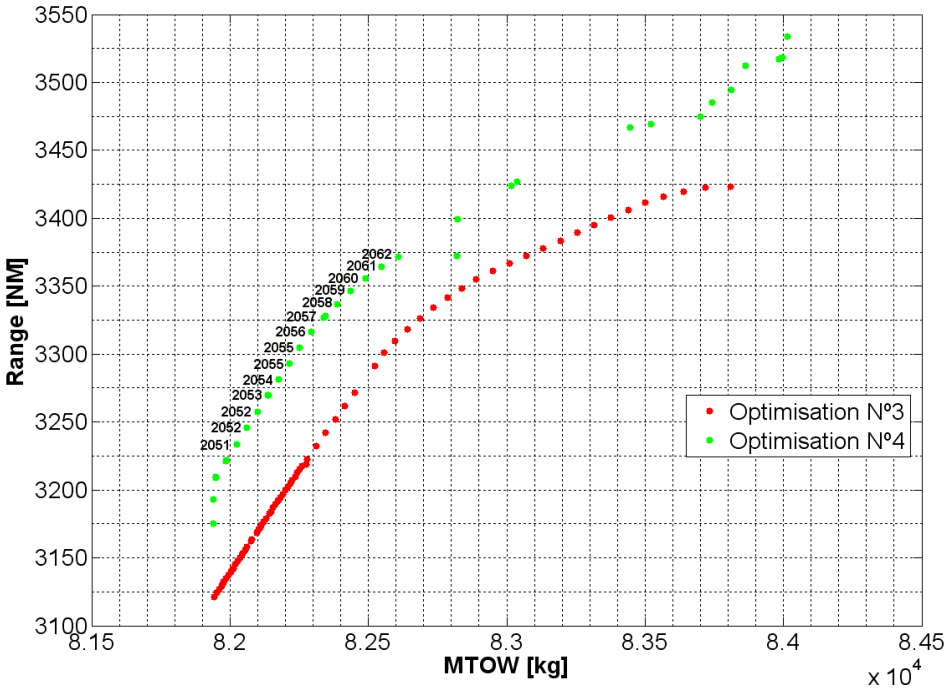

Figure 74. Pareto fronts of Optimisation Nº3 and Optimisation Nº4. Displayed besides each one of the considered points of Optimisation Nº4 is the corresponding *tofl* value.

Mention should be made of the fact that for the optimal solutions obtained from Optimisation Nº4 and featured by a lower *MTOW*, *tofl* is not an active constraint. Although in the problem formulation it has been relaxed from 2000 to 2100 meters, the Pareto points in the lower left-hand corner of the plot present an increment of 50-60 (+2.5-3%) meters with respect to the results of Optimisation Nº3.

Appendix D

Engineering Change Problems that can Potentially Affect Aircraft Conceptual Design

Provided in this section are a number of engineering change scenarios triggered by unplanned design iterations with a potential impact on the conceptual stage of aircraft design. Some examples of real-life problems faced by the aeronautical industry are also provided.

- **Customers' correction of products requirements**. Engineering changes may be required to adapt the design to new needs and requirements specified by the customer. This scenario can turn out to be particularly problematic when there are multiple customers, each with a different set of requirements [28]. An example is the Airbus A350-800 concept, which was revised in 2009 to be developed as a shorter version of the initial A350-900 variant because of the airlines pressure for enhancing commonality capabilities and range [60].

- **Manufacturing specifications**. A considerable number of design changes generally arise during a preliminary determination of manufacturing issues [33]. Modifications are triggered by different design revisions aimed at finding an agreement between designers and production staff. All this can turn out to be even more complicated when multiple assembly lines and factories are involved. For

the production of the Concorde, for example, various issues arose from the fact of having two assembly lines, one in Britain and one in France, each with different production practices [83].

- **Mismatches between expected and real performances**. The need of introducing modifications in the design can derive from testing procedures, which may reveal the non-satisfaction of expected performances. An example is given by the development of the Su-27, which required several redesign actions after its expected air-superiority was not confirmed by comprehensive analyses of performance [112].

- **New legislations and regulations**. The introduction of new legislations and regulations can be one of the reasons of design change. Stricter emission regulations have, for instance, been considered by aircraft manufacturing and airlines industries, the scientific community, and governmental bodies because of the steady increment of fuel use and total emissions in air transport [65]. Stricter regulations have also been introduced in the last thirty years on aircraft noise, in and around airports, and it is expected to continue over the next twenty years [14]. With respect to the latter, for example, one of the most difficult redesign challenges encountered by the engineers in the development of the Concorde was the noise reduction of the Olympus 593 engines, which was dictated by more stringent regulations for subsonic aircraft introduced since the beginning of the project [83].

- **Competitors' products**. Design changes may be required after additional information or considerations about competitors' products come to light. Representative of this case is the strategy of Airbus for gaining a part of Boeing Co.'s home market [94]. The decision of fitting the so-called sharklets to the wings of the largest of Airbus' four narrowbody models (A321) was taken to increase its range, which was shorter than its competitor Boeing 757, thus expecting an increment of 100 nautical miles (or 1,100 payload pounds). Another

example is given by the A380-800 variant, whose weight and performance gain came from customers' requirements against its Boeing competitor [62].

- **Marketing strategy reasons.** Marketing strategy refinements can also result in design changes. One of the marketing strategies nowadays adopted by many engineering companies is based on commonality among its aircraft to reduce design and maintenance costs. In some cases this approach is undertaken by incorporating minor changes to an existing product, rather than developing an optimised variant. With respect to the second member of the A350 family, for instance, a number of customers endorsed the decision of developing a shorter variant of the A350-900 with enhanced commonality capabilities instead of optimising its design around reduced weights [61].

- **Inadequacy of available design methods.** In some cases it may happen that adequate methods and tools for the analysis and development of specific design aspects are not available, especially when addressing unconventional designs. A clear example was the design of the Concorde wing, which required thousands of hours of model testing in wind tunnels and flight testing to reinforce the inadequate theoretical methods that were available. This, coupled with the complicated and conflicting requirements to satisfy, determined the incorporation of continuous aerodynamic improvements up to a late stage of the design through a series of changes in leading-edge camber, plan-form, and overall camber and twist [83].